

# **BULGARIAN CHEMICAL COMMUNICATIONS**

**2024** Volume 56 / Number 2

*Journal of the Chemical Institutes  
of the Bulgarian Academy of Sciences  
and of the Union of Chemists in Bulgaria*



## In memoriam Prof. DSc Ivan Pojarlieff (Johnny)



(03.11.1935 – 03.05.2024)

On May 3, 2024, we lost our teacher, colleague and friend, the corresponding member of the Bulgarian Academy of Sciences Professor DSc Ivan Georgiev Pojarlieff. Tribute to his bright memory!

Prof. Pojarlieff is among the pioneers in the field of mechanistic organic chemistry in Bulgaria. His achievements in stereochemistry, conformational analysis and kinetics and mechanism of organic and bioorganic reactions raised the organic chemistry in the country to a qualitatively new level.

After graduating from the Faculty of Chemistry of the Sofia University in 1958, Ivan Pojarlieff became a full-time graduate student of Acad. Bogdan Kurtev at the Institute of Organic Chemistry at the Bulgarian Academy of Sciences (BAS) and defended his PhD dissertation entitled "Synthesis, stereochemistry and mechanism of cyclization of 3-ureido acids" in 1964. In 1987 he obtained the scientific degree Doctor of Sciences with a dissertation on the „Quantitative dependences of steric effects of substituents in the closing and opening of ring compounds”. In 1971 he became Associate Professor, in 1987 Professor, and in 2004 he was elected Corresponding Member of the BAS. Prof. Pojarlieff published more than 125 publications, which have found a wide response in the world literature, one rationalization, 3 patents and 23 author's certificates.

He specialized in nuclear magnetic resonance and chemical kinetics with Prof. Alan Katritzky at the University of East Anglia and had a long-term collaboration with Cambridge University on enzyme reaction models. During this specialization, he applied modern NMR techniques to clarify problems on Bulgarian topics. With the help of a significant set of dihydrouracils, including model ones, he established the relationship between the proton NMR-parameters and the stereochemistry of the flattened ring. The publication became a primary source in determining configurations and conformations of dihydrouracil systems.

The main achievements of Prof. Pojarlieff in the field of reaction mechanisms are related to his conviction that establishing the mechanism of biochemical reactions is practically possible only if the mechanism of the corresponding non-enzymatic reactions and the ways in which they can be accelerated are known. For this purpose, he organizes and conducts research on the mechanism of acyl group transfer in urea systems; a reaction of special biological interest related to the metabolism of pyrimidine bases and the action of the coenzyme biotin. Kinetic principles and rate-determining stages have been established in relation to the conditions and structure of the substrates: formation or decay of the tetrahedral intermediates, the type of acid-base catalysis, the participation of slow proton transfers and to which atoms they refer. These questions are particularly important for elucidating the catalytic action of the respective enzymes. Crucial is the development of “sterically strained” substrates, in which the accelerations induced by the gem-dimethyl effect are used to study reactions under physiological conditions. Thus, the locations and nature of proton transfers during the interaction of a ureido group with a carboxylate anion, a model of the interaction of biotin with a bicarbonate anion, were established.

For the first time, it was found that steric hindrance of proton transfers between heteroatoms can make them rate-controlling, due to strong retardation contrary to the general case of diffusion control. This explains a number of anomalies in the

gem-dimethyl effect and changes in the rate-determining step in strained substrates. For these scientific results published in a series of articles, J. R. Knowles commented: "To select a single model reaction from a field that has received so much more than its share of attention from the bioorganic community may seem gratuitous, yet Blagoeva, Pojarlieff and Kirby have reported a model reaction of particular appropriateness and simplicity".

The detailed studies of the gem-dimethyl effect, the subject of Prof. Pojarlieff's dissertation for the scientific degree of Doctor of Sciences, prove the enthalpic nature of the effect, contrary to the widespread notions of "stereo population control". The established linear correlations of the free energies, rates - equilibria (Leffler relationship) of the gem-dimethyl effect open up new possibilities for its prediction and understanding. These studies also have a practical application, since based on the gem-dimethyl effect, synthesis can be performed by simply replacing with alkyl groups (most often methyl) substrates of bioorganic reactions, reacting up to  $10^6$  times faster than the unsubstituted example. Thus, the rate of the cyclization reaction can be controlled by the structure of the substrate. Due to the steric nature of the effect, this is a possibly mild perturbation of the molecule, making the conclusions drawn from its study transferable. His top article in the area has been included in the list of excellent publications of the Royal Society of Chemistry.

Prof. Pojarlieff made significant achievements in the field of stereochemistry and conformational analysis. A dramatic example of the demonstration of stereoelectronic effects, a long-time highly debated area, has been found using conformationally constrained systems. Studying compounds with triphenylpropane skeleton, complete inversion of the ratio of migration rates of the acyl transfer upon *N*-methylation is observed, which can be explained only by a "stereoelectronically controlled intermediate cleavage" requirement for two lone Krisztián Buzathe cleaving C-N or C-O bond, i.e. equatorial orientation of the nitrogen lone pair in the tetrahedral intermediates. The main article on the matter is quoted in great details both in the book "Stereoelectronic Effects in Organic Chemistry" by the creator of the theory P. Deslongchamps, and by its main critic M. Sinnott.

For the first time, the role of allylic strain in heterocycles with an endocyclic amide group is shown. Allylic strain has been found to account for

the unexpected axial conformation of substituents adjacent to a substituted trigonal nitrogen atom in several saturated heterocycles. It was established that the preference of gauche conformations in compounds with adjacent phenyl groups is due to a complex of reasons, and not only to favourable non-valent interactions.

Prof. Pojarlieff managed a number of contracts of the Institute with several Bulgarian factories in connection with the development and implementation of the production of additives to galvanic baths, for printed circuit boards, for galvanization, etc. Together with Prof. I. Juchnovski and Prof. S. Rashkov, he was a leader of a significant industrial development, the additives for acid bright copper plating. The Bulgarian team reached a complete replacement of the imported additives in the automobile factories of the former USSR, Czechoslovakia and DDR in 1975. Three additives have been regularly produced for more than 15 years.

Prof. Pojarlieff led the seminars of Academician B. Kurtev's course "Structure and Reactivity of Organic Compounds" in the Faculty of Chemistry of the Sofia University. He took over the regular reading of the course from 1977, which continued until 2003. In the 1980s, the course was significantly modernized and changed to "Physical Organic Chemistry". In 1992 and 1993 he taught the course in the University of Toronto.

Prof. Pojarlieff was the teacher of generations of Bulgarian chemists, from whom they have learned what physical organic chemistry is and how it can be applied in organic and bioorganic chemistry. His textbooks "Physical Organic Chemistry" and "Physical Organic Chemistry and Dynamic Stereochemistry" were the desk books not only of undergraduate organic and bioorganic chemists, but also of established researchers.

Prof. Pojarlieff wrote in a memoir article in 2016: "It was a honour for me to work 47 years at the Institute of Organic Chemistry mostly because of the amazingly large concentration of decent and very talented colleagues". We, in turn, can confidently say that it was a great honour and privilege for us to have a teacher, leader and friend like Johnny.

Farewell, Teacher!

Vanya Kurteva

*Institute of Organic Chemistry with Centre of Phytochemistry, Bulgarian Academy of Sciences.*

## Overview of approaches to obtaining energy from heat including ground-based installation

E. Ganev\*, S. Panyovska, K. Stefanova

*Institute of Chemical Engineering, Bulgarian Academy of Sciences, 1113 Sofia, Bulgaria*

Received: December 1, 2023; Revised: March 29, 2024

Climate changes resulting from the excessive use of fossil fuels and the consequences of their extraction from the earth's bowels motivate the scientific community to develop new concepts for efficient energy management, limiting damage to nature. The present mini-review is motivated by the fact that the last decade has seen significant progress related to the development of reviews, analyses, assumptions, comparisons, research, technological solutions, mathematical models and optimization of supply chains by researchers who consider the problem related to energy efficiency in its various aspects and from different perspectives. Good scientific practice is the use of Computational Fluid Dynamics (CFD) modeling techniques, which can easily and quickly simulate the paths and movements of the various flows, to achieve the above-described objectives. The mini-review aims to review approaches to obtaining electrical energy through heat, including ground-based installations. An original scheme for the production of biogas with geothermal storage with application for greenhouses is presented.

**Keywords:** Sustainable development, Exergy efficiency technologies, CFD, Supply chain

### INTRODUCTION

Along with the rapid development of scientific and technical progress to improve their well-being, modern men are faced with serious challenges related to the future state of nature on earth.

Climate changes resulting from the excessive use of fossil fuels and the consequences of their extraction from the earth's bowels motivate the scientific community to develop new concepts for the efficient management of energy, limiting damage to nature. On the other hand, the use of fossil resources as energy sources is associated with a number of problems related to yield uncertainty, production uncertainties, supply uncertainties, demand uncertainties, geopolitical uncertainties, etc., which create conditions for impaired sustainability and various types dependencies affecting directly or indirectly the price of energy. In this line of thinking, green energy is sustainable energy, guaranteeing the independence of the source from which it is produced [2]. For this purpose, it is necessary to carry out a thorough analysis of the life energy cycle for each specific case and to determine the possibilities for optimal use of the energy input. This analysis will serve the decision-makers to apply it according to the economic, ecological and social aspect to achieve sustainable development of the potential initiatives (Figure 1).

In this context, in 2012 (changed 2018) The Parliament of the European Union has adopted the Directive 2012/27/EU on Energy Efficiency, which regulates definitions, conditions and rules with the aim of making Europe the first climate-neutral continent by 2050 [1].

The aim of the current mini-review is to study the approaches for obtaining mechanical and/or electrical energy, exergy and their applicability in land-based installations. In this regard, and due to purely economic considerations, research interest in the last ten years in this area has increased 3.63 times, according to the data, extracted from ref. [3], *cf.* Figure 2.

In their publications, the authors have carried out reviews, analyses, assumptions, comparisons, research, technological solutions, mathematical models and optimization of supply chains. The problem related to energy efficiency is considered in its various aspects and from different points of view. Regarding the ranking of the individual renewable energy sources, there are a number of disputes and contradictions depending on the viewpoints of the studies, but with regard to solar and geothermal energy, researchers are unanimous and define them as the first on the list. A further point in the implementation of energy efficiency is to pay attention to exergy or the energy-exergy system, aiming to achieve both energy and exergy efficiency [4].

---

\* To whom all correspondence should be sent:  
E-mail: [evgeniy\\_ganev@iche.bas.bg](mailto:evgeniy_ganev@iche.bas.bg)

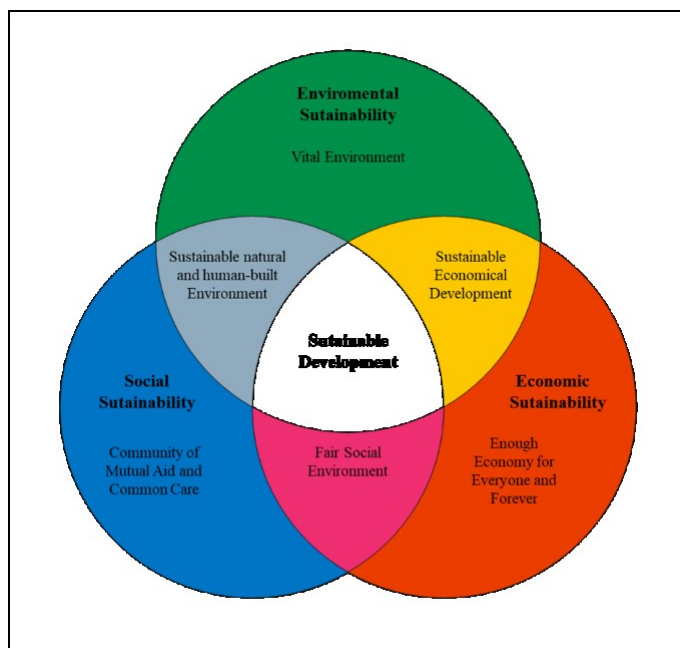


Figure 1. Sustainable development and management concept [1]

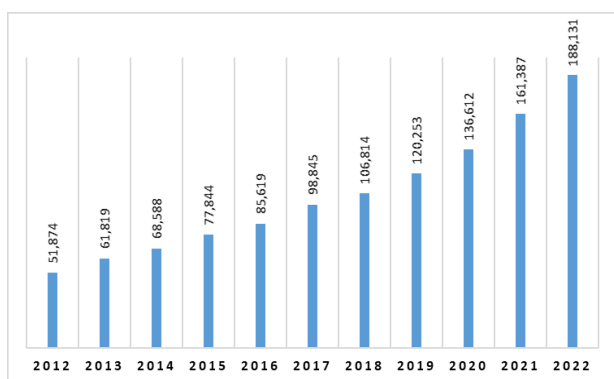


Figure 2. Activity according to the number of scientific publications related to energy efficiency for the period 2012 - 2022.

In developing a methodology for optimal operation of a geothermal power plant, Coskun *et al.* [5] found that when combined in the production of electricity with heating systems in greenhouse production, the exergy efficiency is satisfied at the highest level. The authors proposed seven variants of multi-generator installations for geothermal power plants, reaching 7-80% energy and 10-60% exergy efficiency. Ezzat & Dincer [4] are developing a geothermal energy system that includes solar energy. The authors present a thermodynamic analysis based on the energy and exergy in the system. Within their development, they achieved 69.6% energy and 42.8% exergy efficiency.

Dzhonova-Atanasova *et al.* [6] investigated compact latent heat storage systems for residential buildings to increase their efficiency. According to the authors, for the development of the optimization

model for the design of these systems, certain requirements must be taken into account:

1. Achieving efficiency by combining time periods and cost of heat input.
2. The phase change substance used must meet the conditions to achieve the desired effect, be stable for a long time of operation, be available and have a low cost.
3. The most promising at the moment are heat accumulators with a compact size in a shell-and-tube configuration.
4. The heat accumulator must allow connection to different heat sources, as well as integration to existing heating systems.

## EXERGY EFFICIENCY TECHNOLOGIES

### *Steam turbine*

The steam turbine (Figure 3) consists of: Stator part - highly heated steam under high pressure enters the area of the stator blades, where it swirls and accelerates. Rotor part – the blades in the rotor part receive impulse and reaction forces from the accelerated and swirled steam, generating a torque in the rotor. There is a variety of steam turbines both in terms of number of stages (from 1 to 30 stages) and capacity range (up to 1900 MW).

One of the main applications of the steam turbine is the production of electricity by driving electric generators. As the temperature and pressure of the steam entering the turbine increases, the thermal efficiency also increases. Typically, inlet steam pressures in steam turbines of modern thermal power plants range from 24.1 to 33.0 MPa and temperatures

range from 593°C to 630°C. The unit power of this type of power plants usually ranges from 600 to 1200 MW [7].

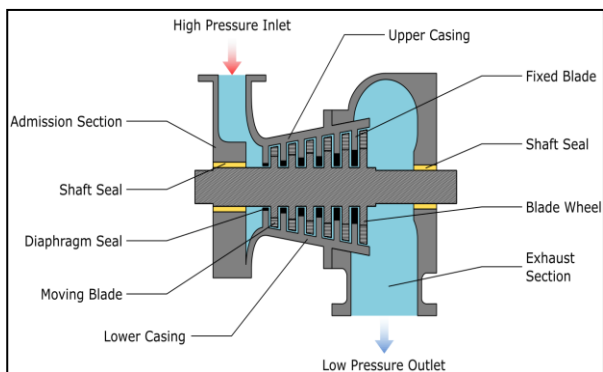


**Figure 3.** Schematic diagram of the operation of the steam turbine [8]

### Thermoelectric method

Thermoelectric generators are devices that directly convert thermal energy into electrical energy. These devices are promising for a number of reasons: they are environmentally friendly, i.e. they do not generate harmful emissions, they are silent during their operation, in terms of construction, they do not have moving parts, i.e. their maintenance costs are low. The principle of operation of these devices is based on the properties of the included P-type and N-type semiconductor elements connected to each other by a wire as shown in Figure 4. Current flows through the n element, passes through the wire to the p element. Under the action of heat, electrons from n elements will move to the coldest place, this will create a current in the wire. The holes in the p cell will move in the same direction as the current. In the presence of a heat source, the device works as an electrical generator. Despite their undeniable qualities, thermoelectric generators cannot provide the necessary efficiency for mass application, which in turn encourages scientific activity in this area [9].

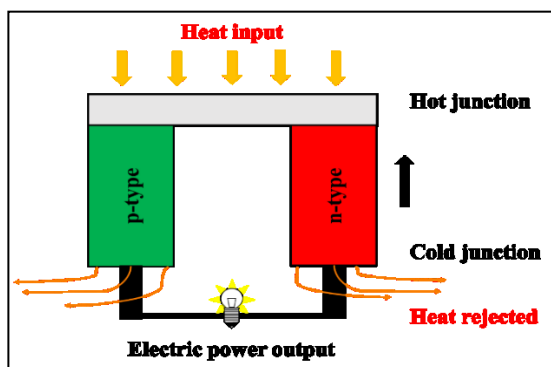


**Figure 4.** Schematic diagram of a thermoelectric generator [9]

### Stirling engine

The Stirling engine itself is an external combustion piston engine. The driving force in it is the change in the pressure of the fluid in the cylinder chamber, as a result of its passage through "warm" and "cold" zones, as well as the alternation of compression and throttling processes. Theoretically, the efficiency of the Stirling machine is equal to that of the Carnot cycle. In terms of construction, there are three types of these machines  $\alpha$ ,  $\beta$  and  $\gamma$  (Figure 5). In the  $\alpha$ -type, the engine is two-cylinder, with cylinders connected in a common volume of working fluid, while  $\beta$ - or  $\gamma$ -type engines are single-cylinder, and the difference between them is in the location of the hot and cold zones [10].

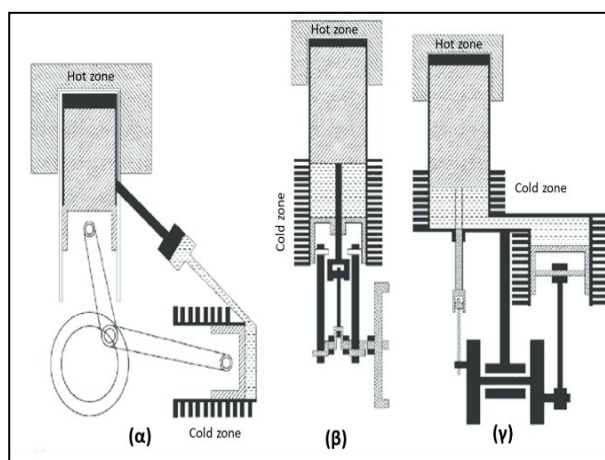


**Figure 5.** Schematic diagram of Stirling engine types [11].

### Heat pumps

The principle of operation of the heat pump is related to the reversal of the direction of the heat flow and is based usually /most often/ mainly on the vapor compression cycle. Characteristic of the vapor compression cycle is the presence of a liquid refrigerant that circulates in the system. Liquid refrigerant absorbs heat from the space where cooling is needed and can also deliver heat to the space where heating is needed. A compression heat pump, as shown in Figure 6, is used for space heating by raising low-temperature energy (from water, ambient air, etc.) to the temperature of the heating system by doing work on the fluid using a compressor.

In terms of waste heat, the heat pump can improve the efficiency to a value that can be more than twice the energy consumed by the device [12].

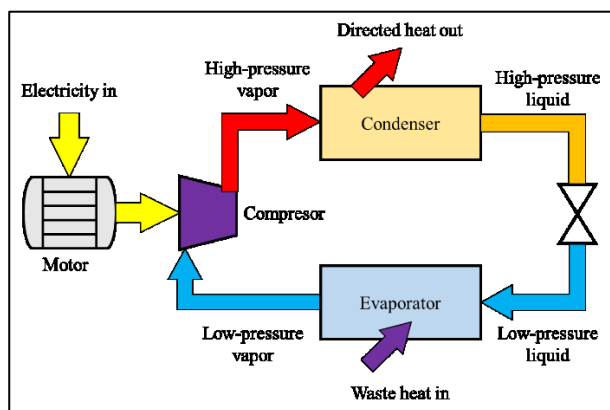


**Figure 6.** Schematic diagram of a compression heat pump.

### RESEARCH ACTIVITY RELATED TO TECHNOLOGIES IN EXERGY EFFICIENCY

The last decade has seen significant progress related to the development of reviews, analyses, assumptions, comparisons, research, technological solutions, mathematical models, and optimization of supply chains by researchers. Table 1 considers the problem related to energy efficiency in its different aspects and from different points of view. The authors present the development of new technologies and the improvement of existing ones to improve their efficiency in order to minimize energy costs and to achieve a nature-friendly economy.

### CFD MODELING FOR ENERGY EFFICIENCY

To achieve the above objectives, it is a good scientific practice to use CFD modeling techniques, which can easily and quickly simulate the paths and movements of the various flows. This is of particular importance in the design of steam turbines, where the driving force is derived from the rate of change of momentum of a high-velocity steam jet impinging on a freely rotating curved blade [41].

Through the use of CFD techniques, different ways to increase the performance of thermoelectric generators can be analyzed, such as efficient direction of heat flows, as well as the construction material, shape and spatial arrangement of heat exchangers [42]. When implementing projects related to the application of the Stirling engine, it is of particular importance to assess which of the types ( $\alpha$ ,  $\beta$ , and  $\gamma$ ) is the most effective for the specific situation and, accordingly, in which it is permissible to be modified. Comparisons can be made in terms of power output, heat transfer and thermal efficiency. For this purpose, a CFD simulation is applied for the three types of Stirling engines in which the respective efficiency is evaluated [43].

**Table 1.** Research contribution in areas related to improvement of classical technologies and development of new ones to improve energy efficiency.

Energy converting machines	References	Scientific direction
Steam turbine	[13], [14], [15]	Using solar energy to generate electricity through a steam turbine and salt tower.
Thermoelectric method	[16], [17], [18], [19], [20], [21], [22], [23], [24], [25]	Using a thermoelectric method to produce electricity from geothermal sources.
Stirling engine	[26], [27], [28], [29], [30], [31], [32], [33], [34], [35]	Using a Stirling engine to convert geothermal energy into mechanical energy and its application.
Heat pumps	[36], [37], [38], [39], [40], [6]	Heat pump application using geothermal energy.

The design of ground-based heat pumps requires consideration of peak heating and cooling loads. It is important for the system to take into account both the input and output energy, as well as the frequency of operation of the heat pump. The intensity, speed and perimeter of heat propagation in the soil where the heat pump is based are investigated. CFD simulation enables the construction of a 3-D model to achieve an objective view of the change in the above-described parameters and the possibilities for the overall optimization of the system [44].

Based on the research done in this way, it can be concluded that in every field of energy-related technologies there is potential for development and improvement. We present a concept (Figure 7) for the improvement of the biogas production and realization technology described by Ganev & Beschkov [1], where the addition of land-based installations is envisaged to improve the exergy efficiency of the project. The excess heat from the cooling of the cogenerator is taken to a horizontally located, ground-based heat exchanger. The goal is to achieve the effect of a heat accumulator. In addition, it is planned to build a greenhouse above the soil where the heat accumulator is located, which will, on the one hand, produce agricultural produce and, on the other hand, play the role of an insulator from atmospheric conditions.

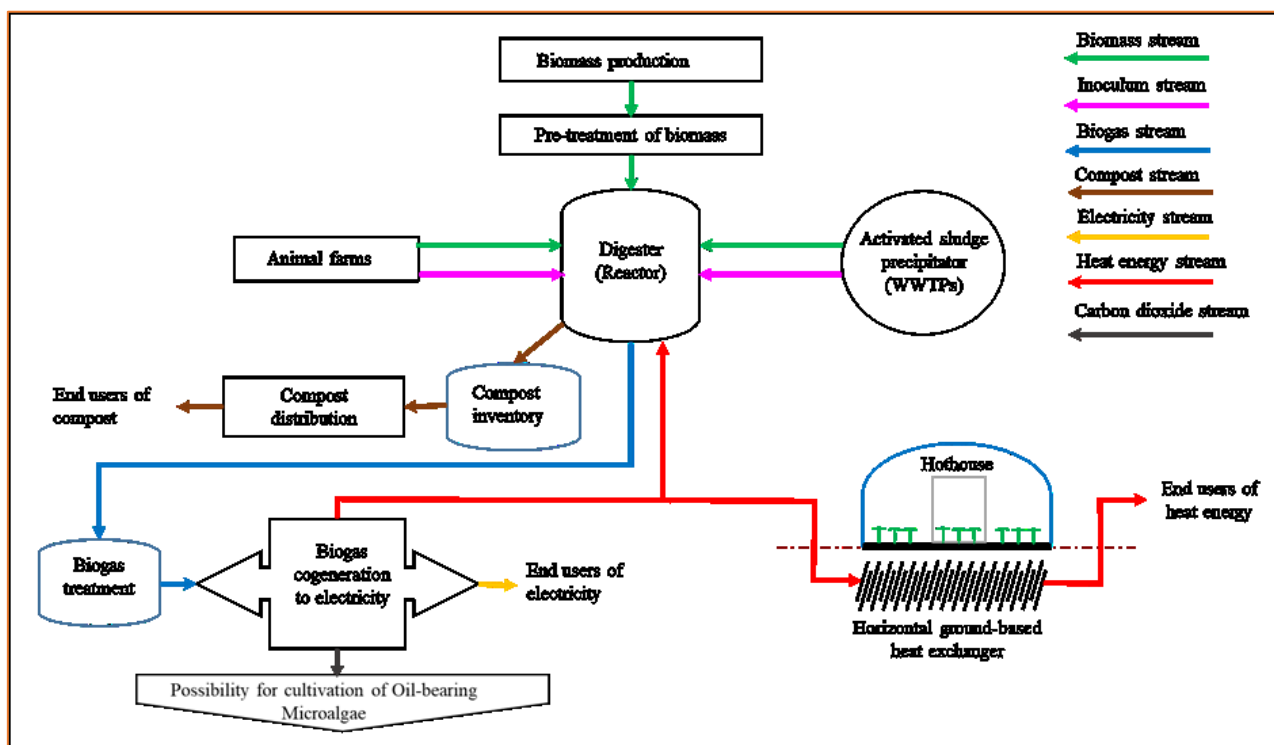


Figure 7. General framework of the biogas supply chain

## CONCLUSIONS

1. Green energy is sustainable energy, guaranteeing the independence of the source from which it is produced.

2. The energy life cycle analysis for each specific case allows optimal use of the energy input. To achieve the goal, it is appropriate to optimize the resource-insurance chain by building a mathematical model, guaranteeing the sustainability of the system from the point of view of ecological, economic and social sustainability.

3. An essential moment in the realization of energy efficiency is to pay attention to exergy or the energy-exergy system to achieve energy and exergy efficiencies.

4. Compiling a CFD simulation model for each specific case can give a clear idea of the distribution of heat flows in the installations and can serve as a tool for improving energy and exergy efficiency.

5. At present, every area of energy-related technologies has potential for development and improvement.

**Acknowledgement:** This study was carried out with the financial support of the National Science Fund, Ministry of Education and Science of the Republic of Bulgaria, Contract No. KII 06-M67/4/13.12.22.

## REFERENCES

1. E. Ganev, V. Beschkov, *Bulg. Chem. Commun.*, **54**, 205 (2022), DOI: 10.34049/bcc.54.3.5483.

2. I. O. Olanipekun, O. Ozkan, G. Olasehinde-Williams, *Energy*, **126949**, (2023), <https://doi.org/10.1016/j.energy.2023.126949>.
3. Science Direct, Elsevier, <https://www.sciencedirect.com/>
4. M. F. Ezzat, I. Dincer, *Solar Energy*, **134**, 95 (2016), <https://doi.org/10.1016/j.solener.2016.04.029>.
5. C. Coskun, Z. Oktay, I. Dincer, *Journal of Cleaner Production*, **32**, 71 (2012), <https://doi.org/10.1016/j.jclepro.2012.03.004>.
6. D. Dzhonova-Atanasova, A. Georgiev, S. Nakov, S. Panyovska, T. Petrova, S. Maiti, *Energies*, **15**, 8269 (2022), <https://doi.org/10.3390/en15218269>.
7. T. Tanuma, *Woodhead Publishing*, **3** (2022), <https://doi.org/10.1016/B978-0-12-824359-6.00024-X>.
8. Steam Turbine, Savree, <https://savree.com/en/encyclopedia/steam-turbine>
9. R. Stobart, A. Wijewardane, C. Allen, *SAE Technical Paper*, 0833 (2010), <https://doi.org/10.4271/2010-01-0833>
10. Ch.-H. Cheng, H.-S. Yang, *Applied Energy*, **92**, 395 (2012), <https://doi.org/10.1016/j.apenergy.2011.11.046>.
11. T. S. Pop, I. Vadan, R. Pop, C. Brad, *Journal of Electrical and Electronics Engineering*, **7**, 111 (2014).
12. C. Ononogbo, E. C. Nwosu, N. R. Nwakuba, G. N. Nwaji, O. C. Nwufu, O. C. Chukwuezie, M. M. Chukwu, E. E. Anyanwu, *Heliyon*, **9**, 2 (2023), <https://doi.org/10.1016/j.heliyon.2023.e13590>.
13. H. Price, D. Kearney, F. Redell, R. Charles, F. Morse, *SolarPACES*, (2017), <http://www.solarpaces.org/wp->

- content/uploads/Hank-Price-Dispatchable-Solar-Power-Plant-.pdf.
14. J. F. Servert, E. Cerrajero, D. López, S. Yagüe, F. Gutierrez, M. Lasheras, G. San Miguel, *Energy Procedia*, **69**, 1152 (2015), <https://doi.org/10.1016/j.egypro.2015.03.187>.
  15. S. Szabó, M. Moner-Girona, I. Kougiyas, et al., *Nat. Energy* **1**, 16140 (2016), <https://doi.org/10.1038/nenergy.2016.140>
  16. L. Catalan, P. Aranguren, M. Araiz, G. Perez, D. Astrain, *Energy Conversion and Management*, **200**, 112061 (2019), <https://doi.org/10.1016/j.enconman.2019.112061>.
  17. P. Alegria, L. Catalan, M. Araiz, *Applied Thermal Engineering*, **200**, 117619 (2022), <https://doi.org/10.1016/j.applthermaleng.2021.117619>.
  18. Y. Lou, G. Liu, A. Romagnoli, D. Ji, *Thermal Engineering*, **226**, 120223 (2023), <https://doi.org/10.1016/j.applthermaleng.2023.120223>.
  19. J. Liu, Z. Wang, K. Shi, Y. Li, L. Liu, X. Wu, *Renewable Energy*, **150**, 561 (2020), <https://doi.org/10.1016/j.renene.2019.12.120>.
  20. P. Alegría, L. Catalán, M. Araiz, Á. Casi, D. Astrain, *Geothermics*, **110**, 102677 (2023), <https://doi.org/10.1016/j.geothermics.2023.102677>.
  21. M. M. Hadjiat, A. Mraoui, S. Ouali, E. H. Kuzgunkaya, K. Salhi, A. Ait Ouali, N. Benaouda, K. Imessad, *International Journal of Hydrogen Energy*, **46** (75), 37545 (2021), <https://doi.org/10.1016/j.ijhydene.2021.06.130>.
  22. E. Assareh, M. Delpisheh, E. Farhadi, W. Peng, H. Moghadasi, *Energy Nexus*, **5**, 100043 (2022), <https://doi.org/10.1016/j.nexus.2022.100043>.
  23. L. Catalan, M. Araiz, P. Aranguren, D. Astrain, *Energy Conversion and Management*, **221**, 113120, (2020), <https://doi.org/10.1016/j.enconman.2020.113120>.
  24. N. Khetani, S. Patel, M. Prankada, N. Bist, A. Sircar, K. Yadav, *Materials Today: Proceedings*, **62**(13), 6918 (2022), <https://doi.org/10.1016/j.matpr.2021.11.453>.
  25. F. Tohidi, S. G. Holagh, A. Chitsaz, *Applied Thermal Engineering*, **201** A, 117793 (2022), <https://doi.org/10.1016/j.applthermaleng.2021.117793>.
  26. S. Guarino, A. Buscemi, G. Ciulla, M. Bonomolo, V. Lo Brano, *Energy Conversion and Management*, **222**, 113228, (2020), <https://doi.org/10.1016/j.enconman.2020.113228>.
  27. G. Moonka, H. Surana, H. R. Singh, *Materials Today: Proceedings*, **63**, 737 (2022), <https://doi.org/10.1016/j.matpr.2022.05.107>.
  28. T. Kumaravelu, S. Saadon, A. R. Abu Talib, *Energy*, **239** A, 121881 (2022), <https://doi.org/10.1016/j.energy.2021.121881>.
  29. K. Laazaar, N. Boutammachte, *Applied Thermal Engineering*, **210**, 118316 (2022), <https://doi.org/10.1016/j.applthermaleng.2022.118316>.
  30. L. Gu, Y. Li, X. Wen, Sh. Zhong, *Energy Conversion and Management*, **249**, 114836 (2021), <https://doi.org/10.1016/j.enconman.2021.114836>.
  31. N. Tongdee, M. Jandakaew, T. Dolwichai, *Energy Procedia*, **105**, 1782, (2017), <https://doi.org/10.1016/j.egypro.2017.03.516>.
  32. Ch.-H. Cheng, H.-S. Yang, Y.-H. Tan, *Energy*, **238** A, 121730 (2022), <https://doi.org/10.1016/j.energy.2021.121730>.
  33. K. Laazaar, N. Boutammachte, *Energy Conversion and Management*, **223**, 113326, (2020), <https://doi.org/10.1016/j.enconman.2020.113326>.
  34. M. Yu, Ch. Shi, J. Xie, P. Liu, Zh. Liu, W. Liu, *International Journal of Heat and Mass Transfer*, **183** C (2022), <https://doi.org/10.1016/j.ijheatmasstransfer.2021.122240>.
  35. A. P. Masoumi, A. R. Tavakolpour-Saleh, A. Rahideh, *Applied Energy*, **268**, 115045 (2020), <https://doi.org/10.1016/j.apenergy.2020.115045>.
  36. O. Arslan, A. E. Arslan, T. E. Boukeliya, *Energy and Buildings*, **282**, 112792 (2023), <https://doi.org/10.1016/j.enbuild.2023.112792>.
  37. G. Chiriboga, S. Capelo, P. Bunces, C. Guzmán, J. Cepeda, G. Gordillo, D. E. Montesdeoca, Gh. Carvajal, *Heliyon*, **7**(12), e08608 (2021), <https://doi.org/10.1016/j.heliyon.2021.e08608>.
  38. L. Liang, X. Wang, X. Zhang, H. Sun, *IFAC-PapersOnLine*, **53**(2), 17125 (2020), <https://doi.org/10.1016/j.ifacol.2020.12.1660>.
  39. J. Fadejev, R. Simson, J. Kurnitski, J. Kesti, T. Mononen, P. Lautso, *Energy Procedia*, **96**, 489 (2016), <https://doi.org/10.1016/j.egypro.2016.09.087>.
  40. O. Arslan, A. E. Arslan, I. Kurtbas, *Journal of Building Engineering*, **73**, 106733 (2023), <https://doi.org/10.1016/j.job.2023.106733>.
  41. C. Rajesh Babu, P. Kumar Hensh, *Materials Today: Proceedings*, **45**(1), 58 (2021), <https://doi.org/10.1016/j.matpr.2020.09.510>.
  42. R. Babu Bejjam, M. Dabot, T. Wondatir, S. Negash, *Materials Today: Proceedings*, **47**(10), 2498 (2021), <https://doi.org/10.1016/j.matpr.2021.04.563>.
  43. A. Abuelyamen, R. Ben-Mansour, *International Journal of Thermal Sciences*, **132**, 411 (2018), <https://doi.org/10.1016/j.ijthermalsci.2018.06.026>.
  44. Y. Cui, J. Zhu, *Applied Thermal Engineering*, **139**, 99 (2018), <https://doi.org/10.1016/j.applthermaleng.2018.04.073>.

# Synthesis, biological evaluation, ADME studies and molecular docking with $\beta$ -tubulin of fused benzimidazole-pyridine derivatives

D. Panchani<sup>1</sup>, S. Maurya<sup>1</sup>, T. Thaker<sup>1\*</sup>, V. Rathod<sup>1</sup>, Sh. Thakur<sup>2</sup>

<sup>1</sup>Department of Chemistry, Parul Institute of Applied Sciences, Parul University, Waghodia, Vadodara-391760, Gujarat, India

<sup>2</sup>Department of Forensic Science, Parul Institute of Applied Sciences, Parul University, Waghodia, Vadodara-391760, Gujarat, India

Received January 25, 2024; Revised: May 21, 2024

After treatment with chloroacetyl chloride, 2-(pyridin-4-yl)-1H-benzo[d]imidazole underwent a reaction to yield 2-chloro-1-(2-(pyridin-4-yl)-1H-benzo[d]imidazol-1-yl) ethan-1-one. The latter intermediately reacted with one equivalent of various primary aromatic amines in the presence of potassium carbonate in chloroform, yielding the respective target amine derivatives of benzimidazole. The structure of the synthesized compounds was established by <sup>1</sup>H NMR, IR, and mass spectrometry. Synthesized compounds were screened for antimicrobial activity by diffusion plate method and most of them showed moderate to good potency against *Staphylococcus aureus*, *Bacillus subtilis*, *Escherichia coli*, and *Pseudomonas aeruginosa*. Compound *3a* showed the best potency compared to others. To predict the pharmacokinetics and drug-like properties of the synthesized substances, absorption, distribution, metabolism, and excretion (ADME) models were employed. Computational methods, along with a set of criteria based on Lipinski and Veber rules, were utilized to anticipate the physicochemical features indicative of drug-likeness for the synthesized molecules. Furthermore, molecular docking tests against 1SA0 ( $\beta$ -tubulin) were conducted, and the results demonstrated favorable interactions of the compounds with the target, with binding energy values approaching 5 Å.

**Keywords:** Benzimidazole, Molecular docking,  $\beta$ -Tubulin, Antibacterial activity.

## INTRODUCTION

The investigation of the biological dynamics of targeted benzimidazoles with  $\beta$ -tubulins through molecular docking and simulations in the context of anthelmintic action is intriguing. Microtubules (MT) are protein polymers characterized by tubular structures composed of tubulin subunits, playing a crucial role in the cell's cytoskeleton. They are essential for maintaining cell shape, facilitating intracellular material movement, and executing mitosis. Additionally, they are integral components connected to the mitotic spindle, centrioles, microtubules, cilia, and flagella [1].

Benzimidazole, featuring a benzene ring fused with imidazole, exhibits a delicate structure and versatile therapeutic benefits. An illustrative example of benzimidazole is cyanocobalamin vitamin [2]. Due to their inhibitory activity and favorable selectivity ratio, benzimidazoles demonstrate significant medicinal potency. Various biochemical and pharmaceutical investigations have highlighted the efficacy of benzimidazole compounds against diverse bacteria [3]. These compounds exhibit antioxidant, antiproliferative [4], anthelmintic, antihypertensive [5], anti-inflamma-

tory, antiparasitic, antineoplastic [6], antiprotozoal [7], anti-HIV [8], and anti-trichinellosis [9] actions, showcasing the versatility of this ring system [10]. The popular medications lansoprazole and esomeprazole contain two heterocyclic moieties, pyridine and benzimidazole [11]. Retinoidal monocationic benzimidazole molecule bears the most potent antimicrobial activity [12]. Moreover, the presence of certain organic groups, such as amino, nitro, hydroxy, methoxy, sulfamide, carboxylic acid, etc., increase the biological activities of the compounds [13].

Consequently, the current study aims to synthesize and evaluate the biological activities of newly derived benzimidazole-pyridine moieties. The synthesized moieties were characterized through various spectroscopic studies. Subsequent ADME studies and molecular docking of novel analogs using beta-tubulin (PDB-1SA0) were undertaken to further elucidate their potential.

## MATERIALS AND METHODS

### General information

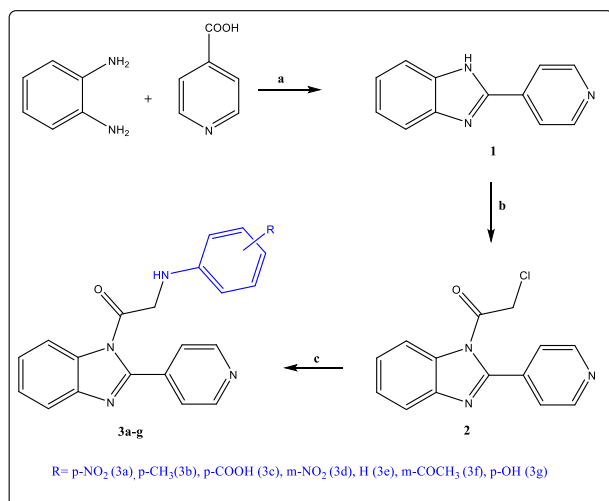
All chemicals were procured from Sigma Aldrich. The solvents used were of analytical reagent (AR) grade. Melting points were determined

\* To whom all correspondence should be sent:  
E-mail: [tirth6582@gmail.com](mailto:tirth6582@gmail.com)

using the Equiptronics model EQ-730 instrument. The reaction was monitored by thin layer chromatography (TLC) and was carried out on Merck silica gel 60 F<sub>254</sub> plates. Visualization of the plates was done using a UV lamp ( $\lambda_{\text{max}} = 254$  or 365 nm). The IR spectra were recorded using KBr pellets on Bruker alpha-II FTIR spectrometer. Deuterated solvents (DMSO-d<sub>6</sub>) were utilized for capturing <sup>1</sup>H NMR spectra on Bruker 400 MHz spectrometer, with tetramethyl silane serving as the internal standard. Mass spectral data were recorded using a Shimadzu LC2010 mass analyzer, and elemental analysis revealed that values were consistent within 0.4% of their theoretical counterparts. C, H, N analyses was conducted using a Perkin Elmer PE 2400.

• *General synthesis of 2-(pyridin-4-yl)-1H-benzo[d]imidazole [compound 1]*

Ortho-phenyl diamine (3 g, 0.0027 moles) and isonicotinic acid (3.41 g, 0.0027 moles) were dissolved in ortho-phosphoric acid (20 ml) and stirred for 24 hours at 130-140°C until the starting material was completely consumed. Subsequently, the mixture was cooled in an ice bath, and pH was maintained at 8-9 by adding 20% NaOH. The resulting precipitate was separated through filtration, washed with methanol, and the solvent was subsequently evaporated.



**Scheme 1.** Reagent and conditions of benzimidazole with pyridine moiety synthesis: (a) ortho-phosphoric acid, 130-140°C, reflux for 24 h; (b) chloroacetyl chloride, diethyl ether, at room temperature, stirred for 24 h; (c) potassium carbonate, chloroform, at 40-50°C and reflux for 12 h.

Yield: 89.88 %; M.P: 208-210 °C; Rf: 0.50; IR (Bruker)  $\nu$  max cm<sup>-1</sup>: 3054.28(m) (N-H Str.), 1607.86 (C=N Str.), 1430.85 (C=C Str.), 1315.31 (C-N Str. aromatic), 1232.30 (C-H o-substituted Bend), 838.16, 742.39; <sup>1</sup>H NMR (DMSO-d<sub>6</sub>, 400

MHz): d = 6.67 (m, 2H, J = 8.4 Hz), 7.10 (d, 2H, J = 8.8 Hz), 7.48 (d, 2H, J = 8.0 Hz), 7.88 (d, 2H, J = 8.4 Hz), 12.56 (s, 1H, -NH); MS (m/z): 196.40; C<sub>12</sub>H<sub>9</sub>N<sub>3</sub> requires 195.08 Anal. calc. for C, 73.83; H, 4.65; N, 21.52; Found C, 72.98; H, 5.03; N, 21.99.

• *General synthesis of 2-chloro-1-(2-(pyridin-4-yl)-1H-benzo[d]imidazol-1-yl)ethan-1-one [compound 2]*

2-(pyridin-4-yl)-1H-benzo[d]imidazole (1 gm, 0.0051 moles) dissolve in diethyl ether (10 ml) and stir spend half an hour in an ice bath, then the addition of chloroacetyl chloride (2 ml, 0.001 moles) dropwise via syringe at 0°C (ice) and stirred for 24 h and ppt separated via filtration and dry the product and recrystallized using ethanol.

Yield: 88.23%; M.P: 219-225°C; Rf: 0.69; IR (Bruker)  $\nu$  max cm<sup>-1</sup>: 1699.25 (C=O str. Imine amide), 1455.21 (CH<sub>2</sub> str.), 1323.20 (C-N str. Aromatic), 1227.57 (C-H O-disubstituted Bend), 878.59, 758.84, 677.47 (C-Cl str.); <sup>1</sup>H NMR (DMSO-d<sub>6</sub>, 400 MHz): d = 4.12 (s, 2H, CO-CH<sub>2</sub>-Cl), 7.25 (m, 2H, J = 9.2, 3.2 Hz), 7.65 (d, 2H, J = 8.8 Hz), 8.10 (d, 2H, J = 5.6 Hz), 8.75 (d, 2H, J = 5.6 Hz); MS (m/z): 272.80; C<sub>14</sub>H<sub>10</sub>ClN<sub>3</sub>O requires 271.70. Anal. calc. for C, 61.89; H, 3.71; N, 15.47; Found C, 61.72; H, 3.02; N, 15.80.

• *General synthesis of 2-((R-substituted phenyl)amino)-1-(2-(pyridin-4-yl)-1H-benzo[d]imidazol-1-yl)ethan-1-one [compounds 3a-g]*

A mixture comprising 2-chloro-1-(2-(pyridin-4-yl)-1H-benzo[d]imidazol-1-yl)ethan-1-one (1 gm, 0.0036 moles), substituted amines (p-nitroaniline, p-toluidine, p-aminobenzoic acid, m-nitroaniline, aniline, p-aminoacetophenone, p-aminophenol) (0.0036 moles), and potassium dichromate (0.49 gm, 0.0036 moles) in 10 ml chloroform at reflux and continuous stirring for 12 hours. The reaction progress was monitored using TLC. Upon completion, the reaction mixture was filtered, and the solvents were evaporated. The resulting product was then dried and subjected to recrystallization in ethanol.

• *2-((4-nitrophenyl)amino)-1-(2-(pyridin-4-yl)-1H-benzo[d]imidazol-1-yl)ethan-1-one [3a]*

Yield: 68.13%; M.P: 290-291°C; Rf: 0.30; IR (Bruker)  $\nu$  max cm<sup>-1</sup>: 3354.14(m) (N-H str.), 1641.50 (C=O str. Imine amide), 1629.54 (C=N), 1585.05 (N=O str.), 1470.61 (CH<sub>2</sub> str.), 1315.31 (N=O str.), 1296.86, 1111.08, 838.00 (C-H bend p-disubstituted), 751.21 (C-H O-disubstituted); <sup>1</sup>H NMR (DMSO-d<sub>6</sub>, 400 MHz): d = 5.63 (s, 2H, CO-CH<sub>2</sub>-NH), 6.60 (d, 2H, J = 9.2 Hz), 7.37 (d, 2H, J = 9.2 Hz), 7.42 (s, 1H, CO-CH<sub>2</sub>-NH), 7.74 (m, 2H, J = 9.2, 3.2 Hz), 7.91 (d, 2H, J = 9.2 Hz), 8.66 (d, 2H, J = 6.0 Hz), 9.01 (d, 2H, J = 6.4 Hz); MS (m/z):

374.54 C<sub>20</sub>H<sub>15</sub>N<sub>5</sub>O<sub>3</sub> requires 373.37. Anal. calc. for C, 64.34; H, 4.05; N, 18.76; Found C, 64.72; H, 4.95; N, 17.96.

• 1-(2-(pyridin-4-yl)-1H-benzo[d]imidazol-1-yl)-2-(p-tolylamino)ethan-1-one [3b]

Yield: 65%; M.P: 201-203°C; Rf: 0.27; IR (Bruker)  $\nu$  max cm<sup>-1</sup>: 3333.40(m) (N-H str.), 3054 (CH<sub>3</sub> str.), 1607.86 (C=O str. Imine amide), 1430.98 (C=C str.), 1314.73 (CH<sub>3</sub> str.), 1232.30, 998.11, 838.53 (C-H bend p-disubstituted), 742.87 (C-H bend o-disubstituted); <sup>1</sup>H NMR (DMSO-d<sub>6</sub>, 400 MHz):  $\delta$  = 2.11 (s, 3H, Ar-CH<sub>3</sub>), 4.79 (s, 2H, CO-CH<sub>2</sub>-NH), 6.46 (s, 1H, CO-CH<sub>2</sub>-NH), 6.82 (d, 2H, J = 8.0 Hz), 7.25 (m, 4H, J = 4.0, 7.2 Hz), 7.66 (m, 2H, J = 9.2, 3.2 Hz), 8.10 (d, 2H, J = 6.0 Hz), 8.76 (d, 2H, J = 8.8 Hz); MS (m/z): 343.53 C<sub>21</sub>H<sub>18</sub>N<sub>4</sub>O requires 342.40. Anal. calc. for C, 73.67; H, 5.30; N, 16.36; Found C, 73.05; H, 5.35; N, 17.05.

• 4-((2-oxo-2-(2-(pyridin-4-yl)-1H-benzo[d]imidazol-1-yl)ethyl)amino) benzoic acid [3c]

Yield: 72.03%; M.P: 143-150°C; Rf: 0.58; IR (Bruker)  $\nu$  max cm<sup>-1</sup>: 3380 (N-H str.), 1641.49 (C=O str. Imine amide), 1615.93 (C=O str. Ar-COOH), 1607.86 (C=N str.), 1431.44 (CH<sub>2</sub> bend), 1315.31 (C-N str. aromatic), 1283.09, 1170.20, 834.35 (C-H bend p-disubstituted), 740.23 (C-H O-disubstituted); <sup>1</sup>H NMR (DMSO-d<sub>6</sub>, 400 MHz):  $\delta$  = 4.33 (s, 2H, CO-CH<sub>2</sub>-NH), 5.87 (s, 1H, CO-CH<sub>2</sub>-NH), 6.58 (d, 2H, J = 9.2 Hz), 7.30 (m, 2H, J = 9.2, 3.2 Hz), 7.64 (d, 2H, J = 12.0, 3.2 Hz), 7.70 (d, 2H, J = 7.2 Hz), 7.77 (d, 2H, J = 6.0 Hz), 8.74 (d, 2H, J = 6.0 Hz), 10.6 (s, 1H, COOH); MS (m/z): 373.12 C<sub>21</sub>H<sub>16</sub>N<sub>4</sub>O<sub>3</sub> requires 372.38. Anal. calc. for C, 67.73; H, 4.33; N, 15.05; Found C, 68.15; H, 4.02; N, 15.76.

• 2-((3-nitrophenyl)amino)-1-(2-(pyridin-4-yl)-1H-benzo[d]imidazol-1-yl)ethan-1-one [3d]

Yield: 96.06%; M.P: 65-72°C; Rf: 0.33; IR (Bruker)  $\nu$  max cm<sup>-1</sup>: 3330.70(m) (N-H str.), 1612.72 (C=O str.), 1519.60 (N=O str.), 1364.75 (CH<sub>2</sub> str.), 1315.31 (C-N str. aromatic), 1072.44, 829.46 (C-H bend p-disubstituted), 735.13 (C-H o-disubstituted); <sup>1</sup>H NMR (DMSO-d<sub>6</sub>, 400 MHz):  $\delta$  = 4.25 (s, 2H, CO-CH<sub>2</sub>-NH), 5.85 (s, 1H, CO-CH<sub>2</sub>-NH), 6.96 (m, 2H, J = 7.6, 1.2 Hz), 7.22 (d, 1H, J = 6.4 Hz), 7.26 (t, 1H, J = 8.8, 1.6 Hz), 7.31 (d, 1H, J = 8.0 Hz), 7.59 (s, 1H), 7.69 (d, 2H, J = 9.2 Hz), 8.19 (d, 2H, J = 6.4 Hz), 8.82 (d, 2H, J = 6.0 Hz); MS (m/z): 374.54; C<sub>20</sub>H<sub>15</sub>N<sub>5</sub>O<sub>3</sub> requires 373.37. Anal. calc. for C, 64.34; H, 4.05; N, 18.76; Found C, 64.12; H, 4.16; N, 18.51.

• 2-(phenylamino)-1-(2-(pyridin-4-yl)-1H-benzo[d]imidazol-1-yl)ethan-1-one [3e]

Yield: 67.79%; M.P: 202-206°C; Rf: 0.44; IR (Bruker)  $\nu$  max cm<sup>-1</sup>: 3365.84(m) (N-H str.), 1610.32 (C=O str. Imine amide), 1576.67 (C=N Str.), 1504.21 (C=C Str.) 1393.17 (C-N str. aromatic),

1314.87 (N=O str.), 1233.29, 745.82 (C-H O-disubstituted), 696.59 (C=C str. Mono substituted); <sup>1</sup>H NMR (DMSO-d<sub>6</sub>, 400 MHz):  $\delta$  = 5.08 (s, 2H, CO-CH<sub>2</sub>-NH), 6.41 (t, 1H, CO-CH<sub>2</sub>-NH), 6.47 (d, 2H, J = 7.2 Hz), 6.61 (t, 1H, J = 8.4 Hz), 6.99 (m, 2H, J = 10.4, 2.8 Hz), 7.09 (m, 2H, J = 8.8, 2.8 Hz), 7.58 (d, 2H, J = 8.8 Hz), 8.16 (d, 2H, J = 5.6 Hz), 8.65 (d, 2H, J = 6.0 Hz); MS (m/z): 329.25 C<sub>20</sub>H<sub>16</sub>N<sub>4</sub>O requires 328.48. Anal. calc. for C, 73.15; H, 4.91; N, 17.06; Found C, 73.10; H, 4.12; N, 17.91.

• 2-((3-acetylphenyl)amino)-1-(2-(pyridin-4-yl)-1H-benzo[d]imidazol-1-yl)ethan-1-one [3f]

Yield: 72%; M.P: 112-115°C; Rf: 0.49; IR (Bruker)  $\nu$  max cm<sup>-1</sup>: 3464.76(m) (N-H str.), 3367.05 (C-H str.), 1641.04 (C=O str. Imine amide), 1595.86 (C=N str.), 1490.56 (C=C str.), 1430.85 (N=O str.), 1355.09 (CH<sub>3</sub> bend), 1319.39 (C-N str. aromatic), 1236.42, 1072.60, 868.73 (C-H bend m-disubstituted), 736.77 (C-H o-disubstituted); <sup>1</sup>H NMR (DMSO-d<sub>6</sub>, 400 MHz):  $\delta$  = 3.31 (s, 3H, CO-CH<sub>3</sub>), 5.32 (s, 2H, CO-CH<sub>2</sub>-NH), 6.80 (m, 2H, J = 7.0 Hz), 7.09 (t, 1H, CO-CH<sub>2</sub>-NH), 7.10 (d, 1H, J = 6.0 Hz), 7.12 (t, 1H, J = 6.6 Hz), 7.16 (d, 1H, J = 6.4 Hz), 7.51 (s, 1H), 8.11 (d, 2H, J = 1.2 Hz), 8.32 (d, 2H), 8.66 (d, 2H, J = 7.2 Hz); MS (m/z): 371.12 C<sub>22</sub>H<sub>18</sub>N<sub>4</sub>O<sub>2</sub> requires 370.41. Anal. calc. for C, 71.34; H, 4.90; N, 15.13; Found C, 71.12; H, 4.71; N, 15.97.

• 2-((4-hydroxyphenyl)amino)-1-(2-(pyridin-4-yl)-1H-benzo[d]imidazol-1-yl)ethan-1-one [3g]

Yield: 88.60%; M.P: 135-137°C; Rf: 0.80; IR (Bruker)  $\nu$  max cm<sup>-1</sup>: 3500-3200(m) (O-H str.), 3278.94 (N-H stretch), 1609.89 (C=O str. Imine amide), 1576.82 (C=N str.), 1508.24 (C=C str.) 1372.01 (C-N str. aromatic), 1233.41, 1003.52, 826.45 (C-H bend p-disubstituted), 741.79 (C-H O-disubstituted); <sup>1</sup>H NMR (DMSO-d<sub>6</sub>, 400 MHz):  $\delta$  = 4.23 (s, 2H, CO-CH<sub>2</sub>-NH), 6.43 (d, 2H, J = 7.7 Hz), 6.48 (d, 2H, J = 8.0 Hz), 6.70 (s, 1H, CO-CH<sub>2</sub>-NH), 7.26 (m, 2H, J = 7.2, 2.2 Hz), 7.68 (m, 2H, J = 7.6, 2.8 Hz), 8.17 (d, 2H, J = 7.2 Hz), 8.74 (d, 2H, J = 7.2 Hz), 9.98 (s, 1H, Ar-OH); MS (m/z): 345.41 C<sub>20</sub>H<sub>16</sub>N<sub>4</sub>O<sub>2</sub> requires 344.13; Anal. calc. for C, 69.76; H, 4.68; N, 16.27; Found C, 69.24; H, 4.70; N, 16.31.

### Biological evaluation

• *In vitro* antibacterial activity

Synthesized compounds were screened for their antimicrobial activity by using the diffusion plate method. A HiMedia blank disc saturated with a measured quantity (25  $\mu$ L) of the sample (5 mM) was placed on a plate (9 cm diameter) containing a solid bacterial medium. The incubation period was 24 h at 37 °C, diameter of the zone of inhibition was measured and showed promising inhibitory power of

the sample against bacterial strains [14]. The title compound's antibacterial efficacy was screened against two Gram-positive bacteria (*Bacillus subtilis*, MTCC 441 and *Staphylococcus aureus*, MTCC 96) and two Gram-negative bacteria (*Pseudomonas aeruginosa*, MTCC 1866, and *Escherichia coli*, MTCC 443). Penicillin G was employed as the standard drug procured from HiMedia.

- *In silico* study

The title compound was subjected to an *in silico* study using the SwissADME software [15]. Nocodazole was employed as a reference standard.

- *Molecular docking*

The molecular modeling studies were performed with Discovery studio2021. The RCSB Protein Data Bank (<http://www.rcsb.org/pdb>) was used to retrieve the X-ray crystallographic structure of the beta-tubulin [16] complex with DAMA-colchicine (PDB: 1SA0). Protein preparation was carried out in AutoDockTools-1.5.6 where standardization of atoms, insertion of missing atoms in the residue, removal of water, addition of polar hydrogen, and addition of Kolman charge were carried out. The nocodazole and 1, 2, 3a-g were drawn through Chemdraw 20.0 and fully minimized and docked using PyRx-Virtual screening tools. Nocodazole is an antiproliferative agent used as a standard, as both tubulin and nocodazole are used to inhibit cell growth.

## RESULTS AND DISCUSSION

### Chemistry

*O*-phenylene diamine and isonicotinic acid were condensed by dissolving in orthophosphoric acid and refluxed for 24 h at 130-140°C to get 2-(pyridin-4-yl)-1H-benzo[d]imidazole (1). Crude product was purified by recrystallization and maroon solid was obtained with 89.88% yield. The IR spectrum of (1) showed -NH (2°amines) at 3054  $\text{cm}^{-1}$ , -C=N of benzimidazole at 1607  $\text{cm}^{-1}$ , and C-N of pyridine at 1315  $\text{cm}^{-1}$ .  $^1\text{H}$  NMR of (1) indicated peak confirmative signals of upfield benzimidazole aromatic protons at 6.67-7.10 ppm, downfield aromatic protons of pyridine at 7.48-7.86 ppm and NH proton at 12.56 ppm. Compound (1) was treated with chloroacetyl dissolved in diethyl ether at 0°C for 24 h to obtain 2-chloro-1-(2-(pyridine-4-yl)-1H-benzo[d]imidazolyl-1-yl) ethan-1-one (2) as green solid with 88.23% yield. IR spectrum of (2) showed disappearance of -NH- (2°amines) peak at 3054  $\text{cm}^{-1}$  of compound (1) and appearance of C=O at 1699.25  $\text{cm}^{-1}$ , CH<sub>2</sub> at 1455  $\text{cm}^{-1}$ , C-Cl at 878.59,

819.33, 758.84 and 677.47  $\text{cm}^{-1}$ .  $^1\text{H}$  NMR of (2) indicated a CH<sub>2</sub> signal at 4.12 ppm (s); benzimidazole aromatic protons at 7.25-7.65 ppm and pyridine protons at 8.10-8.75 ppm. The disappearance of -NH peak at 12.56 ppm of compound (1) confirms the synthesis. Title compounds 3a-g were synthesized by condensation of (2) with aromatic amines in chloroform at reflux over potassium carbonate for 24 h. Reaction was monitored by TLC. RM was filtered, the solvent evaporated and the crude product was recrystallized in ethanol to yield 65-96% of compounds 3a-g. IR of 3a showed -NH at 3354  $\text{cm}^{-1}$ ; C=O at 1641  $\text{cm}^{-1}$ , C=N at 1629  $\text{cm}^{-1}$ , N=O at 1585  $\text{cm}^{-1}$ , CH<sub>2</sub> at 1477  $\text{cm}^{-1}$ ;  $^1\text{H}$  NMR showed 3a peaks at 5.63 ppm for O=C-CH<sub>2</sub>- group, aromatic protons of p-nitroaniline appeared at 6.60-7.37 ppm, aromatic protons of benzimidazole at 7.74- 7.91 ppm and aromatic protons of pyridine appeared at 8.66-9.01 ppm, NH proton at 7.42 confirmed the synthesis. IR spectrum of 3b showed CH<sub>3</sub> at 1314.73  $\text{cm}^{-1}$ , 2° NH at 3333.40  $\text{cm}^{-1}$ , C=O at 1607.14  $\text{cm}^{-1}$ ;  $^1\text{H}$  NMR spectrum of 3b indicated CH<sub>3</sub> at 2.11 ppm; O=C-CH<sub>2</sub> at 4.79, ppm -NH at 6.64 ppm all aromatic protons are observed at 6.82-8.76 ppm; IR spectrum of 3c showed -C=O at 1615.93  $\text{cm}^{-1}$ , CH<sub>2</sub> at 1431.44  $\text{cm}^{-1}$ , -NH at 3380  $\text{cm}^{-1}$ .  $^1\text{H}$  NMR spectrum of 3c indicated signals at 4.33 ppm (-CH<sub>2</sub> peak), 5.87 ppm (-NH peak), and aromatic protons at 6.58 to 8.74 ppm, downfield -COOH at 10.60 ppm.

The IR spectrum of compound 3d showed NH at 3330  $\text{cm}^{-1}$ , C=O at 1612  $\text{cm}^{-1}$ , NO<sub>2</sub> at 1519  $\text{cm}^{-1}$  and CH<sub>2</sub> at 1364  $\text{cm}^{-1}$ .  $^1\text{H}$  NMR of compound 3d indicated CH<sub>2</sub> as a singlet at 4.25 ppm, NH proton appeared as a singlet at 5.85 ppm, and aromatic protons were observed between 6.96 to 8.82 ppm. IR of 3e showed NH at 3365  $\text{cm}^{-1}$ , C=O at 1610  $\text{cm}^{-1}$ , C=N at 1576  $\text{cm}^{-1}$ , aromatic C=C at 1504  $\text{cm}^{-1}$ ; C-N stretch 1393  $\text{cm}^{-1}$ .  $^1\text{H}$  NMR of 3e indicated CH<sub>2</sub> as a singlet at 5.08 ppm, -NH appeared as a singlet at 6.41 ppm and all aromatic protons were observed at 6.47-8.65 ppm. IR of 3f showed NH at 3464  $\text{cm}^{-1}$ , C=O at 1611  $\text{cm}^{-1}$ , C=N at 1595, aromatic ring breathing at 1490. CH<sub>3</sub> at 1355  $\text{cm}^{-1}$ .  $^1\text{H}$  NMR of 3f indicated CH<sub>3</sub> singlet at 3.31 ppm; CH<sub>2</sub> at 5.32 ppm, NH at 7.09 ppm, and aromatic protons at 6.8-8.6 ppm. IR spectrum of 3g showed NH at 3278  $\text{cm}^{-1}$ , OH at 3500-3200  $\text{cm}^{-1}$ . C=O at 1609  $\text{cm}^{-1}$ , C=N at 1576  $\text{cm}^{-1}$ , aromatic ring breathing at 1508.24  $\text{cm}^{-1}$ .  $^1\text{H}$  NMR of 3g indicated CH<sub>2</sub> singlet at 4.23 ppm, NH at 6.70 ppm, aromatic ring at 6.43-8.74 ppm, and OH proton at 9.98 ppm. 3a-g were further confirmed by molecular ion peaks of mass spectra analyses and elemental analyses.

### Biological activity

The antibacterial activity of the novel compounds (1, 2, 3a – 3g) was assessed using the disc diffusion method at a concentration of 5 mM in DMSO (dimethyl sulfoxide) solvent [14]. The synthesized compounds were tested for their antibacterial activity against both Gram-positive bacteria, such as *Staphylococcus aureus* MTCC 96 and *Bacillus subtilis* MTCC 441, and Gram-negative bacteria, including *Pseudomonas aeruginosa* MTCC 1688 and *Escherichia coli* MTCC 443. The reference drug was penicillin g for antimicrobial activity.

The results of antimicrobial screening (Table 1) indicate that the synthesized compounds have a major influence on the antibacterial profile of *P. aeruginosa* and *E. coli* strains (Gram-negative bacteria). Compounds 2, 3a, and 3c showed significant antimicrobial activity against *Bacillus subtilis* as they contain -Cl, -NO<sub>2</sub> and -COOH groups. So, nitro and carboxylic acid groups at para-position enhance antimicrobial activity.

**Table 1.** Antimicrobial activity screening result of synthesized compounds, Gram-negative and Gram-positive bacteria in inhibition zone diameter mm/5 mM.

Antibacterial activity				
Compound no.	Microorganisms and zone of inhibitor (mm/5 mM)			
	Gram-negative bacteria		Gram-positive bacteria	
	<i>P. aeruginosa</i>	<i>E. coli</i>	<i>S. aureus</i>	<i>B. subtilis</i>
1	11	19	12	12
2	17	22	17	27
3a	24	39	19	37
3b	29	24	22	22
3c	20	26	26	35
3d	26	24	24	22
3e	18	20	20	18
3f	24	26	17	22
3g	22	29	24	20
Penicillin-g	15	23	25	25

### ADME Studies

Studies of ADME and toxicity were carried out for these compounds through Absorption, Distribution, Metabolism, and Excretion (ADME) which is a computational approach for assessing

drug-likeness in the bloodstream. Each of these processes can be analyzed independently using specific methods [17]. For example, Lipinski, Ghose, Veber, Egan, Muegge, and the compound's bioavailability score are physiochemical characteristics that provide information on drug-likeness [15]. Based on Egan's multi-statistical graph model 44, the Brain or Intestinal Estimated Permeation makes use of polarity (TPSA) and lipophilicity (WlogP) to forecast CNS access and human intestine absorption (HIA) via a breach in the blood-brain barrier. Thus, the ellipse created by the polarity and lipophilicity profiles intersecting takes into account both strongly and poorly absorbed substances within a human intestine and follows a linear trend. Therefore, the majority populous area of compounds with high HIA, including WlogP values between 0.4 and 6.0 and TPSA lower than 79.2, is indicated by the ellipse created with TPSA less than 142.2 and WlogP between 2.3 and 6.8. The compound's portrayal as a boiled egg provides details about the anticipated Small-molecule penetration of the brain and absorption in the gastrointestinal tract [18]. The scores of all derivatives in the high gastrointestinal absorption (GIA) zone can be seen inside the radar plot of Figure 1, where WlogP values range from 2.62 to 4.09 and TPSA values from 49.57 to 112.32. As a result, all compounds which have the highest oral bioavailability score also have the lowest lipophilicity and polarity index making up the class of compounds with a high GIA.

### Molecular docking

By using Autodock 1.5.7 the target enzyme amylase's (PDB: 1SA0) active site was docked for all of the synthesized variants in this series using molecular docking software [19]. Auto Dock Vina was used to calculate the binding energies of all benzimidazole derivatives, and all binding contacts generated at a distance of 5 Å from the ligand were examined. A standard nocodazole (anti-neoplastic agent) was used for docking. When creating structure-based drug residue, molecular docking is a helpful technique [20]. Figure 2 presents the optimized structures of the three most effective benzimidazole-pyridines employed in the docking investigation. Our research sought to understand how the most potent analog molecules, 3e, 3f, and 3g, interacted with the various amino acids shown in Figure 2 in inappropriate (2D) and (3D) ways. Using energies of -8.1, -8.1, and -8.1 kcal mol<sup>-1</sup>, respectively, Table 3 shows that compounds 3e, 3f, and 3g with strong inhibitory effects occupied acceptable places at the binding center of HPA.

**Table 2:** Estimated absorption and distribution characteristics, as well as anticipated "drug-like" qualities

Compound	Lipinski drug like					Absorption and distribution						
	Mol. wt.	MlogP	H-Bond Acceptors	H-Bond Donors	TPSA	GI	P-gp	BBB	ESOL	WlogP	GI	P-gp
1	195.22	1.66	2	1	41.57	1	Soluble	0.55	2.62	High	Yes	Yes
2	271.7	2.34	3	0	47.78	3	Soluble	0.55	2.98	High	No	Yes
3a	373.36	1.49	5	1	105.63	6	Moderately soluble	0.55	4.09	High	No	No
						5	Moderately soluble					Yes
3c	372.38	0.99	5	2	97.11	6	Moderately soluble	0.56	3.36	High	No	No
						6	Moderately soluble					No
3e	328.37	2.75	3	1	59.81	5	Moderately soluble	0.55	3.66	High	No	Yes
						6	Moderately soluble					Yes
3g	344.37	1.93	4	2	80.04	5	Moderately soluble	0.55	3.37	High	No	No
Std Nocodazole												No

Note: Mol. wt. - Molecular weight, MlogP- Topological method implemented, TPSA- Topological polar surface area, ESOL- Estimated aqueous solubility, WlogP- atomistic method implemented, GI- Gastrointestinal absorption, P-gp- P-glycoprotein substrate, BBB- Blood brain barrier parameter.

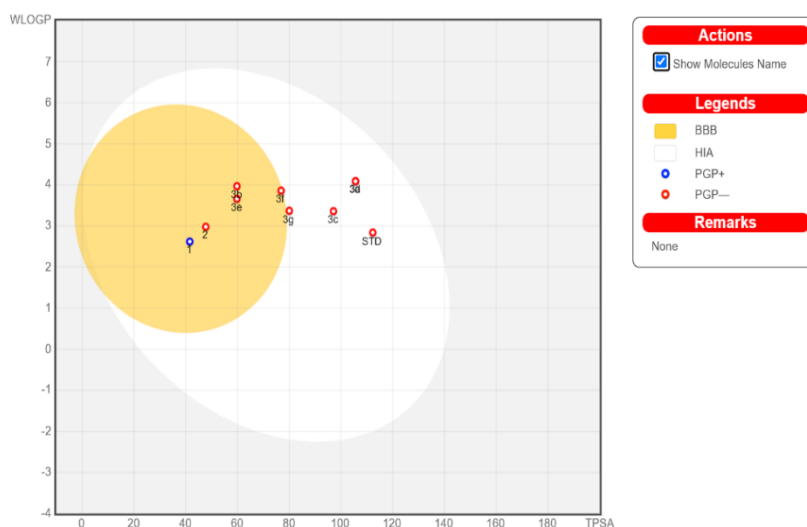


**Figure 1.** BOILED-Egg representation of benzimidazole-pyridine derivatives

**Table 3:** Complexes with 1SA0 docking binding energies (kcal.mol<sup>-1</sup>).

Compounds	1SA0
1	-6.0
2	-6.6
3a	-7.5
3b	-7.7
3c	-7.6
3d	-7.8
3e	-8.1
3f	-8.1
3g	-8.1



antimicrobial potency. A study on the chemicals' absorption, distribution, metabolism, and excretion (ADME) reveals good compatibility and no side effects on the central nervous system (CNS). ADME profiles are moderately water-soluble, blood-brain barrier (BBB) with non-permeant and high GIA absorbance. Molecular docking of the title compounds to tubulin showed that it binds to the colchicine site of tubulin with a binding mode compatible to that of nocodazole. Title compounds provide a promising range of opportunities for future lead optimization of drug development.

**Acknowledgement:** Gratitude is extended to Dr. Devanshu Patel, the President of Parul University, for his generous provision of essential facilities.

#### REFERENCES

1. C. Rao, N. Naidu, J. Priya, K. Rao, K. Ranjith, S. Shobha, B. Chowdary, S. Siddiraju, S. Yadav, *Biomedical Informatics*, **17**, 404 (2021). <https://doi.org/10.6026/97320630017404>
2. M. Andrzejewska, L. Yopez-Mulia, A. Tapia, R. Cedillo-Rivera, A. Laudy, B. Starościak, Z. Kazimierzczuk, *European Journal of Pharmaceutical Sciences*, **21**, 323 (2004). <http://doi.org/10.1016/j.ejps.2003.10.024>
3. K. Ansari, C. Lal, *European Journal of Medicinal Chemistry*, **44**, 4028 (2009). <https://doi.org/10.1016/j.ejmech.2009.04.037>
4. N. Phan, T. Huynh, H. Nguyen, Q. Le, N. Nguyen, K. Ngo, T. Nguyen, K. Ton, K. Thai, T. Hoang, *ACS Omega*, **8**, 28733 (2023). <https://doi.org/10.1021/acsomega.3c03530>
5. E. Mulugeta, Y. Samuel, *Biochemistry Research International*, **13**, 1 (2022). <https://doi.org/10.1155/2022/7255299>
6. V. Grenda, R. Jones, G. George, M. Sletzin, *ACS Publication*, **30**, 259 (1965). <http://doi.org/10.1021/jo01012a061>
7. S. Thurston, G. Hite, A. Petry, R. Sidhartha, *Elsevier B.V.* **37**, 321 (2015). <http://doi.org/10.1016/bs.seda.2015.08.008>
8. P. Zhan, C. Pannecouque, E. Clercq, X. Liu, *Journal of Medicinal Chemistry*, **59**, 2849 (2016). <https://doi.org/10.1021/acs.jmedchem.5b00497>
9. S. Hussain, M. Taha, F. Rahim, S. Hayat, K. Zaman, N. Iqbal, M. Selvaraj, M. Sajid, M. Bangesh, F. Khan, K. Khan, N. Uddin, S. Shahi, M. Ali, *Journal of Molecular Structure*, **1232**, 1 (2021). <https://doi.org/10.1016/j.molstruc.2021.130029>
10. N. Thi, E. Pozioc, N. Van De, N. Praet, P. Pezzotti, S. Gabriel, M. Claes, N. Thuya, P. Dorny, *Acta Tropica*, **139**, 93 (2014). <https://doi.org/10.1016/j.actatropica.2014.07.012>
11. K. Ansari, C. Lal, *European Journal of Medicinal Chemistry*, **44**, 4028 (2009). <https://doi.org/10.1016/j.ejmech.2009.04.037>
12. L. Gatta, F. Perna, N. Figura, C. Ricci, J. Holton, L. D'Anna, M. Miglioli, D. Vaira, *J. Antimicrob. Chemother.*, **51**, 439, (2003). [doi:10.1093/jac/dkg085](https://doi.org/10.1093/jac/dkg085)
13. Z. Ates-Alagöz, M. Alp, C. Kus, S. Yildiz, E. Buyukbingöl, H. Göker, *An International Journal of Pharmaceutical and Medicinal Chemistry*, **339**(2), 74, (2006). <https://doi.org/10.1002/ardp.200500168>
14. M. Marinescu, C. V. Popa, *International Journal of Molecular Sciences*, **23**(10), 5659, (2022). <https://doi.org/10.3390/ijms23105659>
15. B. Srinivas, M. Subramanyam, G. K. Srinivasulu, K. Prabhakara Rao, *Bulg. Chem. Commun.*, **53**(1), 10 (2021). <https://doi.org/10.34049/bcc.53.1.5165>
16. A. Daina, O. Michielin, V. Zoete, *J. Chem. Inf. Model.*, **54**, 3284 (2014). <https://doi.org/10.1021/ci500467k>
17. M. Argirova, M. Guncheva, G. Momekov, E. Cherneva, R. Mihaylova, M. Rangelov, N. Todorova, P. Denev, K. Anichina, A. Mavrova, D. Yancheva, *Molecules*, **28**(1), 291 (2022). <https://doi.org/10.3390/molecules28010291>
18. M. Hay, D. Thomas, J. Craighead, C. Economides, J. Rosenthal, *Nature Biotechnology*, **32**, 40 (2014). <https://doi.org/10.1038/nbt.2786>
19. J. Silva, M. Rocha, E. Marinho, *J. Anal. Pharm. Res.*, **10**, 177 (2021). <https://doi.org/10.15406/japlr.2021.10.00384>
20. L. Aroua, A. Alosaimi, F. Alminderej, S. Messaoudi, H. Mohammed, S. Almahmoud, S. Chigurupati, A. Albadri, N. Mekni, *Pharmaceutics*, **15**, 457 (2023). <https://doi.org/10.3390/pharmaceutics15020457>

## Synthesis, biological evaluation, ADME studies and molecular docking with $\beta$ -tubulin of fused benzimidazole-pyridine derivatives

D. Panchani<sup>1</sup>, S. Maurya<sup>1</sup>, T. Thaker<sup>1\*</sup>, V. Rathod<sup>1</sup>, Sh. Thakur<sup>2</sup>

<sup>1</sup>Department of Chemistry, Parul Institute of Applied Sciences, Parul University, Waghodia, Vadodara-391760, Gujarat, India

<sup>2</sup>Department of Forensic Science, Parul Institute of Applied Sciences, Parul University, Waghodia, Vadodara-391760, Gujarat, India

### Table of contents

1.	IR Spectrum of 2	S1
2.	<sup>1</sup> H NMR Spectrum of 2	S2
3.	IR Spectrum of 2	S3
4.	<sup>1</sup> H NMR Spectrum of 2	S4
5.	IR Spectrum of 3a	S5
6.	<sup>1</sup> H NMR Spectrum of 3a	S6
7.	IR Spectrum of 3b	S7
8.	<sup>1</sup> H NMR Spectrum of 3b	S8
9.	IR Spectrum of 3c	S9
10.	<sup>1</sup> H NMR Spectrum of 3c	S10
11.	IR Spectrum of 3d	S11
12.	<sup>1</sup> H NMR Spectrum of 3d	S12
13.	IR Spectrum of 3e	S13
14.	<sup>1</sup> H NMR Spectrum of 3e	S14
15.	IR Spectrum of 3f	S15
16.	<sup>1</sup> H NMR Spectrum of 3f	S16
17.	IR Spectrum of 3g	S17

**Spectral Data:**

**Compound 1:**

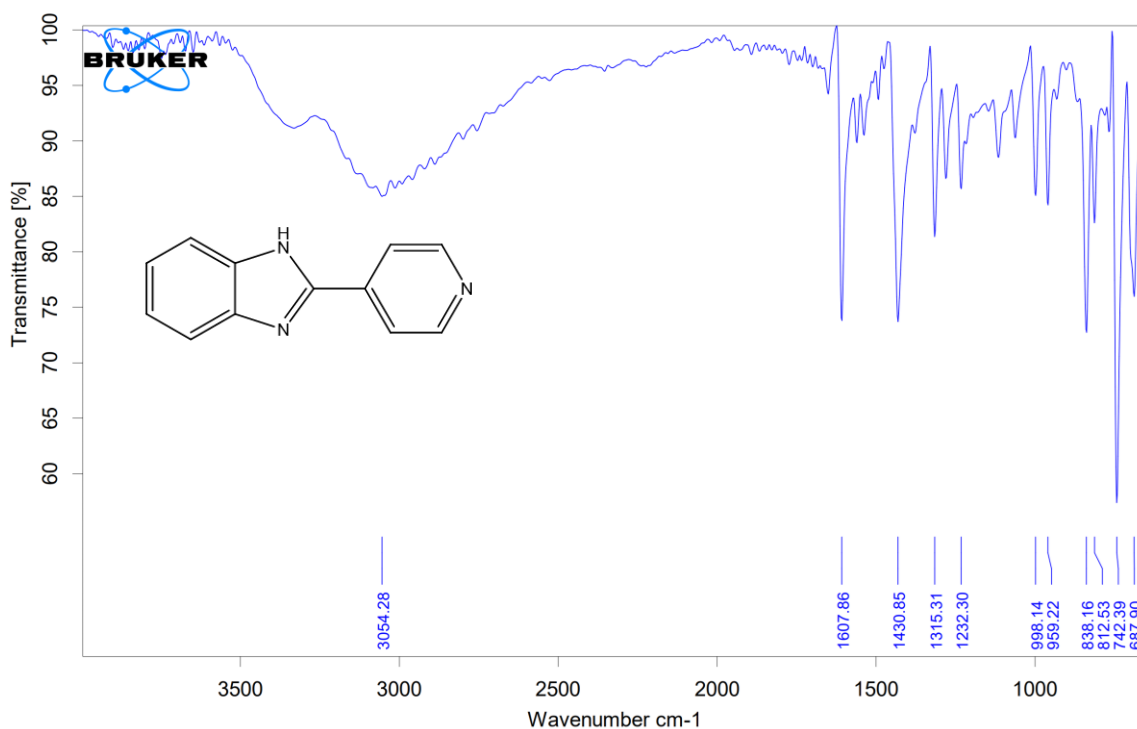


**Figure S1:** IR DATA of 2-(pyridin-4-yl)-1H-benzo[d]imidazole (1)

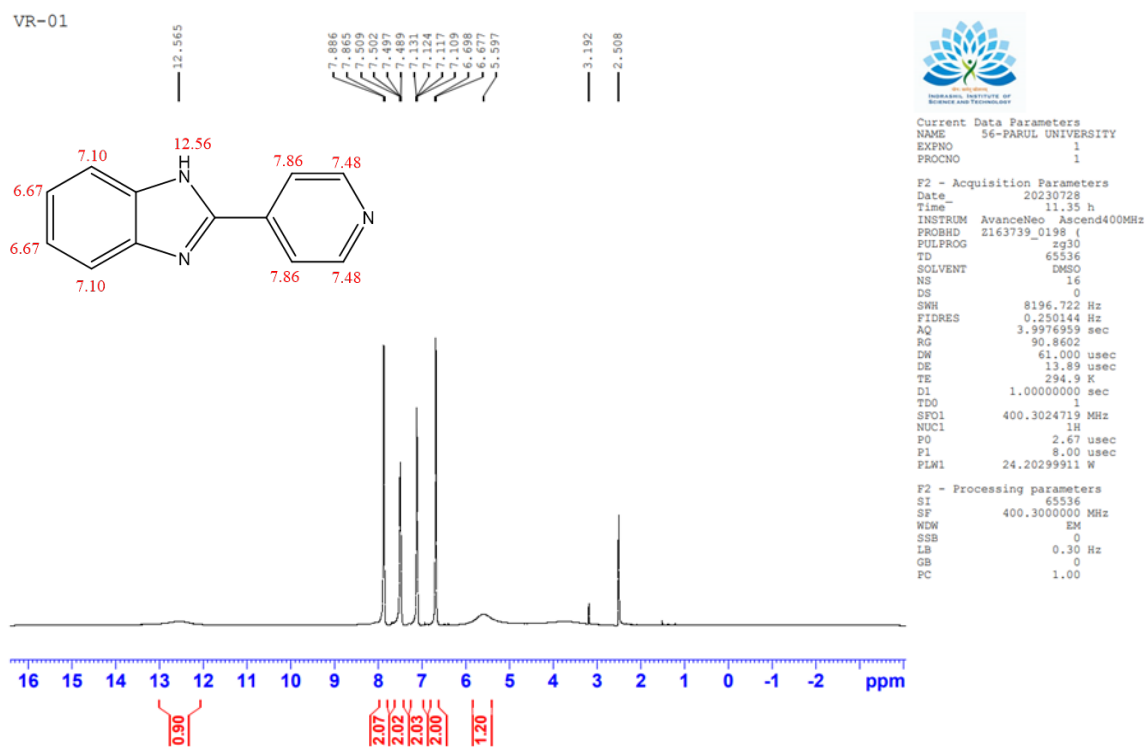


**Figure S2:**  $^1\text{H}$  NMR DATA of 2-(pyridin-4-yl)-1H-benzo[d]imidazole (1)



### Compound 3a

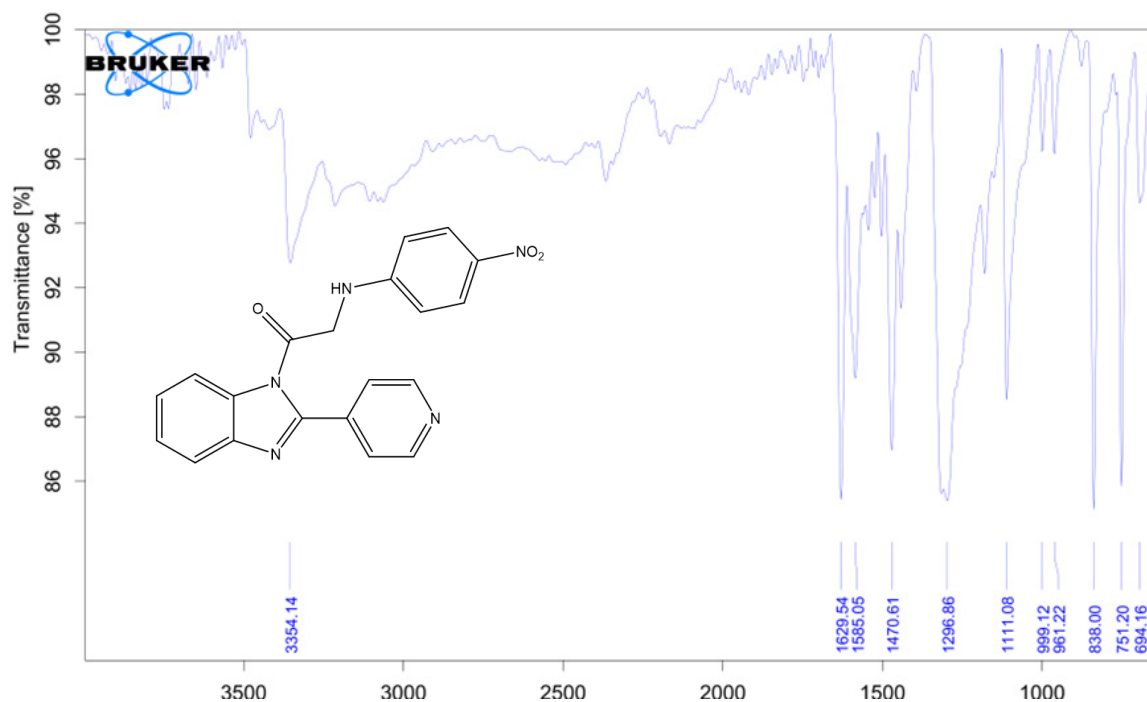


**Figure S5:** IR DATA of 2-((4-nitrophenyl)amino)-1-(2-(pyridin-4-yl)-1H-benzo[d]imidazol-1-yl)ethan-1-one (3a)

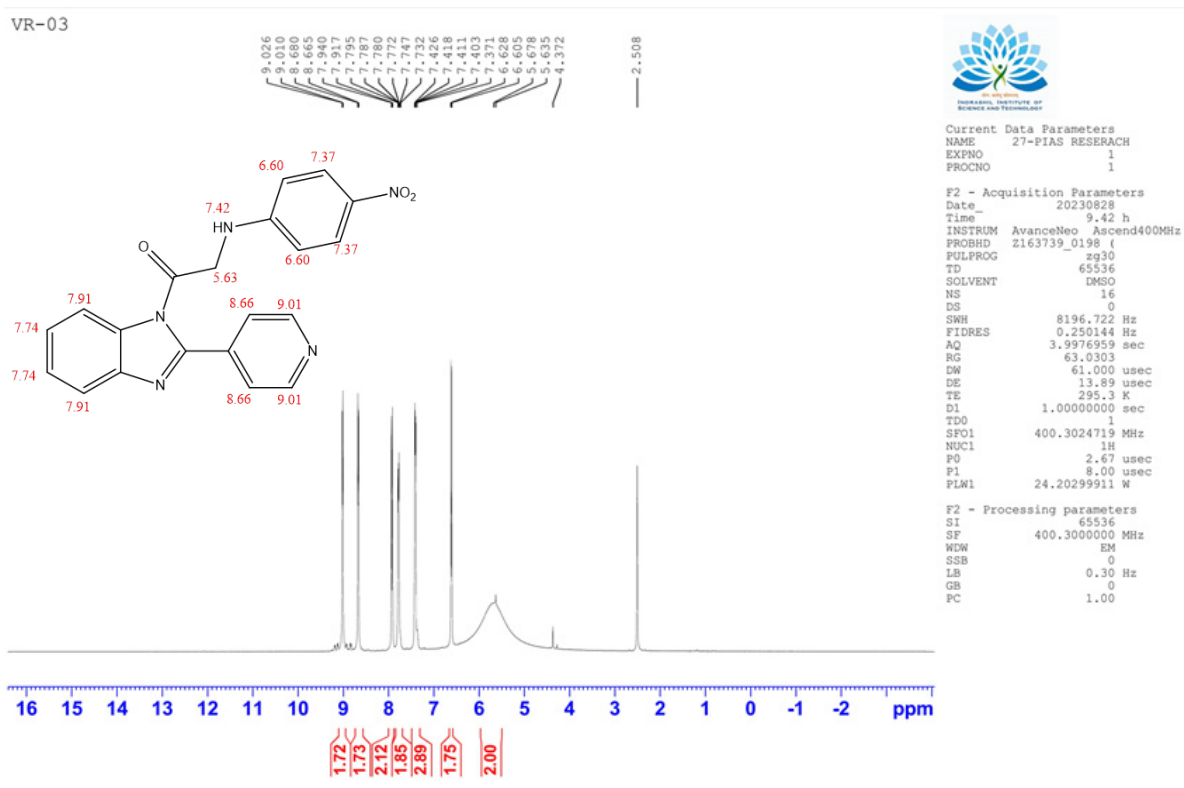


**Figure S6:**  $^1\text{H}$  NMR DATA of 2-((4-nitrophenyl)amino)-1-(2-(pyridin-4-yl)-1H-benzo[d]imidazol-1-yl)ethan-1-one (3a)

### Compound 3b

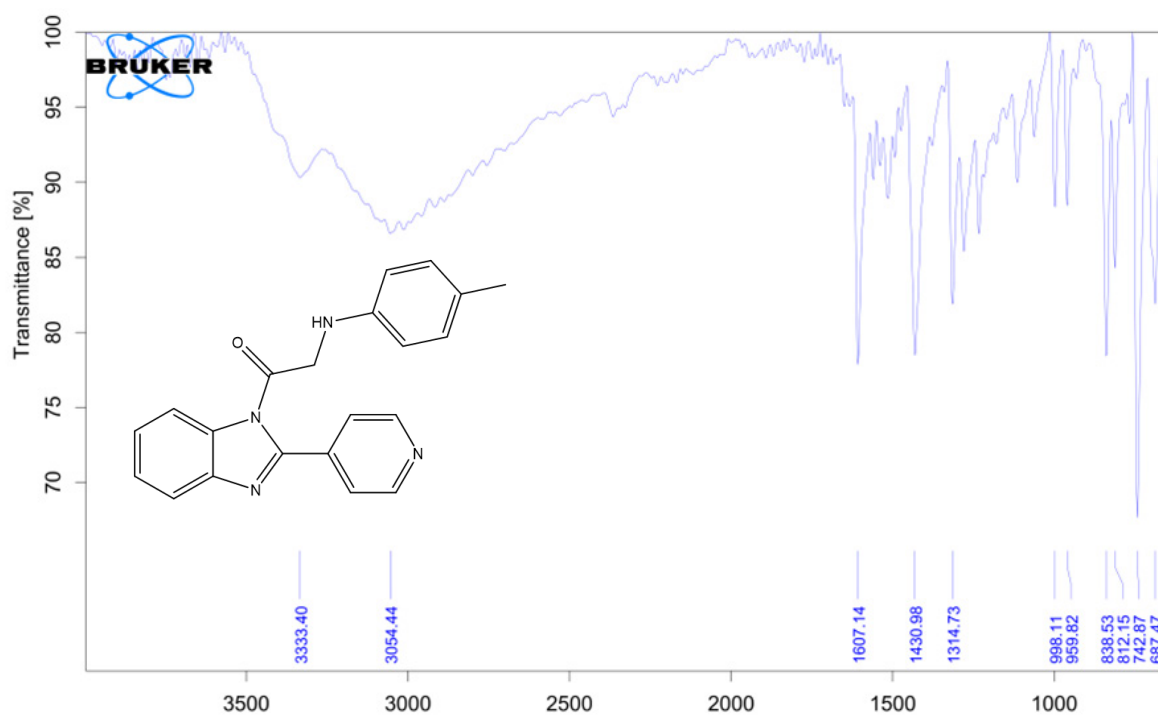


**Figure S7:** IR DATA of 1-(2-(pyridin-4-yl)-1H-benzo[d]imidazol-1-yl)-2-(p-tolylamino)ethan-1-one (3b)

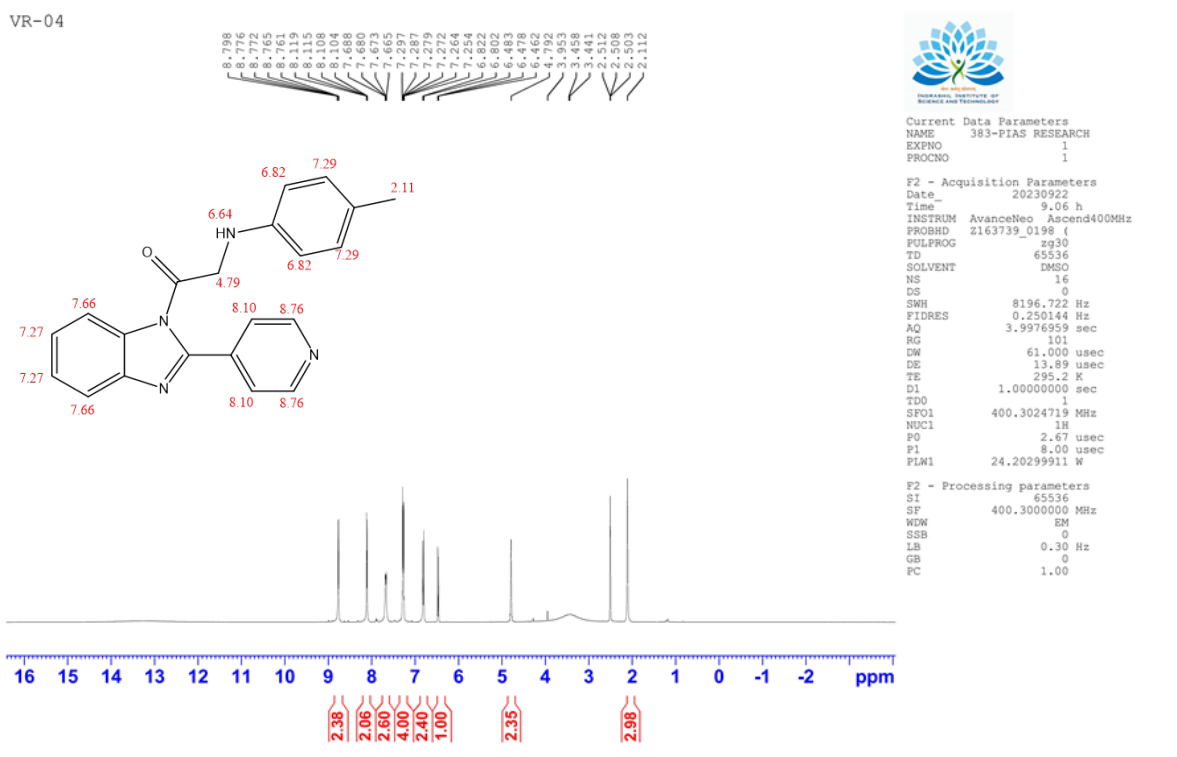


**Figure S8:**  $^1\text{H}$  NMR DATA of 1-(2-(pyridin-4-yl)-1H-benzo[d]imidazol-1-yl)-2-(p-tolylamino)ethan-1-one (3b)



### Compound 3d

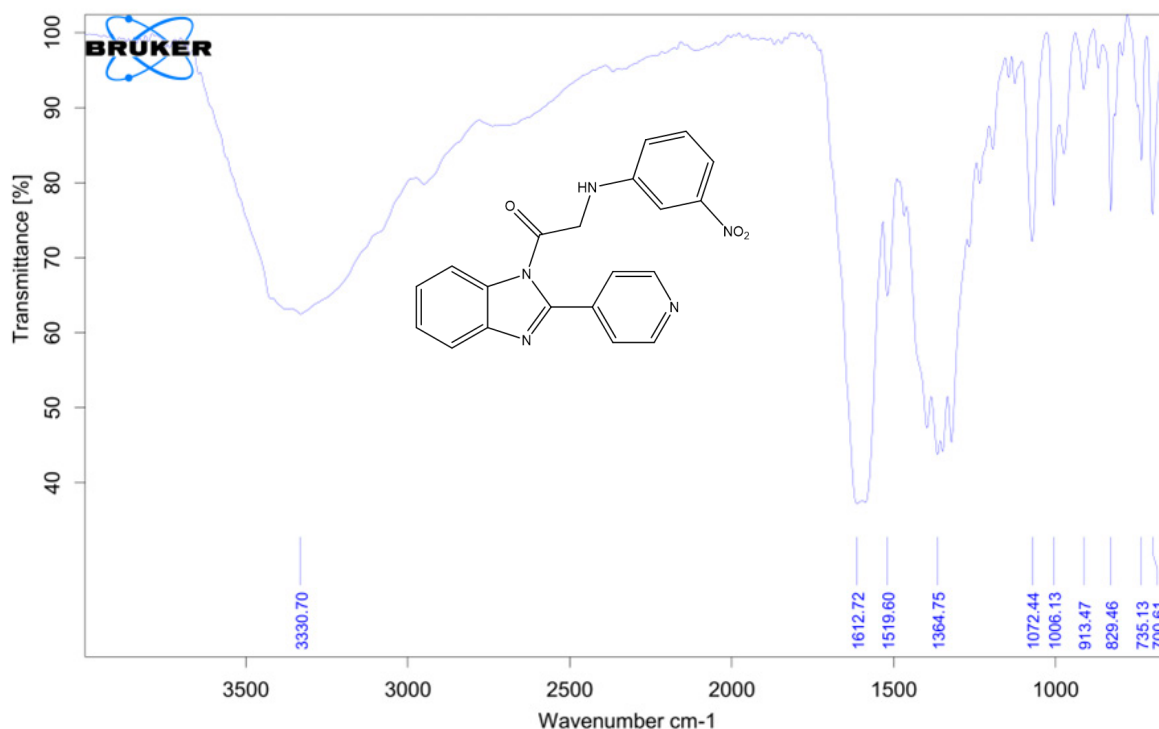


**Figure S11:** IR DATA of IR data of 2-((3-nitrophenyl)amino)-1-(2-(pyridin-4-yl)-1H-benzo[d]imidazol-1-yl)ethan-1-one (3d)

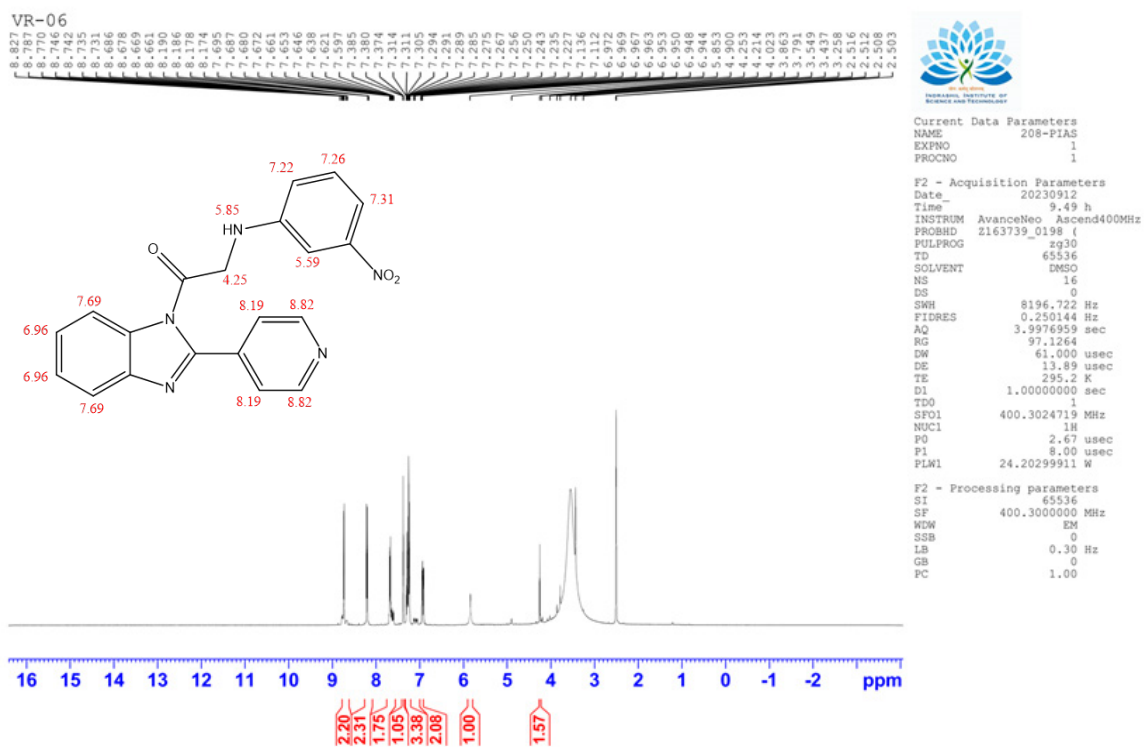


**Figure S12:**  $^1\text{H}$  NMR DATA of IR data of 2-((3-nitrophenyl)amino)-1-(2-(pyridin-4-yl)-1H-benzo[d]imidazol-1-yl)ethan-1-one (3d)

### Compound 3e

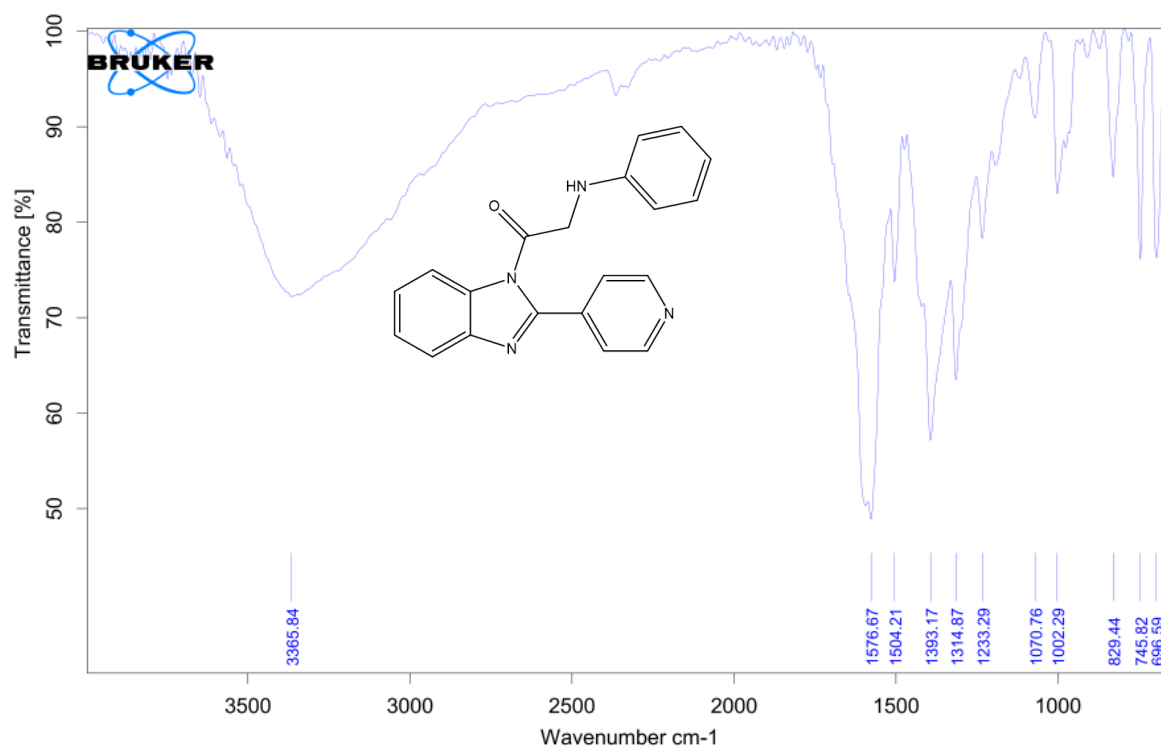


**Figure S13:** IR DATA of 2-(phenylamino)-1-(2-(pyridin-4-yl)-1H-benzo[d]imidazol-1-yl)ethan-1-one (3e)

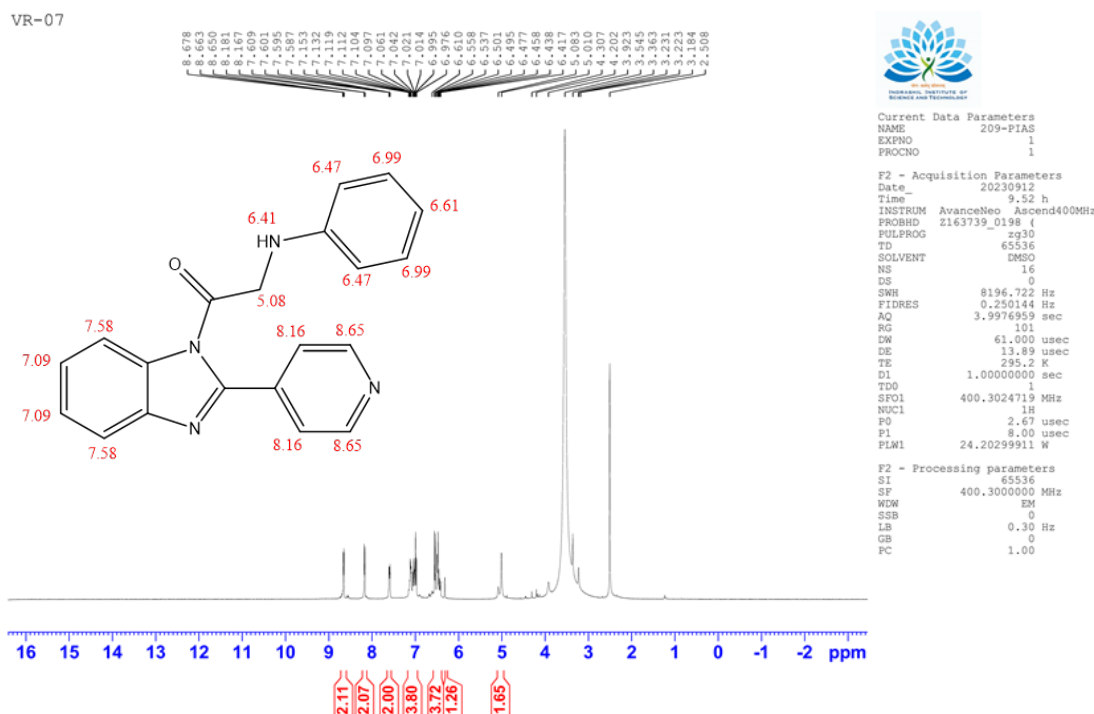


**Figure S14:**  $^1\text{H}$  NMR DATA of 2-(phenylamino)-1-(2-(pyridin-4-yl)-1H-benzo[d]imidazol-1-yl)ethan-1-one (3e)



### Compound 3g

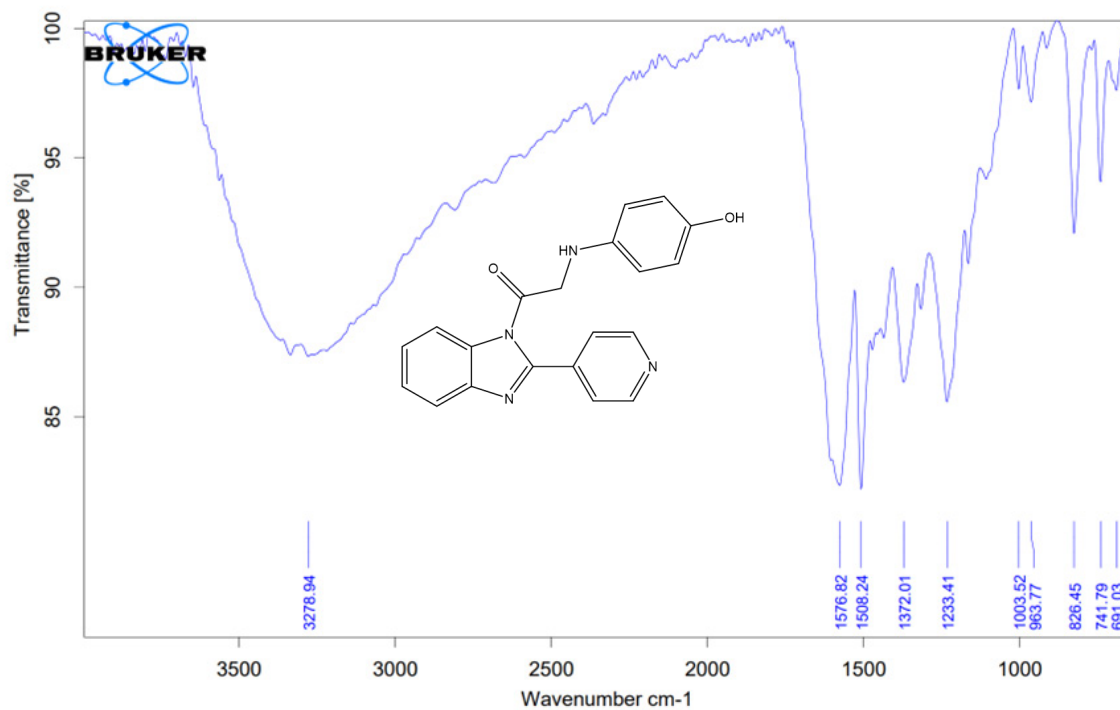


**Figure S17:** IR DATA of 2-((4-hydroxyphenyl)amino)-1-(2-(pyridin-4-yl)-1H-benzo[d]imidazol-1-yl)ethan-1-one (3g)

## Cobalt complexes of pyridine carboxaldehyde Schiff bases as cholinesterase inhibitors and anti-proliferative activity

A. Naseer<sup>1,2</sup>, A. Naz Awan<sup>1\*</sup>, J. Iqbal<sup>3</sup>, S. Habib<sup>4</sup>, A. Javed<sup>4</sup>

<sup>1</sup>Department of Pharmaceutical Chemistry, Faculty of Pharmacy and Pharmaceutical Sciences, University of Karachi, Karachi 75270, Pakistan

<sup>2</sup>College of Pharmacy – Isra University, Hyderabad, Pakistan

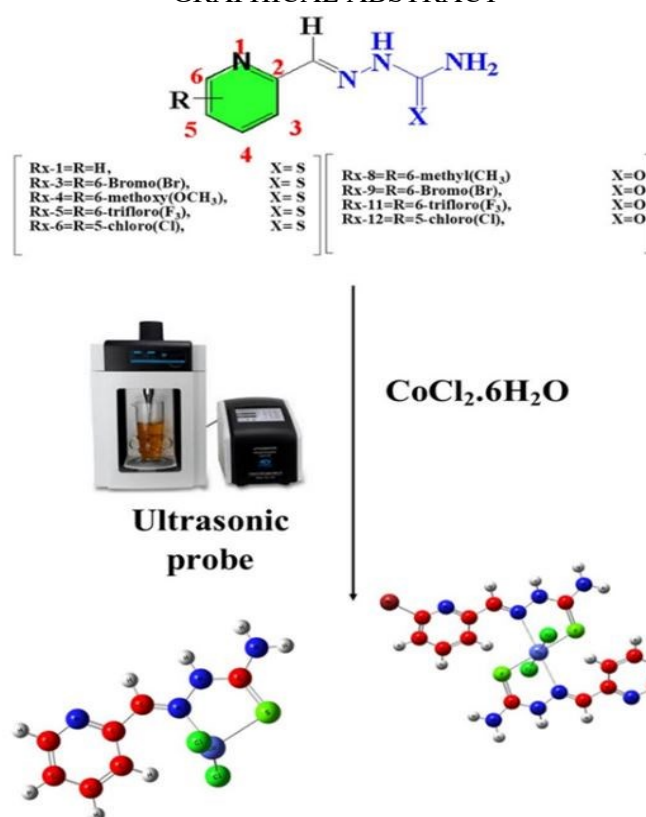
<sup>3</sup>Center for Advanced Drug Research, COMSATS University Islamabad, Abbottabad Campus, Abbottabad 22060, Pakistan

<sup>4</sup>Healthcare Biotechnology, Atta-ur-Rahman School of Applied Biosciences, National University of Science and Technology, Islamabad, Pakistan

Received: January 25, 2024; Revised: May 15, 2024

Novel cobalt complexes of pyridine carboxaldehyde were meticulously designed, synthesized, and subsequently screened to assess their broad spectrum of biological potential. Pyridine carboxaldehyde semicarbazone, thiosemicarbazone, and cobalt chloride served as the initial materials, which were subjected to ultrasonication for the synthesis of the cobalt complexes. Characterization of the obtained compounds was conducted using FTIR, <sup>1</sup>H-NMR, elemental analysis, and both *in-silico* and *in-vitro* assessments were performed to evaluate their cholinesterase inhibition and anti-proliferative properties. It was found that all synthesized molecules selectively inhibited acetylcholinesterase within a range of IC<sub>50</sub> values from 0.97±0.02 to 6.47±0.71 μM. Notably, CoRx-1Cl<sub>2</sub> exhibited non-selective inhibition against both acetylcholinesterase and butyrylcholinesterase, with IC<sub>50</sub> values of 1.91±0.08 and 12.97±2.46 μM, respectively. Subsequent MTT assays and cytotoxic studies were carried out on U-87 and HEK-293 cell lines, revealing that all synthesized compounds were non-toxic to the normal cell line HEK-293. Conversely, cell viability in U-87 cells ranged from 20.93% to 92.9%. These findings suggest that the synthesized cobalt complexes possess a multi-targeting effect and hold potential for use in the management of conditions such as Glioblastoma and Alzheimer's diseases.

### GRAPHICAL ABSTRACT



**Keywords:** Schiff bases; Cobalt complexes; Ultrasonic probe; Cholinesterase inhibition; MTT assay.

\* To whom all correspondence should be sent:  
E-mail: asia.naz@uok.edu.pk

## INTRODUCTION

The enzymes acetylcholinesterase (AChE) and butyrylcholinesterase (BuChE) belong to the class of serine hydrolases [1, 2]. They can hydrolyze acetylcholine (ACh) and a few other choline esters, albeit with varying degrees of relative efficiency. Additionally, cholinesterases may exhibit peptide hydrolysis or aryl acyl amidase activity [3]. In the modern world, conditions such as Alzheimer's disease (AD) and cancer are prevalent and often fatal illnesses, posing significant societal and economic challenges [4, 5]. AD is characterized by the loss of cholinergic neurons, leading to alterations in the concentrations of AChE and BuChE [6, 7], while cancer represents a global health concern due to its unique nature characterized by the uncontrolled growth of abnormal cells [8]. Although cancer research has yielded numerous novel and effective treatments, the drugs currently employed to address these conditions have evident limitations [9, 10].

Improving and stabilizing the symptoms of AD may be achievable by maintaining the level of this essential neurotransmitter in brain tissues [2, 11]. Additionally, acetylcholinesterase (AChE) may play a significant role in cancer development and could potentially serve as a target for treatment, given its involvement in non-neuronal processes such as the regulation of cell proliferation, differentiation, and apoptosis [12]. One possible mechanism linking neurodegeneration and malignancy involves the non-enzymatic binding of AChE to an allosteric site on the nicotinic  $\alpha$ -7 receptor, which operates at both neuronal and non-neuronal levels. Furthermore, AChE may be crucial for the migration of cancer cells, suggesting a pathway that intersects neurodegeneration and carcinogenesis [13, 14].

Semicarbazone (SC) and thiosemicarbazone (TSC) represent classes of Schiff bases derived from the condensation of aldehydes [15] or ketones with semicarbazide and thiosemicarbazide, respectively, wherein the carbonyl group is replaced by an imine bond. Schiff bases constitute an exceptional category of ligands that demonstrate remarkable coordination modes towards transition metals owing to their diverse array of donor atoms [16, 17]. In the formation of metallic complexes, SC and TSC ligands often coordinate to transition metals through their oxygen, nitrogen, and sulfur donor atoms, adopting either their (N, S) bidentate form or (N, N, S or O, N, S) tridentate form [18, 19]. These complexes may exhibit bioactivities that surpass those of the free ligands, including acting as DNA binding agents [20], antiviral [21], antifungal [22], antimicrobial [23, 24], anticancer [23, 25], SARS-

CoV-2 inhibitors [26], inhibitors of topoisomerase II $\alpha$  [27], and monoamine oxidase-B inhibitors [28], as well as displaying acetylcholinesterase inhibition properties [28, 29].

Previous research [30] has utilized experimental approaches to assess the biological activity of compounds against enzymes. Scientists continuously seek innovative compounds to enhance biological activity, often linking metal atoms and ligand molecules to synthesize novel complexes. Researchers have discovered that these metal complexes exhibit greater biological activity compared to their ligands [31, 32], thereby demonstrating more potent inhibition against enzymes.

In the present study, conventional methods such as sol-gel or thermal degradation for synthesizing complexes have been replaced with ultrasonication. This alternative technique offers several advantages, including cost efficiency, environmental friendliness, and the ability to perform treatments on-site. Specifically, this research focuses on the ultrasound-assisted fabrication of cobalt complexes derived from recently reported pyridine carboxaldehyde semicarbazone and thiosemicarbazone [33]. These complexes are subsequently examined to assess their inhibitory effect on cholinesterase enzymes, as well as their anti-proliferative effect against both the U-87 cancer cell line and the HEK-293 normal cell line.

## RESULTS AND DISCUSSION

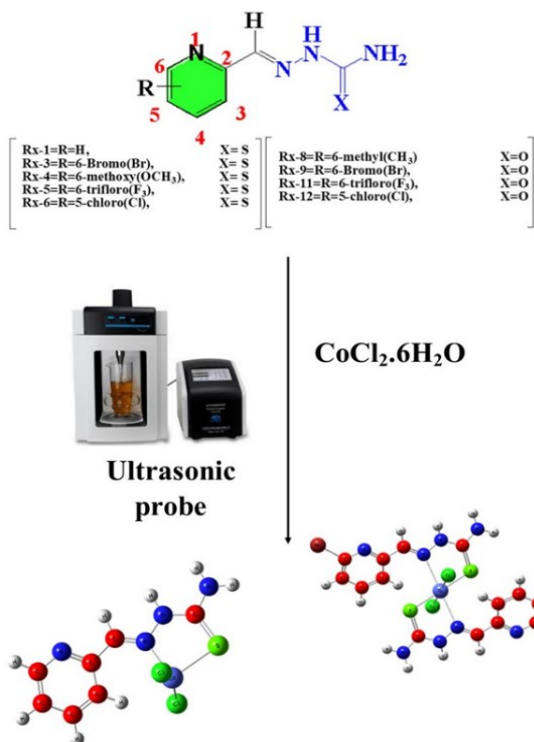
The 0.001 molar water/ethanolic solutions of substituted semicarbazone and thiosemicarbazones were added dropwise to a 0.001 molar cobalt chloride solution while keeping it in a high-density ultrasonic probe. Sonication was continued for 30 minutes, after which the product was precipitated out, filtered, washed with ethanol, and dried, then stored in a closed container for further study.

A cobalt complex of pyridine carboxaldehyde thiosemicarbazone was discussed here as an example for spectral studies. The NH peak appeared at  $3390\text{ cm}^{-1}$ , indicating the presence of one free primary amino group. Peaks at  $1581\text{ cm}^{-1}$  and  $837\text{ cm}^{-1}$  were observed for the stretching of C=N and C=S, respectively, which were slightly shifted to lower wavelengths compared to the respective pyridine carboxaldehyde thiosemicarbazone, which exhibited peaks at  $1622\text{ cm}^{-1}$  and  $877\text{ cm}^{-1}$ . These findings from FTIR suggest the bidentate behavior of pyridine carboxaldehyde thiosemicarbazone, involving the azomethine group (-C=N-) and sulfide group (-C=S-) moieties interacting with the core cobalt metal ions. The  $^1\text{H-NMR}$  results also

confirmed the FTIR findings. The aromatic ring proton appeared at  $\delta$  7.369 (t, 1H), 7.821 (t, 1H), 8.272 (d, 1H), 8.557 (d, 1H), while the CH-N appeared at  $\delta$  8.082 (s, 1H), NH appeared at  $\delta$  11.642 (s, 1H), and the terminal amine appeared at  $\delta$  8.180 (s, 1H).

The solubility study revealed that the obtained complexes are insoluble in diethyl ether, ethanol, and acetonitrile, slightly soluble in chloromethane and carbon tetrachloride, and soluble in DMSO and DMF.

A series of cobalt complexes of pyridine carboxaldehyde semicarbazone and thiosemicarbazone were synthesized according to the details provided in Scheme 1.



**Scheme 1.** Synthesis of cobalt complexes of pyridine carboxamide and carbothioamide.

#### Shape and surface topography

The surface topography and shape of the cobalt complexes of pyridine carboxaldehyde semicarbazone and thiosemicarbazone were characterized using an atomic force microscope (AFM). The study revealed the presence of polydisperse particles ranging in size from 11 to 60 nm. Upon inserting metal into the pyridine carboxaldehyde semicarbazone and thiosemicarbazone complexes, surfaces were transformed into uniformly sized smooth shapes, as depicted in the figures presented in the supplementary data.

Specifically, complexes such as CoRx-1Cl<sub>2</sub>, CoRx-3Cl<sub>2</sub>, CoRx-4Cl<sub>2</sub>, CoRx-5Cl<sub>2</sub>, CoRx-6Cl<sub>2</sub>, CoRx-8Cl<sub>2</sub>, CoRx-9Cl<sub>2</sub>, and CoRx-11Cl<sub>2</sub> exhibited surfaces that were more uniform in small needle-like structures, while the CoRx-12Cl<sub>2</sub> complex displayed a smooth, ball-like structure.

#### Cholinesterase inhibition potential

The newly synthesized cobalt complexes of pyridine carboxaldehyde semicarbazone and thiosemicarbazone underwent screening for cholinesterase inhibition potential, specifically targeting AChE and BuChE. The summarized results are presented in Table 1. Compounds demonstrating more than 50% inhibition were further assessed for their IC<sub>50</sub> values. The findings indicated that all synthesized compounds selectively inhibited AChE, with IC<sub>50</sub> values ranging from submicromolar to micromolar concentrations (0.97±0.02  $\mu$ M to 6.47±0.71  $\mu$ M), except for CoRx-1Cl<sub>2</sub>, which exhibited inhibition of both AChE and BuChE, with IC<sub>50</sub> values of 1.91±0.08  $\mu$ M and 12.97±2.46  $\mu$ M, respectively.

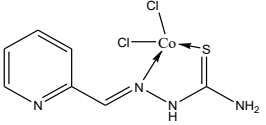
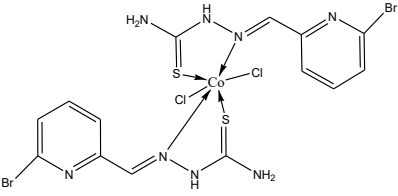
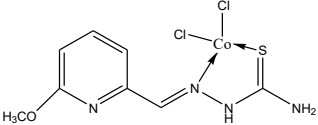
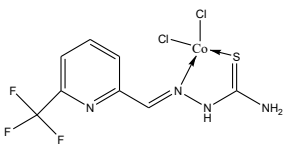
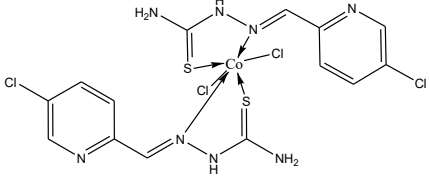
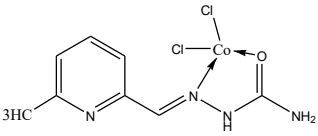
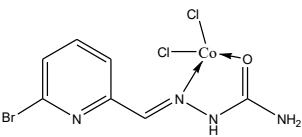
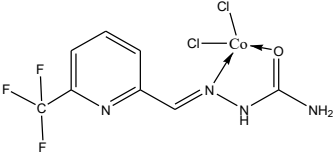
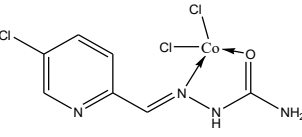
In this study, donepezil was utilized as a positive control, showing inhibition with IC<sub>50</sub> values of 0.03±0.01  $\mu$ M and 6.41± 0.34  $\mu$ M for AChE and BuChE, respectively. The IC<sub>50</sub> values of the synthetic inhibitors and the standard (donepezil) for AChE were ranked as follows: CoRx-8Cl<sub>2</sub> > CoRx-12Cl<sub>2</sub> > CoRx-5Cl<sub>2</sub> > CoRx-1Cl<sub>2</sub> > CoRx-3Cl<sub>2</sub> > CoRx-11Cl<sub>2</sub> > CoRx-4Cl<sub>2</sub> > CoRx-6Cl<sub>2</sub> > donepezil. Inhibiting the enzyme leads to acetylcholine accumulation, overstimulation of nicotinic and muscarinic receptors, and disruption of neurotransmission, which may improve the symptoms of Alzheimer's disease patients by restoring synaptic levels of this neurotransmitter.

#### • Structure-activity relationship

Among the tested compounds, only CoRx-1Cl<sub>2</sub> exhibited significant inhibition of both AChE and BuChE, with IC<sub>50</sub> values of 1.91±0.08  $\mu$ M and 12.97±2.46  $\mu$ M, respectively. This could be attributed to the presence of a non-substituted pyridine ring in the structure.

CoRx-6Cl<sub>2</sub> demonstrated the most potent and selective inhibition of AChE, with an IC<sub>50</sub> value of 0.97±0.02  $\mu$ M. The presence of a chlorine (Cl) group substitution on the 5<sup>th</sup> position of the pyridine ring may contribute to this enhanced potency by reducing the electron density from the aromatic ring. This substitution strategy appears to be more effective compared to compounds with no substitution or substitution at the C-6 position of the pyridine ring.

**Table 1.** Cholinesterase inhibition assay results of cobalt complexes of pyridine carboxaldehyde

Sr. no	Compound name	Structure	AChE	BuChE
			IC <sub>50</sub> ± SEM (μM) or (% inhibition ± SD)*	
1.	CoRx-1Cl <sub>2</sub>		1.91±0.08	12.97±2.46
2.	CoRx-3Cl <sub>2</sub>		1.42±0.10	14%
3.	CoRx-4Cl <sub>2</sub>		1.23±0.47	19%
4.	CoRx-5Cl <sub>2</sub>		2.59±0.12	11%
5.	CoRx-6Cl <sub>2</sub>		0.97±0.02	13%
6.	CoRx-8Cl <sub>2</sub>		6.47±0.71	16%
7.	CoRx-9Cl <sub>2</sub>		36%	14%
8.	CoRx-11Cl <sub>2</sub>		1.25±0.29	21%
9.	CoRx-12Cl <sub>2</sub>		3.07±0.56	27%
10.	Donepezil		0.03±0.01	6.41± 0.34

Other compounds, including CoRx-4Cl<sub>2</sub> (IC<sub>50</sub> = 1.23±0.47 μM), CoRx-11Cl<sub>2</sub> (IC<sub>50</sub> = 1.25±0.29 μM), CoRx-3Cl<sub>2</sub> (IC<sub>50</sub> = 1.42±0.10 μM), CoRx-5Cl<sub>2</sub> (IC<sub>50</sub> = 2.59±0.12 μM), CoRx-12Cl<sub>2</sub> (IC<sub>50</sub> = 3.07±0.56 μM), and CoRx-8Cl<sub>2</sub> (IC<sub>50</sub> = 6.47±0.71 μM), also showed selective inhibition of AChE.

• *Docking study*

One of the most significant methods employed in structure-based drug design is molecular docking, which analyzes atomic-level interactions between a protein and a small molecule. In our study, we conducted docking analyses on the most potent cobalt complexes of pyridine carboxaldehyde thiosemicarbazone against AChE to establish a meaningful association between *in-vitro* and *in-silico* studies. The objective was to gain a deeper understanding of the essential relationships between active scaffolds and the enzyme's active sites.

During the analysis, active residues such as Tyr124 and Tyr337 exhibited hydrogen bonding with sulfur (S) and chlorine (Cl) atoms, while Trp286 showed hydrogen-arene interaction with the pyridine ring of CoRx-4Cl<sub>2</sub>. Similarly, CoRx-6Cl<sub>2</sub> demonstrated binding interactions with Ser293 and Trp286, interacting with sulfur and chlorine atoms, while His287 exhibited hydrogen-arene interaction with the pyridine ring, as depicted in Figures 1 and 2.

According to literature, Tyr337 serves as an entrance point for the catalytic anionic binding site (CAS) for acetylcholine binding, while Trp286 is a principal component of the peripheral anionic site (PAS) that regulates the accessibility of small molecules to the active site and contributes to allosterism. Arene interactions with the Trp286 residue modulate inhibition constants for some AChE inhibitors [34-35]. CoRx-6Cl<sub>2</sub> exclusively demonstrated binding interactions at PAS, whereas CoRx-4Cl<sub>2</sub> exhibited binding interactions at both CAS and PAS by interacting with Tyr337 and Trp286, thereby enhancing its potency and selectivity.

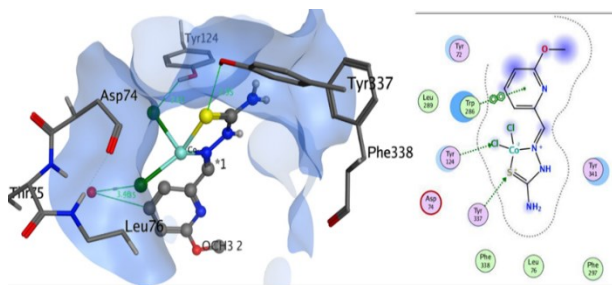


**Figure 1.** Docked image of CoRx-4Cl<sub>2</sub> at the active pocket site of AChE.

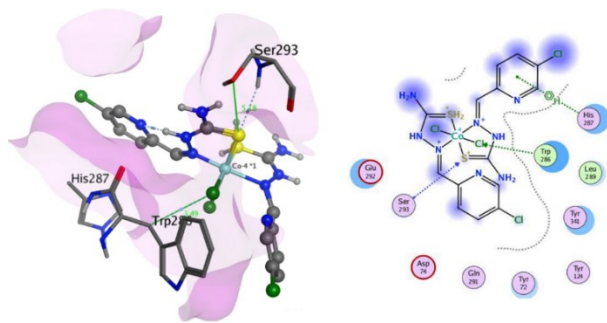


**Figure 2.** Docked image of CoRx-6Cl<sub>2</sub> at the active pocket site of AChE.

• *Kinetic study*

The Lineweaver-Burk plot of CoRx-6Cl<sub>2</sub> was generated to assess the competitive mode of inhibition between the tested molecule and the standard substrate, as illustrated in Figure 3. Kinetic studies revealed that as the concentration increases, K<sub>m</sub> also increases, with only minor differences observed, while V<sub>max</sub> remains constant without significant changes in slopes. This suggests that the substrate and inhibitor compete to bind at the active pocket.

The identified inhibitors demonstrated strong binding at the active pocket of AChE, a finding further validated through molecular docking studies [36].

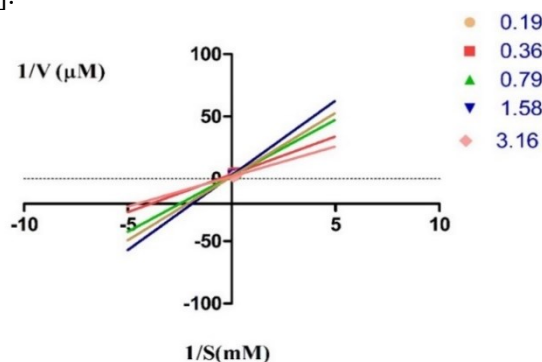


**Figure 3.** Lineweaver-Burk plot of CoRx-6Cl<sub>2</sub>.

*Anti-proliferative potential*

The MTT assay was utilized to assess the anti-proliferative activity of cobalt complexes of pyridine carboxaldehyde semicarbazone and thiosemicarbazone using the glioblastoma cell line (U87), while the cytotoxic activity was evaluated on the normal cell line HEK-293, as presented in Table 2. This cell line was chosen due to the compounds' potential efficacy against many enzymes associated with neurodegenerative diseases, suggesting they might also exhibit anti-proliferative potential.

**Table 2.** MTT assay result of cobalt complexes of pyridine carboxaldehyde semicarbazone and thiosemicarbazone.

Sr. no	Compound name	Structure	% Cell viability	
			HEK-293	U87
1.	CoRx-1Cl <sub>2</sub>		215.05	52.1
2.	CoRx-3Cl <sub>2</sub>		303.32	92.9
3.	CoRx-4Cl <sub>2</sub>		212.3	87.9
4.	CoRx-5Cl <sub>2</sub>		129.52	20.93
5.	CoRx-6Cl <sub>2</sub>		136.34	23.46
6.	CoRx-8Cl <sub>2</sub>		217.58	62.27
7.	CoRx-9Cl <sub>2</sub>		246.08	384.84
8.	CoRx-11Cl <sub>2</sub>		313.26	81.36
9.	CoRx-12Cl <sub>2</sub>		185.03	82.47
10.	Doxorubicin		82.2594	59.8512

The study revealed that all synthesized compounds were non-toxic to the normal cell line, as evidenced by cell viability increasing above 100% after 48 hours of incubation. This suggests that the tested molecules did not affect the growth of the normal cell line. In fact, upon incubation, the number of normal cell line cells doubled compared to the initially incubated cells. Conversely, in the case of U-87 cells, viability decreased from 100%. Among them, CoRx-5-Cl<sub>2</sub> and CoRx-6-Cl<sub>2</sub> showed the most

potent results, indicating moderate to low anti-proliferative activity.

Metal complexes exhibited a stronger potential anti-proliferative effect due to the positive charge of the metal ions enhancing the acidity of the coordinated ligand. This facilitated the ligands carrying hydrogen ions to form stronger hydrogen bonds with the negatively charged DNA of cancer cells.

• *Structure-activity relationship*

The structure-activity relationship analysis revealed that the parent cobalt complex of pyridine carboxaldehyde thiosemicarbazone exhibited moderate anti-proliferative activity, with a cell viability of 52.1%. Substitution of bromo and methoxy groups at the 6<sup>th</sup> position of the pyridine ring of thiosemicarbazone led to a decrease in proliferative action, with cell viabilities of 92.9% and 87.9%, respectively. Conversely, substitution of trifluoro group at the 6<sup>th</sup> position and chloro group at the 5<sup>th</sup> position of the pyridine ring of thiosemicarbazone remarkably increased proliferative activity, with cell viabilities of 20.93% and 23.46%, respectively, even surpassing the standard drug doxorubicin, which showed 59.85% cell viability.

## MATERIALS AND METHODOLOGY

The starting materials were purchased from Sigma-Aldrich and utilized directly without additional purification. Synthesis of the cobalt complexes was carried out using an ultrasonic probe, and their characterization was conducted using AFM, FTIR, and <sup>1</sup>H-NMR spectroscopy.

### *Synthesis of cobalt complexes of pyridine carboxaldehyde semicarbazone and thiosemicarbazone*

The precursor ligand solution was prepared by dissolving the pyridine semicarbazone and thiosemicarbazone [30] in an ethanol/water solution. Due to their low water solubility, they were initially dissolved in a small volume of ethanol and then the solution was made up with water to achieve a concentration of 0.001 molar. This solution was then added dropwise into a solution of cobalt chloride hexahydrate (CoCl<sub>2</sub>.6H<sub>2</sub>O) of the same concentration. The mixture was placed in a high-density ultrasonic probe with an operating frequency of 37 kHz and a force output of 320 W. After sonication for a full half hour, the products were precipitated out, filtered, washed with ethanol, allowed to air-dry, and finally stored in a closed container.

*CoRx-1Cl<sub>2</sub> (C<sub>7</sub>H<sub>8</sub>Cl<sub>2</sub>CoN<sub>4</sub>S)* Molecular weight = 310 g/mol; yellow color; yield = 74%; melting point = 270°C, FTIR (KBr, cm<sup>-1</sup>): 837 (C=S), 1581 (C=N), 3390 (NH); Elemental analysis (calculated): C = 27.03, H = 2.92, N = 18.01, S = 10.31, Co = 18.94, Cl = 22.79; <sup>1</sup>H-NMR 500 MHz, DMSO-*d*<sub>6</sub>; δ<sub>H</sub> = 7.369 (t, 1H), 7.821 (t, 1H), 8.082 (s, 1H), 8.180 (s, 1H), 8.272-8.286 (d, 1H), 8.557 (d, 1H), 11.642 (s, 1H).

*CoRx-3Cl<sub>2</sub> (C<sub>14</sub>H<sub>14</sub>Br<sub>2</sub>Cl<sub>2</sub>CoN<sub>8</sub>S<sub>2</sub>)* Molecular weight = 650 g/mol; brown color; yield = 63%; Melting point = 255°C; FTIR (KBr, cm<sup>-1</sup>): 793 (C=S), 1451 (C=N), 3344 (NH); Elemental analysis (calculated): C = 25.86, H = 2.48, Br = 24.58, N = 17.24, S = 9.86, Co = 9.07, Cl = 10.91; <sup>1</sup>H-NMR 500 MHz, DMSO-*d*<sub>6</sub>; δ<sub>H</sub> = 7.6150-7.6279 (d, 2H), 7.767-7.792 (t, 2H), 7.976 (s, 1H), 8.263 (s, 2H), 8.325-8.338 (d, 2H), 11.741 (s, 1H).

*CoRx-4Cl<sub>2</sub> (C<sub>8</sub>H<sub>11</sub>Cl<sub>2</sub>CoN<sub>4</sub>OS)* Molecular weight = 341 g/mol; peach color; Yield = 54%; Melting point = 280°C, FTIR (KBr, cm<sup>-1</sup>): 799 (C=S), 1612 (C=N), 3371 (NH); Elemental analysis (calculated): C = 28.17, H = 3.25, N = 16.43, O = 4.69, S = 9.40, Co = 17.28, Cl = 20.79; <sup>1</sup>H-NMR 500 MHz, DMSO-*d*<sub>6</sub>; δ<sub>H</sub> = 4.009 (s, 3H), 7.012-7.025 (d, 1H), 7.357-7.376 (d, 1H), 7.944-7.971 (t, 1H), 8.2032 (s, 1H), 8.587 (s, 1H), 13.84 (s, 1H).

*CoRx-5Cl<sub>2</sub> (C<sub>8</sub>H<sub>8</sub>Cl<sub>2</sub>CoF<sub>3</sub>N<sub>4</sub>S)* Molecular weight = 379 g/mol; light pink; Yield = 60%; melting point = 263°C, FTIR (KBr, cm<sup>-1</sup>): 818 (C=S), 1595 (C=N), 3426 (NH); Elemental analysis (calculated): C = 25.35, H = 2.13, F = 15.04, N = 14.78, S = 8.46, Co = 15.55, Cl = 18.70; <sup>1</sup>H-NMR 500 MHz, DMSO-*d*<sub>6</sub>; δ<sub>H</sub> = 7.868-7.881 (d, 1H), 8.084-8.130 (q, 2H), 8.348 (s, 1H), 8.488 (s, 1H), 11.817 (s, 1H).

*CoRx-6Cl<sub>2</sub> (C<sub>14</sub>H<sub>16</sub>Cl<sub>4</sub>CoN<sub>8</sub>S<sub>2</sub>)* Molecular weight = 561 g/mol; brown color; Yield = 82%; melting point = 230°C, FTIR (KBr, cm<sup>-1</sup>): 828 (C=S), 1444 (C=N); Elemental analysis (calculated): C = 29.96, H = 2.87, N = 19.97, S = 11.43, Co = 10.50, Cl = 25.27; <sup>1</sup>H-NMR 500 MHz, DMSO-*d*<sub>6</sub>; δ<sub>H</sub> = 7.980 (d, 2H), 8.068 (s, 2H), 8.272 (s, 2H), 8.350-8.397 (d, 2H), 8.610 (s, 2H), 11.693 (s, 1H).

*CoRx-8Cl<sub>2</sub> (C<sub>8</sub>H<sub>10</sub>Cl<sub>2</sub>CoN<sub>4</sub>O)* Molecular weight = 308 g/mol; dirty white; Yield = 73%; melting point = 310°C, FTIR (KBr, cm<sup>-1</sup>): 1542 (C=N), 1662 (C=O); Elemental analysis (calculated): C = 31.19, H = 3.27, N = 18.19, O = 5.19, Co = 19.13, Cl = 23.02; <sup>1</sup>H-NMR 500 MHz, DMSO-*d*<sub>6</sub>; δ<sub>H</sub> = 2.452 (s, 3H), 6.596 (s, 1H), 7.173-7.186 (d, 1H), 7.661-7.687 (t, 1H), 7.825 (s, 1H), 7.934-7.947 (d, 1H), 10.475 (s, 1H).

*CoRx-9Cl<sub>2</sub> (C<sub>7</sub>H<sub>7</sub>BrCl<sub>2</sub>CoN<sub>4</sub>O)* Molecular weight = 372 g/mol; light pink; Yield = 64%; melting point = 240°C, FTIR (KBr, cm<sup>-1</sup>): 1540 (C=N), 1695 (C=O); Elemental analysis (calculated): C = 22.55, H = 1.89, Br = 21.43, N = 15.02, O = 4.29, Co = 15.80, Cl = 19.01; <sup>1</sup>H-NMR 500 MHz, DMSO-*d*<sub>6</sub>; δ<sub>H</sub> = 6.705 (s, 1H), 7.572 (d, 1H), 7.752-7.778 (q, 2H), 8.202 (s, 1H), 10.641 (s, 1H).

*CoRx-11Cl<sub>2</sub> (C<sub>8</sub>H<sub>7</sub>Cl<sub>2</sub>CoF<sub>3</sub>N<sub>4</sub>O)* Molecular weight = 360 g/mol; peach color; Yield = 69%; melting point = 240°C, FTIR (KBr, cm<sup>-1</sup>): 1584 (C=N), 1714 (C=O); Elemental analysis

(calculated): C= 26.54, H= 1.95, F= 15.74, N= 15.48, O= 4.42, Co=16.28, Cl= 19.59,; <sup>1</sup>H-NMR 500 MHz, DMSO-*d*<sub>6</sub>;  $\delta_H$  = 6.771 (s,1H),7.82 (d,1H), 7.90 (s,1H), 8.09(t,1H), 8.497 (d,1H), 10.726 (s,1H).

CoRx-12Cl<sub>2</sub> (C<sub>7</sub>H<sub>7</sub>Cl<sub>3</sub>CoN<sub>4</sub>O) Molecular weight = 328 g/mol; off white; Yield = 71%, melting point= 320°C, FTIR (KBr, cm<sup>-1</sup>): 1586 (C=N), 1698 (C=O); Elemental analysis (calculated): C= 25.60, H= 2.15, N= 17.06, O= 4.87, Co= 17.94, Cl= 32.38; <sup>1</sup>H-NMR 500 MHz, DMSO-*d*<sub>6</sub>;  $\delta_H$  = 6.690 (s,1H), 7.860 (s, 1H), 7.941 (d, 1H), 8.224 (d,1H), 8.573 (s, 1H), 10.570 (s,1H).

#### Cholinesterase inhibition assay

Ellman's method [37] was employed to assess the inhibitory potential of AChE (acetylcholinesterase) with EC Number: 3.1.1.7 and BuChE (butyrylcholinesterase) with EC Number: 3.1.1.8, with minor modifications. For the assay, 10  $\mu$ L of the test molecule (1 mM, 10% DMSO), 50 mM phosphate buffer (KH<sub>2</sub>PO<sub>4</sub>) at pH 7.8, and 10  $\mu$ L of the enzymes (0.029 and 0.5 U/mL of AChE or BuChE, respectively) were combined and incubated for 10 minutes at 37°C. Following this, 10  $\mu$ L of 1 mM acetylthiocholine iodide or butyrylthiocholine chloride and 10  $\mu$ L of 5,5-dithiobis-2-nitrobenzoic acid reagent (5 mM) were added to each individual enzyme solution. Enzymatic reactions were measured using a microplate reader (FLUOstar Omega, BMG Labtech, Germany) at 405 nm following a 30-minute incubation period at 37°C. The IC<sub>50</sub> values of compounds showing more than 50% inhibition in three replicates were calculated by further diluting the compound into eight different concentrations.

#### • Docking study

The most potent inhibitors among the tested compounds underwent molecular docking investigations using Molecular Operating Environment software (MOE version 2019, Chemical Computing Group, Montreal, QC, Canada). Prior to docking, the Chem 3D v20.0 software was utilized to minimize the energy of the drawn structure. The Force-Field-based parameterization and energy minimization was done by using the MMFF94x force field. Crystal structures of AChE (PDB ID; 4EY4) and BuChE (PDB ID; 1P0I) were downloaded from the RSCB database (<https://www.rcsb.org/>).

The default parameters (T: 300, pH:7, Salt: 0.1, Dielectric: 2, Cutoff(A) 15, solvent: 89 van der Waals; 800r3, Electrostatic; GB/VI) for docking in the MOE software were applied to the crystal structures. Active amino acid residues were selected using the site finder tool for active site identification

after removal of the standard ligand and co-factor from the active pocket. Rapid preparation of the crystal structure was then completed. Docking was performed with default parameters, and the top 20 poses were selected for further analysis.

#### • Kinetic study

To elucidate the mechanism of inhibition for AChE and BuChE, the most potent inhibitor was utilized in enzyme kinetic investigations. The experiment involved testing various concentrations of the test chemicals (0.19  $\mu$ M, 0.36  $\mu$ M, 0.79  $\mu$ M, 1.58  $\mu$ M, 3.16  $\mu$ M in DMSO), along with different amounts of the substrate, namely Donepezil (0 mM, 5 mM, 10 mM, 15 mM, and 20 mM).

#### Anti-proliferative activity

The synthetic compounds' antiproliferative activity was assessed using HEK-293 and U-87 cells, with doxorubicin serving as a positive control. These cells were seeded in 96-well plates at a density of approximately 10,000 cells per well and incubated for 24 hours to achieve a uniform single layer of cells. Subsequently, the cell lines were treated in triplicate with the tested drugs at various doses (i.e., 1, 2.5, 5, 10, 15, 20, and 25  $\mu$ M in DMSO) and incubated under a flow of carbon dioxide for 48 hours at 37°C.

Following the incubation period, the cells were treated with 30  $\mu$ L of MTT solution (5 mg/ml) and incubated for additional 4 hours at 37°C. The absorbance of the MTT formazan formed was quantified using an ELISA plate reader set to 540 nm.

$$\% \text{ Cell viability} = \frac{(A \text{ sample} - A \text{ blank})}{(A \text{ control} - A \text{ blank})} \times 100$$

#### CONCLUSION

In conclusion, given the absence of a cure for Alzheimer's disease (AD), cholinesterase inhibitors like Donepezil have been employed to delay its progression. Currently, second-generation cholinesterase inhibitors such as rivastigmine and galantamine are utilized in AD treatment. The objective of this research is to identify novel inhibitors to further advance AD treatment by leveraging the intriguing properties of transition metal complexes. To assess their potential as multi-targeting medications, acetylcholinesterase (AChE), butyrylcholinesterase (BuChE), and proliferative *in-vitro* assays were employed to evaluate each compound. Analysis of the structure-activity relationships revealed that variations in activities were attributable to the various substituent patterns at different positions on the pyridine ring. Among the compounds tested, CoRx-6Cl<sub>2</sub> was identified as

the most potent AChE inhibitor and also demonstrated moderate anti-proliferative activity by inhibiting the U-87 cell line. This suggests its potential as a promising candidate for further investigation as a therapeutic agent for AD and potentially other related conditions.

**Conflict of interest:** Authors declare no conflict of interest.

**Acknowledgement:** Asia Naz Awan designed the study, Ayesha Naseer performed the synthesis and characterization study of the synthesized compounds, writeup the first draft of the manuscript, Sabahat Habib helped out to carry out proliferative assay, Jamsheed Iqbal and Aneela Javed reviewed the final manuscript.

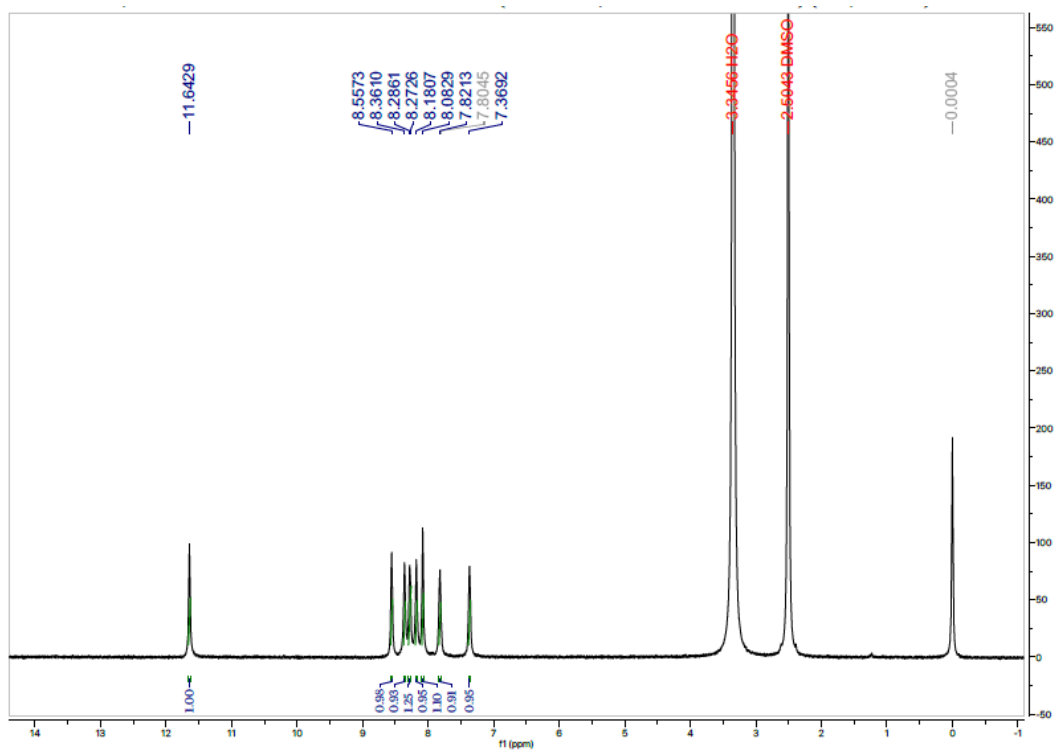
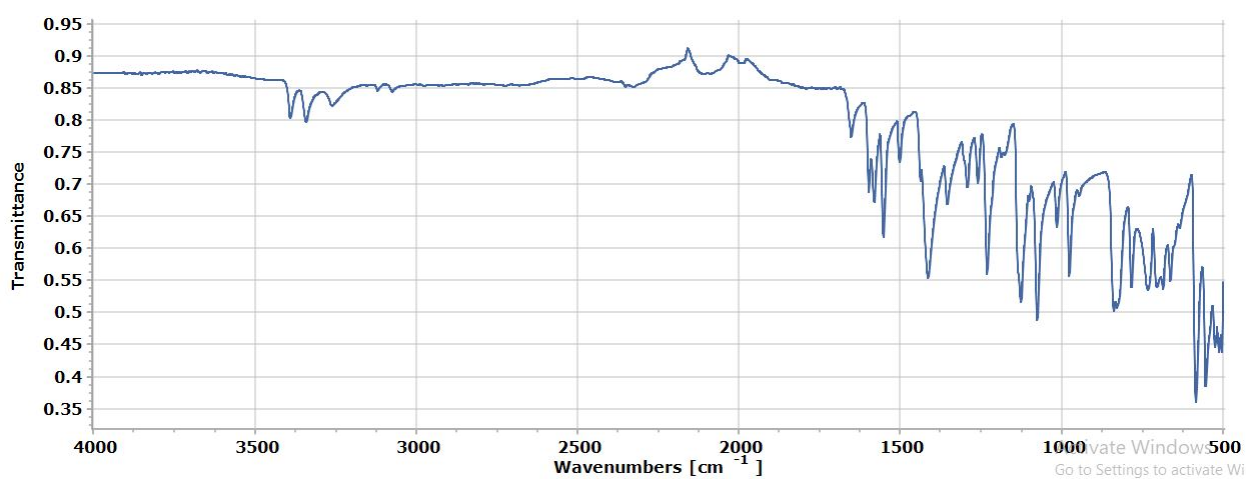
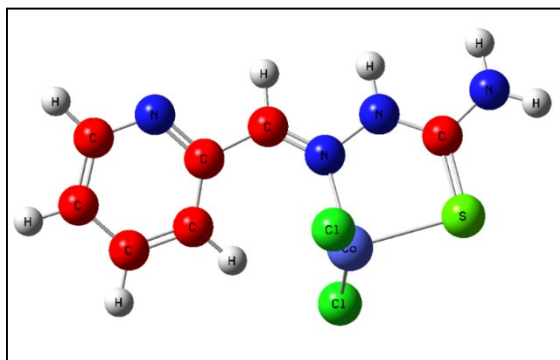
**Supportive/supplementary material:** The AFM images, FTIR, <sup>1</sup>H-NMR, structures are presented in the supplementary file.

#### REFERENCES

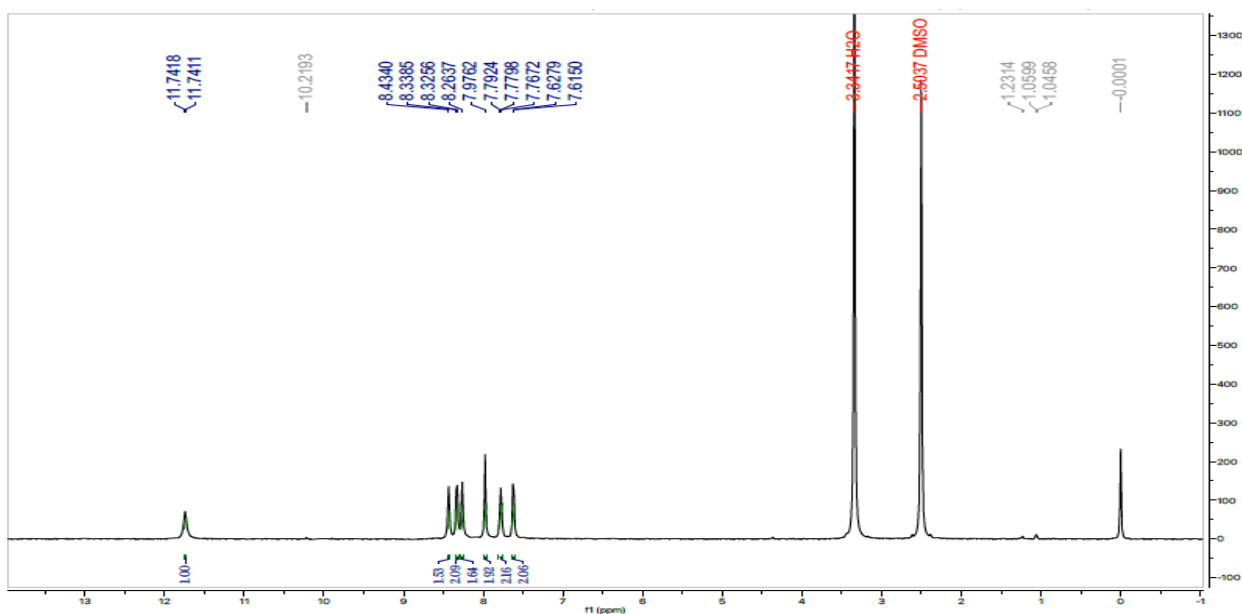
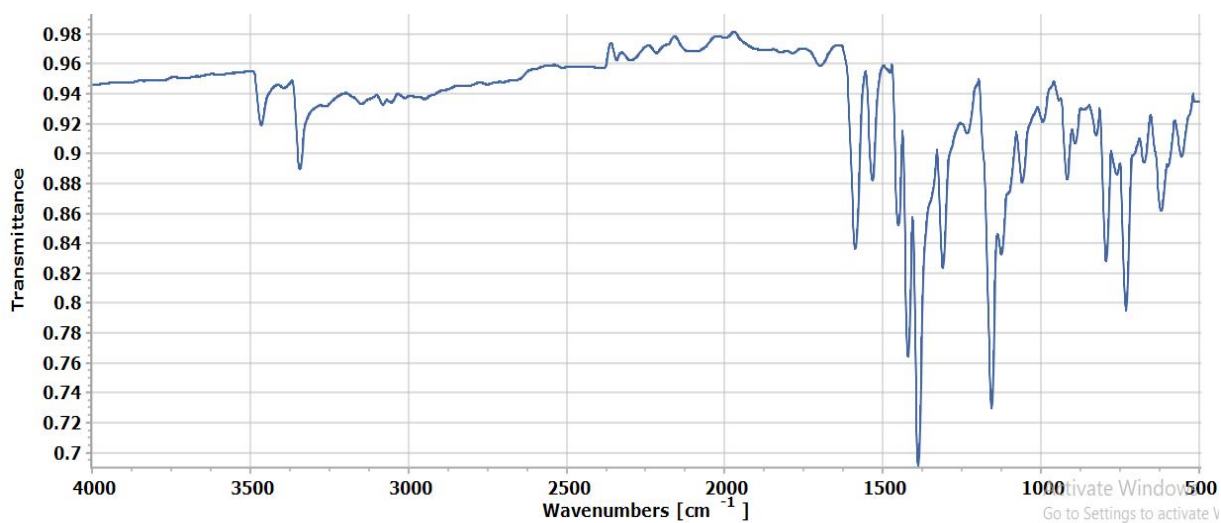
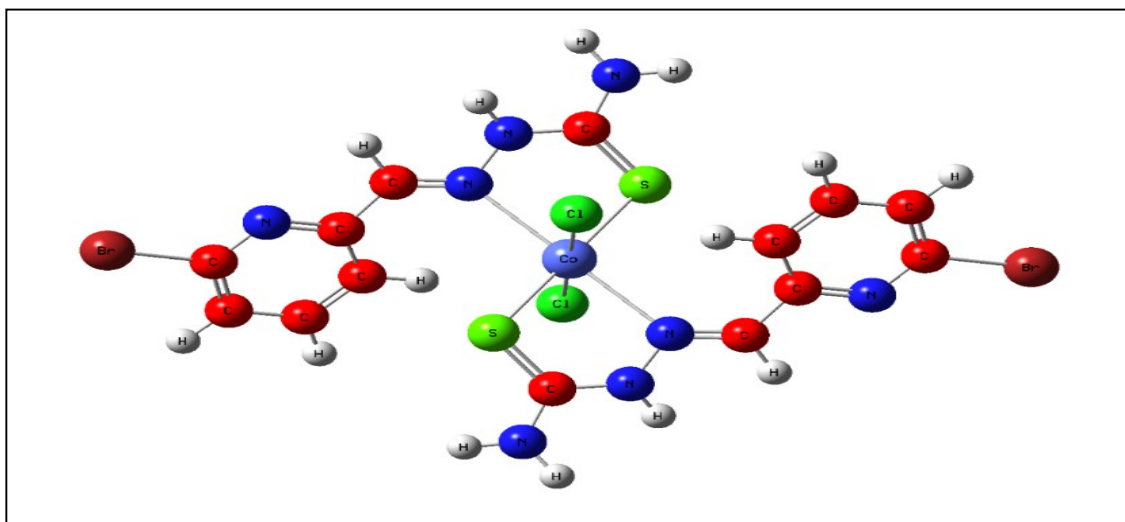
1. D. Small, Z. Ismael, I. J. N. Chubb, *Neuroscience*, **19**(1), 289 (1986).
2. K. J. M. Sharma, *Molecular Medicine Report*, **20**(2), 1479 (2019).
3. L. Jaganathan, R. J. B. Boopathy, *BMC Biochemistry*, **1**(1), 1 (2000).
4. J. A. Driver, A. Beiser, R. Au, B. E. Kreger, G. L. Splansky, T. Kurth, D. P. Kiel, K. P. Lu, S. Seshadri, P. A. J. B. Wolf, *BMJ*, **344**, (2012).
5. F. Catalá-López, B. Crespo-Facorro, E. Vieta, J. M. Valderas, A. Valencia, R. J. N. Tabarés-Seisdedos, *Neuroepidemiology*, **42**(2), 121, (2014).
6. H. Hussain, S. Ahmad, S. W. A. Shah, M. Ghias, A. Ullah, S. U. Rahman, Z. Kamal, F. A. Khan, N. M. Khan, J. J. M. Muhammad, *Molecules*, **26**(23), 7168 (2021)..
7. H. Hussain, S. Ahmad, S. W. A. Shah, A. Ullah, N. Ali, M. Almeahadi, M. Ahmad, A. A. K. Khalil, S. B. Jamal, H.J.M. Ahmad, *Molecules*, **27**(8), 2468 (2022)..
8. K. Papat, K. McQueen, T. W. Feeley, *Best Practice & Research Clinical Anaesthesiology*, **27**(4), 399 (2013)..
9. J. B. J. S. Gibbs, *Science*, **287**(5460), 1969 (2000).
10. H. J. S. Varmus, *Science*, **312**(5777), 1162 (2006).
11. M. Khudhayer Oglah, Y. J. M. C. R. Fakri Mustafa, *Medicinal Chemistry Research*, **29**(3), 479, (2020).
12. H. J. Xi, R. P. Wu, J. J. Liu, L. J. Zhang, Z. S. J. T. C. Li, *Thoracic Cancer*, **6**(4), 390 (2015).
13. O. I. Okereke, M. E. Jno Meadows, *Jama Network Open*, **2**(6), e196167 (2019).
14. J. Jończyk, J. Godyń, E. Stawarska, B. Morak-Młodawska, M. Jeleń, K. Pluta, B. J. M. Malawska, *Molecules*, **25**(11), 2604 (2020).
15. A. Daina, O. Michielin, V. J. S. Zoete, *Scientific Reports*, **7**(1), 1 (2017).
16. G. G. Mohamed, B. *Spectrochim. Acta A: Molecular and Biomolecular Spectroscopy*, **64**(1), 188 (2006).
17. M. T. H. Tarafder, M. A. Ali, N. Saravanan, W. Y. Weng, S. Kumar, N. Umar-Tsafe, K. A. Crouse, *Transition Metal Chemistry*, **25**(3), 295 (2000)..
18. H. Wilfredo, P. J. J. C. S. Juan, *Journal of Chemical Science*, **14**, 10 (2006)..
19. T. R. Todorović, J. Vukašinović, G. Portalone, S. Suleiman, N. Gligorijević, S. Bjelogrić, K. Jovanović, S. Radulović, K. Anđelković, A. J. M. Cassar, *MedChemComm*, **8**(1), 103 (2017)..
20. S. M. Dawoud, *Journal of Physics: Conference Series*, IOP Publishing, 022059 (2021).
21. H. Beraldo, D. J. M. Gambino, *Mini-Reviews in Medicinal Chemistry*, **4**(1), 31 (2004).
22. D. C. Quenelle, K. A. Keith, E.R. Kern, *Antiviral Research*, **71**(1), 24 (2006).
23. S. A. Andres, K. Bajaj, N. S. Vishnosky, M. A. Peterson, M. S. Mashuta, R. M. Buchanan, P. J. Bates, C. A. Grapperhaus, *Inorganic Chemistry*, **59**(7), 4924 (2020).
24. D. C. Reis, A. A. R. Despaigne, J. G. D. Silva, N. F. Silva, C. F. Vilela, I. C. Mendes, J. A. Takahashi, H. J. M. Beraldo, *Molecules*, **18**(10), 12645 (2013).
25. M. Mackenzie, D. Saltman, H. Hirte, J. Low, C. Johnson, G. Pond, M. J. Moore, *Investigational New Drugs*, **25**(6), 553 (2007).
26. A. A. Aly, E. M. Abdallah, S. A. Ahmed, M. M. Rabee, E.-S. Abdelhafez, *Journal of Molecular Structure*, 133480, (2022).
27. B. M. Zeglis, V. Divilov, J. S. Lewis, *Journal of Medicinal Chemistry*, **54**(7), 2391 (2011)..
28. D. Osmaniye, B. Kurban, B. N. Sağlık, S. Levent, Y. Özkay, Z. A. Kaplançıklı, *Molecules*, **26**(21), 6640 (2021).
29. R. Jawaria, M. Hussain, H. B. Ahmad, M. Ashraf, S. Hussain, M. M. Naseer, M. Khalid, M. A. Hussain, M. Al-Rashida, M.N. Tahir, *Inorg. Chim. Acta*, **508**, 119658 (2020).
30. M. S. Ağırtaş, *Heterocyclic Communications*, **23**(1), 7 (2017).
31. I. Ali, Haque, A. Wani, W. A. Saleem, K. Al Za'abi, M., *Biomedical Chromatography*, **27**(10), 1296 (2013).
32. I. Ali, W. A. Wani, K. Saleem, M. F. Hsieh, *RSC Advances*, **4**(56), 29629 (2014).
33. A. Naseer, F. A. Odra, A. N. Awan, A. Imran, A. Hameed, S. A. Ali Shah, *et al. Pharmaceuticals*, **15**(10), 1288(2022).
34. J. L. Sussman, M. Harel, F. Frolow, C. Oefner, A. Goldman, L. Toker, I. Silman, *Science*, **253**(5022), 872 (1991).
35. A. Štalić, Z. Grubić, M. Šentjuric, S. Pečar, M. K. Gentry, B. P. Doctor, *Enzymes of the Cholinesterase Family*, **125** (1995).
36. N. A. Khan, I. Khan, S. Abid, S. Zaib, A. Ibrar, H. Andleeb, *et al., Medicinal Chemistry*, **14**(1), 74 (2018).
37. A. Komersova, K. Komers, A. Čegan, *Zeitschrift für Naturforschung C*, **62**(1-2), 150, (2007).

## Supplementary data

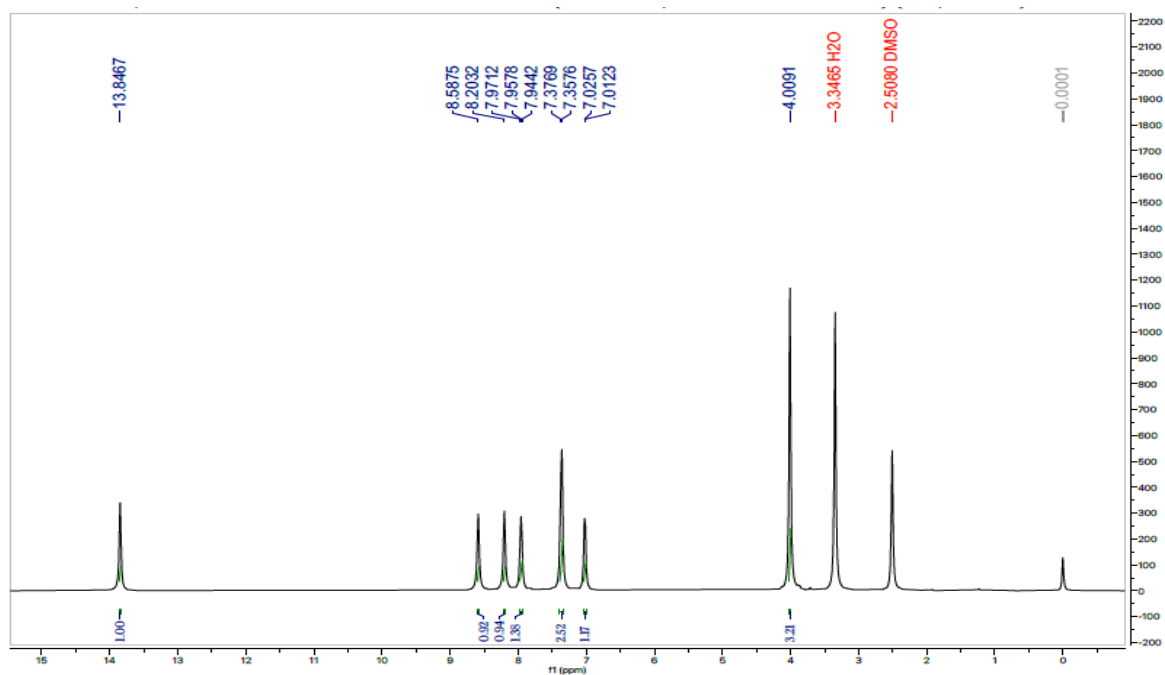
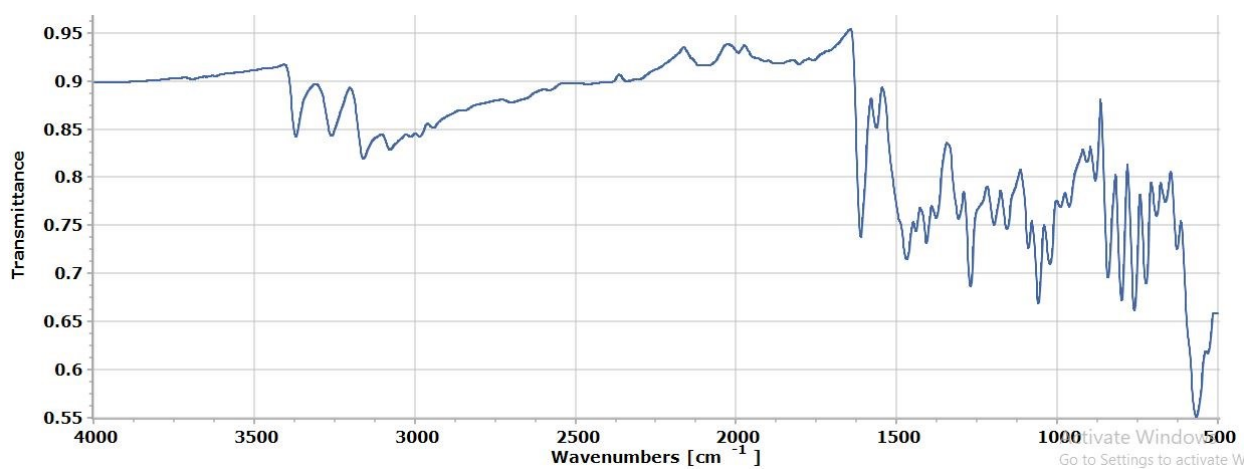
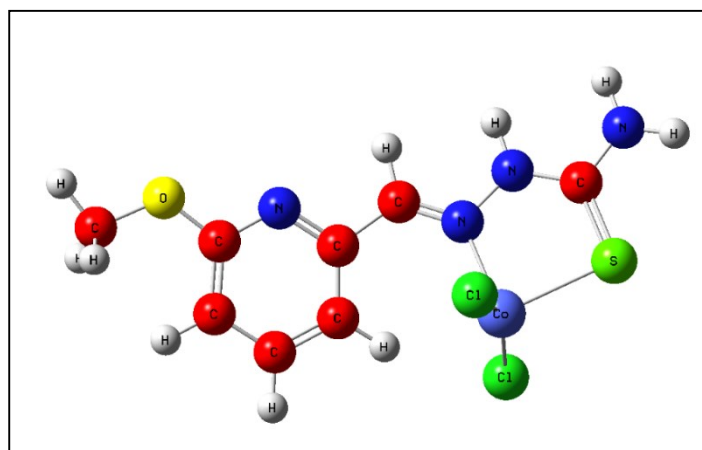
### CoRx-1-Cl<sub>2</sub>



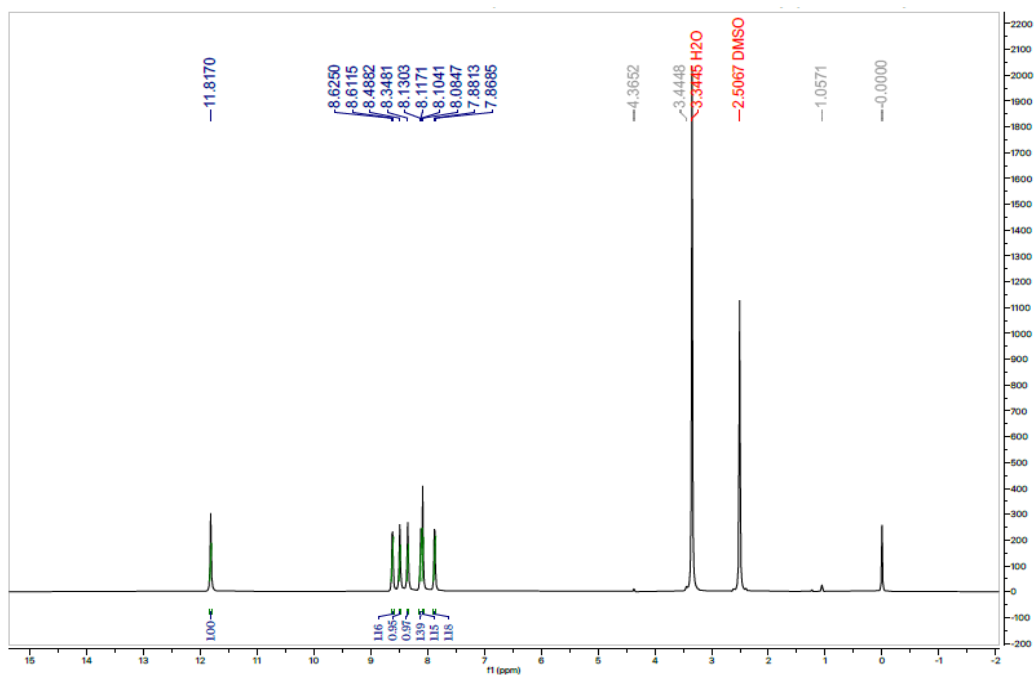
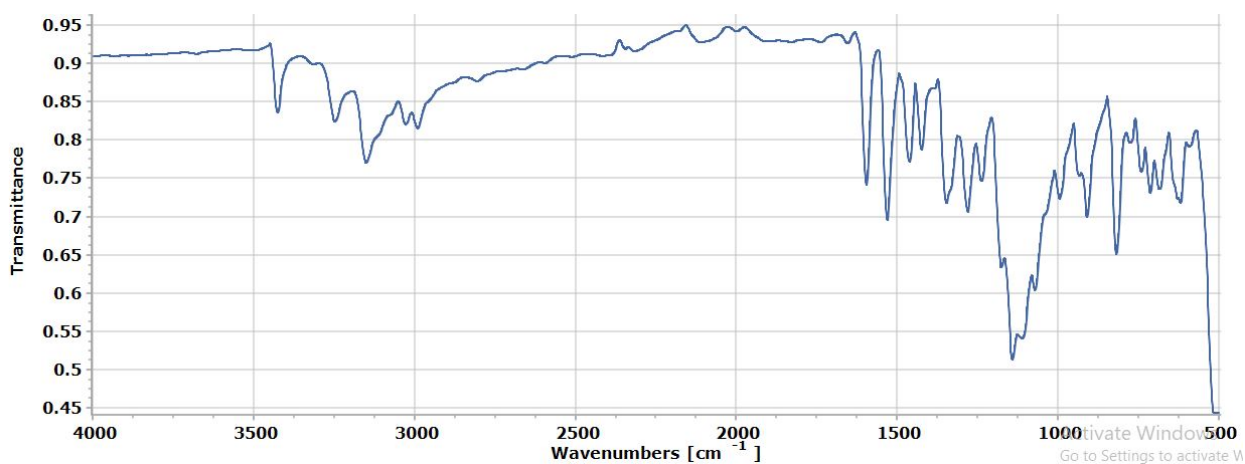
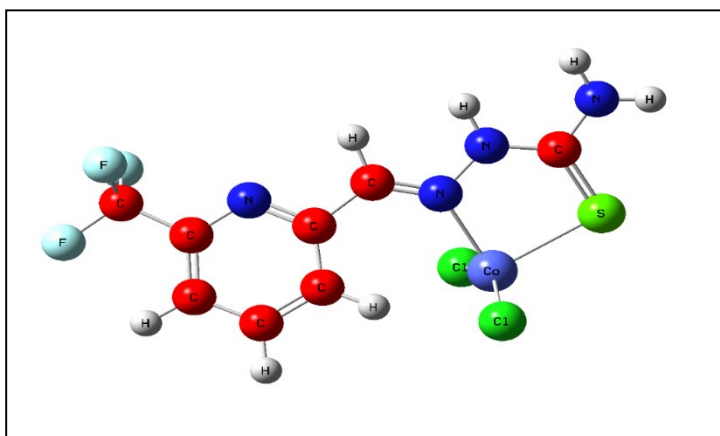
CoRx-3-Cl<sub>2</sub>



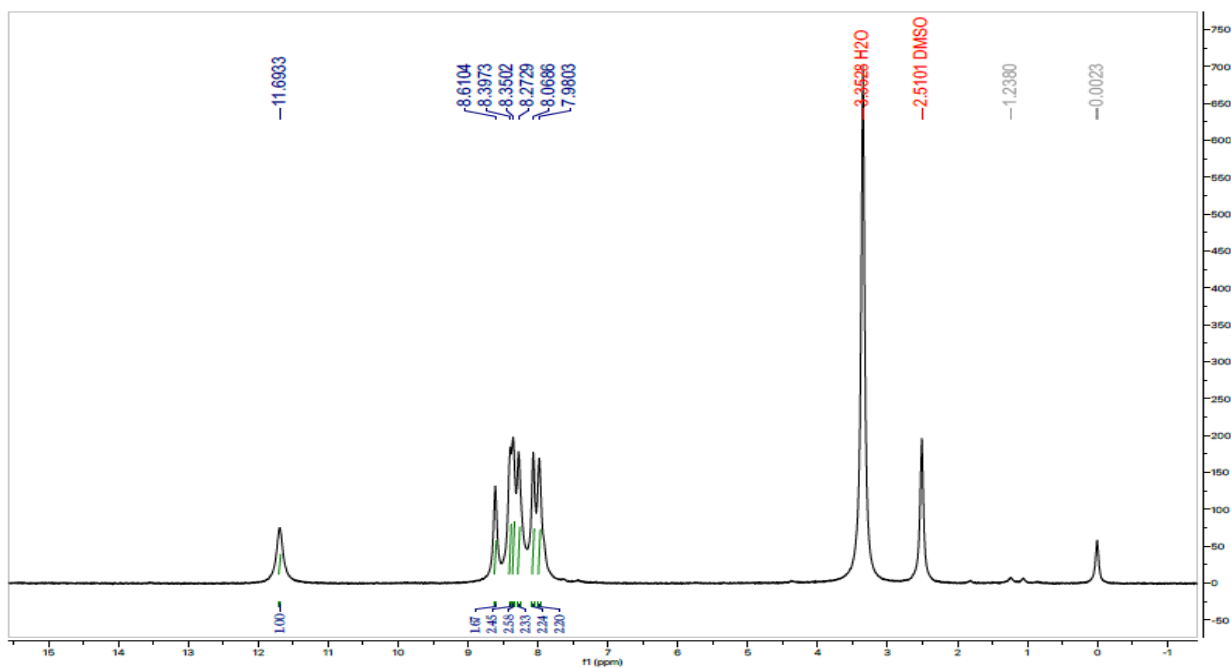
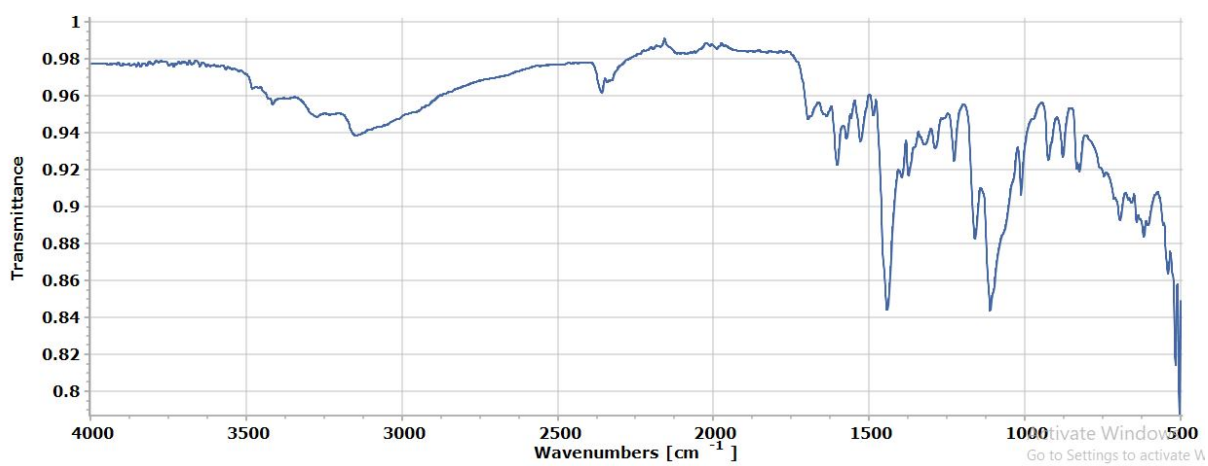
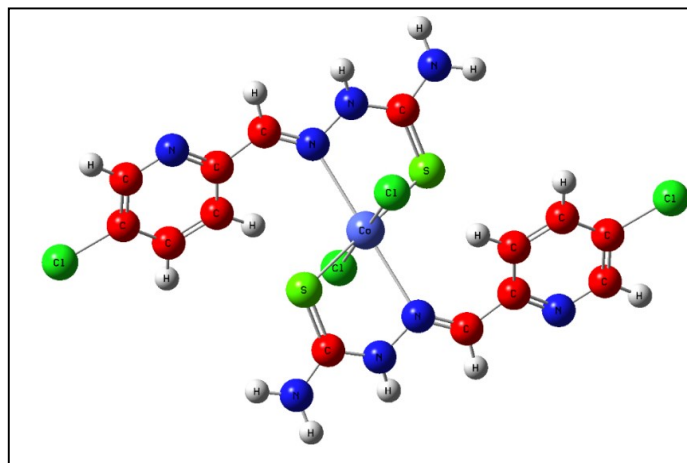
### CoRx-4-Cl<sub>2</sub>



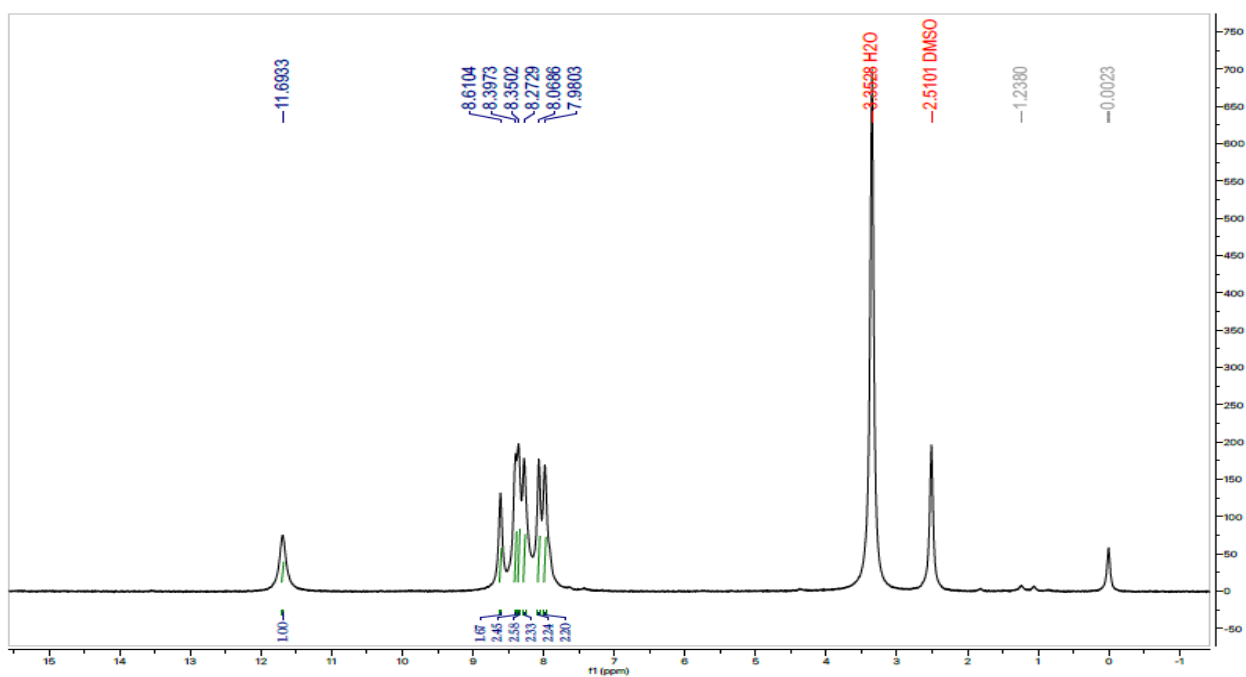
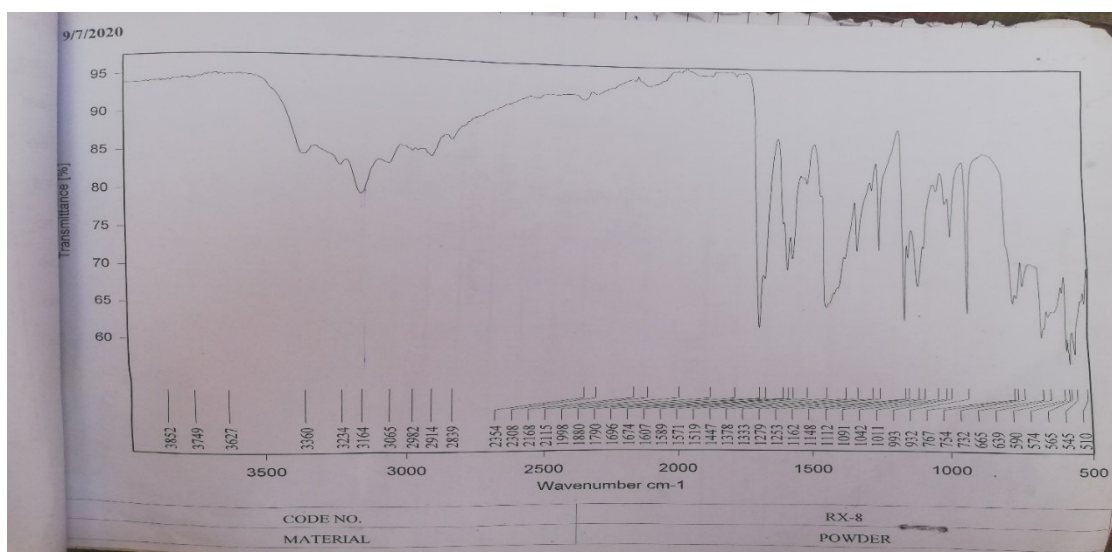
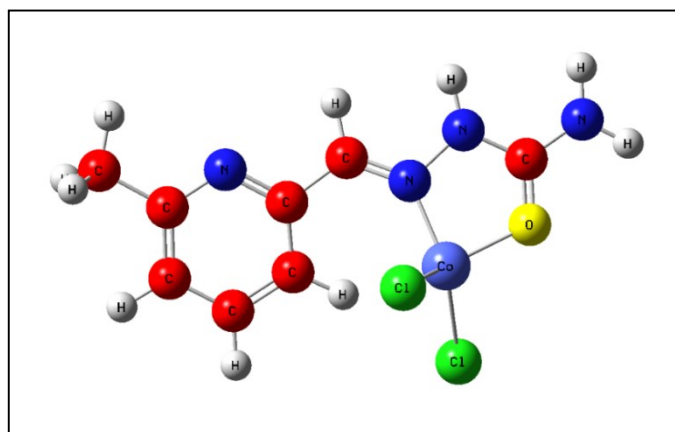
CoRx-5-Cl<sub>2</sub>



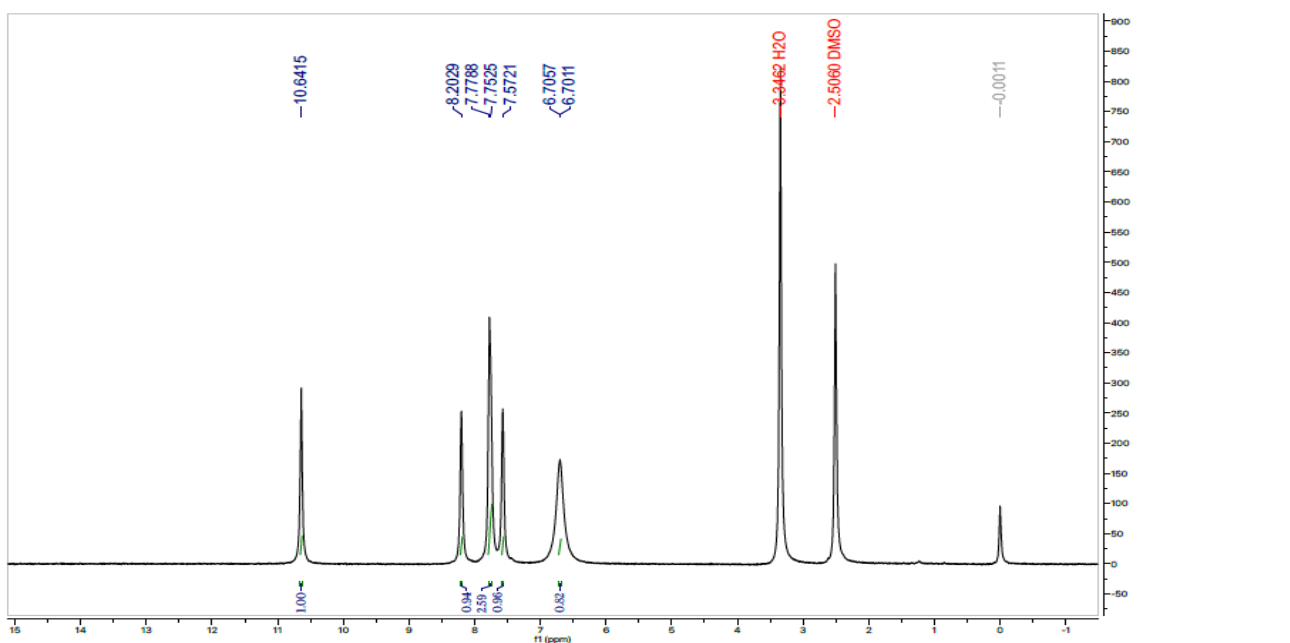
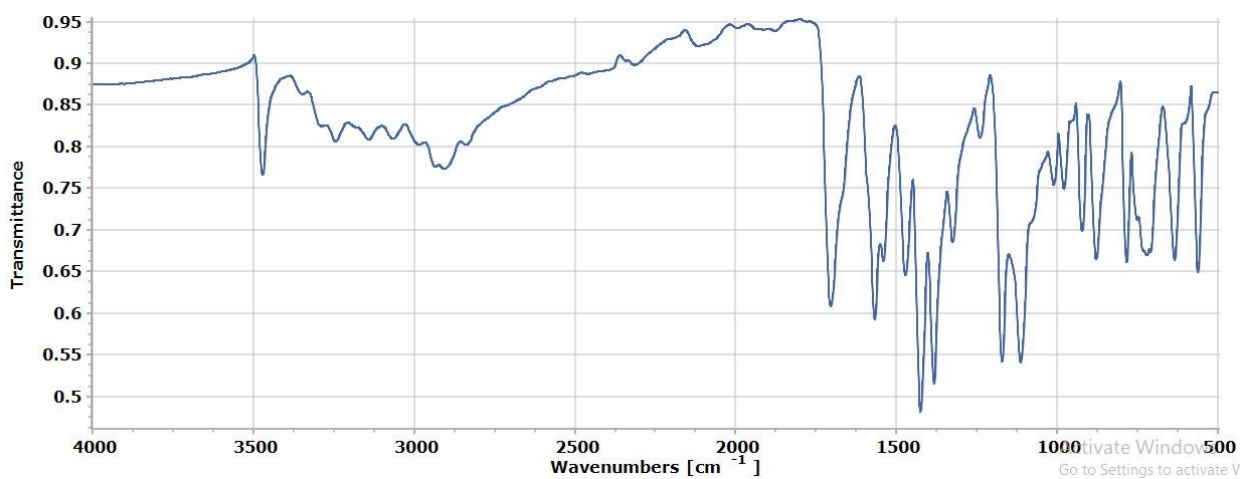
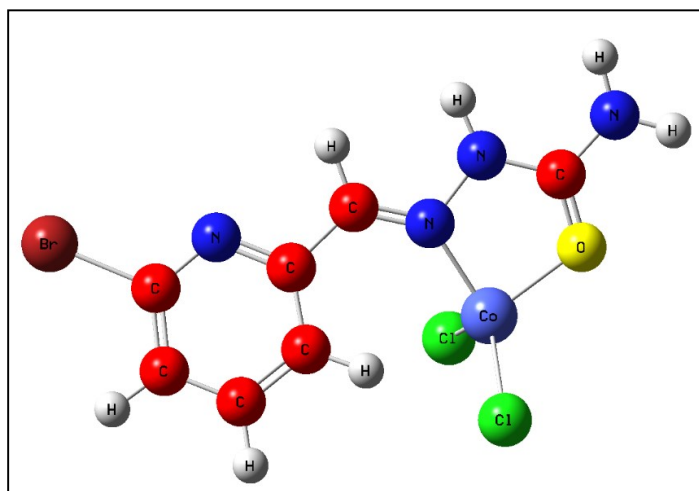
### CoRx-6-Cl<sub>2</sub>



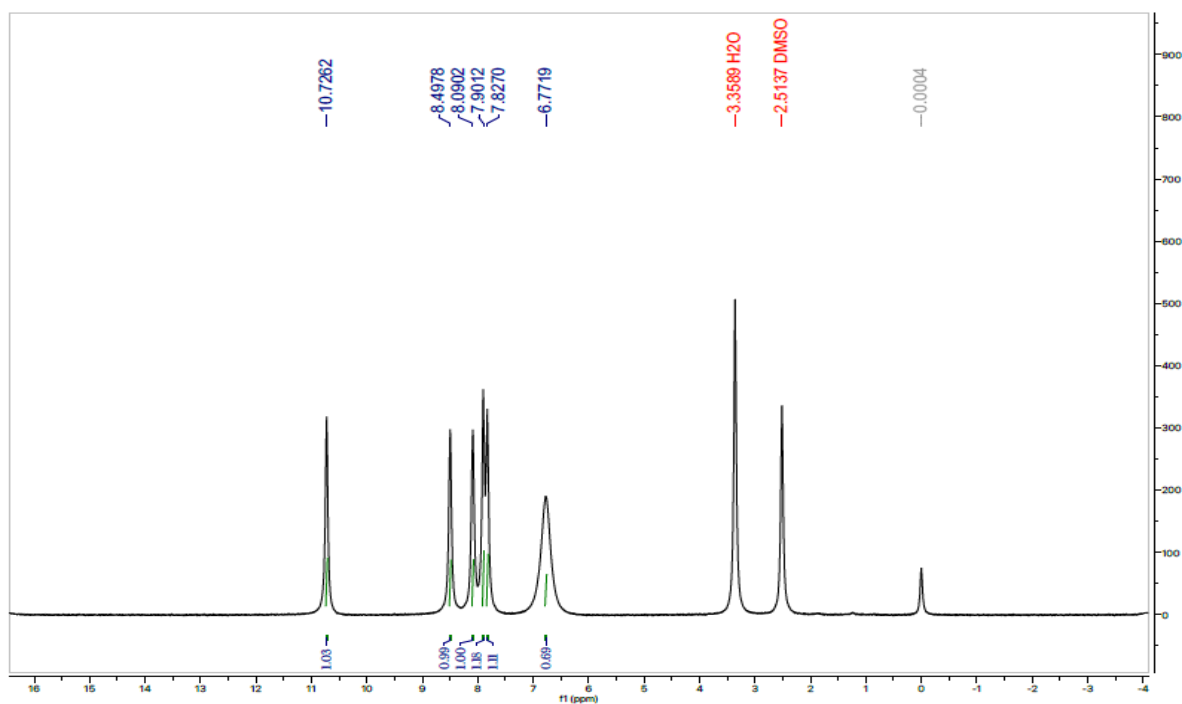
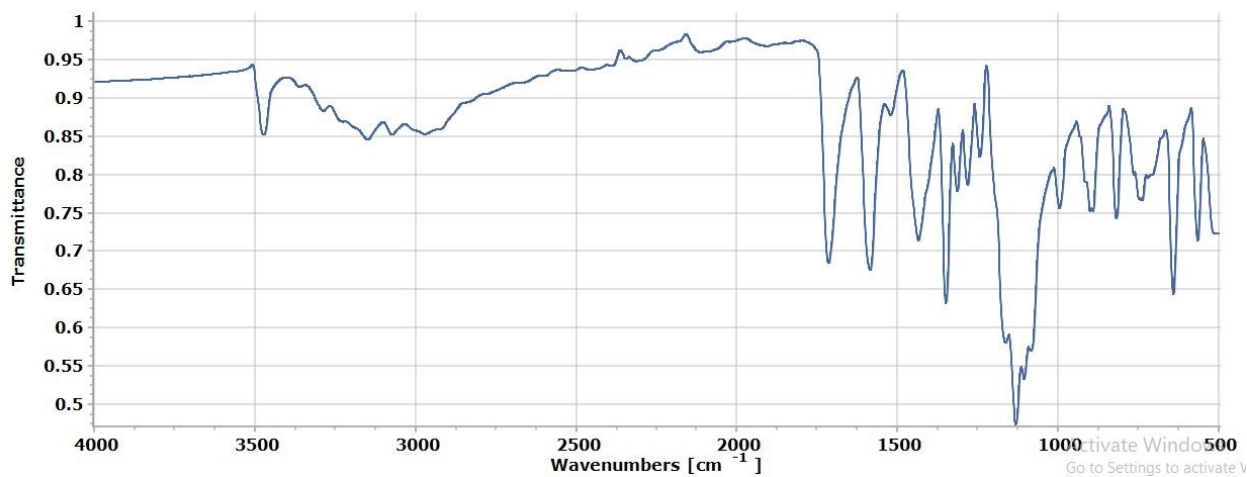
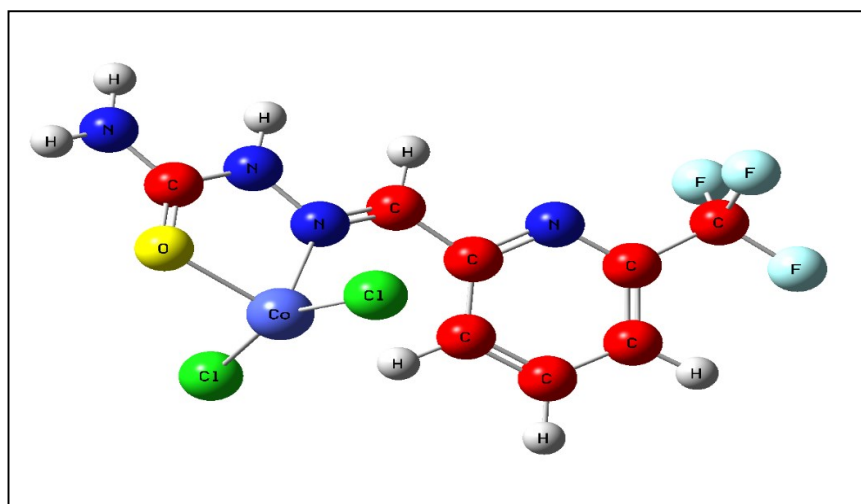
**CoRx-8-Cl<sub>2</sub>**



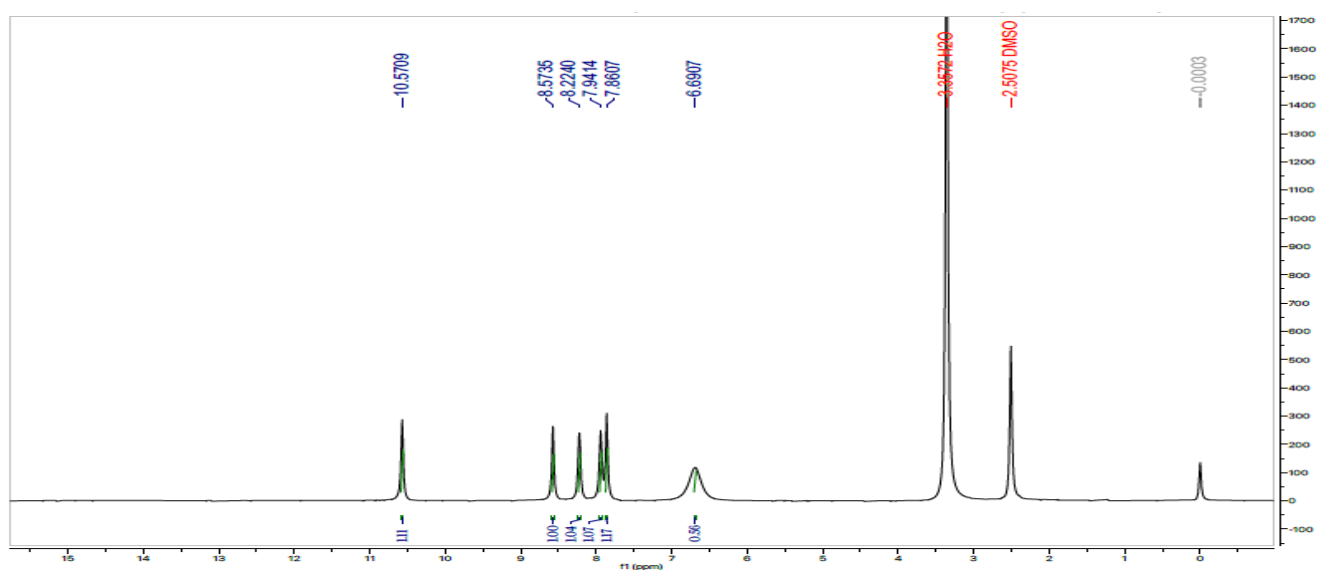
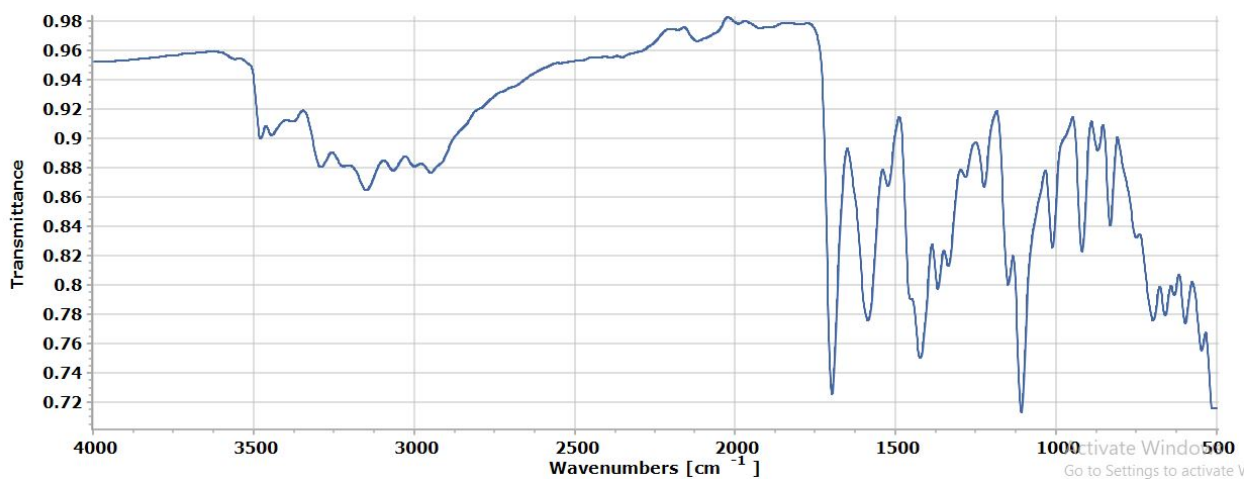
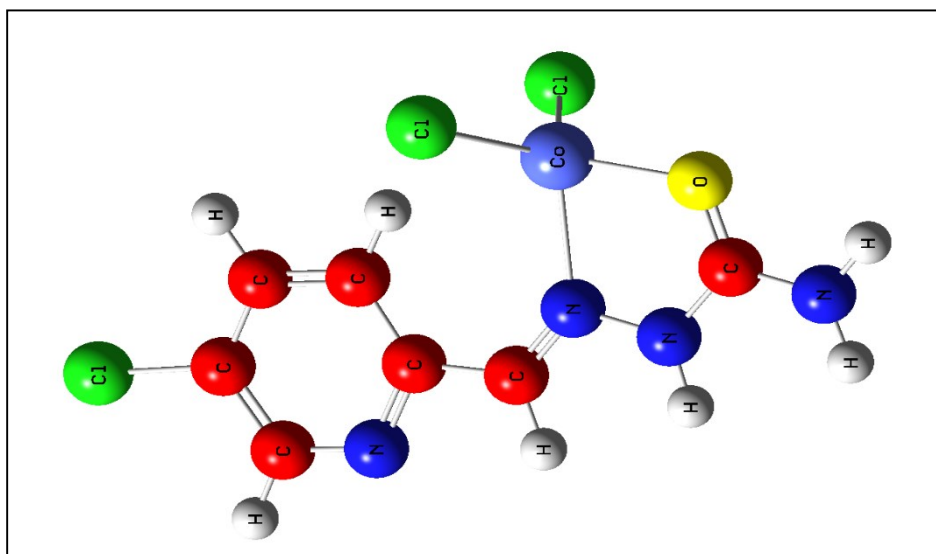
### CoRx-9-Cl<sub>2</sub>



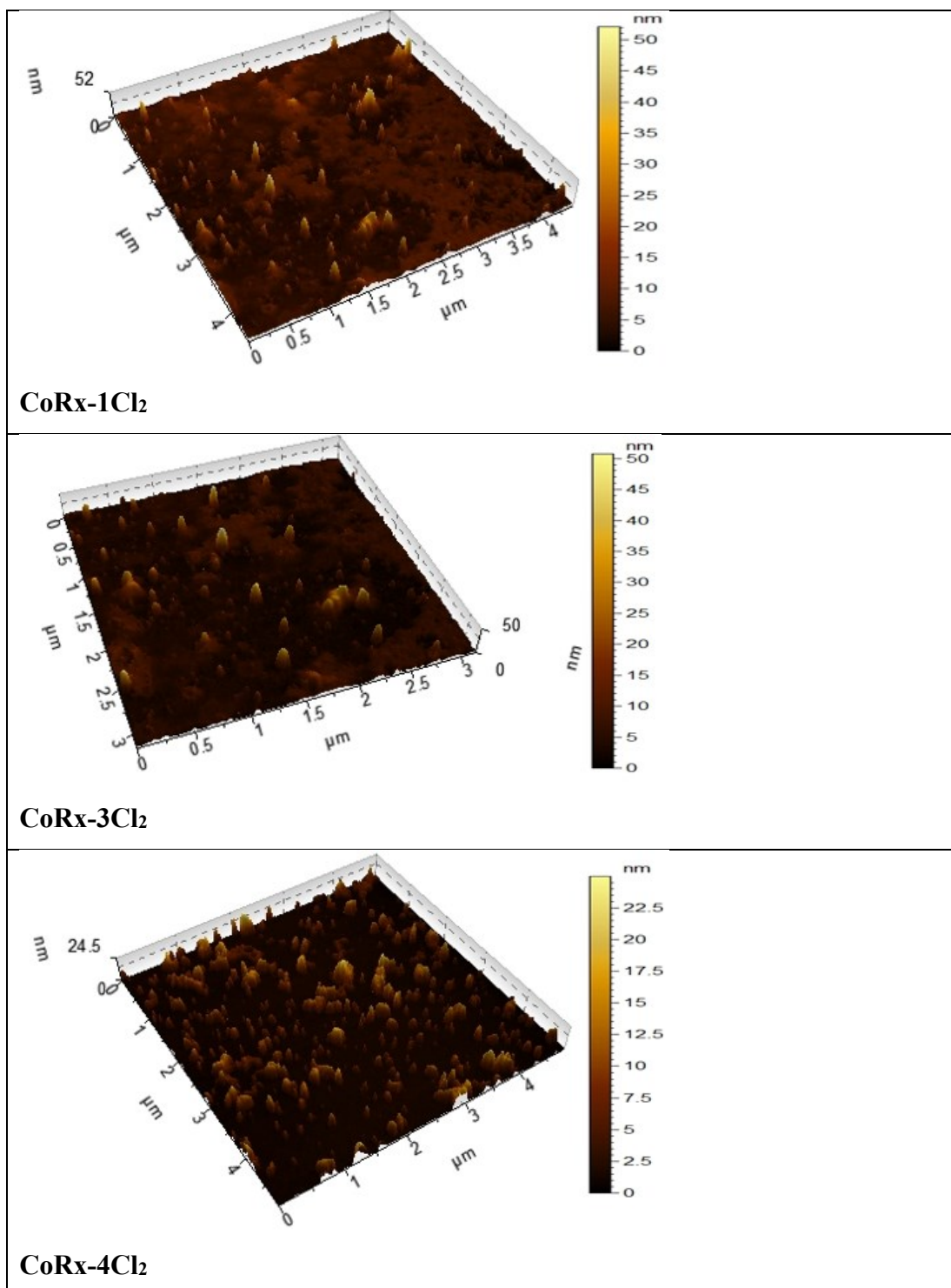
### CoRx-11-Cl<sub>2</sub>

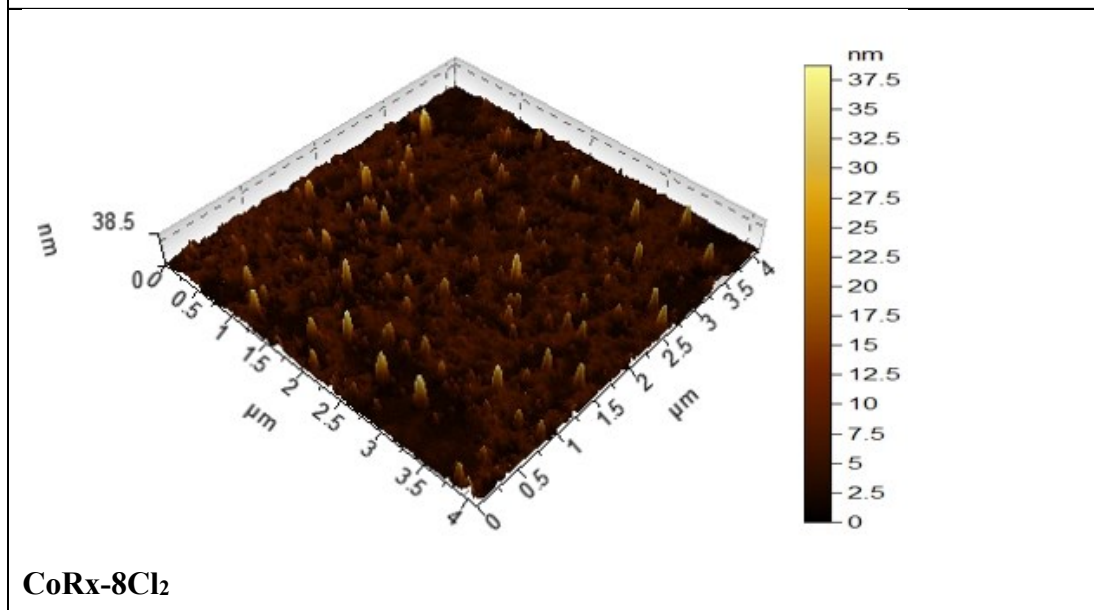
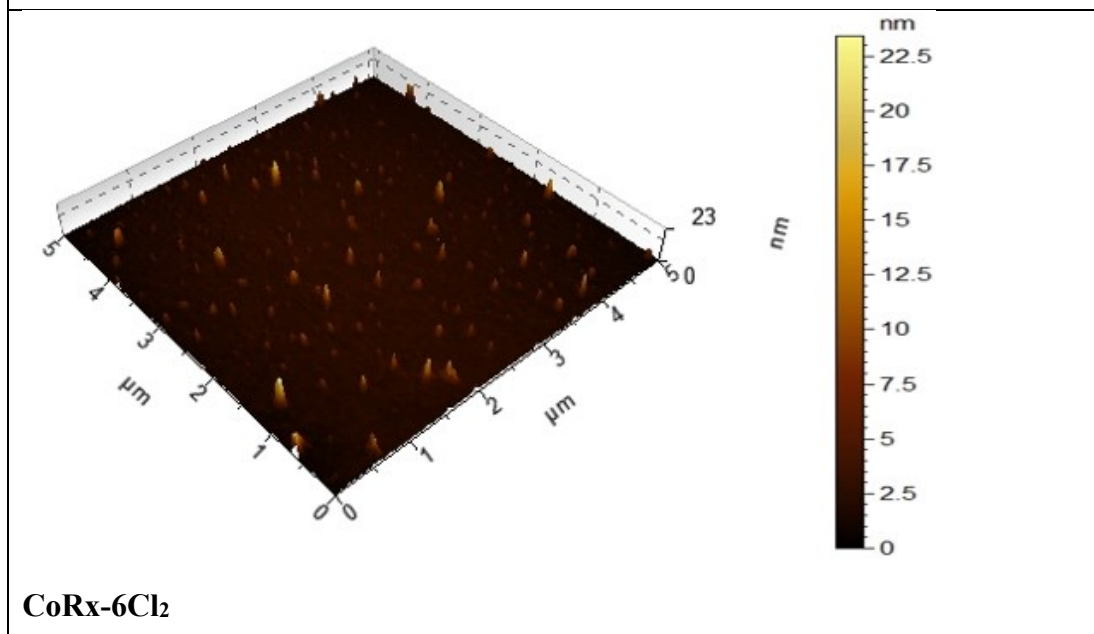
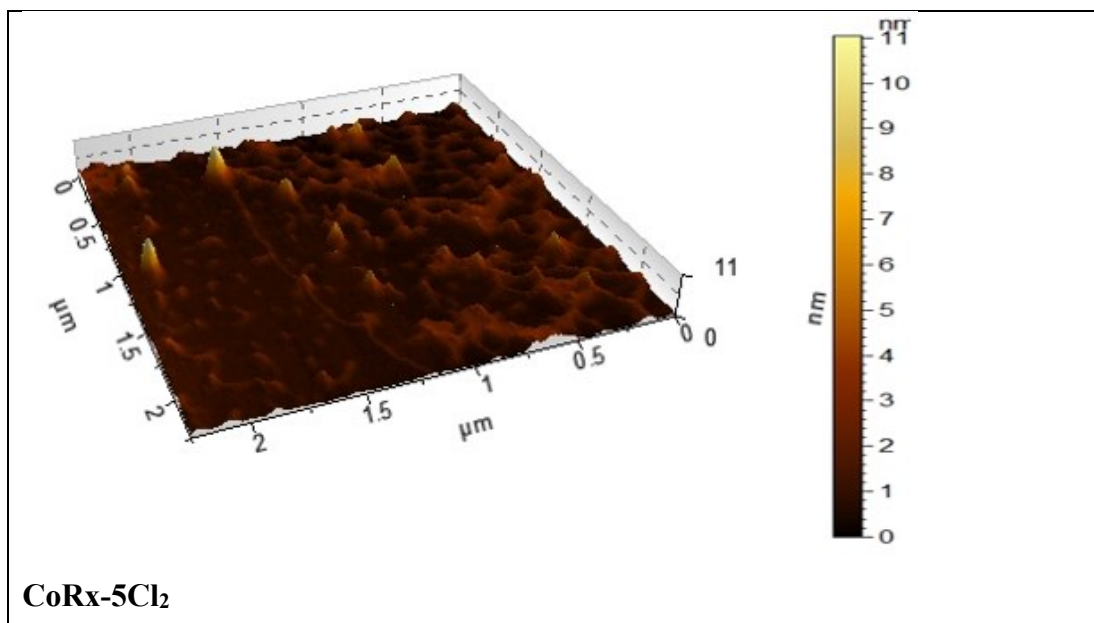


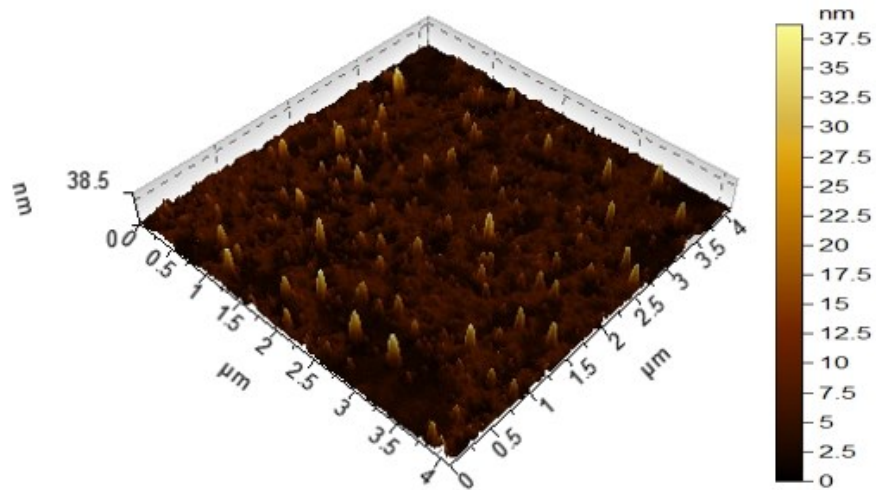
### CoRx-12-Cl<sub>2</sub>



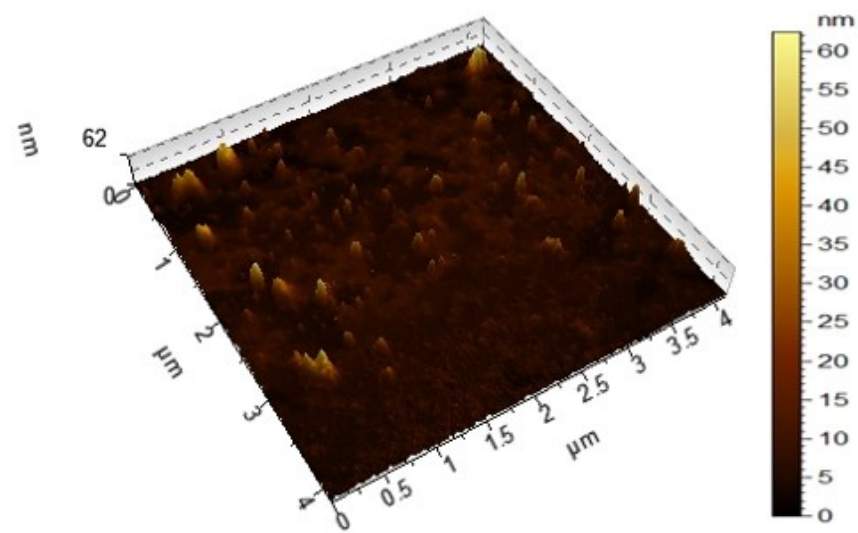
### AFM images of nano-sized cobalt complexes of pyridine carboxaldehyde



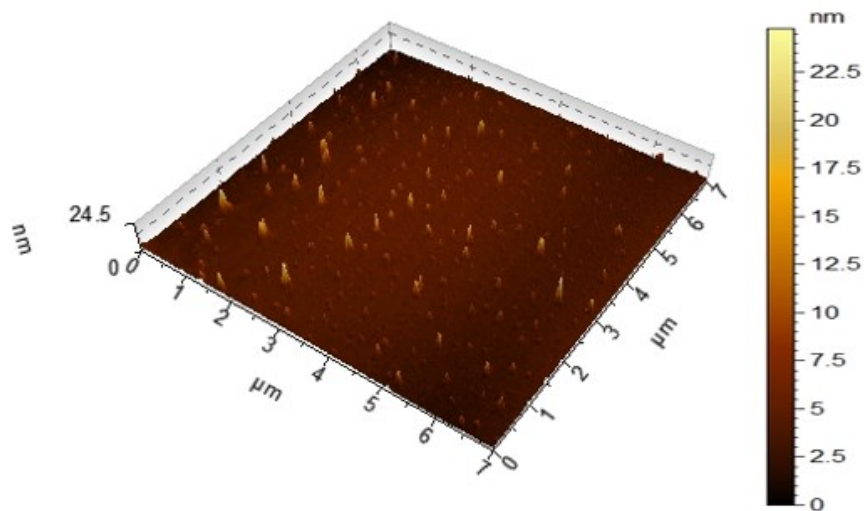




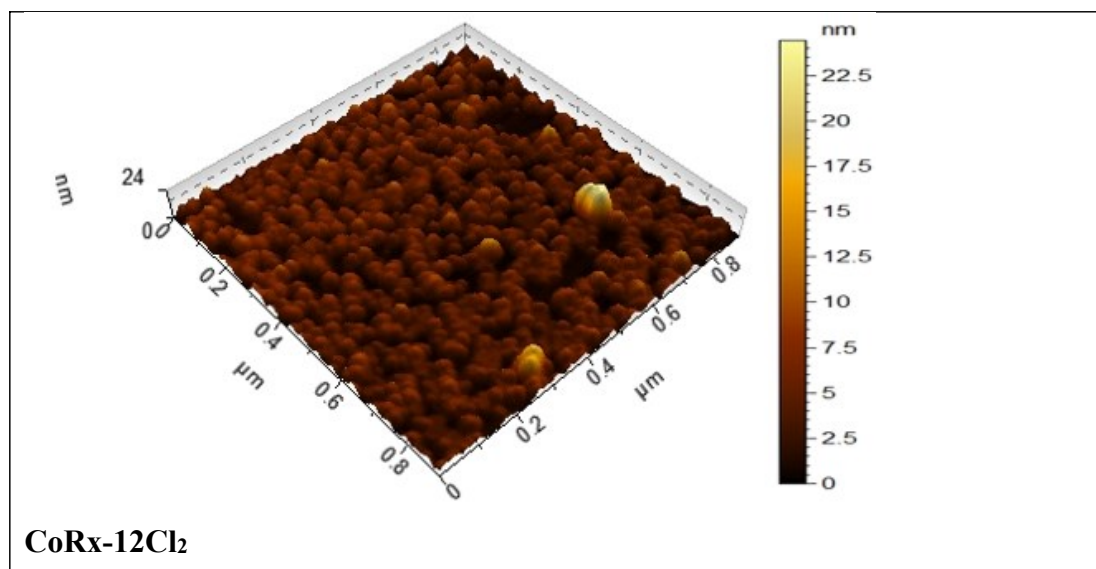
**CoRx-8Cl<sub>2</sub>**



**CoRx-9Cl<sub>2</sub>**



**CoRx-11Cl<sub>2</sub>**



# A multi-objective robust optimization to design a sustainable dairy supply chain under uncertain product demands, economic and social consideration. A real case study from Bulgaria

R. Vladova\*, T. Petrova, E. Kirilova

*Institute of Chemical Engineering, Bulgarian Academy of Sciences, Acad. G. Bontchev, Str., Bl. 103, 1113 Sofia, Bulgaria*

Received: March 13, 2024; Accepted: May 21, 2024

The operation of dairy supply chains (DSCs) is associated with the generation of significant amounts of wastewater pollutants and CO<sub>2</sub> emissions. The presence of uncertainty regarding various parameters of the considered DSCs has an additional impact on their sustainability. The most efficient way to improve the sustainability of DSCs is by applying mathematical modeling approaches for optimal design of sustainable DSCs operating under uncertain conditions. The present study proposes an optimal model for design of a sustainable DSC for the production of two types of dairy products with a technology selection, which includes economic, environmental and social impact models, as well as dairy production model. The optimization model takes into account uncertainty in products demands, raw materials and products prices and social costs. The effectiveness of the proposed approach is proved in a real case of a DSC from Bulgaria, which includes suppliers of two types of milk and dairy plants for the production of two types of dairy products and markets. The obtained optimal values of the economic, environmental and social costs show that the application of the optimization approach results in sustainable solutions that do not significantly change with an increase in the uncertainty level of consideration of the uncertain parameters.

**Keywords:** robust optimization; optimal design; uncertain conditions; economic, environmental and social sustainability improvement; dairy supply chain

## INTRODUCTION

Increasing dairy products production, population growth and changing consumer habits lead to an increased market volume for dairy products, which rises concerns about possible environmental impacts, increased dairy production costs and negative social impact [1]. The latter requires the implementation of the strategy of sustainable management of the DSCs, which takes into account all activities across the network - from the supply of raw materials, through the production itself, products transportation and their delivery to customers. The design of sustainable SCs is directly related to making important decisions that can be taken into account at different levels such as strategic, tactical and operational of the design and management of SCs activities. This includes: choosing suppliers, determining the purpose and location of facilities, allocating production capacity, choosing technologies for manufacturing products, creating a transportation network for supplies, purchasing raw materials, planning production, planning supplies and stocks, etc. On the other hand,

to get an overall advantage for the DSCs efficiency, it is important to consider all aspects of sustainability - economic, environmental and social - in the decision-making process. The uncertainties regarding various parameters of the considered DSCs such as products demands, raw materials and products prices, operating costs, transportation costs, etc., has an additional impact on their sustainability. It is very important to predict how these uncertainties affect the overall sustainability of DSCs to avoid potential risks. They can be: generation of large amounts of pollutants with a harmful impact on the environment, loss of raw materials and products along the supply chain, high energy consumption, lowering of economic indicators (profit from productions, losses in markets for selling the products), social dissatisfaction (spoilage of dairy products due to their perishable nature), etc. Therefore, dealing with uncertainty plays a crucial role in supply chain design and management. One of the most effective ways to improve the sustainability of the considered DSCs operating under uncertain conditions is to optimize all network activities while satisfying economic,

\* To whom all correspondence should be sent:  
E-mail: r.vladova@iche.bas.bg

environmental and social aspects [2]. A large part of the developed mathematical approaches for optimal DSCs design are based on robust [3-6], fuzzy [7-9], chance-constrained [10] and stochastic optimization [11] models. The researchers have chosen to satisfy economic [3, 7, 9], environmental and social criteria, or most often a combination of economic and environmental [4, 12] or the three dimensions of sustainability –economic, environmental and social [6, 13]. The developed approaches aim optimization of material, energy and waste flows and include as optimization criteria - maximization of production profit, minimization of total costs, reduction of energy consumption, reduction of greenhouse gas emissions due to transport, storage and packaging, achievement of maximum social satisfaction, etc. Some of the developed approaches have taken into account the impact of uncertainty on products demands, transport, production and storage costs, capacity of facilities, life (durability) of products. There are no approaches in the literature that consider three aspects of sustainability in the design of optimal DSCs operating under uncertainty, which produce different products according to different technologies and to include not only the impact of CO<sub>2</sub> emissions but also of industrial wastewater.

This paper is organized as follows. A literature review positioning the research in the field is given. In the next sections the proposed robust multi-objective optimization approach is described, an illustrative case study is presented and the obtained results are described and discussed. Finally, the main conclusions are given.

## LITERATURE REVIEW

The literature review part of this study is divided into two sections. Methods for sustainable supply chain management under uncertainties found in the literature are presented. Then, approaches for wastes reduction in dairy supply chain operating under uncertain conditions are given.

### *Sustainable DSCs management under uncertainties*

The dairy market occupies a significant share in the global food sector. This necessitates the application of effective optimization techniques to improve production efficiency and sustainability in the dairy industry. The varied parameters of the considered DSCs complicate their implementation. The latter requires the creation and application of special methods for the optimization of DSCs operating under uncertain conditions. Jouzdani *et al.* [7] applied a fuzzy mixed-integer programming approach to solve an optimization problem for dynamic optimal dairy facility location and supply

chain planning under uncertain products demands. The formulated optimization problem includes as an objective function: minimization of costs of traffic congestion, facility location, transportation of raw/processed milk and dairy products. Sel *et al.* [10] considered a planning and scheduling problem in the dairy industry and proposed a chance-constrained programming model accounting for uncertainty in quality deterioration of intermediate mixture. The lifetime of intermediate products and the quality deterioration of perishable intermediate mixture are considered as uncertain parameters and Weibull distribution is used to determine the waste generated in two-stage semi-continuous production and packaging set of the yogurt production process. Jouzdani *et al.* [3] addressed a robust supply chain network design optimization problem considering multiple products, multiple transportation modes, monetary value of time and uncertainty in transportation costs, demand and supply. The approach is implemented on a case study from Iran of a dairy packaging and distribution network. Jouzdani and Govindan [13] developed a multi-objective mathematical programming model to optimize the cost, energy consumption, and the traffic congestion associated with such supply chain operations. The uncertainty of product lifetime is modeled as a Weibull random variable, and food perishability is assumed to be affected by vehicle refrigerator utilization. The three aspects of sustainability are explored. The weighted multi-objective function is defined by minimizing the net present value of SC total cost, total road traffic congestion, and the total fuel consumption in the considered multi-period multi-product DSC. Yavari and Geraeli [14] investigated a green closed-loop multi-period and multi-product supply chain network design for perishable products under uncertain products demands, rate of return and the quality of returned products. They proposed a mixed-integer linear programming (MILP) model to minimize the total cost of the supply chain and the amount of environmental pollution along the supply chain. Furthermore, they developed a robust approach for the considered problem to deal with uncertainty. Gitinavard *et al.* [15] applied several approaches for optimal allocation of distribution centers in a dairy company under uncertain parameters such as products demands and transportation time. They are: mixed-integer programming model for the distribution center location problem solution; a fuzzy method for ranking the resulting Pareto optimal solutions and chance-constrained programming technique for dealing with uncertain parameters. The

minimization of the transportation costs and the deviation of delivered products for important customers and candidate customers with respect to their demands to increase their satisfaction are considered as optimization criteria. Guarnaschelli *et al.* [11] used a two-stage hierarchical stochastic and decomposition approach for optimal planning and distribution of multi-product two-echelon supply chain under uncertain products demands and supply aiming maximizing the expected net benefit. Roa *et al.* [4] proposed an effective methodology for the robust design of a first-mile logistics system for the storage and cooling of milk as a perishable product taking into account decisions related to open facilities and the flow of products, including sustainability indices. The authors defined milk production and milk price as uncertain parameters. The proposed model is solved using the Epsilon constraints method, and the sustainability is calculated considering an extension of the FePIA methodology for a bi-objective function: maximization of profit and minimization of CO<sub>2</sub> emissions. Hemmati *et al.* [16] proposed a robust bi-level mathematical model for economic and environmental optimization of a multi-echelon perishable dairy supply chain under uncertain products demands, transportation costs and the lifetime of perishable dairy products. Zarei-Kordshouli *et al.* [9] applied a fuzzy goal programming method to solve the supply chain design problem to minimize the total costs, maximize the suppliers' sustainability and resiliency, and maximize the distribution centers' resiliency.

The use of weights in front of the objective functions in the considered problems for the optimal design of DSCs under uncertain conditions has a significant impact on the obtained solutions. Breen *et al.* [12] developed a weighted multi-objective optimization method based on a genetic algorithm for obtaining the optimal dairy farm equipment, management practices and electricity tariffs. Changing the weights for the economic and environmental costs in the weighted objective function leads to different solutions for the optimal combination of equipment.

Touil *et al.* [8] applied the credibility-based fuzzy mathematical programming model and the crisp equivalent model to solve the problems of integrating production and distribution in the SC planning of the dairy industry in Morocco. They used a weighted Hurwicz criterion for a single objective function to maximize the total profit including the total costs for a three-echelon multi-product milk supply chain. Production cost, inventory holding and transport costs, products

demands, production capacity, and safety stock level are considered as uncertain (fuzzy numbers). Gholizadeh *et al.* [5] used heuristic robust optimization and an extended  $\varepsilon$ -constraint approach for optimal design of a multi-period multi-product closed loop DSC under uncertain total costs, capacities of facilities, return rate of products, and products demands. A weighted objective function for maximizing total profit and minimizing environmental impact is considered. Several scenarios were created and a sensitivity analysis of the profitability of the closed-looped supply chain with respect to the product lifetimes was applied. Shafiee *et al.* [6] applied a multi-objective mathematical model to design a multi-period and multi-product DSC composed of suppliers, producers, and retailers to minimize the total costs and the environmental impacts and maximize the social impacts. The authors applied a robust optimization approach to deal with uncertainty associated with demand, transportation costs, production costs, holding costs, and facilities' capacity. A hybrid method based on a heuristic algorithm, and an augmented  $\varepsilon$ -constraint method are developed to solve the proposed model.

#### *Wastes reduction in DSCs operating under uncertain conditions*

Wastes and losses of raw materials and dairy products along the supply chain are a growing problem due to environmental, social and economic impacts. The presence of uncertainties regarding various DSC parameters further affects these losses. Recently, more attention has been paid to this issue, looking for opportunities to reduce waste by proposing solutions to improve the sustainability of dairy supply chains. Ebrahimi *et al.* [17] developed a stochastic DSC valorization optimization model under uncertain raw material price and products demands. The model takes into account the multipurpose and batch characteristics of dairies and the time resource distribution over the processing nodes and products. As a result of its implementation, food waste and supply chain costs have been reduced and the profit function and the overall structure of the chain have been obtained. For model analysis, three different scenarios were designed under different conditions with and without accounting for by-products. Kazancoglu *et al.* [18] applied the Grey prediction method to predict the potential milk losses over a long period, according to triple bottom line (TBL) and considering the uncertainty of data for raw milk losses in the supply chain in Turkey.

In summary, the main focuses of the reviewed past researches are listed below:

➤ Most previous studies focused on minimizing the costs and environmental impact of the considered DSCs and did not consider social costs in their model.

➤ All studies provided environmental impact assessments only in terms of greenhouse gas emissions related with transport or raw material and products and consumed energy by dairy production. There is a lack of approaches to assess the environmental impact of dairy industry in terms of wastewater from the production of dairy products and those related to the processing of the used raw materials – different types of milk.

➤ The uncertainties taken into account most often relate to product demands, transport and production costs, facility capacity, transport traffic, etc.

Recently, Kirilova *et al.* [19] proposed a deterministic approach for optimal design of sustainable DSC for the production of different types of dairy products according to different technologies while meeting economic, environmental and social criteria defined from a cost perspective. The environmental criterion includes assessments of pollutant emissions in relation to two areas of impact - air and water. The model [19] was extended with a Robust Counterpart (RC) for uncertain product demands [20] using the approach [21]. It was solved by considering economic and environmental criteria for a case study, consisting of two suppliers, two dairies and two markets. Based on previous studies, the present study represents an implementation of Kirilova *et al.* [20] approach to an illustrative case study from Bulgaria of DSC consisting of three suppliers, two dairies and three markets. The three dimensions of the sustainability are considered. Products demands, raw materials prices, products prices and social costs are considered as uncertain parameters.

## ROBUST MULTI-OBJECTIVE OPTIMIZATION APPROACH

### *General formulation of the optimization problem*

A robust optimization model was developed to design a sustainable three-echelon DSC for the production of different products according to different technologies (recipes) while meeting economic, environmental and social criteria. Products demands, raw materials prices, products

prices and social costs are considered as uncertain parameters. It includes models for: (i) the production of the products according to the recipes; (ii) the design of DSC; (iii) environmental and (iv) social performance of the DSC. The environmental impact of DSC is assessed in terms of two areas: wastewater generated in each processing task of the production recipes, including those related to the used raw materials; CO<sub>2</sub> emissions related to the energy consumed by the dairies and CO<sub>2</sub> emissions generated due to transportation of raw materials and products. Biochemical Oxygen Demand during 5 days (BOD<sub>5</sub>) is used to evaluate wastewater generated from dairy production. Pollution taxes are imposed on dairies to keep the wastewater and CO<sub>2</sub> emissions below set acceptable levels. The social impact of the DSC is related to the employees hired by the three echelons of the considered DSC. The optimization problems are completed with constraints on the realization of the production portfolio over time horizon, the planned amounts of products and the environmental impact costs that must be paid to treat pollutants. The optimization criterion represents a revenue from the total profit after deducting production costs, raw materials costs, transportation costs, environmental costs and social costs.

### *Needed data*

In order to develop the mathematical models, three sets of data must be known: 1). Data on raw materials and products - composition of used raw materials and target products; 2). DSC data – data for production system; markets demands; capacities of the milk suppliers; prices of milk and products; production costs, distances between suppliers, dairies and markets; transportation costs; vehicles' types capacities; 3). Environmental data - related to pollutants generated in DSC; 4). Social data – related to employees (job positions) hired by suppliers, dairies and markets. These are the costs for salaries, benefits, working clothing, medical care and insurance and the average amounts of raw materials/products processed by employees.

### *Decision variables*

The following decision variables are defined:

1) Binary variables to define a DSC; 2) Continuous variables defining the raw materials and products flows between different DSC sites; 3) Continuous variables determining the milk fat content of the raw materials used; 4) Integer variables determining the number of employees (job positions) depending on processed quantities of raw materials/products.

### Mathematical models

➤ *Models of production recipes.* The production of two types of cottage cheese - low-fat content and high-fat content takes place according to two production recipes (PR1 and PR2) as each of them uses different raw material for production of both products - standardized whole milk (raw material 1 – RM1) and skimmed condensed milk (raw material 2 – RM2). The PRs include different production tasks conducted in different equipment units. PR1 includes three production tasks: milk pasteurization (Task 1); acidification to produce a raw dairy product (Task 2); draining to produce target dairy product (Task 3). PR2 involves one more production task: milk dilution (Task 1); milk pasteurization (Task 2); acidification (Task 3) and draining (Task 4).

The mathematical description of the production recipes includes:

1) Dependencies for determination of the protein, casein and lactose concentrations in raw materials:

*Production recipe 1:* Skimming of whole standardized milk.

$$\begin{aligned} MP(x(r_p)) &= MP \left[ 1 + \frac{MF - x(r_p)}{CF - MF} \right], (\%), \\ MC(x(r_p)) &= MC \left[ 1 + \frac{MF - x(r_p)}{CF - MF} \right], (\%), \\ ML(x(r_p)) &= ML \left[ 1 + \frac{MF - x(r_p)}{CF - MF} \right], (\%), \\ r_p &= 1, \forall p, p \in P. \end{aligned} \quad (1)$$

*Production recipe 2:* Dilution of skimmed condensed milk.

$$\begin{aligned} MP(x(r_p)) &= MP \frac{x(r_p)}{MF}, (\%), \\ MC(x(r_p)) &= MC \frac{x(r_p)}{MF}, (\%), \\ ML(x(r_p)) &= ML \frac{x(r_p)}{MF}, (\%), \\ r_p &= 2, \forall p, p \in P. \end{aligned} \quad (2)$$

where MF (%), MP (%), MC(%) and ML (%) are the concentrations of milk fat content, proteins, casein and lactose in the used raw materials. CF(%) is cream fat content.  $MP(x(r_p))$  (%),  $MC(x(r_p))$  (%) and  $ML(x(r_p))$  (%) are the concentrations of proteins, casein and lactose in the skimmed milk.  $r_p$  is the recipe used for the production of the dairy product  $p$ .

2) Equations for target products yield  $YP(x(r_p))$  (kg) describing the compositions as functions of the fat content in used raw materials [22]:

$$\begin{aligned} YP(x(r_p)) &= \frac{\left[ RF(x(r_p)) \cdot x(r_p) + \right. \\ &\quad \left. + RC_p \cdot MC(x(r_p)) \right] \cdot RS_p}{PS_p}, (\text{kg}), \\ r_p &= 1, 2; r_p \in R_p, \forall p, p \in P \end{aligned} \quad (3)$$

where  $PS_p$  (%) is the solids' content in products and  $RC_p$  (%) and  $RS_p$  (%) are the recovery factors for casein and all solids.  $RF(x(r_p))$  (%) is the milk fat recovery factor.

3) Equations for quality of target products - Determination of Fat in Dry Matter -  $FDM_p$  (%) [22] used as an indicator for curd quality:

$$FDM_p = \frac{PF_p}{PS_p}, (\%), \forall p, p \in I \quad (4)$$

where  $PF_p$  is fat content of the product, (%).

Production times and equipment used to perform the production tasks, as well as the fractions of the processed raw materials, raw products and target products, referred to 1 kg milk and 1 kg cottage cheese - target product in PR2, are given in [19].

The equations (1-4) presented above refer to 1 kg milk and 1 kg target product. Production recipe models provide a relationship between the production tasks by calculating size factors representing the “volumes” of materials that must be processed in production tasks to produce 1 kg of target products. The size factors together with the quantities of produced products related to the products portfolio and production tasks are used to determine the constraints for realization of the production portfolio over the time horizon. They are described in details in [23].

### ➤ Model of DSC

The mathematical description of the DSC includes:

1) Mass balance equations for the subsystems suppliers-dairies and dairies-markets to prevent from the accumulation of raw materials  $QM(r_p)_i$  (kg) in the suppliers and products  $QP(r_p)_i$  (kg) in the dairies.  $YY(r_p)_{i,s}$  (kg) are the quantities of raw materials bought by dairies  $i$  from the suppliers  $s$ ,  $XX(r_p)_{i,m}$  (kg) are the quantities of products  $p$  produced in dairies  $i$  and sold at markets  $m$ ,  $\gamma_{i,s}$  and  $\chi_{i,m}$  are binary variables for defining links between suppliers and dairies and dairies and markets in the DSC.

$$QM(r_p)_i = \sum_{s=1}^S YY(r_p)_{i,s} \cdot \gamma_{i,s}, \text{ (kg)},$$

$$QP(r_p)_i = \sum_{m=1}^M XX(r_p)_{i,m} \cdot \chi_{i,m}, \text{ (kg)},$$

$$\forall i, i \in I; \forall r_p, r_p \in R_p; \forall p, p \in P. \quad (5)$$

➤ *Model of supply chain environmental impact*

The environmental impact model includes equations for:

1) BOD<sub>5</sub> associated with the wastes generated during conducting of all production tasks in both recipes and introduced from outside related to the pre-processing of used raw materials.

$$BOD_M(x(r_p)) = \left[ \begin{array}{l} 0.89 \cdot x(r_p) + \\ + 1.031 \cdot MP(x(r_p)) + \\ + 0.69 \cdot ML(x(r_p)) \end{array} \right] \cdot 10^{-2}$$

(kg O<sub>2</sub> /kg milk),  $\forall r_p, r_p \in R_p, \forall p, p \in P. \quad (6)$

$$BOD_{Cu}(x(r_p)) = \frac{BOD_M(x(r_p))}{YP(x(r_p))}, \quad (7)$$

(kg O<sub>2</sub> /kg product),  $\forall r_p, r_p \in R_p, \forall p, p \in P.$

where  $BOD_M(x(r_p))$  is the BOD load related to spills of skim milk during implementation of Task 1 in PR1 and Task 2 in PR2 as a function of milk fat content  $x(r_p)$ .  $BOD_{Cu}(x(r_p))$  is the BOD load related to losses of cottage cheese during implementation of Task 3 in PR1 and Task 4 in PR2 as a function of milk fat content  $x(r_p)$ .  $YP(x(r_p))$

is the yield of cottage cheese produced according to production recipes as a function of milk fat content  $x(r_p)$  in used milk.

The total environmental impact assessment  $PBOD_p$  for production of 1 kg of each type of cottage cheese is:

$$PBOD(x(r_p)) = \sum_{w=1}^W BOD_w \sum_{l=1}^{L(r_p)} m(x(r_p))_{w,l}, \quad (8)$$

(kg O<sub>2</sub>),  $\forall p, p \in P.$

where  $m(x(r_p))_{w,l}$  ( $\forall w, w \in W; \forall l, l \in L(r_p);$

$\forall r_p, r_p \in R_p; \forall p, p \in P$ ) are environmental impact indices determining the mass of each type of waste  $w$  generated in any production task  $l$  related to 1 kg target product. For their determination In/Out fractions, target products yield (Eq. 3) and the eligible levels of losses listed in Table 1 are used [23].

It can be seen from Table 1 that  $BOD_{Pa}$  is the BOD load related to deposits on the pasteurizer walls during pasteurization of the skim milk (Task 1 in PR1 and Task 2 in PR2),  $BOD_{Wh}$  is the BOD load related to spills of whey produced as by-product during discharging of the cottage cheese vats (Tasks 2, 3 in PR1 and Tasks 3, 4 in PR2).  $LS_{SM}$  represents losses of skim milk in milk pasteurization (Task 1 in PR1 and Task 2 in PR2).  $LS_{Wh}$  represents losses of whey in acidification and draining of the produced cottage cheese (Tasks 2, 3 in PR1 and Tasks 3, 4 in PR2), while  $LS2_{Cu}$  and  $LS3_{Cu}$  represent losses of cottage cheese (Tasks 2, 3 in PR1 and Tasks 3, 4 in PR2).

**Table 1.** BOD<sub>5</sub> load related to wastes, production tasks and eligible levels of losses.

Type of wastes	BOD <sub>5</sub> load, (kg O <sub>2</sub> /kg milk(product))	Recipe 1		Recipe 2	
		generated waste, (%)	“introd.” waste, (%)	generated waste, (%)	“introd.” waste, (%)
Spills of skimmed milk	$BOD_M(x(r_p))$	Task 1; $LS_{SM}=1.2$		Task 2; $LS_{SM}=1.2$	
Deposits on units walls	$BOD_{Pa} = 1.5 \cdot 10^{-3}$	Task 1		Task 2	
Spills whey	$BOD_{Wh} = 32 \cdot 10^{-3}$	Task 2, 3; $LS_{Wh}=1.6$		Task 3, 4; $LS_{Wh}=1.6$	
Cottage cheese losses	$BOD_{Cu}(x(r_p))$	Task 2, $LS2_{Cu}=0.3$ Task 3, $LS3_{Cu}=0.5$		Task 3, $LS3_{Cu}=0.3$ Task 4, $LS4_{Cu}=0.5$	
RM1	0.1%		Task 1, $LS_{SM}=1$		
RM2	0.146%			Task 1, $LS_{SM}=1$	Task 1, $LS_{SM}=1$

2) Equations for the impact of CO<sub>2</sub> emissions associated with heating and cooling of milk referred to 1 kg milk as follows:

$$EIMCO2(\mathbf{x}(r_p)) = \frac{(EH + EC) \cdot ECO_2}{\left( \frac{CF - MF}{CF - \mathbf{x}(r_p)} \right)}, \quad (9)$$

(kg CO<sub>2</sub> /kg cottage cheese),  
 $\forall r_p, r_p \in R_p, \forall p, p \in P$ .

where  $EH$  and  $EC$  is needed energy by the heating and cooling processes during pasteurization task in (kWh/kg milk),  $ECO_2$  is the mass of CO<sub>2</sub> emissions associated with the energy consumption (kg CO<sub>2</sub>/kWh).

3) Equations for the impact of CO<sub>2</sub> emissions associated with the transport of raw materials and products, referred to 1 kg from both:(kg CO<sub>2</sub> /km·kg cottage cheese):

$$TMCO2 = 2 \cdot \frac{TCO_2}{VCm}, \quad (\text{kg CO}_2 / \text{km} \cdot \text{kg milk}),$$

$$TPCO2 = 2 \cdot \frac{TCO2}{VCp}, \quad (\text{kg CO}_2 / \text{km} \cdot \text{kg product}) \quad (10)$$

where  $TCO_2$  is the quantity of CO<sub>2</sub> emissions produced by fuel combustion (kg CO<sub>2</sub>/ km) and  $VCm$  (kg) and  $VCp$  (kg) are the payload capacities of used vehicles for transportation of raw materials and products.

#### ➤ Model of supply chain social impact.

The supply chain social impact model includes equations for the numbers of employee that will be hired by the suppliers Eq. (11), dairies Eq. (12) and markets Eq. (13). They depend on the average quantities of raw materials/products processed by employees in suppliers, dairies and markets.

$$NE\_S = \sum_{i=1}^I \sum_{s=1}^S \sum_{r=1}^R \frac{YY_{i,s,r} \cdot \gamma_{i,s,r}}{AQ_s \cdot NWD}, \quad (11)$$

$\forall i \in I, s \in S, \forall r, r \in R$ .

$$NE\_P = \sum_{i=1}^I \sum_{p=1}^P \sum_{m=1}^M \sum_{r=1}^R \frac{XX_{i,p,m,r} \cdot \gamma_{i,p,m,r}}{AQ_p \cdot NWD}, \quad (12)$$

$\forall i \in I, p \in P, \forall m, m \in M, \forall r, r \in R$ .

$$NE\_M = \sum_{i=1}^I \sum_{p=1}^P \sum_{m=1}^M \sum_{r=1}^R \frac{XX_{i,p,m,r} \cdot \gamma_{i,p,m,r}}{AQ_m \cdot NWD}. \quad (13)$$

$\forall i \in I, p \in P, \forall m, m \in M, \forall r, r \in R$ .

where  $NE\_S$ ,  $NE\_P$ ,  $NE\_M$  are the numbers of employees (job positions) that will be hired by suppliers  $s$ , dairies  $i$  and markets  $m$ .  $AQ_s$ ,  $AQ_p$ ,  $AQ_m$  (kg) are the average quantities of raw materials/products that employees can process per

day in the different echelons of the DSC.  $NWD$  is the number of working days per month,  $XX_{i,p,m,r}$  (kg) are the quantities of product  $p$  produced according to recipe  $r$  in dairy  $i$  and sold at market  $m$ ,  $\gamma_{i,p,m,r}$  is binary variable used to structure the supply chain between the dairies and markets.

#### Constraints

To estimate the feasibility of the obtained sustainable product portfolios, the following constraints are introduced for: 1). Realization of the production portfolio in the time horizon; 2). Capacity of the suppliers; 3). Capacity of the markets; 4). Environmental impact costs that must be paid for treatment of the pollutants released in air and water. These are the costs for BOD removal in the wastewater treatment plants (WWTPs) and the CO<sub>2</sub> costs associated with the production of the products in the dairies and the transportation of raw materials and products.

#### Optimization criterion

A single objective optimization function is used  $F_{profit}$  (BGN) as an optimization criterion. It represents the difference between the production profit and the economic, environmental and social costs, as follows:

$$F_{Profit} = F_R - (F_{P\_Costs} + F_{M\_Costs} + F_{T\_Costs} + F_{BOD\_Costs} + F_{CO_2\_E\_Costs} + F_{CO_2\_T\_Costs} + F_{Social\_Costs\_Suppliers} + F_{Social\_Costs\_Dairies} + F_{Social\_Costs\_Markets}) \quad (14)$$

where  $F_R$  (BGN) is the income from the sale of products in the markets;  $F_{P\_Costs}$  (BGN) are the total production costs for the dairies;  $F_{M\_Costs}$  (BGN) are the total costs of the dairies for purchasing the required quantities of both types of milk from suppliers for the production of the products;  $F_{T\_Costs}$  (BGN) are the total costs for the transportation of the milk and products between suppliers, dairies and markets;  $F_{BOD\_Costs}$  (BGN) are the total costs for BOD<sub>5</sub> paid for treatment of wastewater generated during the production of the products;  $F_{CO_2\_E\_Costs}$  (BGN) are the total costs for CO<sub>2</sub> emissions associated with the energy consumed by pasteurization process;  $F_{CO_2\_T\_Costs}$  (BGN) are the total costs associated with CO<sub>2</sub> emissions of pollutants generated during milk and products transportation;  $F_{Social\_Costs\_Suppliers}$ ,  $F_{Social\_Costs\_Dairies}$  and  $F_{Social\_Costs\_Markets}$  are costs related to the number of employees (job positions) that will be hired by the suppliers, dairies and markets.

The latter terms of the optimization criterion (14) are the following:

$$F_{Social\_Costs\_Suppliers} = NE\_S \cdot (CS_{suppliers} + CWCI_{suppliers} + CSB + CMI), \quad (\text{BGN}), \quad (15)$$

$$F_{Social\_Costs\_Dairies} = NE\_S \cdot (CS_{dairies} + CWCI_{dairies} + CSB + CMI), \quad (\text{BGN}), \quad (16)$$

$$F_{Social\_Costs\_Markets} = NE\_S \cdot (CS_{markets} + CWCI_{markets} + CSB + CMI), \quad (\text{BGN}), \quad (17)$$

Here,  $CS$ ,  $CWCI$ ,  $CSB$ ,  $CMI$  are costs for salaries, working clothing, benefits and medical insurance related to employees (job positions) that will be hired by the suppliers, dairies and markets.

The objective function (14) is subject to maximization:

$$MAX (F_{Profit}) \quad (18)$$

The formulated optimization problem belongs to the MINLP. It contains both binary and continuous variables, sets of modeling equations and inequality constraints. A detailed description of the optimization approach presented above with models for i) the production of the products; ii) planning of activities in SCs; iii) describing the environmental impact of SCs is given in [23].

#### Robust optimization model

The deterministic model presented above is extended with Robust Counterpart to cope with uncertain products demands, raw material prices, product prices and social costs. For this purpose, the robust optimization approach of Ben-Tal *et al.* [21] was applied. The general formulation of a compact robust optimization problem is as follows:

$$\max \quad ax + by \quad (19)$$

$$s.t. \quad bx \leq c$$

$$bx = dy$$

$$a, c, d \in U$$

where  $a$ ,  $c$  and  $d$  are the model parameters that vary under a given uncertainty set  $U$ . A vector  $x$  is a robust feasible solution to problem if it satisfies all realizations of the constraints from the uncertainty set  $U$ .

Each uncertain parameter is assumed to vary in a specified closed bounded box as follows:

$$u_{Box} = \left\{ \theta \in R^n : |\theta_t - \bar{\theta}_t| \leq \rho G_t \right\}, \quad t = 1, \dots, n \quad (20)$$

where  $\bar{\theta}_t$  is the nominal value of  $\theta_t$  as  $t$ -th parameter of vector  $\theta$ .  $G_t$  and  $\rho$  are positive numbers representing the so called ‘‘uncertainty

scale’’ and ‘‘uncertainty level’’. According to that, the RC model can be stated as follows:

$$\max \quad z \quad (21)$$

$$s.t. \quad ax + by \leq z \quad \forall a \in u_{Box}^a$$

$$bx \leq c \quad \forall c \in u_{Box}^c$$

$$bx = dy \quad \forall d \in u_{Box}^d$$

$$y \in \{0, 1\} \quad X \in R^+$$

The RC model (21) can be converted to a tractable equivalent model where  $U_{Box}$  is replaced by a finite set  $U_{Extr}$  consisting of the extreme points of  $U_{Box}$  as follows:

$$ax \leq z - by, \quad \forall a \in u_{Box}^a / u_{Box}^a = \left\{ a \in R^{n_a} : |a_t - \bar{a}_t| \leq \rho_a G_t^a \right\}, \quad t = 1, \dots, n_a \quad (22)$$

The left-side of inequality (22) contains the vector of uncertain parameters, while all parameters of the right-hand side are certain. Thus, the tractable form of the above semi-infinite inequality can be written as follows:

$$\sum_t (\bar{a}_t x_t + y_t) \leq z - by, \quad (23)$$

$$\rho_a G_t^a x_t \leq y_t \quad \forall t \in \{1, \dots, n_a\}$$

$$\rho_a G_t^a x_t \leq -y_t \quad \forall t \in \{1, \dots, n_a\}$$

Similarly, the equality and inequality constraints in Eq. (21) can be converted to their tractable equivalent equations through extending the use of the extreme points of  $U_{Box}$ .

Finally, the tractable form of the robust compact model can be presented as follows:

$$\max \quad z$$

$$s.t. \quad \sum_t (\bar{a}_t x_t + y_t) \leq z - by$$

$$\rho_a G_t^a x_t \leq \gamma_t, \quad \forall t \in \{1, \dots, n_a\}$$

$$\rho_a G_t^a x_t \leq -\gamma_t, \quad \forall t \in \{1, \dots, n_a\}$$

$$b_k x \leq \bar{c}_k + \rho_c G_k^c \quad \forall k \in \{1, \dots, n_c\}$$

$$b_j x \leq \bar{d}_j y + \rho_d G_j^d \quad \forall j \in \{1, \dots, n_d\}$$

$$y \in \{0, 1\} \quad X, \gamma \in R^+$$

It can be used for modeling the uncertain products demands, raw material prices, product prices and social costs in the considered dairy DSC.

#### CASE STUDY

The presented above robust optimization approach is applied in a real case study from Bulgaria including production of two types of cottage cheese (P1 and P2) according two production technologies using standardized whole milk and

skimmed condensed milk as raw materials (RM1 and RM2). The production of both types of products is conducted in two dairies (D1 and D2). Three suppliers provide the raw materials for the dairies (S1, S2 and S3). The produced products are supplied to three markets (M1, M2 and M3). The products production is realized in a time horizon of one month. The production units used and their summarized volumes are listed in Table 2, [24].

**Table 2.** Equipment units with summarized volumes, (m<sup>3</sup>).

	Milk tanks	Pasteurizers	Cottage cheese vats	Drainers
D1	1,450	800	950	300
D2	1,450	950	1,050	340

Capacities of the three suppliers (kg) are presented in Table 3 [25]. Distances (km) between suppliers, dairies and markets are listed in Table 4.

**Table 3.** Capacities of suppliers (kg).

	Capacity (kg)	
	RM 1	RM 2
S1	97,000	57,000
S2	100,540	54,500
S3	113,000	78,000

**Table 4.** Distances between suppliers, dairies and markets (km).

	S1	S2	S3	M1	M2	M3
D1	10	15	20	98	136	46
D2	20	10	15	22	23	75

Table 5 presents the data on the vehicles used for transportation of raw materials and products. They are used for calculation of the CO<sub>2</sub> emissions associated with transportation and transportation costs. The latter in BGN/kg.km are calculated by multiplication of the vehicle's fuel consumption (L/100 km), the vehicle's fuel price (BGN/L) and the number of vehicles' courses. The latter is divided by the total quantities of raw materials or products (kg).

**Table 5.** Data about used vehicles for transportation of raw materials and products.

Vehicles used for transportation	Payload capacity, (L/kg)	Energy of fuel, (kWh/L)	CO <sub>2</sub> emissions generated from fuel combustion, (kg CO <sub>2</sub> /kWh)	Fuel consumption, (L/100 km)	Fuel price, (BGN/L)
Milk tanker truck with petrol engine	2,500	8.056	0.249	32	2.22
Refrigerator truck with diesel engine	4,000	9.583	0.267	23	2.27

The environmental costs associated with transportation are obtained using data listed in Table 5 and the price of CO<sub>2</sub> emissions which is 0.174 BGN/kg CO<sub>2</sub>. The energy consumed in both recipes for heating of 1 kg milk is  $8.333 \times 10^{-3}$  kWh/kg milk, and for cooling is  $6.333 \times 10^{-2}$  kWh/kg milk [26]. The CO<sub>2</sub> emissions associated with both processes is 0.46 kg CO<sub>2</sub>/kWh [27]. The costs of CO<sub>2</sub> are 0.00998 BGN/kg CO<sub>2</sub>. The price of BOD<sub>5</sub> paid to WWTPs from Dairy 1 is 2.9 BGN/kg, while from Dairy 2 it is 3.5 BGN/kg. The production costs are obtained based on the energy used for production of the products with an energy price of 0.14072 BGN/kWh. The average quantities (kg) of raw materials or products that employees can process per day in suppliers, dairies and markets are 500 kg milk, 150 kg products and 40 kg products/day. The average costs (BGN) according to Eqs. (15-17), related to the number of employees (job positions) to be hired by the suppliers, dairies and markets are taken from [28]. They include costs for salaries (BGN) [29], work clothes (BGN), social benefits (BGN) and medical insurance (BGN).

## RESULTS AND DISCUSSION

The proposed robust optimization approach is implemented in a real case study from Bulgaria. DSC includes three suppliers, two dairies and three markets. Uncertain products demands, raw material prices, product prices and social costs are considered as uncertain parameters. Several robust optimization problems were formulated and solved under nominal data and two different uncertainty levels (UL) ( $\rho = 0.5$  and 1). At each uncertainty level, ten random realizations were uniformly generated within the following uncertainty set:  $[nominal\ value \pm \rho \cdot SD]$ , where SD is the standard deviation of the obtained results. The optimization models were solved using GAMS® optimization software-BARON solver as all calculations were carried out on an AMD 7 3700X 8-CORE (3.6/4.4. GHz, 32 MB, AM4) CPU with 16 GB DDR4 3600 MHz RAM. Two performance measures were used to evaluate the models: mean and standard deviation of the obtained results.

The optimization problems are formulated and solved with fixed values for the environmental cost constraints, as follows: cost for treatment of wastewater generated in both dairies - 4,500 BGN and costs for treatment of CO<sub>2</sub> emissions of pollutants associated with transportation of raw materials and products between suppliers, dairies and markets and energy consumed by production facilities - 13,000 BGN. The optimization problems were formulated and solved at given boundaries of varying of the products demands as follows: Product 1, Market 1 – 25,000 ÷ 35,000 kg; Product 1, Market 2 – 15,000 ÷ 25,000 kg; Product 1, Market 3 – 20,000 ÷ 30,000 kg; Product 2, Market 1 – 5,000 ÷ 15,000 kg; Product 2, Market 2 – 35,000 ÷ 45,000 kg; Product 2, Market 3 – 20,000 ÷ 30,000 kg. On the other hand, the raw materials prices vary in the following boundaries: Supplier 1, Recipe 1 - 1.40 ÷ 2.40 BGN; Supplier 2, Recipe 1 - 1.30 ÷ 2.30 BGN; Supplier 3, Recipe 1 - 1.50 ÷ 2.50 BGN; Supplier 1, Recipe 2 - 2.30 ÷ 3.30 BGN; Supplier 2, Recipe 2 - 2.40 ÷ 3.40 BGN; Supplier 3, Recipe 2 - 2.50 ÷ 3.50 BGN. Products prices vary in the following boundaries: Product 1, Market 1 - 10.80 ÷ 20.80 BGN; Product 1, Market 2 – 12.30 ÷ 22.30 BGN; Product 1, Market 3 – 12.70 ÷ 22.70 BGN; Product 2, Market 1 – 12.10 ÷ 22.10 BGN; Product 2, Market 2 – 11.40 ÷ 21.40 BGN; Product 2, Market 3 – 12.50 ÷ 22.50 BGN. The social costs vary in the following boundaries: Suppliers - 1350 ÷ 2150 BGN; Dairies - 2150 ÷ 3150 BGN and Markets - 1850 ÷ 2650 BGN.

The obtained results for model solutions are shown in Figs. 1 and 2. From Fig. 1 it can be seen that the higher level of uncertainty ( $\rho=1$ ) is associated with larger economic, environmental, social cost values, and profit. At the higher level of uncertainty, there is an increase in the standard deviation values of the economic costs and the DSC profit by 5.7% and 6.5% and a decrease in the standard deviation values of the environmental and the social costs by 2.8% and 4.7%. One can see that this large variation in the level of uncertainty does not lead to a large difference in the standard deviations of the values mentioned above. The obtained optimal solutions for the number of employees to be hired from the suppliers, dairies and markets in the DSC at the both uncertainty levels are represented in Fig. 2.

It can be seen that the number of the employees to be hired by suppliers, dairies and markets is held constant under the different uncertainty levels, except for the case of the markets.

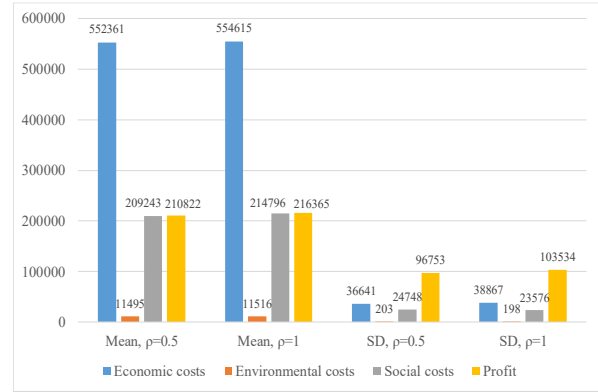


**Figure 1.** Optimal solutions for the mean and standard deviation values of the economic, environmental, social costs and profit of the DSC at both uncertainty levels –  $\rho=0.5$  and  $\rho=1$ .

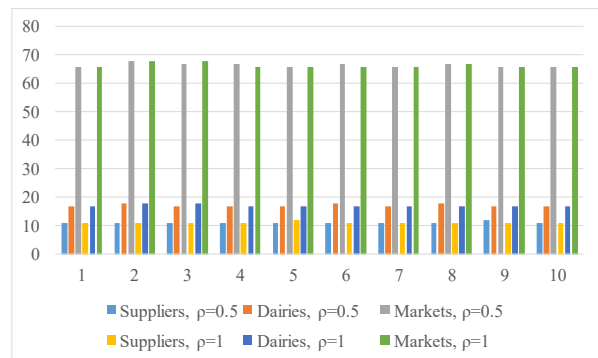


**Figure 2.** Optimal solutions for the number of employees to be hired from the suppliers, dairies and markets in the DSC at both uncertainty levels –  $\rho=0.5$  and  $\rho=1$ .

In the latter, at the higher level of uncertainty, an increase in the values of the standard deviation with 17.7% was observed. Regarding the obtained results for the optimal product portfolios of the two dairies under the different scenarios and levels of uncertainty, the following conclusions can be drawn. The first dairy produces only Product 1 according to the second recipe, which is distributed only to Market 3, and this type of portfolio does not change across scenarios at this level of uncertainty. In the second dairy, with very few exceptions, one type of portfolio is also obtained in the different scenarios, in which both products are produced according to Recipe 2, with Product 1 being distributed to Market 2 and Product 2 to Market 1. Regarding the suppliers of the two types of milk, in the different scenarios with very few exceptions, a solution is obtained, according to which the first dairy is supplied with the second type of raw material only from Supplier 1, while the second dairy is supplied with the second type of milk from all three suppliers. For one of the solutions obtained at the lower level of uncertainty, an optimization problem was formulated and solved using different weights for the three types of costs –

economic, environmental, social. The latter was done to see how the use of weighting factors with the objectives would affect the obtained optimal solutions for the product portfolios of the two dairies and the values of the optimization criterion. Figs. 3 and 4 below show the resulting solutions.

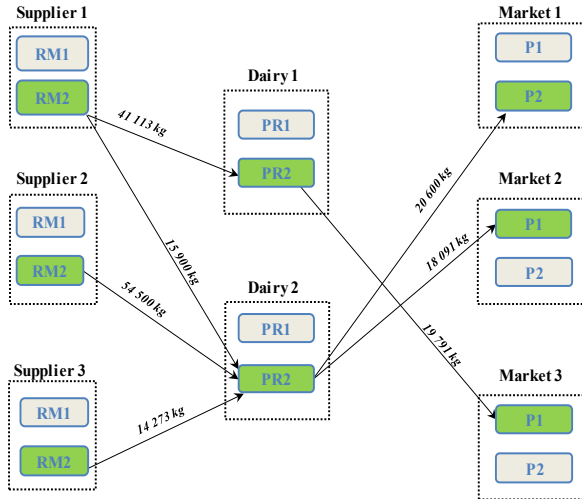


**Figure 3.** Products portfolio of an obtained optimal solution at an uncertainty level of  $\rho=0.5$ .

Figs. 3 and 4 show that the use of weights in front of the objective functions - economic, environmental and social costs leads to different portfolios for the two dairies both in terms of the supply of the two types of raw materials from suppliers of the dairies and in relation to the distribution of the produced output in the markets.

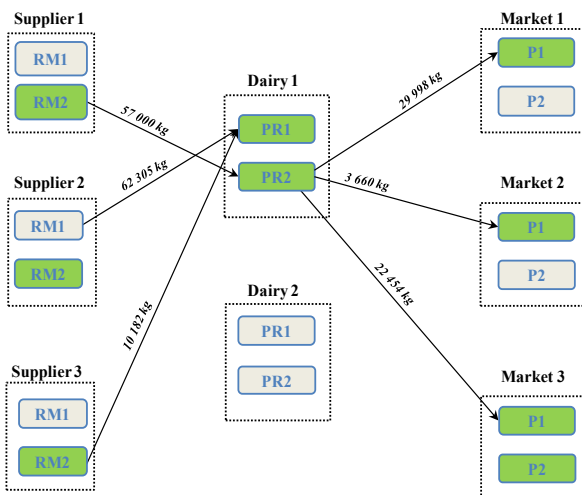


**Figure 4.** Products portfolio of an obtained optimal solution at an uncertainty level of  $\rho=0.5$  with weights of 0.6, 0.3 and 0.1 for the economic, environmental and social costs.

The portfolio presented in Fig. 3 is related to obtaining a profit from the production of the two products in the amount of BGN 117,394, with values for economic, environmental and social costs of BGN 519,304; BGN 11,410 and BGN 192,627. The

number of workers employed by suppliers, dairies and markets for this solution is: 11, 17 and 66, respectively. While the solution presented in Fig. 4, obtained using weights for economic, environmental and social costs of 0.6, 0.3 and 0.1 is associated with a much larger profit of BGN 939,246, as well as larger values for economic, environmental and social costs of BGN 859,819; BGN 14,655 and BGN 313,024. The number of workers employed by suppliers, dairies and markets are: 16, 22 and 83. The latter shows that the use of weights in front of the objectives leads to obtaining completely different solutions. Also, the obtained results enable managers and decision makers in DSC optimization to obtain model predictions when their needs and preferences change in the future. By varying the weights in the objective function under consideration, different scenarios can be played out, preferring each of the three criteria according to the specific case.

### CONCLUSIONS

The study represents the implementation of a robust optimization approach for the optimal design of sustainable dairy SC for production of two types of cottage cheese according to two technologies, under uncertain products demands, raw materials prices, products prices and social costs. The considered DSC includes three milk suppliers, two dairies and three markets. The dairy products production is associated with the release of emissions of pollutants into the air and water. Several robust optimization problems were formulated and solved under different random realizations of the uncertain parameters taking into account economic, environmental and social considerations. The nominal data for the products demands, raw materials prices, products prices and social costs were randomly generated under two uncertainty levels using a uniform distribution in a given uncertainty set. Two performance measures were used to evaluate the optimization models: the mean and standard deviation of the objective function values under random realizations. Moreover, for one of the solutions obtained at the lower level of uncertainty, an optimization problem was formulated and solved with different weights for the three types of costs – economic, environmental, social, such as 0.6, 0.3 and 0.1, respectively. The latter was done with a purpose to show how the use of weights with the objective function would affect the obtained optimal solutions for the product portfolios of the two dairies and the values of the optimization criterion. The obtained results show that the higher level of uncertainty is associated with larger economic, environmental, social cost values,

and profit. At the higher level of uncertainty, there was an increase in the standard deviation values of the economic costs and the profit of the DSC by 5.7% and 6.5% and a decrease in the standard deviation values of the environmental and the social costs by 2.8% and 4.7%. Similar is the case with the results obtained for employees to be hired by the suppliers, dairies and markets. In them, at the higher level of uncertainty, the largest increase in the values of the standard deviation of the obtained results of 17.7% is related with employees to be hired by the markets. The resulting types of product portfolios under the two levels of uncertainty do not differ significantly for the different randomly generated scenarios. On the other hand, the use of weights with the objectives leads to completely different solutions. The use of weights with the objectives has a very large influence on the obtained optimal values for the parameters of a given decision. This enable managers and decision makers in the future to play out different scenarios, favoring each of the three criteria according to the specific case and the needs of the DSC. Generally, it can be concluded that the obtained optimal values of the economic, environmental and social costs show that the optimization approach implementation results in sustainable solutions that do not significantly change with an increase in the uncertainty level of consideration of the uncertain parameters.

**Acknowledgment:** The study represents results obtained under project “Sustainable supply chains in terms of environmental, economic and social criteria” funded by the Bulgarian Science Fund under Contract No. KII-06-H37/5/06.12.19.

#### REFERENCES

1. M. B. Beck, R.V. Walker, *Front Environ Sci Eng*, **7(5)**, 626 (2013).
2. M. Malik, V. K. Gahlawat, R. S. Mor, V. Dahiya, M. Yadav, *Logistics*, **6**, 74 (2022).
3. J. Jouzdani, M. Fathian, A. Makui, M. Heydari, *Oper Res Int J*, **20(3)**, 1811 (2018).
4. A. P. Roa, J. W. Escobar, M. P. Montoya, *Heliyon*, **9**, e18444 (2013).
5. H. Gholizadeh, H. Jahani, A. Abareshi, M. Goh, *Computers and Industrial Engineering*, **157**, 107324 (2021).
6. F. Shafiee, A. Kazemi, A. J. Chaghooshi, Z. Sazvar, H. A. Mahdiraji, *Journal of Cleaner Production*, **294**, 126230 (2021).
7. J. Jouzdani, S. J. Sadjadi, M. Fathian, *Applied Mathematical Modelling*, **37**, 8467 (2013).
8. A. Touil, A. Echchatbi, A. Charkaoui, *International Journal of Supply and Operations Management*, **6(1)**, 30 (2019).
9. F. Zarei-Kordshouli, M. M. Paydar, S. Nayeri, *Clean Technologies and Environmental Policy*, **25**, 2903 (2023).
10. C. Sel, B. Bilgen, J., Bloemhof-Ruwaard, *Applied Mathematical Modelling*, **51**, 129 (2017).
11. A. Guarnaschelli, H. E. Salomone, C. A. Méndez, *Computers and Chemical Engineering*, **140**, 106966 (2020).
12. M. Breen, M. D. Murphy, J. Upton, *Applied Energy*, **242**, 1697 (2019).
13. J. Jouzdani, K. Govindan, *Journal of Cleaner Production*, **278**, 123060 (2021).
14. M. Yavari, M. Geraeli, *Journal of Cleaner Production*, **226**, 282e305 (2019).
15. H. Gitinavard, S. H. Ghodsypour, M. A. Shirazi, *Scientia Iranica E*, **26(5)**, 2952 (2019).
16. M. Hemmati, M. Rabbani, M.R. Mehregan, *Journal of Industrial and Systems Engineering*, **15(1)**, 134 (2023).
17. S.R. Ebrahimi, F. Khoshalhan, H. Ghaderzade, in: Proceedings of the 2nd International Conference on Industrial Engineering and Operations Management, Paris, France, July 26-27, 2018, article ID 235.
18. Y. Kazancoglu, Y.D. Ozkan-Ozen, M. Ozbiltekin, *Resources, Conservation and Recycling*, **139**, 270 (2018).
19. E. Kirilova, N. Vaklieva-Bancheva, R. Vladova, T. Petrova, B. Ivanov, D. Nikolova, Y. Dzhelil, *Clean Technologies and Environmental Policy*, **24(1)**, 213 (2022a).
20. E. Kirilova, N. Vaklieva-Bancheva, R. Vladova, T. Petrova, D. Nikolova, E. Ganev, Y. Dzhelil, *Chemical Engineering Transactions*, **94**, 547 (2022b).
21. A. Ben-Tal, B. Golany, A. Nemirovski, J.P. Vial, *Manufacturing and Service Operations Management*, **7(3)**, 248 (2005).
22. M. Johnson, Curd clinic, *Dairy Pipeline*, **12(2)**, 9 (2000).
23. E. Kirilova, N. Vaklieva-Bancheva, *Journal of Cleaner Production*, **167**, 493 (2017).
24. COWI Consulting Engineers and Planners AS, 2000, Overview of Dairy Processing, Cleaner Production Assessment in Dairy Processing, 2000, p. 7.
25. [https://agriculture.ec.europa.eu/system/files/2023-07/eu-raw-milk-prices\\_en.pdf](https://agriculture.ec.europa.eu/system/files/2023-07/eu-raw-milk-prices_en.pdf)
26. D. Maslarski, V. Tomova, Technological Equipment of Dairy Industry, Hristo Danov Publisher, Plovdiv, Bulgaria, 1980.
27. <https://eu-mayors.ec.europa.eu/en/home>
28. [https://eures.ec.europa.eu/living-and-working/living-and-working-conditions/living-and-working-conditions-bulgaria\\_en](https://eures.ec.europa.eu/living-and-working/living-and-working-conditions/living-and-working-conditions-bulgaria_en)
29. [https://www.zaplatomer.bg/zaplati/selsko-stopanstvo-khranitelna-promishlenost?global\\_currency=BGN](https://www.zaplatomer.bg/zaplati/selsko-stopanstvo-khranitelna-promishlenost?global_currency=BGN)

# Inductively heated fluidized beds and their potential for energy savings and efficient process control

V. V. Idakiev<sup>1,2\*</sup>, L. Mörl<sup>3</sup>

<sup>1</sup>University of Chemical Technology and Metallurgy, St. Kliment Ohridski Blvd. 8, 1756 Sofia, Bulgaria

<sup>2</sup>Institute of Catalysis, Bulgarian Academy of Sciences, Acad. G. Bonchev Str., Bl. 11, 1113 Sofia, Bulgaria

<sup>3</sup>Otto von Guericke University Magdeburg, Universitätsplatz 2, 39106 Magdeburg, Germany

Received: January 17, 2024; Accepted: March 18, 2024

This article presents a novel method with the necessary equipment for introducing contactless energy into heated fluidized beds, enabling improved energy utilization and consistent quality of the manufactured product. Inductive energy input serves as an alternative to convective heating. In contrast to conventional heat supply, where the heated fluidization gas acts as the energy carrier, electrically conductive particles are used here. These electrically conductive, yet chemically inert particles, are introduced into the fluidized bed and fluidized together with the substrate to be treated. An integrated inductor within the system applies an electromagnetic alternating field to the fluidized bed, thus inductively heating it.

The heated inert particles are intended to release their heat from the interior of the fluidized bed over a very large surface area to the material being treated. This results in a high energy density and, ultimately, highly efficient heat transfer. This is especially relevant for batch processes that are evaluated for efficiency and cost-effectiveness. The fast and precise temperature control in inductively heated fluidized beds is also particularly beneficial for thermolabile materials.

**Keywords:** Fluidized bed; inductive heating; contactless energy input; heat exchange; precise temperature control

## INTRODUCTION

The phenomenon of solid fluidization exhibits distinct characteristics and manifestations that can be strategically leveraged across various processes. Notably, the heightened intensity of heat and mass transport processes in fluidized beds renders them advantageous in numerous industrial applications. The intensified processes often permit substantial reductions in apparatus constructions. Fluidized beds are increasingly utilized in diverse economic sectors for processes such as solid heating, drying, particle granulation and coating, as well as the combustion of solid, liquid, or gaseous substances. They play a role in the pyrolysis or gasification of solids and in the classification or sorting of particle mixtures. In recent years, fluidized beds have become prevalent in environmental technology processes, including adsorptive or absorptive gas purification within a fluidized bed, and the fluidization of immobilized microorganisms in a liquid phase for the preparation of active compounds or wastewater purification.

Alongside the manifold application processes in fluidized beds, a multitude of apparatus-specific solutions have been developed for their implementation. Extensive literature and patent research indicate that the number of publications and

patents related to fluidized beds has already surpassed five figures. It is no longer feasible for a single expert to encompass all developments in this field. Nevertheless, we have yet to explore all the potential applications of fluidized bed technology, and ongoing innovations are anticipated [1, 2].

The customary approach to heat a fluidized medium within a fluidized bed involves indirect convective heating through an upstream heater. Another commonly employed strategy to augment heat transfer to the fluidized bed involves contact heating through the utilization of vapor-heated pipes within the chamber or by heating the walls of the apparatus. Energy conservation plays a pivotal role in facilitating the economic and ecologically sustainable design of fluidized bed processes. Nevertheless, an alternative method for heating the fluidized medium may be necessary to achieve this objective. Alternatively, inductive heating utilizing electro-conductive and chemically inert particles or other electro-conductive elements provides a means for energy input into a fluidized bed. In inductive heating, the primary heat source does not stem from a fluid or heated surfaces, it arises from the interaction of electro-conductive objects within an electromagnetic field, leading to the contactless heating of these objects. These electro-conductive objects can be, for example, moving iron hollow

\* To whom all correspondence should be sent:

E-mail: [idakiev@uctm.edu](mailto:idakiev@uctm.edu)

[idakiev86@ic.bas.bg](mailto:idakiev86@ic.bas.bg)

balls (IHB) or other stationary iron tubes inside the fluidized bed chamber. In this scenario, as the heat is directly and contactless transmitted into the electro-conductive fluidized particles (for example, IHB) across a significantly expanded heat transfer surface, it enables achieving a high energy density and more efficient heat transfer in comparison to conventional heating methods.

The concept of contactless energy transfer using iron hollow balls (IHB) within a magnetic field was first experimentally validated on a fluidized bed by Stresing *et al.* in 2011 [3]. The results confirmed the feasibility of energy input into the fluidized bed through an induction coil and IHB. Subsequently, Idakiev *et al.* delved deeper into the fluidization behavior of beds, incorporating additional inert particles. Non-conductive particles such as glass, alumina, or plastic were mixed with the IHB, and experiments were conducted with inductive energy input. Experimental findings indicate that an increase in the proportion of inert particles correlates with a rise in process temperature [4, 5].

Generally, the use of induction technology enables rapid heating and cooling of the fluidized bed. Additionally, it facilitates targeted heating of the fluidized bed, allowing for precise adjustment of gas temperature. This capability is particularly crucial for temperature-sensitive materials.

## EXPERIMENTAL

For the implementation of the above-mentioned process or objective, several fluidized bed systems were developed and tested. However, all of them operate in the same way. In Figure 1, the functioning of such a fluidized bed with inductive heating is illustrated. The figure shows a cylindrical fluidized bed apparatus with direct non-contact heating of electro-conductive particles fluidized together with the substrate to be treated in the fluidized bed chamber. This fluidized bed chamber is surrounded by three induction coils switched in parallel, each with three windings, so that the electro-conductive material inside the chamber can be subjected to an alternating electromagnetic field, whereby this material should be inductively heated directly and contactless. The building material (copper) used for the induction coil has a high purity and also very good electrical conductivity. In order to avoid heating or overheating of this building material, the coils are continuously cooled with cold water. In this way, the electrical conductivity of the copper used is kept stable.

For the inductive energy input into the apparatus, an alternating current induction generator TruHeat

MF3040, TRUMPF Hüttinger Elektronik GmbH, with a maximum power of 40 kW, is used.

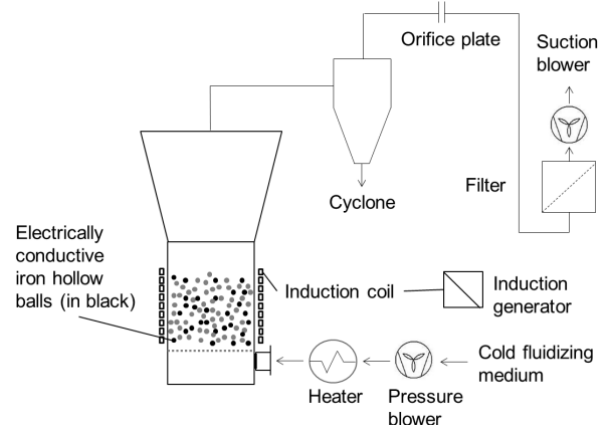


**Figure 1.** Graphic illustration of a cylindrical fluidized bed with direct contactless inductive heating of the electro-conductive particles inside the fluidized bed chamber.

Figure 2 shows a real picture of the cylindrical fluidized bed apparatus shown in Figure 1. This picture depicts the chamber surrounded by three parallel switched induction coils, each with three windings. The copper coil generates an electromagnetic field, leading to the inductive heating of the electro-conductive particles inside the apparatus chamber.

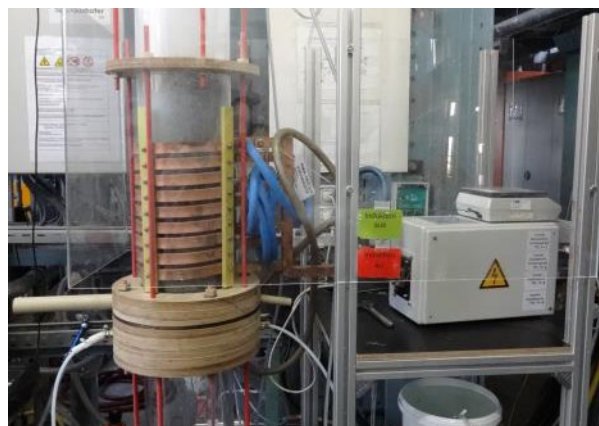


**Figure 2.** Picture of the cylindrical fluidized bed apparatus from Figure 1. Shows the fluidized bed chamber surrounded with the copper induction coil.

For a direct comparison between the novel energy input into the fluidized bed and the conventional method (*via* preheated fluidization gas), this system is equipped with a convective heater, installed at the gas inlet before the fluidized bed chamber. The plant can be operated in both suction and pressure modes, as well as with the simultaneous use of the suction and pressure fan, however, this has no effect on the energy input discussed in this paper.

For the realization of particle formulation processes in the inductively heated fluidized bed, a two-fluid nozzle Mod. 940 from the company Schlick is mounted as a bottom spray. This nozzle allows the injection of different liquids and their fine distribution thanks to the second channel with compressed air atomization. During the development phase of the process involving inductive heating of fluidized beds, typical fluidized bed processes such as drying, granulation, coating, agglomeration, and roasting were implemented in fluidized beds with inductive heating and compared with convective heating. For the cleaning of the fluidization medium in particle formulation processes in this fluidized bed apparatus with inductive heating, cyclones and filters are available [6].

## RESULTS AND DISCUSSION

The most significant advantage of the inductively heated fluidized bed is the precise control of gas temperature, particularly crucial for temperature-sensitive materials. The utilization of induction technology allows for extremely short heating and cooling durations in the fluidized bed, leading to a notable reduction in energy consumption. For a better representation of these advantages and of the actual temperature profile of a induction fluidized bed apparatus, Figure 3 displays an experimental image captured with a thermal camera.

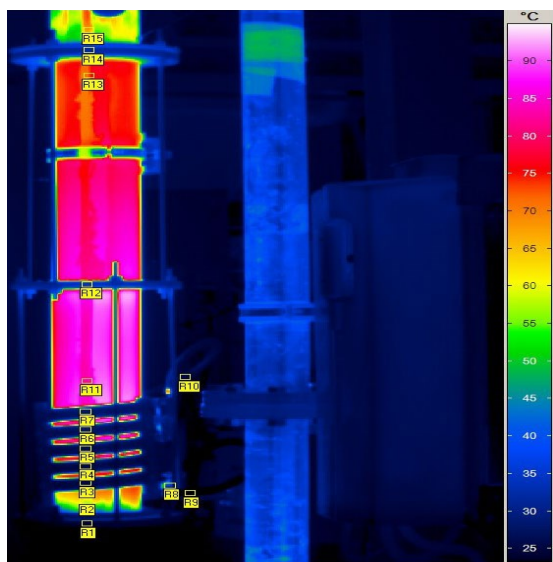


**Figure 3.** Picture taken with a thermal camera depicting the heat concentration in the chamber of the induction fluidized bed, external view of the apparatus.

In this case, it concerns a different fluidized bed system with inductive heating. In comparison with the apparatus shown in Figure 2, the induction coil here has 5 turns. The functionality of this presented induction fluidized bed is the same. As seen in this image, cold air enters the fluidized bed chamber from below, where the electro-conductive elements (for example iron hollow balls) in a fluidized state are exposed to an external electromagnetic field, resulting in heat generation directly within the fluidized bed chamber. Thus, non-contact energy input is achieved, and heat is generated precisely where it is needed – directly in the chamber of the fluidized bed.

By precisely controlling the supplied energy (in kW, up to a maximum of 40 kW) through the connected induction generator TruHeat MF3040, only the amount of energy necessary for the processes occurring in the fluidized bed is provided.

The following pictures (Figures 4, 5, and 6), taken with a thermal camera, directly depict the heat profile of the fluidized bed in comparison to picture 3, where the induction fluidized bed apparatus is shown from the outside. In these specific experiments, the thermal camera was carefully mounted directly within the fluidized bed reactor above the fluidized electro-conductive iron hollow balls. The left window in each image displays the color representing the heat directly generated within the fluidized bed. The right window correlates 1 to 1 with the left window and graphically displays the corresponding temperature of the non-contact and inductively heated fluidized bed of iron hollow balls. Both windows are scaled up to 220 °C. Picture 4 illustrates the cold fluidized bed (about 20 °C) in an initial state, prior to the input of energy and serves as a benchmark. Figure 5 indicates a warming of the layer and the corresponding rapidly increasing temperature. The layer reaches a temperature of approximately 170 °C for only about 15 seconds. The supplied power is 5 kW in this case.

By using cold fluidization medium, in this example ambient air with a temperature of approximately 20 °C, the layer can also cool down very rapidly when the induction is turned off, what is shown in Figure 6. This rapid temperature adjustment in inductively heated fluidized beds can be of significant importance for temperature-sensitive products.

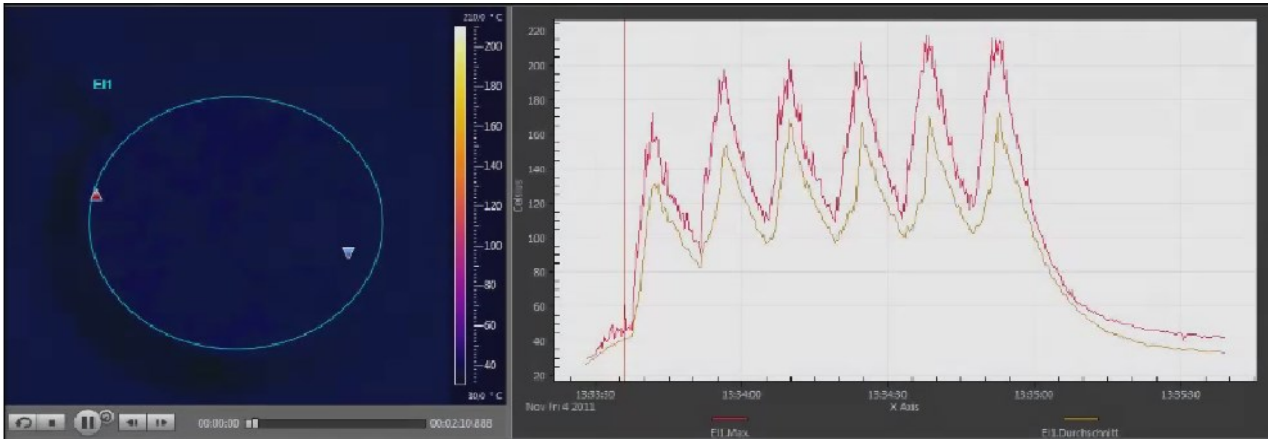


Figure 4. Picture taken with a thermal camera. Top internal view of the fluidized bed chamber, 0 kW input power

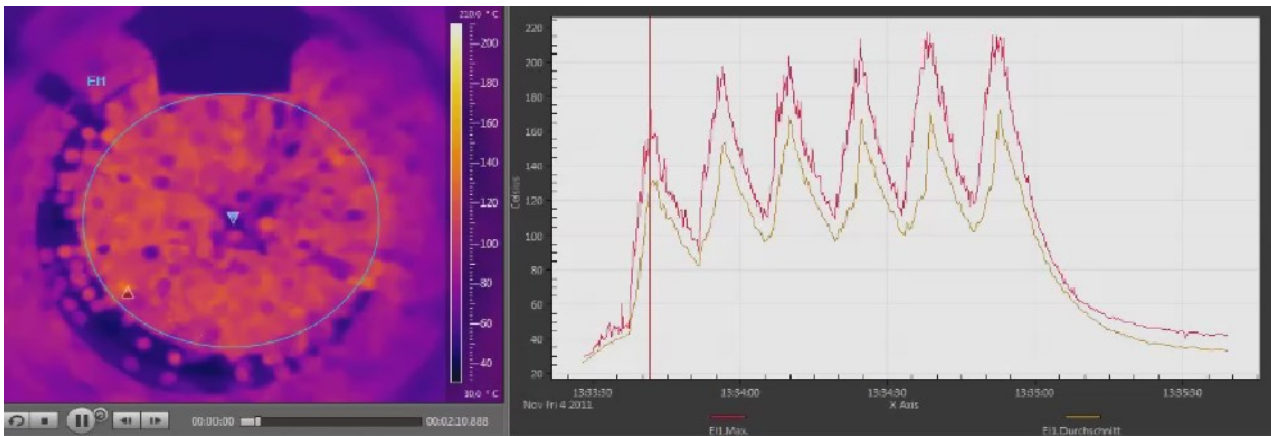


Figure 5. Picture taken with a thermal camera. Top internal view of the fluidized bed chamber, 5 kW input power

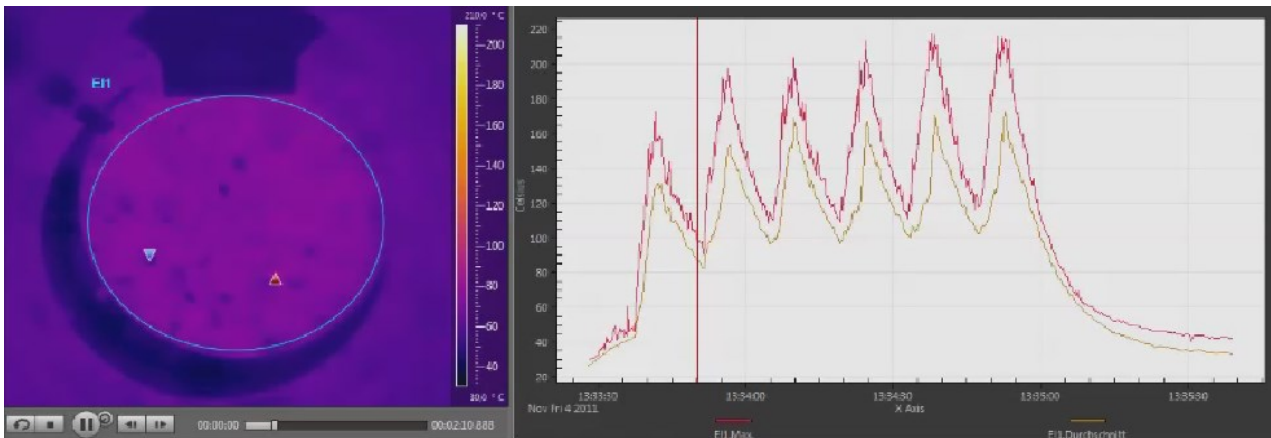


Figure 6. Picture taken with a thermal camera. Top internal view of the fluidized bed chamber, 0 kW input power

It should be noted that the purpose here is to illustrate the speed and precise control of the heating process in induction fluidized beds. The induction fluidized beds shown here are deliberately not insulated to gain a better understanding of the heating process. The introduction of insulation is mandatory for safety reasons and energy conservation, and it was implemented in later research.

## CONCLUSIONS

The main focus of this research was the introduction of an alternative method for conventional energy supply in fluidized beds. The research conducted within the framework of these extensive investigations encompassed the implementation of all common fluidized bed processes, such as drying, coating, granulation, agglomeration, or roasting, using fluidized beds with inductive, non-contact heating. This innovative

method allows for non-contact energy input directly into the fluidized bed chamber through the use of ferromagnetic objects (such as iron hollow balls) located in the fluidized bed chamber along with the substrate to be treated. The electrically conductive, ferromagnetic iron hollow balls fluidize together with the substrate to be treated. In this case, the iron hollow balls serve as a movable (mobile) heat exchanger directly in the fluidized bed chamber. Since they release heat directly through contact and convection in the fluidized bed chamber, the heating process can be additionally intensified. Additionally, instead of iron hollow balls, a securely fixed, stationary object (for example, a securely fixed ferromagnetic iron tube) in the center of the fluidized bed chamber can be used as a stationary heat exchanger.

It can be summarized that the conducted research using fluidized beds with inductive heating shows a significant reduction in heating and cooling phases, resulting in precisely controlled temperature profiles for fluidized bed processes. This allows for the shortening of costly and time-consuming startup procedures in a batch process design within the fluidized bed.

The presented work confirms the potential of the inductive energy input in fluidized beds. The use of fluidized beds with inductive heating opens up new possibilities for the treatment of industrial products

that require rapid and precise adjustment of the temperature profile or are thermolabile.

**Acknowledgement:** This research work was supported with funding from the Federal Ministry of Education and Research (BMBF) as part of the "InnoProfile Transfer" program of the BMBF-Innovationsoffensive Neue Länder „Unternehmen Region“ with project number 03IPT701A.

#### REFERENCES

1. W. Michel, Wirbelschichttechnik in der Energiewirtschaft, Deutscher Verlag für Grundstoffindustrie, 1992.
2. H. Uhlemann, L. Mörl, Wirbelschicht-Sprühgranulation, Springer, 2000.
3. A. Stresing, L. Mörl, J. Neum, M. Jacob, K. Walther, Non-contact energy transfer to a fluidized bed, in: European Drying Conference - EuroDrying 2011, p. 26.
4. V. V. Idakiev, S. Marx, A. Roßau, A. Bück, E. Tsotsas, L. Mörl, Inductive heating of fluidized beds: Influence of fluidization behavior, *Powder Technology*, 286, (2015).
5. V. V. Idakiev, A. Bück, E. Tsotsas, L. Mörl, Modellbasierte Untersuchung des Wärmeübergangs in einer induktiv beheizten Wirbelschicht, *Chemie Ingenieur Technik*, **88** (5), 1 (2016).
6. V. V. Idakiev, Induktiv beheizte Wirbelschichten und deren Anwendungsmöglichkeiten, Doctoral Thesis, Otto-von-Guericke University Magdeburg, Germany, 2019.

## PLA/PVP/bio-synthesized hydrozincite nanocomposite films – photocatalytic and antibacterial activity

K. L. Zaharieva<sup>1\*</sup>, S. S. Dimova<sup>2</sup>, R. T. Eneva<sup>3</sup>, V. N. Hubenov<sup>3</sup>, I. D. Stambolova<sup>4</sup>, D. D. Stoyanova<sup>4</sup>, F. S. Ublekov<sup>2</sup>, O. S. Dimitrov<sup>5</sup>, H. P. Penchev<sup>2</sup>

<sup>1</sup>*Institute of Mineralogy and Crystallography “Acad. I. Kostov”, Bulgarian Academy of Sciences, Acad. G. Bonchev Str., Bl. 107, 1113 Sofia, Bulgaria*

<sup>2</sup>*Institute of Polymers, Bulgarian Academy of Sciences, Acad. G. Bonchev Str., Bl. 103A, 1113 Sofia, Bulgaria*

<sup>3</sup>*The Stephan Angeloff Institute of Microbiology, Bulgarian Academy of Sciences, Acad. G. Bonchev Str., Bl. 26, 1113 Sofia, Bulgaria*

<sup>4</sup>*Institute of General and Inorganic Chemistry, Bulgarian Academy of Sciences, Acad. G. Bonchev Str., Bl. 11, 1113 Sofia, Bulgaria*

<sup>5</sup>*Institute of Electrochemistry and Energy Systems, Bulgarian Academy of Sciences, Acad. G. Bonchev Str., Bl. 10, 1113 Sofia, Bulgaria*

Received: January 18, 2024; Revised: March 27, 2024

Nanocomposite films based on biodegradable polylactic acid (PLA) and PLA/polyvinylpyrrolidone (PVP) with embedded stabilized Hydrozincite powder were synthesized by solution casting method. The Hydrozincite was prepared by plant extract-mediated hydrothermal synthesis. Powder X-ray diffraction analysis and Fourier-transform infrared spectroscopy were used to establish the phase composition and structure of the films. The photocatalytic activity of the obtained nanocomposite films was tested and compared in the reaction of degradation of Malachite Green dye under UV illumination. The photocatalytic results revealed that the PLA/PVP-containing Hydrozincite nanocomposite film leads to a higher degree of degradation of the Malachite Green dye (87 %) after 150 minutes in comparison to that of PLA/Hydrozincite (31%). The antibacterial activity of the prepared nanocomposite films against an *Escherichia coli* control strain was also discussed. The investigated biocomposite films demonstrated high antibacterial efficiency. It was found that the concentration of viable bacterial cells decreases by about 99% after 1 hour of contact time for both investigated composites.

**Keywords:** PLA/PVP/Hydrozincite, nanocomposite, photocatalyst, Malachite Green, antibacterial activity:

### INTRODUCTION

The polymeric/inorganic nanocomposites have a wide variety of applications in photocatalysis, engineering technology and medicine, due to their suitable electronic, optical and mechanical properties [1-3]. Polylactide (PLA) is an environmentally friendly, economical and commercially available polymer that can be used as disposable packaging material [4]. PVP is one of the most widely used vinyl polymers possessing very interesting properties, such as: extremely low cytotoxicity, high chemical and thermal resistance, bio- and hemocompatibility, good environmental stability [5]. Hydrozincite ( $Zn_5(CO_3)_2(OH)_6$ ) is a known carbonate mineral of zinc which can be formed synthetically or naturally (geologically and biologically) [6]. Organic contaminants such as dyes released from textile, pharmaceutical and other industries have caused serious water pollution problems. Previous investigations have revealed that the photocatalytic degradation process is one of the

effective, low-cost and green solutions to resolve these problems [7]. The photocatalytic properties and/or antibacterial efficiency of various hybrid composites such as PLA/ZnO, PLA/ZnO/TiO<sub>2</sub>, PLA/ZnO:Cu/Ag, PVP/ZnO, Cd/Ag/ZnO/PVP, PVP/SnO<sub>2</sub>/TiO<sub>2</sub> have been discussed in the literature [8-15].

The development of novel polymers and polymer-based materials with antibacterial properties is useful in many different applications, such as biomedicine (drug delivery systems), food science and technology, etc. [16]. One of the strategies to enhance the antimicrobial properties of composite polymers is the incorporation of non-toxic oxide nanoparticles (e.g. ZnO, TiO<sub>2</sub>) in the polymer matrix. Biocompatible polymers filled with antibacterial particles (Ag, Cu, TiO<sub>2</sub>, ZnO) are preferred; for instance, those based on polyhydroxyalkanoates such as polyhydroxybutyrate (PHB) and biodegradable polyesters like polylactic acid (PLA) and polyglycolic acid (PGA) [17].

\* To whom all correspondence should be sent:  
E-mail: zaharieva@imc.bas.bg

The aim of this study is to prepare nanocomposite films based on polylactic acid (PLA) and PLA/polyvinylpyrrolidone (PVP) matrix, containing Hydrozincite green synthesized particles. The phase composition and structure were studied using powder X-ray diffraction analysis and Fourier-transform infrared spectroscopy. The photocatalytic behavior of the obtained hybrid materials in the degradation reaction of Malachite Green (MG) dye under UV light and their antibacterial properties against the pathogen *Escherichia coli* were investigated.

## EXPERIMENTAL

### Materials

The polymers, poly(D,L-lactide) (PLA),  $M_w = 60.520 \text{ g.mol}^{-1}$ , Shenzhen Esun Industrial Co., Ltd. and polyvinylpyrrolidone (PVP),  $M_w = 360.000$ , Fluka AG, dichloromethane (Valerus Co.), ethanol (96 % Fisher Scientific, U.K). All chemicals were of analytical grade and were used as received without any further purification.

*Preparation of PLA/Hydrozincite and PLA/PVP/Hydrozincite films.* Films of nanocomposite blend (PLA-PVP) with incorporated hydrozincite (5 wt.%) were prepared by a solution

casting method (Figure 1). For the film preparation, PLA stock solution was prepared by dissolving 1 g of PLA in 30 mL of dichloromethane (DCM). Hydrozincite nanoparticles (5 wt.%) prepared using *Mentha arvensis* plant extract-mediated hydrothermal synthesis [18], were well dispersed in 10 mL of DCM by magnetic stirring for 30 min at room temperature followed by sonication (frequency, 20 kHz; power, 200 W).

For PLA/Hydrozincite nanocomposite film preparation, these two solutions were mixed together with magnetic stirring.

For PLA/PVP/Hydrozincite film preparation, a stock solution of PVP, 0.1g in 10 mL ethanol was prepared and mixed with the Hydrozincite suspension in DCM. In the next step, the solution of PLA and the suspension of PVP-stabilized Hydrozincite were vigorously mixed by vortex. Finally, both PLA/Hydrozincite and PLA/PVP-Hydrozincite dispersions were sonicated for 30 min until a homogenized blend was obtained. The resulting solutions were poured into a Teflon mold ( $8 \times 4 \times 1.5 \text{ cm}$ ) and rested under hood till the solvent was completely evaporated, resulting a dry  $60 \mu\text{m}$  thick film.

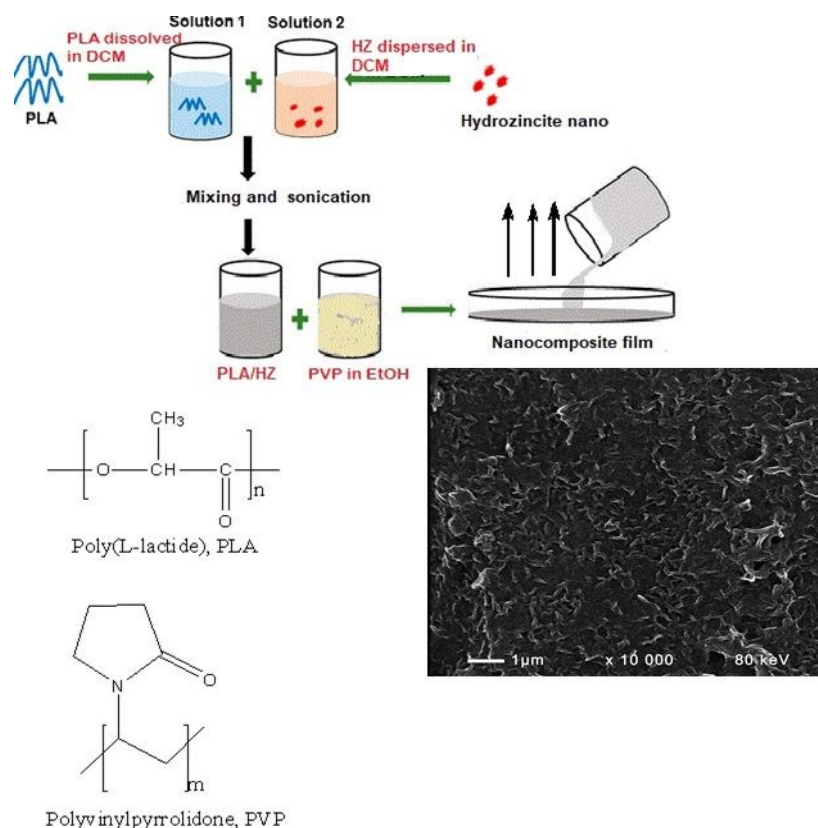


Fig. 1. Preparation of the PLA/PVP/Hydrozincite nanocomposite films

### Physicochemical characterization

The physicochemical characterization of the samples was performed using FT-IR spectroscopy and powder X-ray diffraction analysis (PXRD). PXRD analysis was carried out on a Bruker D8 Advance ECO diffractometer in reflection mode with Ni-filtered Cu K $\alpha$  radiation at 40 kV. The FT-IR spectroscopy was carried out on a Fourier infrared spectrometer Bruker-Vector 22 in the range 400-4000 cm<sup>-1</sup>. The FT-IR spectra of the samples were registered using KBr tablets.

### Photocatalytic tests

The oxidative photodegradation of an aqueous solution of Malachite Green dye with concentration of 5 ppm was investigated in a semi-batch slurry reactor using the synthesized PLA/Hydrozincite and PLA/PVP/Hydrozincite films as catalyst and 60 ml of dye solution under constant stirring in an air flow. The photocatalytic tests were carried out using UV-Vis absorbance spectrophotometer in the wavelength range from 200 to 800 nm ( $\lambda_{\text{max}} = 615$  nm) and polychromatic UV-A lamp illumination (18W) with maximum of the emission at 365 nm and intensity of illumination 0.66 mW.cm<sup>-2</sup>. The tested systems were left in the dark for about 30 min before switching on the UV irradiation for 2 hours and 30 minutes in order to reach adsorption-desorption equilibrium state. Periodically sample aliquots were taken from the solution. The degree of dye degradation was calculated using the dependence:  $((C_0 - C)/C_0) \times 100$ , where  $C_0$  and  $C$  are initial concentration before turning on the illumination and residual concentration of the dye solution after illumination for a selected time interval.

### Antibacterial ability

The antimicrobial activity was determined by placing an appropriate amount of the polymer sample in contact with a microbial suspension of a certain cell density. A modification of the ASTM standard test method E 2149-10 was used, which consisted of placing a 0.1 g sample of the composite film in contact with 1 ml of a microbial suspension of *E. coli* (ATCC 25922) in a well of a 24-well test plate (Techno Plastic Products AG, Switzerland). During cultivation, the plate was placed on an Advantage-Lab shaker apparatus, AL05-06, which provided continuous agitation at 150 rpm. Cultivation was carried out at a constant temperature of  $20 \pm 1^\circ\text{C}$  provided in a thermostated room. The antimicrobial effect was determined by counting the number of colony-forming units (CFU) in aliquots of

the microbial suspension that was in contact with the composite film at certain time intervals after the start of cultivation (1 h, 24 h, 48 h and on the fifth day).

The bacterial suspension used in the experiment was prepared from an 18-hour shake culture of *E. coli* (ATCC 25922). The composition of the nutrient medium used for the development of the strain is as follows (for 1 L): 10 g of tryptone, 5 g of yeast extract and 10 g of sodium chloride. The 18 h culture grown in the indicated medium was centrifuged at 3500 rpm/10 min. The collected cell pellets were washed and resuspended in a sterile buffer with the following composition (for 1 liter): 0.150g KCl, 2.25g NaCl, 0.05g NaHCO<sub>3</sub>, 0.12g CaCl<sub>2</sub>.6H<sub>2</sub>O (pH 7.0). The final concentration of the bacterial cell suspension should be in the range of  $1.5\text{-}3.0 \times 10^6$  CFU [19].

## RESULTS AND DISCUSSION

The PXRD patterns of the investigated samples are presented on Figure 2.

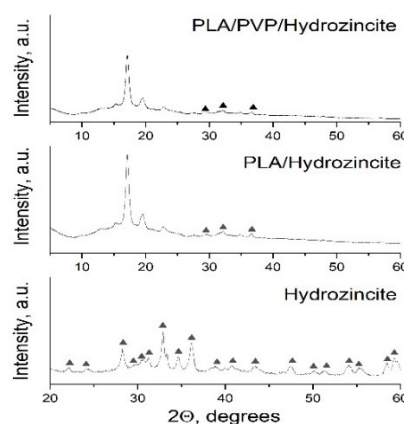


**Fig. 2.** PXRD patterns of PLA/Hydrozincite, PLA/PVP/Hydrozincite films and Hydrozincite.

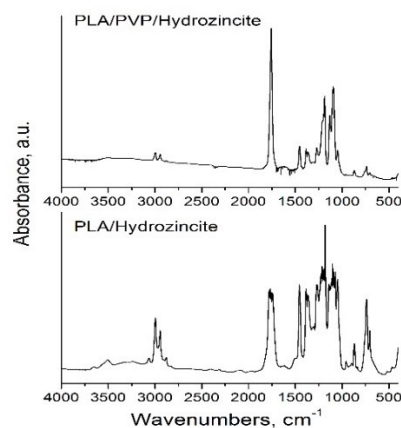


**Fig. 3.** FT-IR spectra of PLA/Hydrozincite and PLA/PVP/Hydrozincite films.

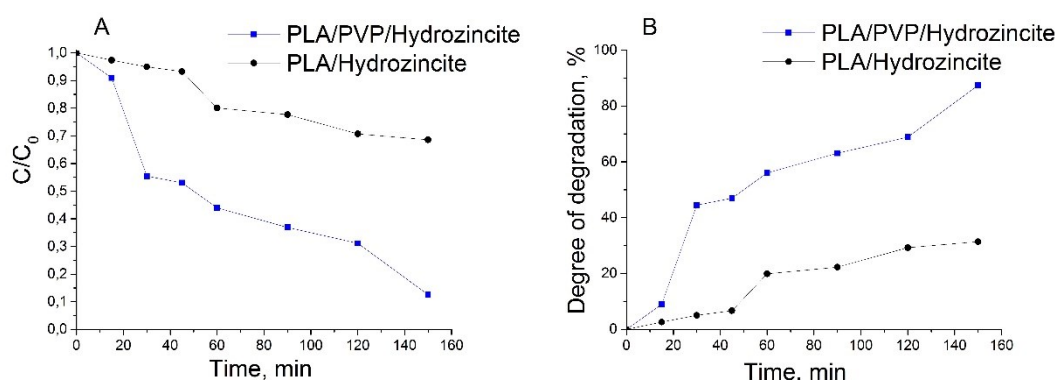
The PXRD analyses of PLA/Hydrozincite and PLA/PVP/Hydrozincite films established diffraction peaks, corresponding to an orthorhombic crystal structure of PLA. The PXRD patterns of PLA/Hydrozincite and PLA/PVP/Hydrozincite films showed additional three diffraction peaks, corresponding to hydrozincite phase (JCPDS 72-1100) at  $29.02^\circ$ ,  $33.06^\circ$  and  $36.95^\circ$   $2\theta$ . Due to the amorphous nature of PVP and its small quantity, its presence was not registered.

Figure 3 represents the FT-IR spectra of PLA/Hydrozincite and PLA/PVP/Hydrozincite films obtained in the range of  $400\text{--}4000\text{ cm}^{-1}$  at room temperature. Characteristic absorption peaks were found around  $1750\text{ cm}^{-1}$  which correspond to the stretching vibration of  $\text{C}=\text{O}$  and a peak at  $1260\text{ cm}^{-1}$ , which was attributed to the bending vibration of the  $\text{CH}(\text{CH}_3)$  plane. The bending vibration at  $1090\text{ cm}^{-1}$  is due to the presence of ester groups  $\text{C}-\text{O}$ , which belong to PLA [20]. The absorption peak at  $2883\text{ cm}^{-1}$  is due to the  $\text{C}-\text{H}$  stretching vibrations and the peak registered at  $1346\text{ cm}^{-1}$  corresponds to the  $\text{C}-\text{O}-\text{H}$  bending vibrations. The peak at  $1180\text{ cm}^{-1}$  could be attributed to the  $\text{C}-\text{O}-\text{C}$  stretching vibrations. The peaks around  $2900\text{--}2850\text{ cm}^{-1}$  are due to the  $\text{C}-\text{H}$  stretching vibrations and the peak observed at  $1400\text{ cm}^{-1}$  corresponds to the PVP [21]. The absorption bands at  $830$ ,  $1383$ ,  $1510\text{ cm}^{-1}$  are assigned to the characteristic vibrations of hydrozincite [22].

The photocatalytic activities of the prepared PLA/Hydrozincite and PLA/PVP/Hydrozincite nanocomposite films were tested and compared in the reaction of degradation of MG dye as model

pollutant in aqueous solutions under UV irradiation. Figures 4A and 4B present the concentration changes  $C/C_0$  and the degree of degradation of MG dye with time of UV illumination, respectively. The photocatalytic results revealed that PLA/PVP/Hydrozincite nanocomposite photocatalysts demonstrate higher photocatalytic activity in MG dye degradation (87%) in comparison to that of PLA/Hydrozincite films (31%). The values of apparent rate constants (calculated using logarithmic linear dependence:  $-\ln(C/C_0) = k.t.$ ) of the studied PLA/PVP/Hydrozincite and PLA/Hydrozincite catalysts are  $12.3 \times 10^{-3}\text{ min}^{-1}$  and  $2.7 \times 10^{-3}\text{ min}^{-1}$ , respectively. It could be supposed that the PVP surface stabilized Hydrozincite and the improved PVP/Hydrozincite dispersibility into the PLA matrix plays a significant role for the enhanced photocatalytic activity of these composite films. Other research groups have also established an improvement of the catalytic activity towards degradation of both sulfamethoxazole and Reactive Red-141 dye in the presence of PVP-surface stabilized ZnO [23, 24].

The antimicrobial properties of the investigated materials were evaluated with *E. coli* (ATCC 25922) strain. A standardized suspension of *E. coli* strain was used as a control and PLA foil immersed in buffer solution was used as a blank and was found to contain  $5.9 \cdot 10^6$  CFU/mL. Both composites exhibit high antimicrobial activity against *E. coli* and above 99 % of reduction in CFU number since the first sampling after 1 hour of cultivation of the bacterial suspension in contact with the material (Table 1).



**Fig. 4.** A) The concentration ratio  $C/C_0$  and B) Degree of degradation of Malachite Green dye with time of UV illumination.

The antibacterial efficiency of the obtained hybrid films might be due to the release of zinc ions from the hydrozincite particles, which can pass through the cell membrane, causing oxidative damage. These processes might be responsible for

the enhanced antibacterial activity of the PLA/PVP/Hydrozincite and PLA/Hydrozincite nanocomposite films [25, 26].

**Table 1.** Log reduction of colony-forming units (CFU) in *E. coli* K-12 suspension placed in contact with different biopolymer composites.

Cultivation time, h	Control ( <i>E. coli</i> ) Log Reduction	Biocomposite samples	
		PLA/hydrozincite Log Reduction	PLA/PVP/hydrozincite Log Reduction
0	0	0	0
1	0	4.071	3.771
24	0	4.771	4.771
48	0	4.771	4.771
120	0	4.771	4.771

### CONCLUSIONS

A solution casting method was successfully used to prepare PLA/Hydrozincite and PLA/PVP/Hydrozincite films. The PLA/PVP/Hydrozincite hybrid photocatalysts demonstrated enhanced photocatalytic activity towards degradation of MG dye (87%) after 150 minutes of UV irradiation. The obtained composite PLA/PVP/Hydrozincite could be applied for purification of water polluted with Malachite Green textile dye. Both PLA and PLA/PVP-embedded bio-synthesized hydrozincite composites have excellent bactericidal activity against *E. coli* (90% after 1 hour of contact time). The prepared polymer/inorganic nanocomposite films are promising candidates as alternative materials in various food packing applications.

**Acknowledgement:** The authors express their gratitude to the project with the Fund “Scientific Investigations”, Bulgaria, KP-06-N69/8 (KII-06-H69/8), “Novel polymer-hybrid materials containing (bio)synthesized metal oxide particles with improved photocatalytic and antimicrobial potential” for the financial support.

### REFERENCES

- A. F. Moreno, M. F. González Pérez, *J. Mater. Sci. Eng. A*, **10**, 111 (2020).
- V. Melinte, L. Stroea, A. L. Chibac-Scutaru, *Catalysts*, **9**, 986 (2019).
- A. Shakeel, K. Rizwan, U. Farooq, S. Iqbal, A. A. Altaf, *Chemosphere*, **294**, 133772 (2022).
- R. Pantani, G. Gorrasi, G. Vigliotta, M. Murariu, P. Dubois, *Eur. Polym. J.*, **49**, 3471 (2013).
- M. Teodorescu, M. Bercea, S. Morariu, *Biotechnol. Adv.*, **37**, 109 (2019).
- E. Turianicová, M. Kaňuchová, A. Zorkovská, M. Holub, Z. Bujňáková, E. Dutková, M. Baláž, L. Findoráková, M. Balintová, A. Obut, *J. CO<sub>2</sub> Util.*, **16**, 328 (2016).
- S. L. Lee, C.-J. Chang, *Polymers*, **11**, 206 (2019).
- S. Abdolalian, M. Taghavijeloudar, *J. Clean. Prod.*, **365**, 132833 (2022).
- I. Kim, K. Viswanathan, G. Kasi, K. Sadeghi, S. Thanakkasaranee, J. Seo, *Polymers*, **11**, 1427 (2019).
- W. J. Chong, S. Shen, Y. Li, A. Trinchì, D. Pejak, I. L. Kyrtzis, A. Sola, C. Wen, *J. Mater. Sci. Technol.*, **111**, 120 (2022).
- D. Virovska, D. Paneva, N. Manolova, I. Rashkov, D. Karashanova, *Appl. Surf. Sci.*, **311**, 842 (2014).
- A. Tajdari, A. Babaei, A. Goudarzi, R. Partovi, *J. Plast. Film Sheeting*, **36**, 285 (2020).
- C. Vasile, M. Răpă, M. Ștefan, M. Stan, S. Macavei, R. N. Darie-Niță, L. Barbu-Tudoran, D. C. Vodnar, E. E. Popa, R. Ștefan, G. Borodi, M. Brebu, *EXPRESS Polym. Lett.*, **11**, 531 (2017).
- S. Selvam, M. Sundrarajan, *Carbohydr. Polym.*, **87**, 1419 (2012).
- S. Vignesh, S. Suganthi, J. K. Sundar, V. Raj, P. R. I. Devi, *Appl. Surf. Sci.*, **479**, 914 (2019).
- M. R. E. Santos, A. C. Fonseca, P. V. Mendonça, R. Branco, A. C. Serra, P. V. Morais, J. F. J. Coelho, *Materials*, **9**, 599 (2016).
- D. Olmos, J. González-Benito, *Polymers*, **13**, 613 (2021).
- D. Stoyanova, I. Stambolova, V. Blaskov, P. Georgieva, M. Shipochka, K. Zaharieva, O. Dimitrov, P. Markov, V. Dyakova, Y. Kostova, R. Mladenova, G. Tzvetkov, N. Boshkova, N. Boshkov, *Appl. Sci.*, **12**, 1096 (2022).
- A. Marra, C. Silvestre, D. Duraccio, S. Cimmino, *Int. J. Biol. Macromol.*, **88**, 254 (2016).
- H. Khalil, H. M. Hegab, L. Nassar, V. S. Wadi, V. Naddeo, A. F. Yousef, F. Banat, S. W. Hasan, *J. Water Process Eng.*, **45**, 102510 (2022).
- L. Saravanan, S. Diwakar, R. Mohankumar, A. Pandurangan, R. Jayavel, *Nanomater. Nanotechnol.*, **1**, 42 (2011).
- M. Y. Nassar, M. M. Moustafa, M. M. Taha, *RSC Adv.*, **6**, 42180 (2016).
- M. Darwish, A. Mohammadi, N. Assi, *Bull. Mater. Sci.*, **40**, 513 (2017).
- K. Singh, Nancy, M. Bhattu, G. Singh, N. M. Mubarak, J. Singh, *Sci. Rep.*, **13**, 13886 (2023).
- D. Q. Khai, H. H. Chi, N. H. Duong, N. T. Trong, M. H. Hanh, *VNU Journal of Science: Natural Sciences and Technology*, **39**, 20 (2023).
- L. Zhang, Y. Ding, M. Povey, D. York, *Prog. Nat. Sci.*, **18**, 939 (2008).

## Preparation and antimicrobial activity of silver nanoparticles impregnated with halloysite clay

K. L. Zaharieva<sup>1\*</sup>, R. T. Eneva<sup>2</sup>, S. L. Mitova<sup>2</sup>, O. S. Dimitrov<sup>3</sup>, H. P. Penchev<sup>4</sup>

<sup>1</sup>*Institute of Mineralogy and Crystallography "Acad. I. Kostov", Bulgarian Academy of Sciences, Acad. G. Bonchev Str., Bl. 107, 1113 Sofia, Bulgaria*

<sup>2</sup>*The Stephan Angeloff Institute of Microbiology, Bulgarian Academy of Sciences, Acad. G. Bonchev Str., Bl. 26, 1113, Sofia, Bulgaria*

<sup>3</sup>*Institute of Electrochemistry and Energy Systems, Bulgarian Academy of Sciences, Acad. G. Bonchev Str., Bl. 10, 1113 Sofia, Bulgaria*

<sup>4</sup>*Institute of Polymers, Bulgarian Academy of Sciences, Acad. G. Bonchev Str., Bl.103A, 1113 Sofia, Bulgaria*

Received: February 08, 2024; Revised: May 10, 2024

In the present work, nanotubular halloysite clay was ultrasonically treated and impregnated with silver nanoparticles. The citrate surface-stabilized silver nanoparticles dispersion was prepared using an effective method of electrochemical synthesis. The elemental and phase composition, and the structure of the obtained AgNPs-impregnated and pristine halloysite were investigated by various methods such as X-ray fluorescence (XRF), powder X-ray diffraction analyses and Fourier-transform infrared spectroscopy. The Ag-loaded halloysite sample with 0.454 wt.% silver content was confirmed by the XRF analysis. The antimicrobial activity of the pristine and the AgNPs-impregnated halloysite clay was tested against *Escherichia coli* ATCC 25922 (Gram-negative) and *Bacillus subtilis* ATCC 6633 (Gram-positive) strains. The results show that pure halloysite does not exhibit antibacterial activity. The AgNPs-impregnated halloysite demonstrates antibacterial activity against *Escherichia coli* and *Bacillus subtilis* with only bacteriostatic effect.

**Keywords:** halloysite, silver nanoparticles, antimicrobial activity, *Escherichia coli*, *Bacillus subtilis*

### INTRODUCTION

Halloysite nanotubes (HNTs) are clay minerals that belong to the kaolin group of clays. They have been widely investigated due to their interesting structure and properties in recent decades. HNTs are dioctahedral 1:1 clay minerals present in soils. This mineral can be found worldwide, in particular in wet tropical and subtropical regions and weathered rocks. Countries such as Belgium, China, New Zealand and France are rich in this clay [1]. The empirical chemical formula of halloysite nanotube aluminosilicate clay is  $\text{Al}_2\text{Si}_2\text{O}_5(\text{OH})_4 \cdot 2\text{H}_2\text{O}$  [2]. Halloysite consists of hollow cylinders formed by multiple rolled alumino-silicate layers [3]. It is present in two forms, the hydrated form (Halloysite-10 Å) and the dehydrated one (Halloysite-7 Å) [4]. Halloysite-based nano-composites have attracted attention as a potential material for various biological applications as enzyme and antibacterial immobilization, controlled drug delivery, etc. [3]. The profound scientific interest in both natural and synthetic HNTs clays could be attributed to their unique physico-chemical properties: their nanotubular structures, length-to-diameter (L/D) ratio, high specific surface area, hydrophobicity and intercalating properties [3, 5].

The antibacterial application of halloysite-halloysite-based nanocomposites containing different metal nanoparticles such as Ag, Cu, Au, Fe, and Ag-Cu bimetallic nanoclusters or metal oxides ( $\text{ZnO}$ ,  $\text{Fe}_3\text{O}_4$ ,  $\text{CeO}_2$ ,  $\text{MnO}_x$ ) has been studied by many research groups [3, 6-15]. In human daily life, antibacterial agents and nanocomposite materials are widely used and effectively help in society health shielding by preventing the transmission of many existing pathogens and the corresponding infectious diseases. Lately, antibacterial properties of transition metal nanomaterials have become increasingly attractive areas of research, including silver nanoparticles, silver nanorods, copper nanoparticles, etc. Among them, silver attracts attention since it is strongly active against a broad spectrum of fungal and bacterial species, and displays low toxicity, low volatility and high thermal stability. It is also effective against antibiotic-resistant strains of microorganisms [6].

The present paper aims at preparing AgNPs-impregnated halloysite clay. An effective electrochemical method was used for the preparation of citrate surface stabilized concentrated silver nanoparticles dispersion. The phase and elemental composition, and the structure of the AgNPs-impregnated halloysite and pristine halloysite were

\* To whom all correspondence should be sent:  
E-mail: zaharieva@imc.bas.bg

determined using different physicochemical methods. The antimicrobial activity of AgNPs-impregnated halloysite against pathogens *E. coli* and *B. subtilis* was studied as well.

## EXPERIMENTAL

### Preparation of AgNPs- impregnated halloysite material

The halloysite nanoclay ( $(\text{H}_4\text{Al}_2\text{O}_9\text{Si}_2 \cdot 2\text{H}_2\text{O})$ ,  $M = 294.12 \text{ g}\cdot\text{mol}^{-1}$ ) from Sigma-Aldrich was impregnated with a citrate surface-stabilized Ag nanoparticles dispersion. Silver nanoparticles dispersion with total silver concentration of  $400 \text{ mg}\cdot\text{L}^{-1}$  was synthesized using a slightly modified methodology proposed in [16]. The electrochemical reduction method used square-shaped bulk silver (probe 999) electrodes as metal source, 47 V applied DC voltage and dissolved sodium citrate ( $500 \text{ mg}\cdot\text{L}^{-1}$ ) as surface stabilizing agent. The advantage of the electrochemical method is the purity of the obtained colloidal silver and there is no need to purify the product from residual salts as in the case of chemical reduction methods. The impregnation was performed using ultrasonic treatment of 2.1 g of halloysite and 30 ml of AgNPs colloidal dispersion (400 ppm) for 10 minutes followed by stirring (500 rpm) for 5 hours at  $50^\circ\text{C}$  using a magnetic stirrer. After that, the AgNPs-impregnated halloysite was filtered and washed several times with distilled water until neutral reaction and the resultant pale-brown fine powder was dried for 1 hour at  $50^\circ\text{C}$  in a vacuum oven (Figure 1).

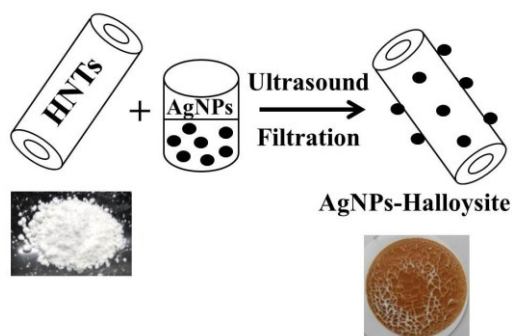


**Fig. 1.** Preparation of AgNPs-impregnated halloysite hybrid.

### Physicochemical characterization

The phase and elemental composition, and the structure of the obtained AgNPs-impregnated halloysite material and the pristine halloysite were determined by powder X-ray diffraction analyses, X-ray fluorescence (XRF) and Fourier-transform infrared spectroscopy (FT-IR). The powder X-ray diffraction analysis (PXRD) of the investigated

samples was performed on an X-ray powder diffractometer "Empyrean" within the range of  $2\theta$  values between  $2^\circ$  and  $70^\circ$  using  $\text{Cu K}\alpha$  radiation ( $\lambda = 0.154060 \text{ nm}$ ) at 40 kV and 30 mA. The phases in the prepared materials were established using the ICDD database. Wave-dispersive X-ray fluorescence (WDXRF) analyses were performed using a Supermini 200 spectrometer (Rigaku, Osaka, Japan). Data collection was performed by wave-dispersed X-ray fluorescence at 50 kV and 4.0 mA. Data processing was performed using the ZSX software package. The analysis used a semi-quantitative method to determine the elemental composition. The results obtained by the method of semi-quantitative analysis "SQX" allow the determination of the chemical composition of samples without the need for comparative materials (standards). The FT-IR spectra of the prepared materials were recorded on a Bruker Tensor 37 spectrometer in the region  $4000\text{--}400 \text{ cm}^{-1}$ , using the KBr pellet technique. The surface morphology of the samples was investigated by scanning electron microscopy (SEM) using Zeiss Evo 10 microscope (Carl Zeiss Microscopy, Oberkochen, Germany). TEM analyses were carried out on an HR STEM JEOL JEM 2100.

### Antimicrobial activity

**Materials and methods.** *Escherichia coli* ATCC 25922 (Gram-negative, G-) and *Bacillus subtilis* ATCC 6633 (Gram-positive, G+) were used as test microorganisms. Overnight cultures in Mueller-Hinton Broth were diluted to approx.  $5 \times 10^5$  colony forming units (CFU)/mL.

The antimicrobial activity of the materials was evaluated by the drop dilution method in a 96-well sterile plate, in the presence of resazurin [17]. Resazurin dye indicates cell viability by changing colour from blue to pink upon chemical reduction resulting from aerobic respiration of growing cells. Halloysite and Ag-halloysite were tested in two-fold decreasing concentrations from 20 to  $0.312 \text{ mg}\cdot\text{mL}^{-1}$ . The lowest concentration of nanoparticle suspension that inhibited cell growth (dye did not convert to pink) was defined as the minimum inhibitory concentration (MIC).

Gentamycin for *E. coli* in concentrations from 0.5 to  $0.008 \text{ mg}\cdot\text{mL}^{-1}$  and erythromycin for *B. subtilis* in concentrations from 20 to  $0.312 \text{ mg}\cdot\text{mL}^{-1}$  were used as positive controls.

## RESULTS AND DISCUSSION

The recorded powder X-ray diffraction patterns of pristine halloysite and AgNPs-impregnated halloysite are presented in Figure 2A.

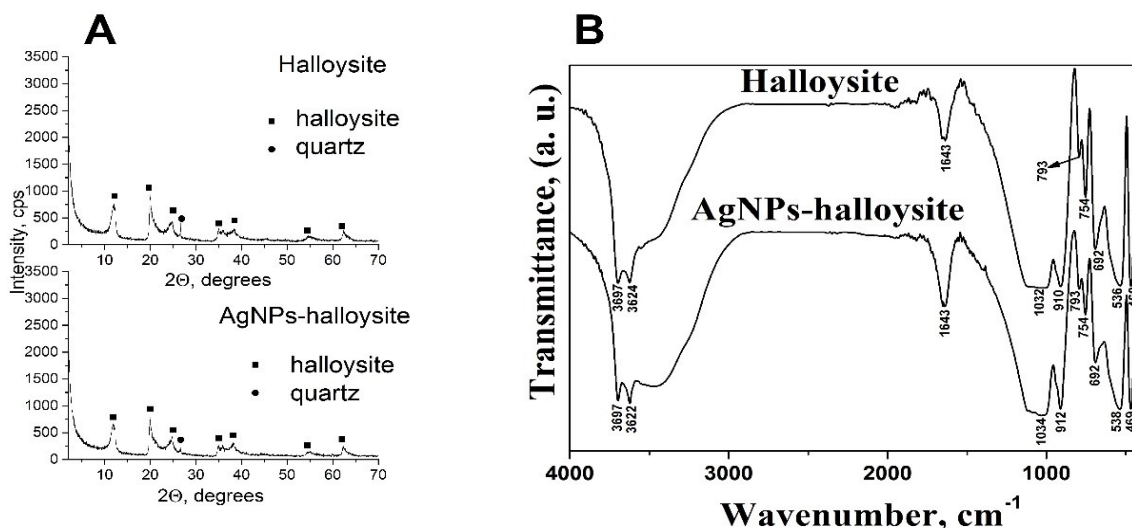


**Fig. 2.** A) XRD patterns of pristine halloysite and AgNPs-impregnated halloysite and B) FT-IR spectra of pure halloysite and AgNPs-impregnated halloysite.

**Table 1.** Elemental composition (wt.%) of pristine halloysite and AgNPs-impregnated halloysite, determined by XRF analysis.

Sample	Si/Al (wt. ratio)	Ag	Al	Si	P	S	K	Ca	Ti	Fe	Ni	Zn
AgNPs-impregnated halloysite	0.68	0.454	38.1	55.7	2.17	0.175	0.193	1.52	0.222	1.36	0.0836	-
halloysite	0.68	-	38.0	56.1	2.15	0.217	0.294	1.46	0.218	1.33	0.0847	0.0228

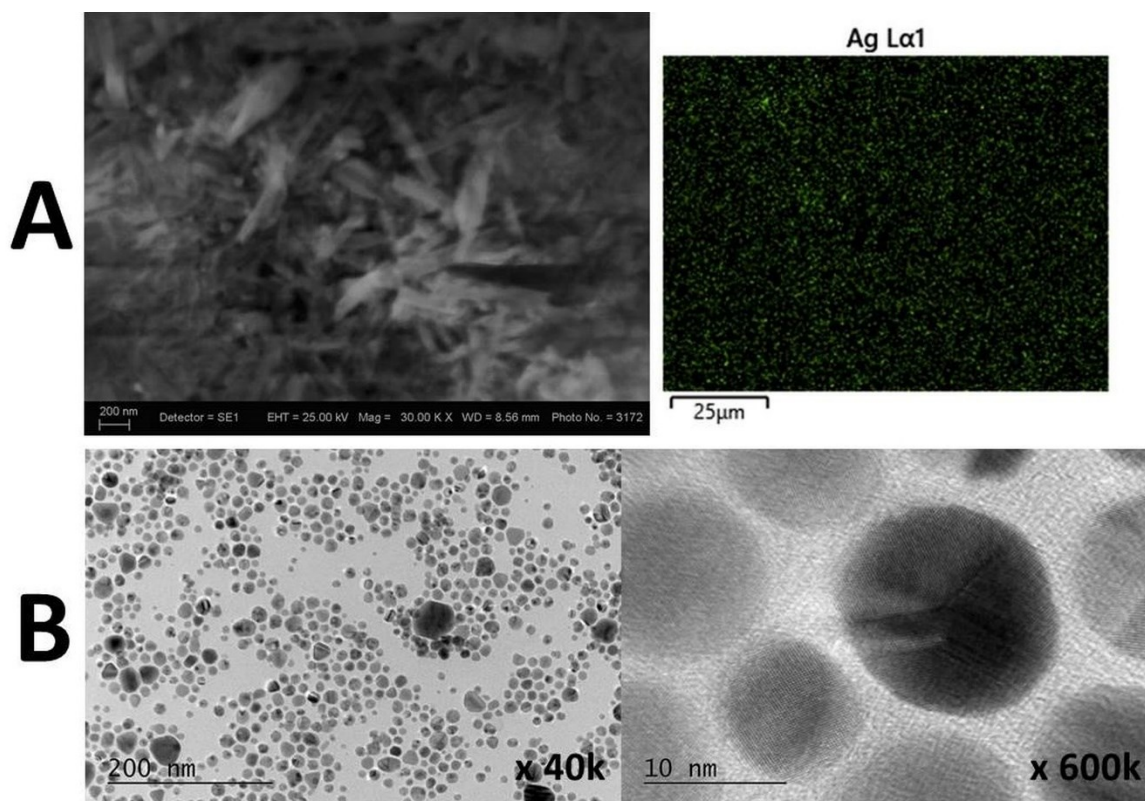


**Fig. 3.** A) SEM images of AgNPs-impregnated halloysite and B) TEM images of AgNPs.

The powder X-ray diffraction analysis of the investigated samples pointed to the presence of halloysite phase (PDF-00-009-0453) in AgNPs-impregnated and pure halloysites. A reflection peak corresponding to the small content of quartz (PDF-00-033-1161) was also found. The silver phase was not established owing to its small amount below the sensitivity threshold. The PXRD results show that the modification of halloysite with silver nanoparticles does not lead to observable structural changes.

The XRF data are displayed in Table 1. The silver content in the AgNPs-impregnated halloysite material is 0.454 wt.%. The Si/Al ratios in the investigated halloysite materials are preserved after impregnation with silver nanoparticles. The results from XRF and PXRD analyses show that after the impregnation, the halloysite structure is retained. Similar structure retention referred to the halloysite clay mineral after impregnation with Cu and Co oxides was established by another research group [18].

Figure 2B shows the FT-IR spectra of the investigated samples. The bands at 3697  $\text{cm}^{-1}$  and 3622-3624  $\text{cm}^{-1}$  correspond to OH stretching vibrations attributed to the inner surface and inter-layer hydroxyl groups of halloysite clay. A characteristic peak was recorded at 1643  $\text{cm}^{-1}$  due to the O-H vibration of adsorbed water on the halloysite surface [19]. The bands at wavenumbers 1032-1034  $\text{cm}^{-1}$  and 910-912  $\text{cm}^{-1}$  were assigned to the stretching vibrations of Si-O-Si and bending modes of Al-O-H [20, 21]. The vibrations observed

at 754 and 692  $\text{cm}^{-1}$  are due to perpendicular Si-O stretching [21]. The band observed at 793  $\text{cm}^{-1}$  was attributed to the symmetric stretching of Si-O. The peaks at 536-538 and 469  $\text{cm}^{-1}$  were attributed to the deformation of both Al-O-Si and Si-O-Si [22]. The data determined by FT-IR spectroscopy are in agreement with results established using powder X-ray diffraction and XRF analyses. The presence of spherical AgNPs with average particle diameter about 20 nm on the surface of tubular shaped halloysite is observed using SEM and TEM studies (Figures 3A and 3B).

Clays are materials with wide application for health purposes, because they are natural, easily available, biocompatible, low-cost, capable of crossing cellular membranes [23]. Some authors assume that, in contrast to other clays, halloysite itself is not considered an antibacterial material. Depending on the goal, it can be used both to maintain a given microbial population and as a carrier of ions or substances with antimicrobial action [24]. On the other hand, Abhinayaa *et al.* [25] compared the antibacterial activity of pristine halloysite with that of halloysite modified with various surfactants and reported inhibition of phytopathogenic G- bacteria at 2.5 mg/mL for halloysite and at 0.3-1.25 mg/mL for its modified forms. In our study, pristine halloysite showed no antibacterial activity, even at a concentration of 20 mg/mL. The AgNPs-loaded form of halloysite displayed inhibitory activity against the tested bacteria at concentrations of 0.312 mg/mL for *E. coli* and 1.25 mg/mL for *B. subtilis* (Figures 4-6).

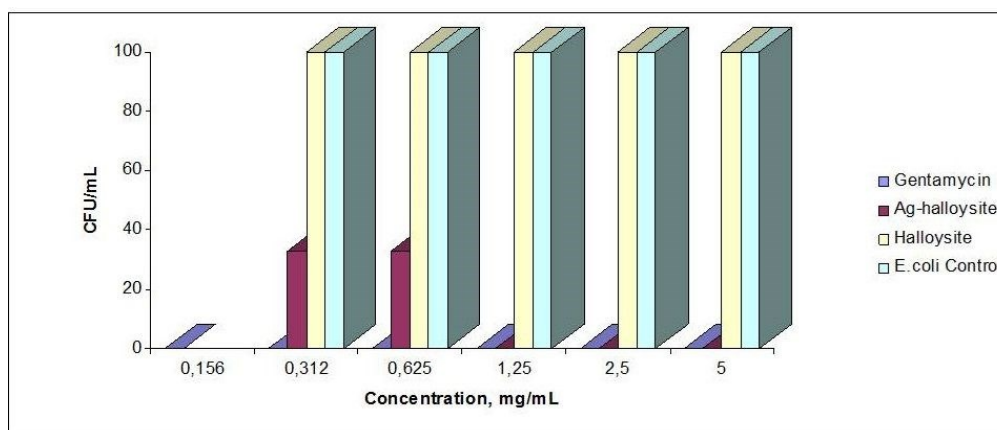
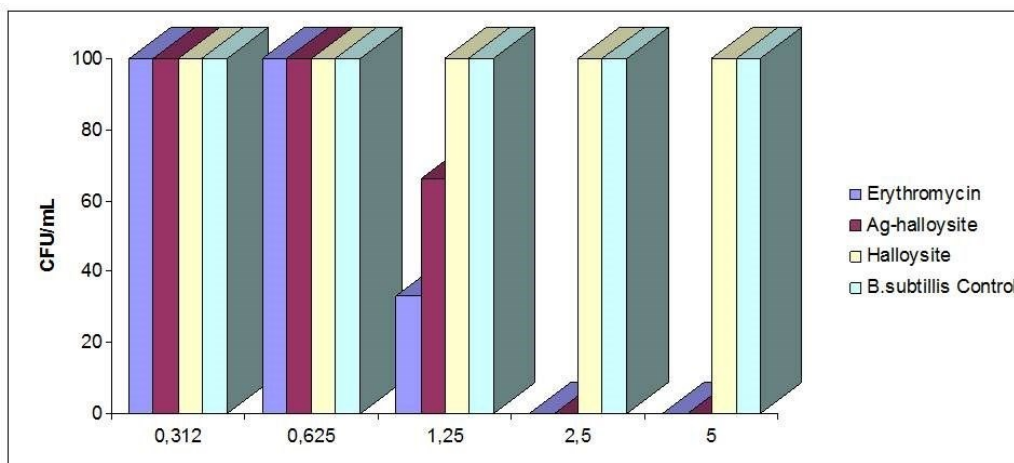
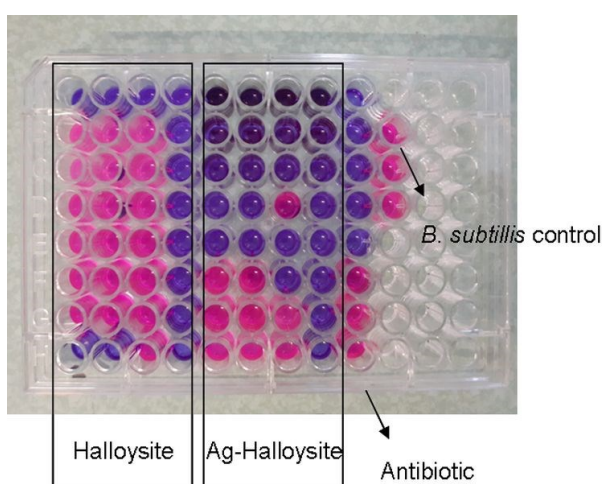


Fig. 4. Antimicrobial activity of AgNPs-impregnated halloysite against *E. coli* ATCC 25922 compared to halloysite.



**Fig. 5.** Antimicrobial activity of AgNPs-impregnated halloysite against *B. subtilis* ATCC 6633 compared to halloysite.



**Fig. 6.** Drop dilution method in a 96-well sterile plate, according to Sarker *et al.* [17]. Antimicrobial activity of halloysite and AgNPs-impregnated halloysite was tested in decreasing concentrations from 20 to 0.312 mg/mL. Wells in magenta contain inhibited bacterial culture; wells in pink contain growing bacteria. The antibiotic tested is erythromycin in the same decreasing concentrations.

These results indicate that the suppressive action is due to the silver nanoparticles. After inoculation on a solid medium of the bacterial cultures containing silver nanoparticles-impregnated halloysite at these concentrations, only a reduction in the number of CFU was observed, and not a lack of growth, which means that the action of silver nanoparticles-impregnated halloysite on the tested strains is bacteriostatic. Both G- and G+ bacteria have a negative charge on the cell surface, suggesting an electrostatic interaction with the positively charged nanoparticles and adhesion on the bacterial cell [24]. This could cause structural changes or functional damage, due to the production of oxygen radicals catalyzed by silver ions [6], which leads to an imbalance in the redox potential of bacterial cells. In our study, the G+ test strain shows

higher resistance. The mechanism of interaction between the prepared AgNPs-impregnated halloysite and the bacterial cells, as well as the ability of *B. subtilis* to tolerate higher concentrations of silver nanoparticles are to be elucidated by further studies. The prepared AgNPs-impregnated halloysite material could find possible applications as antibacterial filter for treatment of contaminated waters and as potential catalyst for oxidation of CO to CO<sub>2</sub>.

## CONCLUSIONS

The silver-impregnated halloysite material was successfully prepared using silver nanoparticles obtained by the electrochemical reduction method. The presence of 0.454 wt.% of silver in the AgNPs-impregnated halloysite sample was determined by XRF analysis. The results from the PXRD analyses show that after the impregnation, the halloysite structure is preserved. Silver-impregnated halloysite demonstrated inhibitory activity against *E. coli* and *B. subtilis* at concentrations of 0.312 and 1.25 mg/mL, respectively. A good antimicrobial activity towards *E. coli* bacteria was displayed by the silver-impregnated halloysite sample. The *B. subtilis* test strain showed higher resistance. The effect of Ag-loaded halloysite against *E. coli* and *B. subtilis* is bacteriostatic. Comparison with pristine halloysite shows that the suppressive action is due to the silver nanoparticles.

**Acknowledgement:** The authors acknowledge the technical support from the project PERIMED BG05M2OP001-1.002-0005/29.03.2018 (2018–2023). H.P. thanks to the National Infrastructure NI SEVE supported by the Bulgarian Ministry of Education and Science under grant agreement N° Д01-385/Д01-18.12.2020. Thanks are due to Liliya

K. L. Zaharieva et al.: Preparation and antimicrobial activity of silver nanoparticles impregnated with halloysite clay  
Tsvetanova for her technical assistance in the XRF analysis.

#### REFERENCES

1. M. Massaro, R. Noto, S. Riela, *Molecules*, **25**, 4863 (2020).
2. M. J. Saif, H. M. Asif, M. Naveed, *J. Chil. Chem. Soc.*, **63**, 4109 (2018).
3. Z. Shu, Y. Zhang, Q. Yang, H. Yang, *Nanoscale Res. Lett.*, **12**, 135 (2017).
4. P. Lampropoulou, D. Papoulis, *Materials*, **14**, 5501 (2021).
5. Y. Zhao, E. Abdullayev, A. Vasiliev, Y. Lvov, *J. Colloid Interface Sci.*, **406**, 121 (2013).
6. Y. Zhang, Y. Chen, H. Zhang, B. Zhang, J. Liu, *J. Inorg. Biochem.*, **118**, 59 (2013).
7. S. Jana, A. V. Kondakova, S. N. Shevchenko, E. V. Sheval, K. A. Gonchar, V. Y. Timoshenko, A. N. Vasiliev, *Colloids Surf. B: Biointerfaces*, **151**, 249 (2017).
8. A. R. Sayfutdinova, K. A. Cherednichenko, A. A. Bezdomnikov, U. P. Rodrigues-Filho, V. V. Vinokurov, B. Tuleubayev, D. Rimashevskiy, D. S. Kopitsyn, A. A. Novikov, *JCIS Open*, **12**, 100098 (2023).
9. X. Ding, H. Wang, W. Chen, J. Liu, Y. Zhang, *RSC Adv.*, **4**, 41993 (2014).
10. X. Xu, Y. Chao, X. Ma, H. Zhang, J. Chen, J. Zhu, J. Chen, *Int. J. Biol. Macromol.*, **258**, 128704 (2024).
11. J. Cervini-Silva, A. N. Camacho, E. Palacios, P. Angel, M. Pentrak, L. Pentrakova, S. Kaufhold, K. Ufer, M. T. Ramirez-Apan, V. Gómez-Vidales, D. R. Montaña, A. Montoya, J. W. Stucki, B. K. G. Theng, *Appl. Clay Sci.*, **120**, 101 (2016).
12. Y. Jin, F. Zhang, J. Fan, H.-J. S. Fan, *Appl. Clay Sci.*, **231**, 106750 (2023).
13. S.-C. Jee, M. Kim, S. K. Shinde, G. S. Ghodake, J.-S. Sung, A. A. Kadam, *Appl. Surf. Sci.*, **509**, 145358 (2020).
14. Z. Shu, Y. Zhang, J. Ouyang, H. Yang, *Appl. Surf. Sci.*, **420**, 833 (2017).
15. J. Wang, S. Wu, W. Zhang, H. Wang, P. Zhang, B. Jin, C. Wei, R. Guo, S. Miao, *Appl. Clay Sci.*, **216**, 106352 (2022).
16. S. Sharma, K. Choudhary, I. Singhal, R. Sain, *Int. J. Pharm. Sci. Rev. Res.*, **28**, 272 (2014).
17. S. D. Sarker, L. Nahar, Y. Kumarasamy, *Methods*, **42**, 4 (2007).
18. A. M. Carrillo, J. G. Carriazo, *Appl. Catal. B: Environ.*, **164**, 443 (2015).
19. S. S. Abdullahi, N. H. Hanif Abu Bakar, A. Iqbal, N. H. Yusof, *Egypt. J. Chem.*, **66**, 345 (2023).
20. H. Cheng, R. L. Frost, J. Yang, Q. Liu, J. He, *Spectrochim. Acta A Mol. Biomol. Spectrosc.*, **77**, 1014 (2010).
21. Y. Zheng, L. Wang, F. Zhong, G. Cai, Y. Xiao, L. Jiang, *Ind. Eng. Chem. Res.*, **59**, 13, 5636 (2020).
22. P. Yuan, P. D. Southon, Z. Liu, M. E. R. Green, J. M. Hook, S. J. Antill, C. J. Kepert, *J. Phys. Chem. C*, **112**, 15742 (2008).
23. M. Notarbartolo, M. Massaro, R. de Melo Barbosa, C. Emili, L. F. Liotta, P. Poma, F. M. Raymo, R. Sánchez-Espejo, R. Vago, C. Viseras-Iborra, S. Riela, *Colloids Surf. B Biointerfaces*, **220**, 112931 (2022).
24. O. P. Setter, E. Segal, *Nanoscale*, **12**, 23444 (2020).
25. R. Abhinayaa, G. Jeevitha, D. Mangalaraj, N. Ponpandian, P. Meena, *Appl. Clay Sci.*, **174**, 57 (2019).

## The history of the first germanium crystals along with a descendant of the novel “Bulgarians of old time”

M. Atanassova<sup>1\*</sup>, N. Todorova<sup>1</sup>, S. Goranova-Markova<sup>2</sup>

<sup>1</sup>University of Chemical Technology and Metallurgy, Department of General and Inorganic Chemistry, 8 Kliment Ohridski Blvd., 1756 Sofia, Bulgaria

<sup>2</sup>National Polytechnic Museum, 66 Opalchenska Str., 1303 Sofia, Bulgaria

Received: November 07, 2023; Accepted: May 23, 2024

This article represents a review of studies on the determination of germanium and the intriguing history behind it. The purpose of this paper is to familiarize readers with one outstanding figure in Bulgaria on the second half of the 19<sup>th</sup> century and his scientific activities - in particular, the Bulgarian trace in the discovery of the element Ge. The advantages of this research item are many and diverse, of course, but the main issue is to get closer for the umpteenth time to the chemistry that was created for us. Since then, the name of Stoycho Karavelov, the first Bulgarian metallurgical engineer, is quite forgotten and is not mentioned or spoken of today. Another positive issue is that inorganic chemistry during the germanium isolation is considered in depth herein including the foundations of chemical science in Bulgaria. In addition, the fascinating story of an incredible tradition and continuity among inorganic chemists in Bulgaria that lasted a hundred years, whose passing an ampoule of crystals from hand to hand is well worth telling.

**Keywords:** discovery of germanium, metallurgy, Clemens Winkler, Stoycho Karavelov, inorganic chemistry.

### INTRODUCTION

In the Bulgarian National Polytechnic Museum in Sofia, a glass container is exhibited in a separate display case, in which a small glass ampoule with several germanium crystals is placed, accompanied by a donation inscription. In fact, these are some of the first experimentally obtained crystals of the chemical element germanium (Fig. 1).

We will try to tell you the exciting story behind

which stands the first Bulgarian metallurgical engineer – Stoycho Dragoev Karavelov. Who is this Bulgarian about whom little is known today? *Quick overview.* He is the founder of the modern Bulgarian mining, born on August 1, 1865 in Koprivshitsa (former Ottoman Empire), in the same house where the popular Lyuben Karavelov museum is located today. He comes from the famous Karavelov family and is first cousin of Lyuben and Petko Karavelov.

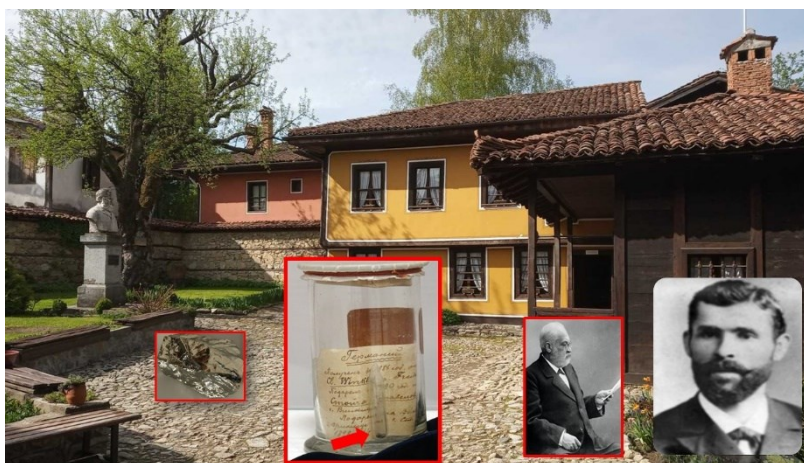


**Figure 1.** The house where Stoycho Karavelov (right photo and prof. Winkler - left photo) was born in Koprivshitsa, as well as the glass container with the ampoule with the first experimentally obtained crystals of the chemical element germanium and the donation inscription.

\* To whom all correspondence should be sent:  
E-mail: [ma@uctm.edu](mailto:ma@uctm.edu)

In fact, almost every Bulgarian student knows the cheerful and romantic love story of Pavlin and Lila from Lyuben Karavelov's novel "Bulgarians of Old Time", which refers to the time of the Bulgarian National Revival, in the 19th century. Considering the world historical periodization, we understand somehow why huge discovery of new elements started in the 19th century [1]. The characters behind this story are real people, close relatives and fellow citizens of Lyuben Karavelov. The prototype of Pavlin's image is Lyuben Karavelov's youngest uncle Dragoya, the father of the engineer Stoycho Karavelov. Dragoya Libenov Karavelov was born in 1820 and was the youngest son of Stoycho's grandfather Liben. Meanwhile, Lila was actually Paraskeva Ivanova Spasova, Nayden Gerov's niece. Nayden Gerov was a Bulgarian linguist, folklorist, writer and public figure during the Bulgarian National Revival. Dragoya and Paraskeva were married in 1842 and had nine children. The youngest one, Stoycho, was named after the father of Lyuben and Petko Karavelov. Generally, the book describes the flaws of Bulgarian society in those distant times, but also represents traditions and some essentials values. The main idea of the book is: "There is no, there is nothing in the world sweeter than to do good to a person." Little Stoycho started school at the age of 9 in his hometown. In 1878, his father had serious financial difficulties that forced him to settle the family somewhere around the town of Montana, where he died after only two years. Later, Stoycho studied II grade in Belogradchik and III grade in Tsaribrod. Left an orphan, he went to study up to the 7th grade at the real gymnasium in Lom located along the Danube River, where in 1885 he graduated with honors. The same year, 1885 he took part in the struggles for the Unification of Bulgaria and was also a volunteer in the Serbo-Bulgarian War. The Unification of Bulgaria was the act of unification of the Principality of Bulgaria and the province of Eastern Rumelia in the autumn of 1885. Both had been parts of the Ottoman Empire, but the Principality had *de facto* functioned independently whilst the Rumelian province was autonomous and had an Ottoman presence. Further on, he won a scholarship from the Ministry of Public Education to the Saxon Mining Academy in Freiberg, Germany, and the same year he went to study metallurgy. Freiberg today is home to the Technische Universität Bergakademie, which is the oldest mining and metallurgy university in the world, established by Prince Franz Xavier in 1765. During his studies in Freiberg (1885-1889), he was probably an assistant of Prof. Clemens Winkler, who was known to be the discoverer of the chemical element germanium. To

be honest, it is not so clear how, and whether Stoycho Karavelov helped Winkler in the discovery of germanium, but he was obviously in some way connected to the scientific activity of the professor. It can only be asserted for sure that between our compatriot and the German scientist, there was more than a simple acquaintance or friendship, because in 1890 Prof. Clemens Winkler gave Stoycho some of the first germanium crystals. We cannot pass over the words of an American student who finished his studies in 1883, that – "He always did all of his experiments himself, rarely calling upon an assistant", which does not mean, however, that Professor Winkler could not count on help in his laboratory, because his "chemical feeling" is *sui generis* [2]. In those days in Freiberg, there were students from all parts of the world: North and South America, England, France, Russia, Sweden, Poland, Austria, Italia, Spain, Greece, Australia even Japan and the Philippine Islands. The first Japanese student studied at the Freiberg Mining Academy in the year 1873 and was followed by 44 more Japanese students until 1939 [2]. Among them was Watanabe Wataru in 1882 who became later the first Japanese professor for mining and metallurgy in Tokyo. For information, around 31.7 % of the students at the Mining Academy Freiberg were students from Russia (1900). The story is impressive for the way the students were taught with lots and lots of experimental work in the labs as no lectures were given in chemical analysis. However, each student was told to provide himself with a copy of C. Remigius Fresenius textbooks, do their task and consult the assistant when in doubt of something. Moreover, considering the enormous amount of laboratory work involved in obtaining this famous extract under the experimental conditions of that time, the crystals of germanium were truly priceless!

#### THE STORY OF THE FIRST GERMANIUM CRYSTALS

*What exactly is a discovery of an element?*

*When the first germanium crystals appeared and how we can claim to know?* In 1886, the German chemist, Professor of Inorganic Chemistry, Clemens Alexander Winkler from the Freiberg Mining Academy has received for analysis the newly discovered silver-rich mineral "argyrodite" from Albin Weisbach (Professor of Mineralogy) from the Himmelsfürst mine near Freiberg. From the start prof. Weisbach was somehow convinced of having a new species in front of him, found in the middle of September 1885, around 460 m underground ( $\text{Ag}_8\text{GeS}_6$ ); because of the apparent high silver

content prompted him to the undefined mineral as early as October 1, to give the characteristic name: argyrodite. In fact, it was Theodor Richter who first determined the exact silver content with the blowpipe to be 73.5 percent, but he also stated to have found some mercury, which was quite surprising owing to the fact that this heavy metal had never been found before in Freiberg ores [3]. Therefore, Prof. Weisbach was not so satisfied with this finding and kindly asked his cousin and friend Clemens Winkler for an analysis of this new mineral. Freiberg, which is located in present-day Saxony near Dresden on the Elbe River, is known as “die Silberstadt” or “The Silver City”, due to its proximity to the Himmelsfürst mine that produced vast amounts of silver-containing ores. Germanium is usually recovered as a by-product from zinc and copper ores and coal. Moreover, the precise analysis shows that almost 7% of argyrodite weight consists of an unknown element. The balance of the contents was identified as silver (75%), sulfur (18%) and some minor impurities, i.e. trace amounts of mercury, iron, and zinc in the ore but all together these made up less than one percent of the composition. As a whole, currently about 30 germanium minerals are known to contain germanium ranging up to 70% in argutite,  $\text{GeO}_2$ . Many are sulfides, underlining the strong chalcophile character of germanium [4]. After doing a number of studies, as well as investigating its properties, after spending four months of solid work, on February 6<sup>th</sup> 1886, Winkler realized that he had discovered the missing element *eka*-silicon (Es) with

properties intermediate between the metal tin and the non-metal silicon (the future germanium), Fig. 2. It is the third of the “big three” elements, i.e. element with sequence number 32 of Dimitri Mendeleev’s Periodic Table of the elements today, whose place was left empty in 1871, in which the Sanskrit prefix meant “one”. That is the element one row beyond silicon. One can see no more than four “?”-s in the first version (1869), left by Mendeleev vacant spaces “gaps” for future newcomers in the table, while nearly eleven “–”-s appeared in the second proposition from 1871 [5, 6].

On February 8, 1886, the editors of the *Berichte der deutschen chemischen Gesellschaft* received Winkler’s article, in which he informed the scientific community about the discovery of this chemical element [7]. He wrote about this discovery as follows: *After several weeks of laborious searching, I can today say with certainty that the argyrodite contains a new element very similar to antimony, but sharply differentiated from it, to which the name “germanium” may be given.* However, at first, Winkler assumed that his new element should chemically be similar to antimony because argyrodite and antimony minerals behaved similarly, but the chemists have to forgive him for the mistake, which was relatively quickly spotted by others. First Victor von Richter, and then Lothar Meyer, pointed out that, according to the plot of atomic volumes, germanium should be low-melting as well as volatile, and identified with *eka*-silicon, prognosticated fifteen years ago by Mendeleev [8].

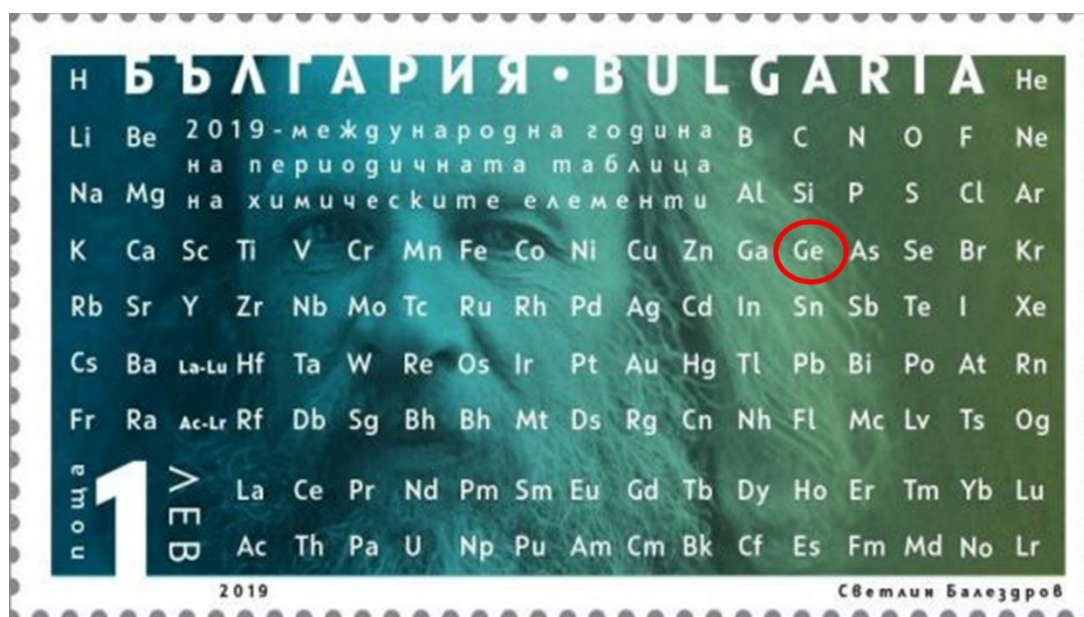
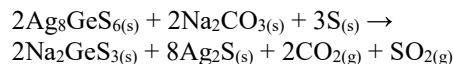
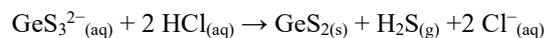


**Figure 2.** International Year of the Periodic Table stamp issued by the Bulgarian Post on 24.06.2019. (The author of the stamp which has a circulation of 5.500 pieces, is Assistant Professor Dr. Svetlin Balezdrov from the National Academy of Arts. It depicts the Periodic Table over the face of Dmitri Mendeleev).

For instance, applying the so-called “Freiberger digestion” in order to analyze the argyrodite, upon digestion process, a soluble sodium thiogermanate is formed that dissolves when water is added after the performed heating process. While, at the same time, the silver sulfide does not dissolve [3, 9]:



However, the aqueous extract also contained the thiosalts  $\text{Na}_3\text{AsS}_4$  and  $\text{Na}_3\text{SbS}_4$  because naturally, the ore in use was contaminated with both elements, i.e. arsenic and antimony. The essential key to isolating the germanium salt was to separate it from these two contaminants. This was somehow ultimately achieved by weakly acidifying the aqueous solution with hydrochloric acid, allowing the solution to sit overnight to form precipitates. Further, the final isolation of germanium was achieved by slow acidification of the obtained inorganic material. Generally, the three anions  $\text{AsS}_4^{3-}$ ,  $\text{SbS}_4^{3-}$ , and  $\text{GeS}_3^{2-}$  are present in solution and the process of slow acidification will result in the precipitation of the two sulfides  $\text{As}_2\text{S}_5$  and  $\text{Sb}_2\text{S}_5$ , respectively, while the  $\text{GeS}_3^{2-}$  ion remains in solution [3, 9]. Perhaps, here it is good to recall the memory of the student from Princeton: “You see, Prof. Winkler said, *the precipitation was not complete. Hereafter, when you have occasion to throw out of a solution a substance, see to it that the proper reagent is added in moderate excess.*” [2]. The main difficulty in isolating this new element, experienced by Winkler, stems from the unusual fact that the sulfide is soluble in dilute acids and water but insoluble in concentrated acids. Therefore, the following addition of excess mineral acids HCl or  $\text{H}_2\text{SO}_4$  then leads to the precipitation of germanium(IV) sulfide:



The sample of  $\text{GeS}_2$ , initially obtained by Winkler, was sealed in a glass tube and is currently exhibited at the Bergakademie (the Mining Academy, the Institute for Inorganic Chemistry) in Freiberg, shown in Fig. 3 [3]. Moreover, a second ampoule ended up in the hands of a Bulgarian student as a gift. It was later determined that washing the solid product of  $\text{GeS}_2$  with sulfuric acid and then alcohol would prevent it from undesirable re-dissolving in water. Moreover, the element itself could be isolated from the sulfide by roasting in oxygen followed by reduction of the resulting oxide by hydrogen gas [3]:

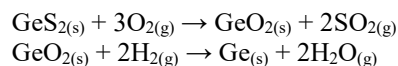


**Figure 3.** Winkler’s sample of  $\text{GeS}_2$  from February 6, 1886, and his gift.

Think of a sulfide which possesses the unique chemical property of being insoluble in strong acids but soluble in dilute acids and water! No wonder why Winkler experienced such difficulty in obtaining it [2]. Thankfully, from this chemical stage on, all was likely more easily. Fortunately, the managing director of the Himmelsfürst mine, Eduard Neubert, was generous and provided Winkler with a total of 5.34 kg of argyrodite, with the stipulation that the silver obtained from this material would be returned [9]. This worthwhile ore ended up yielding about 100 g of germanium. In five months of intense research, Prof. Winkler was able to obtain the majority of the compounds of the element for which Mendeleev had made some predictions. The properties of elemental germanium and those of its compounds agreed very well with those predicted by Prof. Mendeleev, including the determination of its atomic weight of 72.32 g/mol from  $\text{GeCl}_4$ , as well as the oxide  $\text{GeO}_2$ , the sulfides  $\text{GeS}$  and  $\text{GeS}_2$ , as well as the iodide  $\text{GeI}_4$ , Table 1. Thus, surely one of Mendeleev’s greatest triumphs, and perhaps the one that he is best remembered for forever, is the correct prediction of the existence of several new elements [10, 11].

**Table 1.** Predicted and observed properties of *eka-silicon* (germanium).

Properties	1871	1886
Relative atomic mass	72	72.32
Density, $\text{g/cm}^3$	5.5	5.47
Specific heat	0.073	0.076
Atomic volume, $\text{cm}^3$	13	13.22
Color	dark grey	grayish-white
Vaporization energy, $\text{J}\cdot\text{C}^{-1}\cdot\text{g}^{-1}$	0.31	0.32
$T_f$ , $^\circ\text{C}$	high	960
Oxide	$\text{RO}_2$	$\text{GeO}_2$
Oxide density, $\text{g/cm}^3$	4.7	4.703
Chloride	$\text{RCl}_4$	$\text{GeCl}_4$
Boiling point of tetrachloride, $^\circ\text{C}$	100	86

Furthermore, Lecoq de Boisbaudran also received a good sample of germanium and was so eager to subject it to the action of the induction spark, consequently, he is the first person that measured germanium's spark spectrum. A very beautiful spectrum was produced which contains two lines whose brilliancy is above all remarkable: a blue and a violet at 468 and 422 nm, respectively. These lines lay midway between similarly determined lines for silicon and tin, Fig. 4. "*I have measured the two rays with an accuracy already sufficient to enable me to apply my formulas relating the wavelengths of the homologous rays and the atomic weights of bodies which produce them, i.e. 72.27*" [12].

As a matter of fact, Ge as an element is somewhat more reactive and more electropositive than Si, as it slowly dissolves in hot concentrated  $\text{H}_2\text{SO}_4$  and  $\text{HNO}_3$  acids but does not react with water or with dilute acids or alkalis unless an oxidizing agent such as  $\text{H}_2\text{O}_2$  or  $\text{NaOCl}$  is present; fused alkalis react with incandescence to give germanates. Germanium is oxidized to  $\text{GeO}_2$  in air at red heat and both  $\text{H}_2\text{S}$  and gaseous S yield  $\text{GeS}_2$ . Both  $\text{Cl}_2$  and  $\text{Br}_2$  yield  $\text{GeX}_4$  on moderate heating, while HCl gives two compounds,  $\text{GeCl}_4$  and  $\text{GeHCl}_3$  [13].

Despite its spectacular increase in availability during the past few decades from a laboratory rarity to a general article of commerce, Ge and its compounds still are more or less relatively expensive [14]. Actually, germanium, along with selenium, tellurium and helium, is one of the few non-metallic elements to carry the '-ium' suffix in English [5, 10].

Further, Clemens Winkler wrote to Mendeleev in a letter dated February 26, 1886 [8]: *Your Excellency! Allow me to transmit to you this separate reprint of a report according to which I have discovered a new element, germanium, in a silver mineral found here. Initially, I was of the opinion that this element fills the gap between antimony and bismuth in the very ingeniously compiled by you periodic table, that is, that it, therefore, represents your eka-antimony; however, everything points to the fact that here we are dealing with the eka-silicon predicted by you. I hope soon to be able to give you details on a new extremely interesting body; today I will confine myself to informing you of this new triumph of your ingenious research and to pay you my highest respect.*

In June 1886, Dr. G. Quesneville, the editor of the French journal *Moniteur Scientifique*, accused Prof. Winkler of bringing nationalism into science, and insisted that Winkler should give up the name

germanium as opposed, no doubt, to that of gallium, and that the new element should keep the name *eka-silicon*, since that was Mendeleev's name for this predicted element and so the naming of it should be up to him [15].

Over and above, C. Winkler kindly asked Mendeleev, if it was possible to name the element germanium: a manifestation of great respect [8, 11, 16], Fig. 5. Not long after that, the two scientists, the predictor of a new element and the real discoverer of said element, had the opportunity to meet each other in 1900 on the occasion of the 200<sup>th</sup> anniversary of the Prussian Academy of Sciences, Berlin. In fact, four countries, situated in Europe, have chemical elements named after their lands, i.e. Fr, Ga, Ge, Po and Ru. So, France has not only two elements, but its capital Paris (Lutetia) also gave the name of the element No 71 in the Periodic Table [16].

Let's recall that on August 27, 1875, the French chemist Lecoq de Boisbaudran had also discovered the predicted by Mendeleev *eka*-aluminum, i.e. gallium. Mendeleev's prognosis concerning the existence of *eka*-boron also became somehow the truth [17]. In other words, this element was discovered by the Swedish chemist Lars Frederic Nilson in 1879: scandium. It should be mentioned that in a ten-year period from 1880 to 1890 only 6 new chemical elements were discovered, germanium being the only one different among the isolated lanthanoids (Gd, Pr, Nd, Dy and Sm) at that time [1].

Unfortunately, the years following the discovery of Ge did not lead to any major scientific findings or technological applications for this rare, greyish-white, expensive, brittle and metal-like element which has a bright lustre with a diamond structure. It is a metalloid with a similar electrical resistivity to Si at room temperature but with a substantially smaller band gap [18, 19]. As a whole, more than one-half century elapsed after the isolation of germanium before its first commercial application in diodes and transistors [20]. To remind a reader that the chemical element In was also discovered by German scientists Ferdinand Reich (physicist) and Hieronymus Theodor Richter (chemist) during a spectrographic analysis of sphalerite ore samples again from the mines around Freiberg [21], just two decades earlier, 1863. However, they decided to name the element indium after the distinctive indigo-blue line in its emission spectrum. One more time, indium remained only a scientific curiosity for years following its discovery and unfortunately little was known about its occurrence apart from the Freiberg ore too [20].

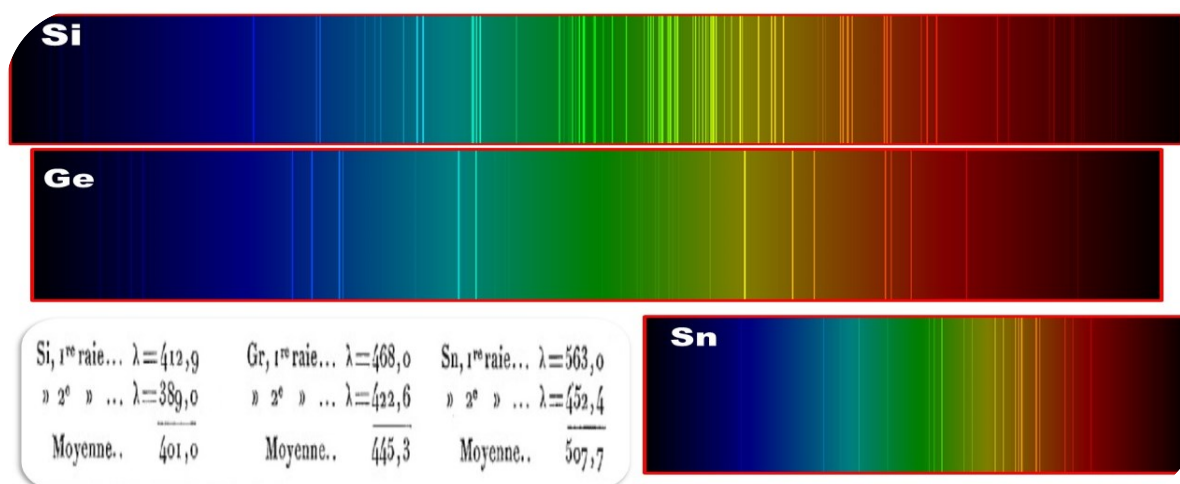


**Figure 4.** Spectral lines of Si, Ge and Sn in the visible spectrum at about 400-700 nm as well as the observed spark spectra applying Boisbaudran’s new experimental apparatus.



**Figure 5.** Winkler and Mendeleev in Berlin in 1900. Monument in honor of Clemens Winkler in Freiberg (Wikipedia).

*The first germanium crystals in Bulgaria. A little more of the story of engineer Stoycho Karavelov.*

In 1890, Stoycho Karavelov returned to Bulgaria and joined the Mining Department of the Ministry of Finance as a mining engineer. In 1893, the Department was transferred to the newly created Ministry of Commerce and Agriculture. In the following years, he held various positions: chemical engineer for mines, head of the chemical laboratory, head of the chemical engineering laboratory, metallurgical engineer, director of mines, head of the department for mines, etc. As an outstanding expert, he was also the main author of the Basic Law on Mines in Bulgaria [22]. This law regulates the relations between mining enterprises and the state. In other words, the state reserves the right to exploit the

main mineral resources on its own. As a person with broad interests, Karavelov also participated in the establishment of the first balneological organization for the use of mineral waters in Bulgaria. The engineer is the author of numerous articles providing information about the state of mining production in the world and in our country, about the production of precious metals in the world, as well as various statistical data on that topic. The works of the engineer also include the translations from German into Bulgarian language of the two books: “Guide to the determination of minerals with the help of the bellows” by Prof. Dr. C. W. C. Fuchs (translation 1892) and “Tables for the determination of minerals by external signs” by Prof. Dr. A. Weisbach (translation 1899), Fig. 6. Of course, these works

were extremely important for that time, as they were the first serious scientific materials on metallurgy and mining in our country and for a long time they satisfied the glaring needs for such kind of literature in the young Bulgarian state. Eng. Stoycho Karavelov was repeatedly authorized to represent Bulgaria abroad [23], e.g., in the making of coin dies, and as state comptroller in the minting of coins at the mints of Vienna and Berlin. For his

extraordinary work, Eng. Karavelov was awarded with several medals: “St. Alexander” 5<sup>th</sup> degree (1892) and “St. Alexander” 4<sup>th</sup> degree (1905), as well as the medal for Civil Merit 4<sup>th</sup> degree (1898) and Civil Merit 3<sup>rd</sup> degree (1914). Examples of medals, that Eng. Stoycho Karavelov was awarded are shown in Fig. 7, as described in his personal business list [24].

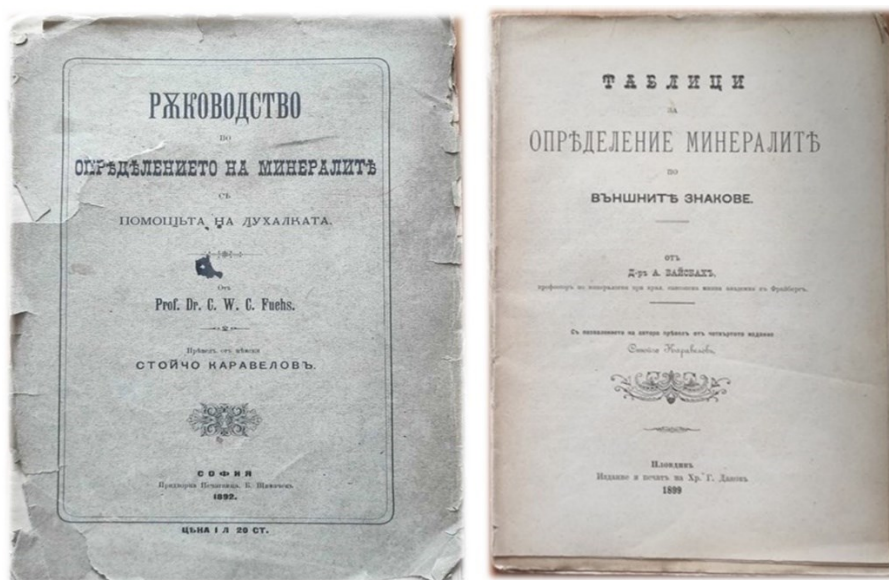
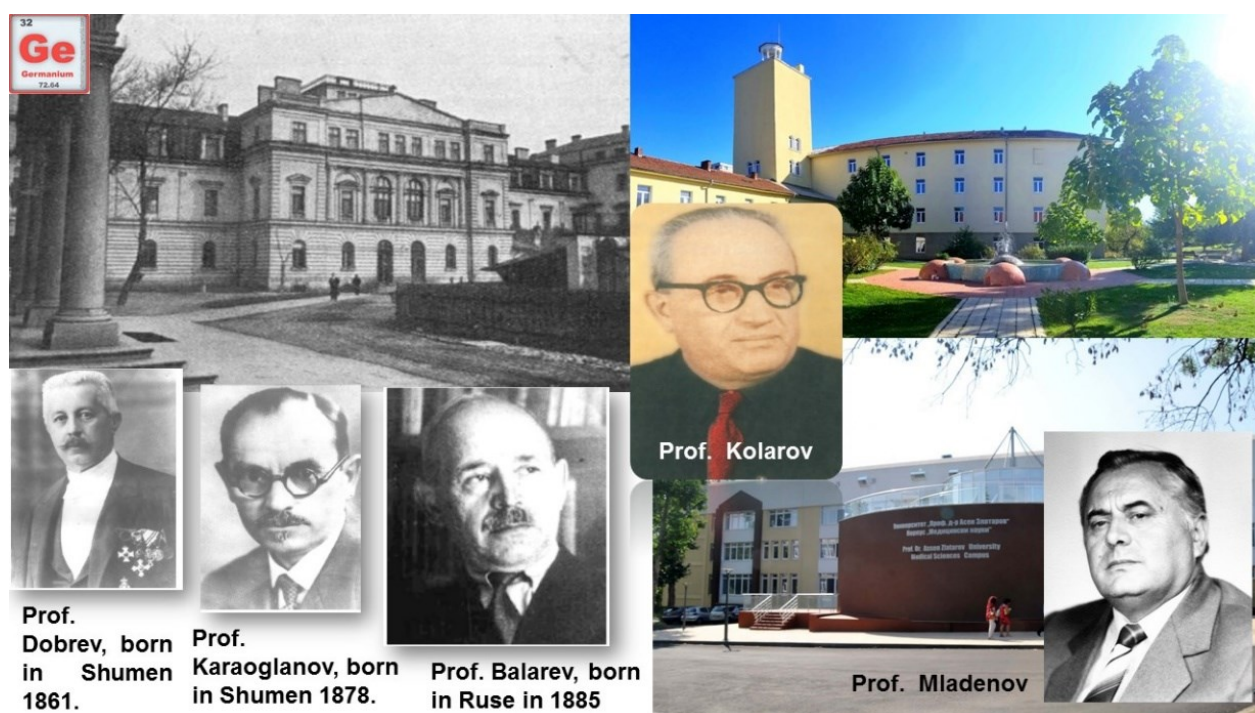


Figure 6. Photos of the two books.



Figure 7. Stoycho Karavelov’s medals.



**Figure 8.** The eminent Bulgarian inorganic chemists, in whose hands has been the ampoule with the first germanium crystals.

In 1915, however, he resigned for health reasons and the following year (October 8) he died in Sofia, only 51 years old, from lung cancer. To mention, on the same date, but 11 years earlier, Professor Clemens Winkler died also because of lung cancer: October 8, 1904.

*However, what is the route of the germanium ampoule and how did it reach to the Bulgarian National Polytechnic Museum?* In 1898, Eng. Karavelov decided to give the ampoule with the first germanium crystals to the First Higher School in Bulgaria, probably to the Chemical Institute of the Faculty of Physics and Mathematics. The ampoule was placed in a glass jar (along with a handwritten donation inscription of Eng. Karavelov) and was kept by some of the distinguished Bulgarian chemists for a whole century. This peculiar relic is carefully preserved to this day. An incredible but real fact that all chemists in Bulgaria highly appreciate (Fig. 8). Prof. Nikola Dobrev, (head of the “Inorganic and Analytical Chemistry” Department in the period 1889-1909) handed it over to Prof. Zahari Karaoglanov (head of the same department in the period 1909-1922), who carefully hid the precious ampoule. Further, in 1922, the department was divided into two: “Inorganic Chemistry” and “Analytical Chemistry”. Thus, the ampoule was

handed over for safekeeping, completely naturally, to the head of the “Inorganic Chemistry” Department, Prof. Dimitar Balarev, who, following the tradition, handed it over to his best student, Prof. Nikola Kolarov. In fact, as an assistant professor, Mr. Kolarov had the opportunity to observe how Prof. Balarev showed the ampoule with germanium to the students, emphasizing with great pride that Winkler gave the first received crystals to a Bulgarian. Since 1958, Prof. Kolarov kept it in the Department of “Inorganic Chemistry” of the State Polytechnic, and later at the Higher Institute of Chemical Technology, nowadays University of Chemical Technology and Metallurgy. Upon his retirement in 1977, he entrusted it to his successor, Prof. Ivan Mladenov, one of the first assistants in the department from 1947 remained until 1953 when he moved in order to be a PhD student in the Department of Plastics Technology. Later, he became the founder and first rector of the Higher Institute of Chemical Technology in the city of Burgas. In July 1993, both Prof. Nikola Kolarov and Prof. Mladenov decided to give the ampoule for storage at the National Polytechnic Museum, thus ending this beautiful tradition and continuity among the inorganic chemists in Bulgaria. Recorded in the inventory book of the museum under No. OF 06564,

the ampoule with germanium and the corresponding donation inscription became part of the permanent exhibition today. The exact text of the donation inscription reads: "Germanium isolated in 1886 by Prof. Winkler in Freiberg. – Gifted in 1890 to Mr. Karavelov by Mr. Winkler. – Gifted to the Higher School by St. Karavelov 1898 – 31/I."

### CONCLUSION

While the name of the eminent German chemist Clemens Winkler is loudly heard among chemists in Germany, that of the Bulgarian is almost forgotten or is little mentioned today. For example, in the present days the Clemens-Winkler gold medal is awarded by the Division of Analytical Chemistry of the German Chemical Society every two years. Undoubtedly, it was a real privilege to study under the direction of an eminent man like Winkler, who inspired his students. *A university has no doctrine to teach. Its special purpose is to investigate what is true in any field. It is the special gift of the great teacher to open the mind of the pupil.* – Jeremiah W. Jones [2]. The intertwining of historical facts and events with the life stories of existing people and/or literary characters from Bulgarian literature makes the experience herein even more memorable, brings the museum narrative to life, makes the memories lasting, and emotional for almost all people, not only students or chemists, but also foreigners. Accordingly, science education should emphasize the major landmarks in our understanding of the natural world, and the major figures and events in the history of science and the cultural significance of scientific achievement as a primary argument. It is our pleasure to recount the past 130 years related to the Bulgarian footprint in the history of germanium.

**Acknowledgement:** This study was supported by the Bulgarian National Science Fund – project title "Green twist to synergistic solvent extraction and separation of rare earth metals", project № KII-06-H69/5(2022) as well as by the European Union-NextGenerationEU, through the National Recovery and Resilience Plan of the Republic of Bulgaria, project № BG-RRP-2.004-0002-C01, "BiOrgaMCT". The authors thank Mr. Borislav Slavov (UCTM) for the technical (informational) assistance provided during the preparation of the material, as well as to the BSc students Ilina Todorova, Katrin Chavdarova and Aleyna Chamdere. We express our sincere gratitude to the entire team working at the National Polytechnic Museum and especially to the Director Dr. Ekaterina Tsekova.

### REFERENCES

1. M. Atanassova, R. Angelov, *Chemistry: Bulg. J. Sci. Edu.*, **23**, 275 (2014).
2. L. W. McCay, *J. Chem. Educ.*, **7**, 108 (1930).
3. M. Haustein, *Chem. Unserer Zeit*, **45**, 398 (2011).
4. G. A. Ruiz, C. P. Sola, N. Palmerola, Germanium: current and novel recovery processes. Chapter 2, Advanced material and device applications with germanium, Intech Open, 2018.
5. M. Atanassova, R. Angelov, *Chemistry: Bulg. J. Sci. Edu.*, **28**, 398 (2019).
6. K. Brad Wray, *Foundations of Chem.*, **21**, 139 (2019).
7. B. Harvey, G. Hermann, R. Hoff, D. Hoffman, E. Hyde, J. Katz, O. Keller, M. Leffort, G. Seaborg, *Science*, **193**, 1271 (1976).
8. A. Szejnberg, *Rev. CENIC Cienc. Quim.*, **53**, 103 (2022).
9. C. Weinert, *Bull. Hist. Chem.* **45**, 8 (2020).
10. M. Atanassova, *Chemistry: Bulg. J. Sci. Edu.*, **24**, 125 (2015).
11. M. Atanassova, R. Angelov, D. Gerginova, A. Zahariev, *Chemistry: Bulg. J. Sci. Edu.* **28**, 807 (2019).
12. P.-E. Lecoq de Boisbaudran, *C. R. Hebdomadaire des Séances*, 1291 (1886).
13. N. N. Greenwood, A. Earnshaw, *Chemistry of the elements*, Butterworth-Heinemann, 1998.
14. F. Melcher, P. Buchholz, Germanium, *Critical Metals Handbook*, G. Gunn (ed.), John Wiley&Sons Ltd., 2014.
15. G. Quesneville, *Moniteur Scientifique*, **16**, 691 (1886).
16. M. V. Orna, M. Fontani, Discovery of three elements predicted by Mendeleev's table: gallium, scandium and germanium, in: 150 Years of the Periodic Table. A commemorative symposium, C. Giunta, V. Mainz, G. Girolami (eds.), Perspectives on the history of chemistry. Springer Nature, Switzerland, 2021.
17. M. Akeroyd, *Foundations of Chem.*, **12**, 117 (2010).
18. T. Gusebnikova, *Talanta*, **251**, 123792 (2023).
19. E. Haller, *Mat. Sci. Semicond. Processing*, **9**, 408 (2006).
20. W. C. Pat Shanks III, B. Kimball, A. Tolcin, D. Guberman, Germanium and Indium. Chapter I of Critical Mineral Resources of the United States—Economic and Environmental Geology and Prospects for Future Supply. K. J. Schulz, J. H. DeYoung, Jr., R. R. Seal II, D. C. Bradley (eds.), Professional Paper 1802–I. U.S. Geological Survey, Reston, Virginia, 2017.
21. F. Reich, H. T. Richter, *Journal für Praktische Chemie*, **89**, 441 (1863).
22. D. Dimitrov, *Young Designer*, **7**, 10 (1986). (Mlad konstruktor, in Bulgarian).
23. A. Valchev, *Young Designer*, **2**, 23 (1987). (Mlad konstruktor, in Bulgarian).
24. V. Denkov, Bulgarian Orders and Medals, Cybele, 2001, (in Bulgarian).

# Digitalization in Bulgarian science education: a comparative analysis of the state of the art

E. Boiadjieva, A. Tafrova-Grigorova\*

*Faculty of Chemistry and Pharmacy, University of Sofia St. Kliment Ohridski, 1 James Bourchier Blvd., 1164 Sofia, Bulgaria*

Received: May 28, 2024; Accepted: June 11, 2024

The paper discusses the use of digital technologies (DT) in Bulgarian school science education through a review and analysis of national and international studies. Both the strengths and weaknesses of the application of DT in the Bulgarian school in a comparative plan with other European countries are highlighted. The findings show that the digital competence of Bulgarian students and teachers related to DigComp and DigCompEdu frameworks is generally lower than the European average despite the confidence in their digital skills. Problematic areas include creating and modifying digital content, collaboration among teachers, identifying fake news, assessing student progress, implementing constructivist approaches in e-learning. The quality of continuing teacher education for digital competences is also a concern. Nevertheless, many Bulgarian teachers express satisfaction with their work in distance learning and believe that the use of DT enhances their lessons. Analysis of digital technology use and student learning achievements in science education shows no clear evidence of a correlation. However, there are potential positive effects of using computers as a supplement to traditional instruction rather than as an alternative to it.

**Keywords:** DigComp; DigCompEdu; digital competence; science education.

## INTRODUCTION

Data on the state of digitalization in Bulgarian school education can be found in some national and cross-national studies, as well as in research papers by individual authors. Some of these data are also valid particularly for science education – in physics, chemistry and biology. These three subjects are primarily experimental sciences as they are based on the collection and analysis of data from empirical studies. With the rapid development of digital technology, it has become possible to visualize and conduct some of the observations and experiments using digital devices and resources. As in other subjects, the search for and systematization of reliable and trustworthy information, the processing of data, and their presentation in the form of tables, charts, diagrams and other representations are important. It is taken, somewhat for granted, that digitalization supports science education and facilitates the work of both teachers and students, which would lead to better achievements in science education. In this paper, sources from national and international studies will be presented and analysed, which provide information on the state of digitalization in science education in Bulgarian schools.

### *Research aim and research questions*

The aim of the present work is to highlight the strengths and weaknesses of the application of

digital technologies in the Bulgarian school in a comparative plan with other European countries through a review and analysis of studies on the digital competences of teachers and students. In line with this aim, two research questions were set:

1) To what extent do the digital competences of Bulgarian teachers and students in the context of science education correspond to the European Digital Framework for citizens (DigComp) and the European Digital Framework for educators (DigCompEdu)?

2) Is there a correlation between the application of digital technologies and students' learning achievements in natural sciences?

### *Research methodology*

In search of answers to the research questions we followed three stages: 1) Review of the European frameworks for digital competence; 2) Search and selection of scientific literature, national and supranational studies on the application of digital technologies in Bulgarian schools and particularly in science education and 3) Data analysis of literature sources and conclusions.

### *Overview of the European digital competence frameworks – DigComp for citizens and DigCompEdu for educators*

These frameworks have been designed by the European Commission (EC) and are used to evaluate and develop people's digital skills.

\* To whom all correspondence should be sent:  
E-mail: exat@chem.uni-sofia.bg

DigComp is the Europe-wide framework for developing and measuring citizens' digital skills. It was created in 2013 [1], and describes key components of digital competence, grouped into five areas: 1) Information and data literacy; 2) Communication and collaboration; 3) Digital content creation; 4) Security; 5) Problem solving. DigComp defines digital competence as „the confident, critical and creative use of ICT to achieve goals related to work, employability, learning, leisure, inclusion and/or participation in society“.

The components of digital competence, also referred to as competences, are total 21 and distributed across the five areas of the framework. They are denoted by two numbers, the first indicating the area and the second showing the competence, e.g. 2.4 is the competence *Collaboration through digital technologies* which is pertinent to area 2. Communication and collaboration.

The content of the framework is structurally presented in 5 dimensions: Dimension 1: the areas in which digital competence is manifested; Dimension 2: the titles and descriptions of the competences in each area; Dimension 3: the levels of proficiency for each competence; Dimension 4: examples of knowledge, skills and attitudes applicable to each competence; Dimension 5: use cases of the competence in different contexts. Dimension 3 includes three levels of proficiency (foundation, intermediate and advanced). Dimensions 4 and 5 give examples of different possible manifestations and applications of the competences of dimension 2, but do not claim to be exhaustive.

The rapid development of digital technologies, the skills to create them and work with them has led to several versions of DigComp, each of which, updates some elements of the Framework and complements it. The first of the updated versions, labeled DigComp 2.0 [2] updates Dimension 1 (the five areas) and Dimension 2 (the titles and descriptors of the 21 competences) in line with the fast development of digitalization. The descriptors of the competences use the terms digital technologies and digital environment. This facilitates the descriptions so that it is not necessary to specify a particular technology, software or app, as well as a particular device. This way, all types of computers and all mobile devices such as smartphones, media players, e.g. game consoles, e-book readers, etc. are included. These terms now also include sensors and all kinds of information transmission devices, more recently known as the Internet of Things – a system of interconnected devices, objects, animals or people that have unique identifiers (UID) and can transmit

data by a network without the need for human-human or human-computer interaction.

The next version DigComp 2.1 [3] details the proficiency levels and they become 8 for each of the 21 competencies, therefore 168 in total. Progress in mastery of the competencies is reported in terms of three components: 1) the complexity of the tasks, 2) the independence with which the tasks are performed, and 3) the need for guidance in completing the tasks.

At the end of 2020, the next update of the DigComp – DigComp 2.2 begins, focusing on Dimension 4, which is complemented by examples of knowledge, skills and attitudes for each of the 21 competences. What is new in this latest version is the consideration of emerging technologies such as artificial intelligence (AI), Internet of Things (IoT), datafication – converting information about subjects, objects, processes into digital data. DigComp 2.2. also reflects the new conditions for remote working, which requires new digital skills of citizens that are different from the previous ones [4]. Dimension 5 is enriched with use cases of digital competences in the context of learning and education.

DigComp 2.2 includes over 250 new examples of knowledge, skills and attitudes to help citizens to engage with digital technologies. Due to the short period since the publication of version 2.2 of the DigComp, we have not yet found any relevant publications on the topic of the present study, so we will refer to previous versions.

The DigCompEdu [5] describes teacher specific digital competences within a progression model that allows teachers to identify and to gradually improve their competencies. 22 core competencies are described and grouped into six areas that focus on different aspects of educators' activities: 1) Professional engagement, 2) Digital resources, 3) Teaching and learning, 4) Assessment, 5) Empowering learners, 6) Supporting learners' digital competence.

The aim of DigCompEdu is to promote the development of digital skills among teachers and to stimulate innovation in education. The core of the DigCompEdu framework is defined by areas 2-5. Together, these areas represent the digital competencies that educators need to use digital technologies effectively and innovatively, and to create and share digital learning resources. Area 1 focuses on educators' own professional development of digital skills in their professional interactions with colleagues, students, parents, and other stakeholders. Area 2 describes the competencies needed to create and share digital resources for learning. Area 3 addresses the

pedagogical skills for managing and organizing the use of digital technologies in learning. Area 4 looks at using digital strategies to improve assessment in education. Area 5 focuses on the potential of digital technologies for learner-centred teaching and learning strategies to promote active and creative engagement in their learning. Area 6 details the specific pedagogical competencies required to support the development of learners' digital competence to use digital technologies effectively and responsibly to find information and resources in digital environments, to communicate, collaborate and actively participate.

*Search and selection of scientific literature, national and supranational studies on the application of digital technologies in Bulgarian schools, in particular in science education*

For articles in scientific journals the international databases (academic databases) ERIC, JSTOR, Scopus, Web of Science with keywords "digital technologies, science education, Bulgaria" and in the National Reference List of Contemporary Bulgarian Scientific Publications with Scientific Review were consulted. Information was also sought from the website of the Ministry of Education and Science of the Republic of Bulgaria, as well as from the websites of the Organisation for Economic Cooperation and Development (OECD), primarily its educational programmes: Programme for International Student Assessment (PISA), Education at Glance (EAG), Teaching and Learning International Survey (TALIS), as well as from UNICEF publications for Bulgaria. Of the huge number of literature sources found, the ones of interest for our study are only those that refer to the first secondary school stage (grades 8-10) and the second secondary school stage (grades 11-12) of secondary education and provide directly or indirectly reliable information about the digital skills of students and/or teachers in the field of science education in the Bulgarian context over the last dozen years. After a careful review and selection of the publications, it turned out that those of them that meet the set criteria are not many, but some of them are of considerable interest for outlining the situation in Bulgarian schools.

*Review and analysis of publications on the digital competences of Bulgarian science teachers and their students according to the European digital frameworks*

In this section, the findings of studies of key relevance for science education according to the

DigComp and DigCompEdu requirements will be followed in turn.

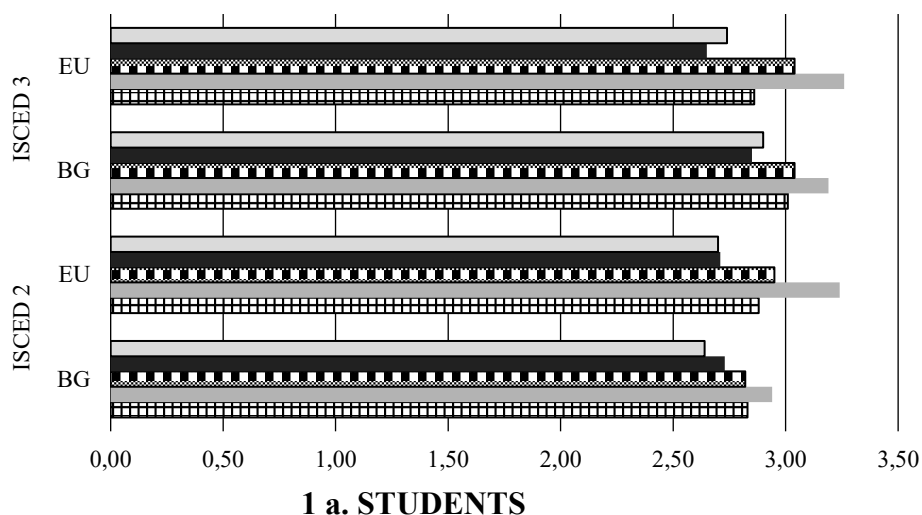
The *2nd survey of schools: ICT in Education* [6] provides information on access, use and attitudes towards the application of technologies in education through an online survey of principals, teachers, students and parents from the EU-28, Norway, Iceland and Turkey, covering three levels of the International Standard Classification of Education (ISCED): ISCED 1 - primary education, ISCED 2 - lower secondary education and ISCED 3 - upper secondary education.

In Bulgaria, the number of schools invited to take part in the survey was 2305, selected at random. Interviews were conducted with 325 principals, 81 primary teachers (ISCED 1) 272 and 217 lower secondary and upper secondary teachers, respectively (ISCED 2 and 3), 2583 students and 1653 parents.

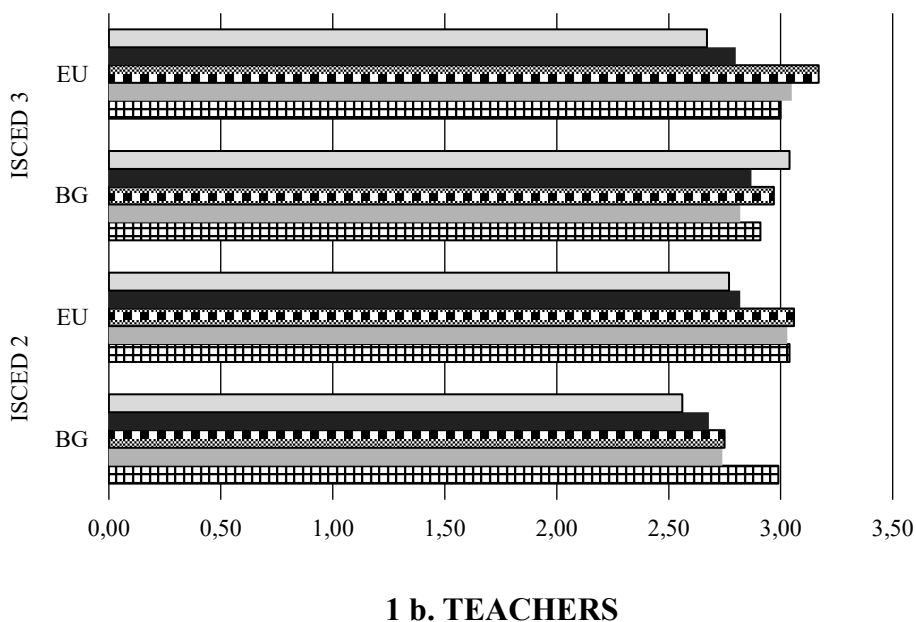
The EC study for Bulgaria, [7] has collected data on the following ten indicators: 1. Highly digitally equipped and connected schools; 2. Schools with high-speed Internet; 3. Students who use a computer at school at least once a week for learning; 4. Use of own digital equipment for learning purposes; 5. Schools supporting digital technology; 6. Students' confidence in their digital competence; 7. Coding/programming activities for female *versus* male students; 8. Teachers' confidence in their digital competence; 9. ICT related teacher professional development; 10. Parents' confidence in teaching their child how to use the Internet safely and responsibly.

In Bulgaria, the number of schools with a high level of digital equipment and connectivity is significantly lower across all ISCED levels compared to the European average, but the share of owned digital devices (tablets, laptops and smartphones) for ISCED levels 2 and 3 is higher in Bulgaria compared to the European average.

Students' confidence in their digital competence (indicator 6) is determined according to the areas of the DigComp framework: 1) information and data literacy; 2) communication and collaboration; 3) digital content creation; 4) safety; 5) problem solving. The data show a lower confidence of students in Bulgaria at ISCED 2 level in all areas of digital competence compared to the European average, but a higher confidence of Bulgarian students at ISCED 3 level in all areas of digital competence except for the areas of "Communication and collaboration" and "Information and data literacy" compared to the European average (Fig. 1).



Digital content creation
  Problem solving  
 Information and data literacy
  Communication and Collaboration  
 Safety



**Confidence:** 1 – Not at all, 2 – A little, 3 – Somewhat, 4 – A lot

**Fig. 1.** Confidence of students (1a) and teachers (1b) in their digital competence

Despite the declared confidence of Bulgarian students, it turns out that in reality their digital competence is not very high. In his study, Tsankov [8] found “a significant discrepancy between students’ self-assessment of their digital competence at the entrance to university education and the actual assessment of their knowledge and skills as basic constructs of their competence”, and “significant deficits in students’ cognitive and practical skills in the context of the application of information and communication technologies and working in a digital environment.”, (p. 338).

Bulgarian teachers’ confidence in their digital competence is lower for all ISCED levels in all areas of digital competence, except for digital content creation (ISCED 3) and problem solving (ISCED 3), compared to the European average. On the 4-level scale, it is between “Somewhat” and “To some extent”, being lower than that of students, except for “Creating resources”, and there is no significant difference in the area of “Problem solving” (ISCED 3), as well as in “Security” for ISCED 2.

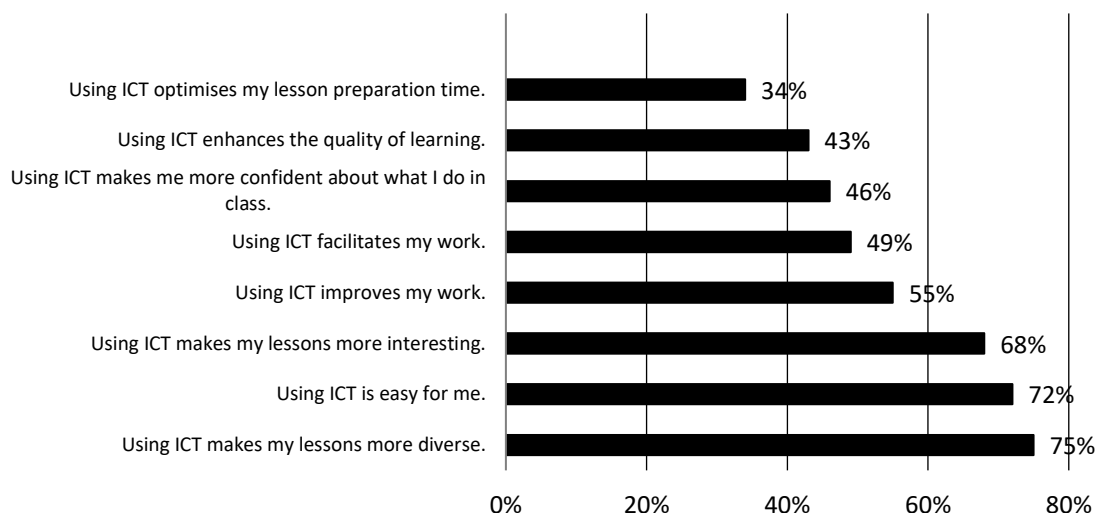


**Fig. 2.** Percentage of teachers who agree or strongly agree with the statements

For coding/programming activities in DigComp area 3 Digital content creation: both female and male students score between 20% and 30% lower than other European countries.

Data on the Bulgarian teachers' critical reflection of their own digital and pedagogical practice (Area 1. Professional Engagement, Indicator 1.3. Reflective Practice: "To individually and collectively reflect on, critically assess and actively develop one's own digital pedagogical practice and that of one's educational community") are presented in a national survey conducted by the Institute for Research in Education (IRE) [9] among 1885 teachers, a quarter of whom are science teachers. A high proportion of teachers (69%) was found to be satisfied with their own work during distance learning, and 22% were critical of their work.

To assess teachers' self-efficacy in using ICT in the educational process, a 5-point Likert scale was applied in several aspects: self-assessment of the use of digital technology (DT) in the educational process (Fig. 2) and self-assessment of their ability to use DT for specific purposes (Fig. 3). As can be deduced from Fig. 2, most teachers are confident that the use of ICT diversifies their lessons and makes them more interesting. Almost one half believe that ICT is a way to facilitate and improve their work. The findings of the study lead to the important conclusion that teachers' attitudes towards DT have a significant impact on the achievement of good outcomes, according to both teachers themselves and their students: "a strong linear relationship was found between teachers' attitudes about the benefits of using technology in the learning process and their self-efficacy in using ICT ( $r=0.74$ ,  $p<0.001$ ). This means that the more positive teachers are about the

use of ICT in learning and teaching, the more optimistic they are about their own ability to work with technology and to achieve good results (for themselves and their students)" [9, p. 100]. In terms of student achievement, the correlation analysis of the researchers cited above shows "moderately positive linear relationships" between teachers' self-efficacy for ICT use on the one hand and students' interest in distance learning ( $r=0.48$ ,  $p<0.001$ ) and their motivation to learn ( $r=0.43$ ,  $p<0.001$ ) on the other. These correlations were slightly weaker in terms of students' adaptation to the distance learning organization ( $r=0.42$ ,  $p<0.001$ ), their acquisition of the learning content without difficulty ( $r=0.41$ ,  $p<0.001$ ) and their engagement with the learning process ( $r=0.39$ ,  $p<0.001$ ).

A study over ten years old [10], presents the results of a nationally representative survey of the competencies and attitudes of science teachers from different types of schools and regions in Bulgaria on the use of ICT in teaching. The aim of the study is to build a general picture of the competencies and views of Bulgarian science teachers on the use of ICT in teaching and learning in secondary school. The data show that the share of teachers using their computer skills in almost all activities (word processing, spreadsheets, working with electronic databases, presentation software, e-mail, Internet) is relatively small (less than 25%). These data are also consistent with teachers' lack of confidence in their ability to use ICT in teaching practice. Teachers' confidence to use digital technology in the presentation of learning content is also low. A small number of teachers surveyed could create and use animations, develop their own presentations and select teaching situations appropriate for ICT use. Comparatively

higher (but below 40%) is the number of those who state that they can use ready-made teaching resources from the Internet. It is noteworthy that teachers see a variety of opportunities for integrating ICT into students' activities. According to the authors of the survey, the low results are due to the fact that in Bulgarian schools there is no practice of using external experts for help, although with the development of videoconferencing technologies such activities are quite possible within the school environment.

A comparison with other similar studies shows that some of the data and results, unfortunately, have not changed, and the authors' recommendations for improving digital skills in specific pedagogical contexts are still relevant today. In the first study carried out for the EC [11], one of the main prerequisites for effectively exploiting the benefits of ICT applications to create opportunities for high quality learning for everyone was "teachers' positive attitudes towards ICT applications and their confidence in their own abilities to use them", as well as students' access to ICT. These findings are consistent with the results of the study by Kirova *et al.* [10]. Six or seven years later, however, in the second study for the EC [6], analysed at the beginning of this paper, the findings are similar.

What is noticeable in the literature reviewed is the discrepancy between teachers' self-assessment of the ease with which they deal with DT and their students' opinions. According to the study cited above [9] the proportion of teachers who think that they easily cope with ICT is high (72%). This proportion is even higher according to a nationally representative UNICEF survey [12] on e-distance learning conducted with 1229 Bulgarian students nationwide (594 aged 5 to 7 grade and 635 aged 8 to 12 grade). 11.7% of them attend specialised science schools. At the same time, however, it is worrying that a relatively high percentage of students indicated that their teachers did not cope well with distance working (28.7%), in contrast to the confidence of almost all teachers (over 98%) that they deal easily with e-learning. Students in the capital are more likely to state that their teachers cannot work well remotely. Nearly 40% of the parents of students surveyed shared a similar opinion: "teachers are not sufficiently prepared to work remotely", and almost half felt that "the teaching content is not adapted to be taught online".

Hristova *et al.* [9] show that according to the DigComp competence 5.4 Identifying digital competence gaps, half of the students stated that they did not need help to work in electronic environments. This is more the case for specialised

natural sciences schools which could be explained by the fact that students in these schools are admitted after selection – by passing exams in Bulgarian language and mathematics with relatively high grades. Students over the age of 16 most often need help with an online tutoring platform and assistance in preparing lessons or homework suitable for specialized online learning software. Despite the confidence of at least half of the respondents, there was a significant discrepancy between students' self-assessment of their digital competence at the entry to university and the actual assessment of their knowledge and skills.

The findings of the same survey related to teachers' ability to use ICT for specific purposes are of particular interest. Fig. 3 presents some of them, in terms of the proportion (%) of teachers who are unconfident or slightly confident in carrying out certain DT activities. Area 2. Digital Resources of DigCompEdu notes that teachers should share resources through links or as attachments e.g. to emails; on online platforms and personal or organisational websites/blogs; to share their own resources database with others, managing their access and rights appropriately. The relatively high proportion of teachers are not confident in fairly simple activities (Competence 2.2. Creating and modifying digital content, Area 2. Digital Resources), e.g., Create a presentation with simple animation functions (24%) and Using ICT to carry out experiments (27%). Slightly less than a third of teachers are unconfident in spotting fake news. Regardless of the subjects they teach, spotting fake news is very important. For science teachers, this is a key issue as their work should be focused on shaping a scientific worldview and developing students' scientific literacy.

Another important skill for science teachers, especially in chemistry and physics, is the use of spreadsheets to create graphs. Natural sciences deal with laws and patterns, plotting research data graphically, interpreting graphs, and drawing relevant conclusions. Despite the fact that the research [9] is not focused only on the skills of science teachers, it is seen that nearly 38% of teachers have difficulties in such activities. A study by Boiadjieva [13] shows similar results, with around 35% of chemistry teachers having difficulties using spreadsheets, and less than 30% able to use animations only to some extent or to select situations appropriate for ICT use. This study also has found that around 40% of chemistry teachers are not confident in using ICT to organise activities involving participation in discussion forums with students as well as with colleagues.

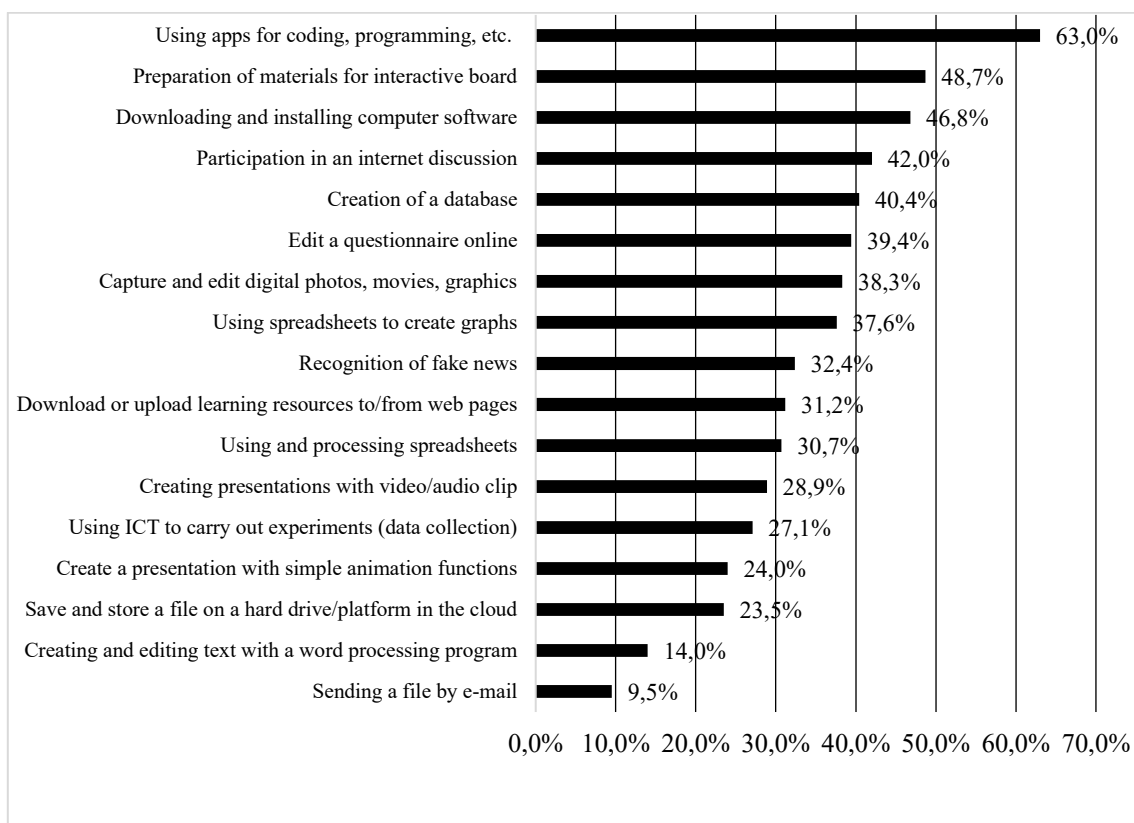


Fig. 3. Self-assessment of teachers' use of ICT for specific purposes.

Obviously, in terms of these particular activities, the situation has not positively changed. The need for training in these fields continues to be on the agenda. Special attention should be paid to the skills outlined above as they play an important role in science education.

The continuing professional education of teachers is also included in Area 1 of DidCompEdu. The effectiveness of distance learning in an e-environment is not just about having equipment, provision of digital devices, internet, and available high-quality electronic platforms. An important condition is the qualifications and experience that teachers have, as well as their commitment, behaviour and attitudes. All of them are related to effective use and integration of technologies, opportunities for active involvement and support of students in learning, adequate and timely feedback [14].

Based on the data in Fig. 3, it can be concluded that despite participation in trainings, there is a deficit in teachers' ability to use DT. A study conducted with 348 Bulgarian biology teachers [15] shows that the highest proportion of teachers experienced difficulties in creating diagnostic and assessment electronic materials (over 85%), followed by the proportion of teachers who had difficulties in developing audio and video resources (over 67%). Over 90% of teachers felt that they

needed training to implement innovative methods using DT. These results confirm the conclusions about the need for targeted qualification courses tailored to the content of the subject area.

A survey of the views of 79 Bulgarian chemistry teachers [16] in two areas: opportunities for ICT application in chemistry classes, and chemistry teachers' competences for integrating ICT in the classroom. The results do not reveal a clear relationship between teachers' views and attitudes on the one hand, and on the other hand with opportunities for using computer technology in chemistry classes in for problem solving; improving communication and collaboration; and developing critical thinking and creativity (Area 6, DigCompEdu). Findings from the study point to the need for further training for chemistry teachers to help them more fully unlock the potential of ICT to enhance teaching and develop key skills for students in a digital society.

According to the Teaching and Learning International Survey (TALIS) of teachers and school leaders on school environments [17], the participation of Bulgarian teachers (ISCED 2) in ICT-related training is 63.3%, which is the same as the average for all teachers who participated in TALIS 2018 (63%). At the same time, 23% of Bulgarian teachers state that they need DT-related training in teaching, while the average for TALIS

2018 is 20%. According to TALIS, even if teachers received professional qualifications in this area years ago, due to the rapid development of ICT and the increasing penetration of digital technologies in teaching, they need to continuously update their knowledge and skills. Distance learning during the pandemic of COVID-19, showed that developing DC should have the highest priority in teachers' professional development.

The IER monitoring report [9] also poses research questions related to an examination of teachers' use of educational resources that meet Area 2. Digital resources from DigCompEdu. Appropriate didactic materials and resources are crucial for the implementation of effective teaching in both traditional and electronic environments. Nearly 15% of the Bulgarian teachers surveyed used available educational resources, with only 17% using educational resources created by colleagues teaching the same subject in their own school.

Other important requirements for this area are: sharing digital content by respecting intellectual property and copyright; complying with any copyright restrictions on the use, reuse and modification of digital resources; citing sources appropriately when resources are shared or published under copyright. The literature search found no evidence for Bulgaria in these aspects. Clearly these requirements are important and could be a subject not only for research but also for targeted training of both teachers and students.

An online survey compiled under the DigCompEdu framework [18] has found that the predominant level of digital competence of 81.8% of teachers surveyed on almost all criteria was A2 Explorer. Teachers identified at A2 level should be aware of the potential of digital technologies and are interested in exploring and mastering them to enhance pedagogical and professional practice. This conclusion coincides with the findings of the international studies presented above as well as the Education and training monitor report on Bulgaria of EC [7].

Many requirements in Area 3. Teaching and Learning of DigCompEdu: 3.1 Teaching; 3.2 Guidance; 3.3 Collaborative learning and 3.4 Self-regulated learning are at the heart of the constructivist approach. Learning in a constructivist environment is the focus of current educational standards and curricula in many countries, including Bulgaria. Researchers find a deep connection between the effective use of ICT in the educational process and the application of constructivist approach in teaching practice. In the spirit of constructivist ideas, therefore, some of the questions

in the IER survey [9] have been selected, while at the same time they can be related to Area 3 of DigCompEdu, namely (a) the way the learning content is presented; (b) the opportunity for students to work independently; (c) the stimulation of students to participate in the construction of knowledge; (d) practices for checking students' work and monitoring their progress; (e) practices for providing additional support to students who are experiencing difficulties. The responses of the Bulgarian teachers on the opportunities they have had to use educational resources and different teaching methods are of particular interest. More than 70% of them say that they had used more educational resources and that they had experimented with using more different teaching methods in the online environment than in face-to-face teaching. However, there is a certain inconsistency in the responses of these teachers with their answers concerning the teaching practices and methods applied. More than 70% of the teachers have declared that they presented and explained the learning content. The same percentage of teachers have sent ready-made learning materials for independent work. The result is similar for teachers who have sent and checked the completed tasks photographed or scanned. A significant proportion of teachers used platforms for these activities, but a relatively small proportion of teachers implemented elements of constructivist learning in an e-environment, and as would be expected, these were most prevalent at the high school level.

Similar results were found in the TALIS 2018 survey [17]: the least common teachers practices in ICSED 2 are using IT in class or for a project – 44.2% of Bulgarian teachers vs. 51.3% on average for TALIS, and having students work in small groups to solve a problem – 48.6% of Bulgarian teachers vs. 52.7% on average for the survey.

Regular assessment of student progress and good quality, relevant and timely feedback are seen as key factors in the process of learning and have one of the most significant impacts on student learning achievements. DT extend opportunities for both summative and formative assessment, feedback and self-assessment skill formation (DigCompEdu, Area 4. Assessment: 4.1. Assessment strategies; 4.2. Analyzing evidence; 4.3. Feedback and Planning). According to the IER survey [9], almost 70% of teachers have carried out assessment-related activities, but the percentage of teachers who have rarely engaged in assessment of their students is not small, at around 30%. E-learning allows the use of different ways to develop self-assessment skills. The IER study mentioned above reports some hesitancy

and uncertainty among teachers about the objectivity of the grades they give students for various reasons, e.g., copying, help from other persons. This feedback from a significant number of practicing teachers casts serious doubt on the real contribution of regular student assessment. In this context, the use of different tools for both assessment and self-assessment can have a positive impact on the effectiveness of monitoring and diagnosis of distance learning.

Understanding the real situation regarding DC is particularly important to develop the digital competences needed for the near future in a society we now call Society 5.0. A study at the University of Maribor, Slovenia has shown that “neither teachers nor students are sufficiently qualified to work in the society of the future, in society 5.0.” [19, p. 118]

#### *Digital technologies and students' academic performance in science*

Digital technologies undoubtedly facilitate teaching and learning in many cases. Without them, distance learning during the COVID-19 pandemic could not have taken place given the extent and duration of school closures. Yet, despite the obvious advantages of DT use in education, it turns out that, in many cases, the use of DT does not improve students' academic performance and sometimes even worsen it.

An OECD [20] study based on PISA 2015 presents data on the availability of digital resources, their use in teaching and learning, and the relationship between ICT use and achievement among 15-year-old students. It may seem a paradox, but the PISA data show that for a given level of per capita gross domestic product (GDP), and after accounting for the initial level of performance, countries that invested less in introducing of computers in schools improved their performance faster on average than countries that invested more. The results are similar for reading, mathematics and science [20, pp. 150-151]. As will become clear later from the analysis of publications of a number of researchers, there is no correlation between student achievement and the use of digital resources. The achievement-digitization relationship in education is multi-component and therefore complex and difficult to study, which is why the results of different studies are contradictory. An analysis of Trends in International Mathematics and Science Study (TIMSS) data [21] compare differences in computer use in mathematics and science with differences in student achievement. It was found that math scores are unrelated to computer use, while science scores are positively linked only in cases

such as looking up ideas and information, and the effect is "detrimental" when DT is used to practice skills and procedures. The authors conclude that the “policymakers and educators all over the world rush to bring computers into every classroom but such enthusiasm and costly investment is hard to reconcile with the available evidence that computer use in schools has little if any effect on student achievement.” After all, “the overall effect of using computers in schools is generally close to zero” (p. 22).

A 2023 literature review [22] has listed a number of studies, some from 2022, that have found positive impacts of DT on science learning and also on subjects in STEM (science, technology, engineering, and mathematics) disciplines.

Another literature review [23] on the impact of computer simulations on science process skills has found that simulations help more in the presentation and understanding of science concepts than traditional teaching methods, but without combining them with other teaching methods they are not effective enough. Virtual laboratories pose problems, e.g. students do not acquire the skills for practical work in a real laboratory environment and the uptake of science process skills is at a low level.

According to Hristova *et al.* [9] “very few teachers, between 4% and 9% strongly agree that distance learning was more effective than face-to-face learning in terms of student outcomes.” Between 21% and 28% of teachers did not express a definite opinion about the effects of distance learning on student interest and motivation. These, as well as the findings of other studies [14, 24], lead to the conclusion that the more positive attitudes teachers have towards the use of ICT, the easier their students adapt to distance learning in an electronic environment, having a greater interest, motivation and engagement in the learning process and learn the teaching material more easily.

Hattie and Yates [25, p. 274] report that if computers are not used as an alternative to traditional teaching, but rather complement it, their impact on student performance is stronger. According to these authors, positive effects were achieved in activities that applied the same instructional principles as traditional teaching. There are topics in science subjects that have abstract or theoretical content where visualization through digital resources helps considerably in understanding and learning. Interactive methods such as computer simulations, animations, and YouTube videos increase interest and understanding of difficult concepts. A common practice in Bulgarian schools is to use You Tube channels such

as Khan Academy (<https://www.khanacademy.org>). However, in these channels, sometimes there are a lot of gaps and inaccuracies in the visualization and explanation of information from a scientific point of view, which can lead to misconceptions. These digital resources should serve as supplementary rather than core didactic material, as is sometimes observed in practice.

Hu *et al.* [26], as well as Petko *et al.* [27], have found that students who use ICT devices at home for entertainment achieve higher science scores while ICT use by students at school correlates negatively with their academic performance. This result seems paradoxical at first, but quite a few other researchers have reported a similar effect. For students from 25 European countries in PISA 2015, medium and high ICT users scored lower in science than those with little ICT use [28]. Other authors [29] have also found that ICT use for entertainment at home is positively correlated with science scores in Turkey but this is not the case in Finland.

In their article “The Relation between ICT and Science in PISA 2015 for Bulgarian and Finnish Students”, Canadian researchers [30] examine the extent to which ICT helps or hinders students’ school achievements in science and the relationship between ICT and student performance in science in two European countries – Bulgaria and Finland. The choice of the two countries – Finland and Bulgaria, for the comparative analysis the authors justify as follows: Finland is considered a digital leader due to its high level of DT, the small gap between high and low technology users, and good welfare in general. In Bulgaria, the gap between high- and low-tech users is large, the DT are relatively late entrants to the free market, and student achievements in school are relatively low. Referring to European Commission reports the authors note that in the high-performing country Finland, the digital competence of students and teachers is higher than both the European and Bulgarian average. Finland is much better equipped with digital technology than Bulgaria, but when it comes to computer use, the two countries show similarities. This study investigates whether ICT-related factors such as availability of digital devices, their use, independent work, interests and competence in DT, and social interactions are associated with higher or lower science scores of Bulgarian and Finnish students. PISA 2015 data for 5,928 Bulgarian students and 5,882 Finnish students aged 16 years 3 months and 16 years 2 months were used. In general, the authors’ literature review shows that the results are inconsistent. In both Bulgaria and Finland, students who perceive themselves as competent and capable of working independently

with ICT, for whom ICT is among their topics of conversation and have a strong interest in DT are positively linked to higher science scores, while the use and availability of ICT technologies at home and at school for academic work or leisure are negatively related to science scores. The study finds no association between science scores in Finland and the availability of ICT devices, and that ICT use does not contribute to higher science scores for the majority of students in Finland.

Why does the use of ICT for learning purposes at school and at home lead to lower science scores? Possible explanations are that students are distracted by ICT while engaged in an activity, or spend more time on extracurricular ICT activities that take them away from academic tasks; or the time spent on ICT is at the expense of academic work. Excessive computer use, especially for non-academic purposes (social media, gaming, etc.), can lead to distractions and decreased focus on students’ learning impacting negatively academic performance. Another possible explanation is that students do not sufficiently mobilize their own mental capacity and knowledge, but rely only on easily accessible information using the Internet, artificial intelligence, and various digital applications.

The only component of ICT for which all studies have found a positive relationship with science achievement is the ability to work independently with ICT. ICT competence is the second factor with a positive relationship. Therefore, the authors believe that it is important to determine which ICT component has a greater impact on student achievements in science and this can serve as a first step in identifying the sources of some of the conflicting results between ICT and science.

## CONCLUSION

The forced shift to e-learning due to the Kovid 19 pandemic has revealed both positive and negative aspects of students’ and teachers’ digital technology skills. It cannot be denied, though, that the situation has resulted in an acceleration of the use of digital resources and technologies and an increase in the digital competencies of teachers and students.

The analysis of the literature has largely made it possible to answer the research questions posed.

Overall, the analysis shows that despite Bulgarian students and teachers declared relatively high confidence to work with DT, in reality their digital competence is lower in most areas reflected in the DigComp and DigCompEdu frameworks compared to the European average.

The survey results outline several problematic areas of digital competences for Bulgarian teachers

according to DigCompEdu. In addition to the difficulties found in activities related to creating and modifying digital content, the lack of collaboration between teachers that is highlighted in much of the research is of concern. The fact that a similar outcome is observed among Bulgarian students is not to be overlooked. From a science perspective, teachers' difficulties in identifying fake news also stand out, which is particularly important for developing a scientific worldview and scientific literacy in their students. Activities related to assessment of students' progress and ensuring high-quality, relevant, and well-timed feedback also emerged as a serious problem.

The quality of continuing teacher education aimed at the development of digital competences is also a problematic area. Regardless of the data on the participation of a high percentage of teachers in such trainings, the existing skills deficit in the use of technology requires training in which DT is targeted to the specific subject area.

However, a large proportion of Bulgarian teachers express satisfaction with their own work during distance learning and this is also evident in their self-efficacy ratings. A good sign is the declared confidence of most teachers that the use of ICT diversifies their lessons and makes them more interesting.

Regarding the second research question related to identifying a correlation between the use of digital technologies and students' science learning achievements, the analysis of the publications does not provide a definitive answer to this question without pretending to the completeness of the study. Much of the studies show a lack of correlation between student performance and the use of digital resources. The reason for this can be sought in different aspects of the achievement-digitalisation relationship, which makes the field complex and difficult to study. The focus is rather on the possible positive effect when computers are used to complement traditional teaching and not as an alternative to it.

**Acknowledgement:** *This study is financed by the European Union-NextGenerationEU, through the National Recovery and Resilience Plan of the Republic of Bulgaria, project No BG-RRP-2.004-0008.*

#### REFERENCES

1. Y. Punie, A. Ferrari, B. Brečko, DigComp: a Framework for Developing and Understanding Digital Competence in Europe, EC Publications Office, 2013. <https://data.europa.eu/doi/10.2788/52966>

2. L. Brande, S. Carretero, R. Vuorikari, DigComp 2.0: the Digital Competence Framework for Citizens, EC Publications Office, 2016. <https://data.europa.eu/doi/10.2791/11517>
3. S. Carretero, R. Vuorikari, Y. Punie, DigComp 2.1: the Digital Competence Framework for Citizens with Eight Proficiency Levels and Examples of Use, EC Publications Office, 2017. <https://data.europa.eu/doi/10.2760/38842>
4. R. Vuorikari, S. Kluzer, Y. Punie, DigComp 2.2, The Digital Competence Framework for Citizens: with New Examples of Knowledge, Skills and Attitudes, EC Publications Office, 2022. <https://data.europa.eu/doi/10.2760/115376>
5. C. Redecker, Y. Punie, European Framework for the Digital Competence of Educators: DigCompEdu, EC Publications Office, 2017. <https://data.europa.eu/doi/10.2760/159770>
6. European Commission, Directorate-General for Communications Networks, Content and Technology, 2nd Survey of Schools: ICT in Education: Objective 1: Benchmark Progress in ICT in Schools, Executive Summary, Publications Office, 2019. <https://data.europa.eu/doi/10.2759/958553>
7. European Commission, Directorate-General for Education, Youth, Sport and Culture, Education and Training Monitor 2022: Bulgaria, Publications Office, 2022. <https://data.europa.eu/doi/10.2766/207>
8. N. S. Tsankov, The Digital Competence of Future Teachers (Growth Design and Development), Academic Publishing House of Thracian Univ., 2023.
9. A. Hristova, S. Petrova, E. Papazova, Evaluation of the Impact of Distance Learning in e-Environment or Other Non-presence Forms on the Effectiveness of School Education, Institute for Research in Education, 2020. [https://ire-bg.org/wpsite/wp-content/uploads/2020/11/Otsenka-vazdeystvieta-na-ORES\\_IIO.pdf](https://ire-bg.org/wpsite/wp-content/uploads/2020/11/Otsenka-vazdeystvieta-na-ORES_IIO.pdf)
10. M. Kirova, E. Boiadjieva, R. Peitcheva-Forsyth, *Chemistry: Bulg. J. Sci. Edu.*, **21**, 282 (2012).
11. European Commission, Directorate-General for the Information Society and Media, Survey of Schools: ICT in Education: Benchmarking Access, Use and Attitudes to Technology in Europe's Schools. Publications Office, 2013. <https://data.europa.eu/doi/10.2759/94499>
12. UNICEF Europe and Central Asia, Assessing the Impact of Covid-19 on Pre-school and School Education in Bulgaria: Students' Perspective, 2020. <https://www.unicef.org/bulgaria/media/8916/file>
13. E. Boiadjieva, in: E-learning, Distance Education...or the Education of 21st Century (Proc. Intern. Conf., April, 6-8, 2011, Sofia), 2011, p. 455.
14. J. Webster, P. Hackley, *Acad. Manag. J.*, **40**, 1282 (1997). <https://www.jstor.org/stable/257034>
15. K. Yotovska, A. Assenova, V. Necheva, *Sci. & Techn.*, **X(7)**, 14 (2020). <https://www.sustz.com/bg/?f=journal&volume=12>
16. M. Kirova, N. Kostova, M. Trendafilova, *Chemistry: Bulg. J. Sci. Edu.*, **24**, 776 (2015).

17. OECD. TALIS 2018 Results (Vol. I) Teachers and School Leaders as Lifelong Learners. TALIS, OECD Publishing, 2019. <https://doi.org/10.1787/1d0bc92a-en>
18. N. Koleva, The Digital Competences of Bulgarian Teachers, Shumen Univ. Konstantin Preslavski Publishing House, 2019.
19. M. Kordigel Aberšek, B. Aberšek, *J. Baltic Sci. Edu.*, **21**, 108 (2022). <https://doi.org/10.33225/jbse/22.21.108>
20. OECD, in: Students, Computers and Learning: Making the Connection, PISA, OECD Publishing, 2015, p.145. <https://doi.org/10.1787/9789264239555-en>
21. O. Falck, C. Mang, L. Woessmann, Virtually no Effect? Different Uses of Classroom Computers and their Effect on Student Achievement. IZA Discussion Paper 8939, 2015. [https://papers.ssrn.com/sol3/papers.cfm?abstract\\_id=2589781](https://papers.ssrn.com/sol3/papers.cfm?abstract_id=2589781)
22. S. Timotheou, O. Miliou, Y. Dimitriadis, S. V. Sobrino, N. Giannoutsou, R. A. Cachia, M. Monés, A. Ioannou, *Edu. and Inform. Techn.*, **28**, 6695 (2023). <https://doi.org/10.1007/s10639-022-11431-8>
23. B. Çelik, *Canadian J. Edu. and Soc. Studies*, **2**(1), 16 (2021). <https://doi.org/10.53103/cjess.v2i1.17>
24. J. Gil-Flores, J. Rodríguez-Santero, J.-J. Torres-Gordillo, *Computers in Human Behaviour*, **68**, 441 (2017). <https://doi.org/10.1016/j.chb.2016.11.057>
25. J. Hattie, G. C. R. Yates, Visible Learning and the Science of How we Learn. Routledge, 2013. <https://doi.org/10.4324/9781315885025>
26. X. Hu, Y. Gong, C. Lai, F. K. S. Leung, *Comp. & Edu.*, **125**, 1 (2018). <https://doi.org/10.1016/j.compedu.2018.05.021>
27. D. Petko, A. Cantieni, D. Prasse, *J. Edu. Comp. Res.*, **54**, 1070 (2017). <https://doi.org/10.1177/0735633116649373>
28. M. Rodrigues, F. Biagi, Digital technologies and learning outcomes of students from low socioeconomic background: An analysis of PISA 2015, JRC Science for Policy Report, 2017. <https://data.europa.eu/doi/10.2760/415251>
29. O. Bulut, M. Cutumisu, *J. Edu. Multimedia and Hypermedia*, **27**, 25 (2018). <https://www.learntechlib.org/p/178514>
30. B. Odel, A. M. Galovan, M. Cutumisu, *Eurasia J. Math, Sci. and Techn. Edu.*, **16**(6) em1846 (2020). <https://doi.org/10.29333/ejmste/7805>

### Instructions about Preparation of Manuscripts

**General remarks:** Manuscripts are submitted in English by e-mail. The text must be prepared in A4 format sheets using Times New Roman font size 11, normal character spacing. The manuscript should not exceed 15 pages (about 3500 words), including photographs, tables, drawings, formulae, etc. Authors are requested to use margins of 2 cm on all sides.

Manuscripts should be subdivided into labelled sections, e.g. INTRODUCTION, EXPERIMENTAL, RESULTS AND DISCUSSION, etc. **The title page** comprises headline, author(s)' names and affiliations, abstract and key words. Attention is drawn to the following:

a) **The title** of the manuscript should reflect concisely the purpose and findings of the work. Abbreviations, symbols, chemical formulae, references and footnotes should be avoided. If indispensable, abbreviations and formulae should be given in parentheses immediately after the respective full form.

b) **The author(s)'** first and middle name initials and family name in full should be given, followed by the address (or addresses) of the contributing laboratory (laboratories). **The affiliation** of the author(s) should be listed in detail (no abbreviations!). The author to whom correspondence and/or inquiries should be sent should be indicated by an asterisk (\*) with e-mail address.

**The abstract** should be self-explanatory and intelligible without any references to the text and containing up to 250 words. It should be followed by keywords (up to six).

**References** should be numbered sequentially in the order, in which they are cited in the text. The numbers in the text should be enclosed in brackets [2], [5, 6], [9–12], etc., set on the text line. References are to be listed in numerical order on a separate sheet. All references are to be given in Latin letters. The names of the authors are given without inversion. Titles of journals must be abbreviated according to Chemical Abstracts and given in italics, the volume is typed in bold, the initial page is given and the year in parentheses. Attention is drawn to the following conventions: a) The names of all authors of a certain publication should be given. The use of "et al." in the list of references is not acceptable; b) Only the initials of the first and middle names should be given. In the manuscripts, the reference to author(s) of cited works should be made without giving initials, e.g. "Bush and Smith [7] pioneered...". If the reference carries the names of three or more authors it should be quoted as "Bush et al. [7]", if Bush is the first author, or as "Bush and co-workers [7]", if Bush is the senior author.

**Footnotes** should be reduced to a minimum. Each footnote should be typed double-spaced at the bottom of the page, on which its subject is first mentioned. **Tables** are numbered with Arabic numerals on the left-hand top. Each table should be referred to in the text. Column headings should be as short as possible but they must define units unambiguously. The units are to be separated from the preceding symbols by a comma or brackets. Note: The following format should be used when figures, equations, etc. are referred to the text (followed by the respective numbers): Fig., Eqns., Table, Scheme.

**Schemes and figures.** Each manuscript should contain or be accompanied by the respective illustrative material, as well as by the respective figure captions in a separate file. As far as presentation of units is concerned, SI units are to be used. However, some non-SI units are also acceptable, such as °C, ml, l, etc. Avoid using more than 6 (12 for review articles) figures in the manuscript. Since most of the illustrative materials are to be presented as 8-cm wide pictures, attention should be paid that all axis titles, numerals, legend(s) and texts are legible.

**The authors are required to submit the text with a list of three individuals and their e-mail addresses that can be considered by the Editors as potential reviewers. Please note that the reviewers should be outside the authors' own institution or organization. The Editorial Board of the journal is not obliged to accept these proposals.**

The authors are asked to submit **the** final text (after the manuscript has been accepted for publication) in electronic form by e-mail. The main text, list of references, tables and figure captions should be saved in separate files (as \*.rtf or \*.doc) with clearly identifiable file names. It is essential that the name and version of the word-processing program and the format of the text files is clearly indicated. It is recommended that the pictures are presented in \*.tif, \*.jpg, \*.cdr or \*.bmp format. The equations are written using "Equation Editor" and chemical reaction schemes are written using ISIS Draw or ChemDraw programme.

## EXAMPLES FOR PRESENTATION OF REFERENCES

### REFERENCES

1. D. S. Newsome, Catal. Rev.–Sci. Eng., 21, 275 (1980).
2. C.-H. Lin, C.-Y. Hsu, J. Chem. Soc. Chem. Commun., 1479 (1992).
3. R. G. Parr, W. Yang, Density Functional Theory of Atoms and Molecules, Oxford Univ. Press, New York, 1989.
4. V. Ponec, G. C. Bond, Catalysis by Metals and Alloys (Stud. Surf. Sci. Catal., vol. 95), Elsevier, Amsterdam, 1995.
5. G. Kadinov, S. Todorova, A. Palazov, in: New Frontiers in Catalysis (Proc. 10th Int. Congr. Catal., Budapest (1992), L. Guzzi, F. Solymosi, P. Tetenyi (eds.), Akademiai Kiado, Budapest, 1993, Part C, p. 2817.
6. G. L. C. Maire, F. Garin, in: Catalysis. Science and Technology, J. R. Anderson, M. Boudart (eds.), vol. 6, Springer Verlag, Berlin, 1984, p. 161.
7. D. Pocknell, GB Patent 2 207 355 (1949).
8. G. Angelov, PhD Thesis, UCTM, Sofia, 2001, pp. 121-126.
9. JCPDS International Center for Diffraction Data, Power Diffraction File, Swarthmore, PA, 1991.
10. CA 127, 184 762q (1998).
11. P. Hou, H. Wise, J. Catal., in press.
12. M. Sinev, private communication.
13. <http://www.chemweb.com/alchem/articles/1051611477211.html>.

***Texts with references which do not match these requirements will not be considered for publication!!!***

CONTENTS

<i>V. Kurteva</i> , In memoriam Prof. DSc Ivan Pojarlieff (Johnny).....	99
<i>E. Ganev, S. Panyovska, K. Stefanova</i> , Overview of approaches to obtaining energy from heat including ground-based installation.....	101
<i>D. Panchani, S. Maurya, T. Thaker, V. Rathod, Sh. Thakur</i> , Synthesis, biological evaluation, ADME studies and molecular docking with $\beta$ -tubulin of fused benzimidazole-pyridine derivatives.....	107
<i>A. Naseer, A. Naz Awan, J. Iqbal, S. Habib, A. Javed</i> , Cobalt complexes of pyridine carboxaldehyde Schiff bases as cholinesterase inhibitors and anti-proliferative activity.....	125
<i>R. Vladova, T. Petrova, E. Kirilova</i> , A multi-objective robust optimization to design a sustainable dairy supply chain under uncertain product demands, economic and social consideration. A real case study from Bulgaria.....	147
<i>V. V. Idakiev, L. Mörl</i> , Inductively heated fluidized beds and their potential for energy savings and efficient process control.....	159
<i>K. L. Zaharieva, S. S. Dimova, R. T. Eneva, V. N. Hubenov, I. D. Stambolova, D. D. Stoyanova, F. S. Ublekov, O. S. Dimitrov, H. P. Penchev</i> , PLA/PVP/bio-synthesized hydrozincite nanocomposite films – photocatalytic and antibacterial activity.....	164
<i>K. L. Zaharieva, R. T. Eneva, S. L. Mitova, O. S. Dimitrov, H. P. Penchev</i> , Preparation and antimicrobial activity of silver nanoparticles impregnated with halloysite clay.....	169
<i>M. Atanassova, N. Todorova, S. Goranova-Markova</i> , The history of the first germanium crystals along with a descendant of the novel “Bulgarians of old time”.....	175
<i>E. Boiadjieva, A. Tafrova-Grigorova</i> , Digitalization in Bulgarian science education: a comparative analysis of the state of the art.....	184
<i>INSTRUCTIONS TO AUTHORS</i> .....	196